Report on the Production of Landsat Overpass and Monthly Evapotranspiration Maps for the Beryl Junction area of Utah for Years 2020 and 2021 using the METRIC^{tm} Model

a component of the
Agricultural Water Optimization Task Force Depletion Accounting Case Study

submitted to
Utah State University

by
Dr. Richard Allen
Dr. Wenguang Zhao
Dr. Ayse Kilic
Evapotranspiration, Plus
Lincoln, NE

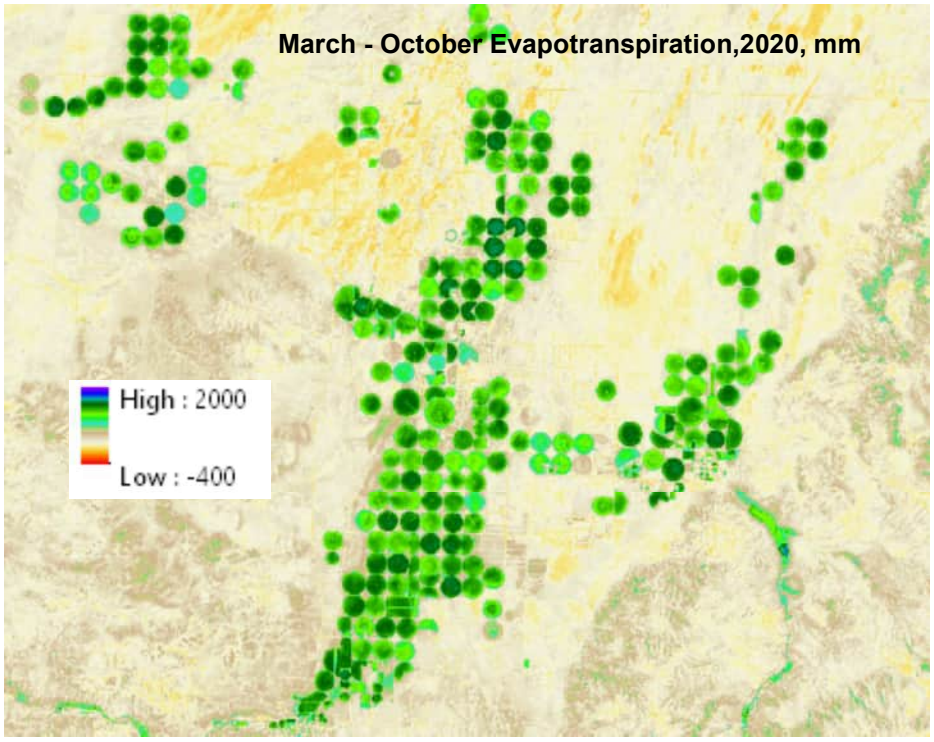

June 2022

Cover Graphic: March-October ET from irrigated areas near Beryl Junction, Utah during 2021 showing higher evapotranspiration as dark green. Beige colored areas have low ET.

Contents

1. Introduction

This report provides a description of the procedures and products used during processing of satellite, weather and land-use data for the Beryl Junction region of Utah to produce spatial maps of monthly evapotranspiration (ET) for the region and nearby surrounding. The products represent ET information presented at 30 m resolution in the form of ET (mm per month) and also presented as a fraction of reference evapotranspiration (ET_rF) based on the alfalfa reference crop. The processed region lies in the overlap of two Landsat paths (38 and 39) as shown in Figure 1. The location in the path overlap area provided for Landsat imagery from both paths. This effectively doubled the potential for obtaining clear (cloud-free) images for the area that could then be processed by the METRIC process. The study domain was contained in row 34 of Landsat.

ET was produced using the METRIC model developed by the University of Idaho (Allen et al. 2007a,b; 2011). The METRIC procedure utilizes visible, near-infrared and thermal infrared energy spectrum bands from Landsat satellite images and weather data to calculate ET on a 30 m pixel by pixel basis. ET is estimated from a surface energy balance, where net radiation at the surface (R_n), comprised of both both solar and thermal radiation, is partitioned into ground heat flux (G) and sensible heat flux (H) and ET, as described later. The impact of topography of the region on the surface energy balance is incorporated into METRIC via a digital elevation model (DEM), and is used to account for impacts of slope and aspect on solar radiation absorption and impacts of elevation on surface temperature. The surface energy balance in METRIC was uniquely calibrated for each image date using ground based meteorological information and identified 'anchor' or 'endpoint' conditions (the cold and hot pixels of METRIC) present in each image. A detailed description of METRIC can be found in Allen et al. (2007a,b; 2011).

The METRIC model has been in existence since year 2000 and has found wide use in the states of Idaho, California, Oregon, Nevada, New Mexico, Montana, Wyoming, Texas and Nebraska for determining spatial distribution of consumptive use associated with water rights administration, crop water modeling and ground-water model operation. Many applications in the western US and internationally are described in Serbina and Miller (2014). A strong advantage of using energy balance is that actual ET is computed rather than estimating a potential ET based on amount of vegetation. As a result, reductions in ET caused by shortages of soil moisture or other factors are identified. METRIC™ utilizes spectral raster images from the visible, near infrared, and thermal infrared energy spectrum to compute the energy balance on a pixel-by-pixel basis. General accuracy of ET estimated by METRIC has been estimated to be +/- 5 to 15% over a growing season for specific fields when applied by expert users (Allen et al., 2011).

For the year 2020 and 2021 processing, an ERDAS-Imagine implementation of METRIC code was utilized. That implementation allows for image-by-image processing with user selection of calibration points, as well as review of calibration results and adjustment based on expert overview. The ERDAS scripts are described in the METRIC user manual (Allen et al., 2016).

2. Image Selection and pre-processing

Imagery from Landsat satellites is processed into evapotranspiration (ET) due to the relatively high resolution of 30 m and the presence of a thermal band on the Landsat satellites. The 30 m resolution provides ET information at the sub-field scale, which is important for agricultural water management and for water rights management. The thermal information permits application of a surface energy balance that is able to determine ET under both well-watered and stressed conditions. For 2020 and 2021, images from both Landsat 8 and Landsat 7 satellites were processed. Landsat 7 was launched in 1999. Landsat 8 was launched in February 2013. Landsat 7 was retired in February 2022 and was replaced at that time by the newly launched Landsat 9.

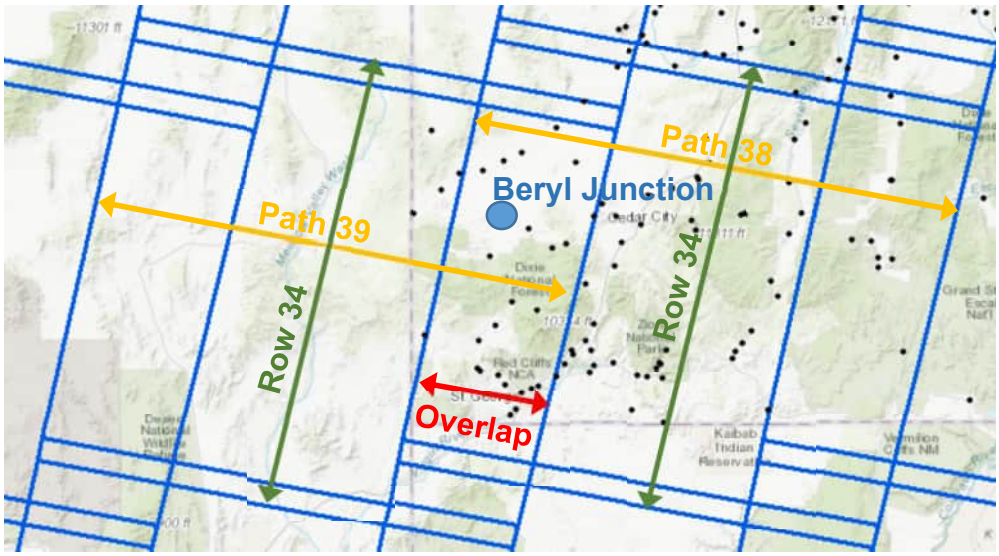

Figure 1. Overlays of Landsat WRS2 path and row extents onto the Beryl Junction region of Utah, and showing where path 38 and path 39 overlap relatively to the location of Beryl Junction. Every landsat path overlaps the adjacent paths. Rows have a smaller overlap.

Landsat 7 images acquired after May 2003 are less preferred than from Landsats 8. This is due to an anomaly with the Landsat 7 satellite caused by the malfunction of the scan line corrector (SLC-off) beginning in May 2003. As a consequence, Landsat 7 images processed for years 2020 and 2021 are "SLC-off" images that contain wedge shaped gaps extending from the edges of the image and stretching towards the centers, as shown later in Figure 8. The gaps in ET_rF (ET as a fraction of reference ET) maps produced by METRIC from Landsat 7 were therefore filled in during post-processing using the natural neighbor tool of Arc-GIS. Experience has shown that filling gaps with the natural neighbor tool produces better information in gaps that keys off from ET_rF values and patterns adjacent to the gaps.

Images to process during the two years was based on time between image dates and cloud conditions over the area of interest (irrigated fields in the Beryl Junction area). Landsat 7 and 8 are polar orbiting satellites and each revisit a specific location every 16 days. Landsat 7 is scheduled 8 days prior to and following Landsat 8 so that a Landsat 7 or Landsat 8 image is available every 8 days. The path 38 adjacent to path 39 has a Landsat 8 image that is 7 days later than the path 39 Landsat 8, and therefore 1 day prior to a Landsat 7 image. This is useful, as in effect, there is the

possibility of having Landsat 8 images that are 7 or 9 days apart in time. The 1-day separation between Landsat 8 on one path and Landsat 7 on the adjacent path means that a Landsat 8 can potentially be processed, if clear, rather than a Landsat 7 image, occurring one day earlier or later, with its SLC-off gaps. As a consequence, the processing for 2020 and 2021 was able to use a majority of Landsat 8 images and a minority of Landsat 7.

An important criterion for image selection is an assessment of cloud conditions at the time of the satellite overpass. The clearness of the atmosphere is impacted by clouds, including thin cirrus clouds, and jet contrails, smoke and haze. The occurrence of these conditions over an area of interest can render that part of the image unusable for processing in METRIC. Even very thin cirrus clouds can indicate lower surface temperature than the actual ground surface. Because METRIC uses surface temperature estimates to solve the energy balance, areas having cloud cover create error in the ET estimates. In addition, areas recently shaded by moving clouds may appear to be cooler than other sunlit areas because they have not yet reached a thermal equilibrium corresponding to the clear sky energy loading. These areas adjacent to clouds and shadows are generally masked out of the processed images and replaced with information from other image dates, as described later. Initial cloud assessment was done by viewing Landsat preview images at http://glovis.usgs.gov/ and noting the amount of cloud cover in the image, especially over irrigated regions in the scene. Special preference was given for clearness over irrigated areas of the study area.

The following tables list Landsat overpass dates processed for each year as well as whether they were used during time integration of ET_rF from overpass dates into monthly ET, as described later. The ET from individual fields in the study area tend to vary substantially in time during the growing season due to alfalfa cuttings, rapid development of annual crops and rain events. Therefore, a high frequency of image processing is valuable for defining time-based changes in ET rates. In 2020, there was sufficient spacing of Landsat 8 images in time, so that no Landsat 7 images were needed. In 2021, four Landsat 7 images were included for processing, but only one was included in the time integration step due to lack of confidence in the ET produced for the SLC-off gaps of three of the Landsat 7 images during the gap filling step, and the proximity of clear Landsat 8 image dates.

Table 1. Landsat images processed for year 2020.

Image No.	Year	MoDa	Sat.	Path	Used for Monthly
1	2020	0331	L8	P39	X
2	2020	0425	L8	P38	X
3	2020	0502	L8	P39	X
4	2020	0511	L8	P38	X
5	2020	0527	L8	P38	X
6	2020	0612	L8	P38	X
7	2020	0619	L8	P39	X
8	2020	0628	L8	P38	X
9	2020	0705	L8	P39	X
10	2020	0714	L8	P38	X
11	2020	0730	L8	P38	X
12	2020	0806	L8	P39	X
13	2020	0815	L8	P38	X
14	2020	0822	L8	P39	X
15	2020	0831	L8	P38	X
16	2020	0916	L8	P38	X
17	2020	0923	L8	P39	X
18	2020	1002	L8	P38	X
19	2020	1018	L8	P38	X
20	2020	1119	L8	P38	X

Use?

Table 2. Landsat images processed for year 2021.

Image no.	Year	MoDa	Sat.	Path	Used for Monthly
1	2021	327	L8	P38	X
2	2021	404	L7	P38	no
3	2021	412	L8	P38	X
4	2021	419	L8	P39	X
5	2021	505	L8	P38	X
6	2021	514	L8	P39	X
7	2021	521	L8	P38	X
8	2021	606	L8	P39	X
9	2021	615	L8	P38	no
10	2021	708	L8	P39	X
11	2021	717	L8	P38	X
12	2021	724	L8	P39	X
13	2021	802	L8	P38	X
14	2021	810	L7	P38	X
15	2021	826	L7	P38	no
16	2021	903	L8	P38	X
17	2021	919	L8	P38	X
18	2021	926	L8	P39	X
19	2021	927	L7	P38	no
20	2021	1021	L8	P38	X
21	2021	1028	L8	P39	X

The geometric projection for the Path 38 images as obtained from the USGS EROS data center is UTM zone 12 and the projection for the Path 39 image is UTM zone 11. Therefore the Path 39 images were reprojected to zone 12 prior to processing with METRIC to produce a common projection for later time integration of ET data.

A total of 20 Landsat images were processed for paths 38 and 39 and used in time integration of monthly ET for 2020 and 17 were processed and used for 2021. The selection of image dates was according to clearness of the images over irrigated areas and the dates of the images relative to other images.

General features of the study area

The Beryl Junction area of Utah has a semi-arid climate with low amounts of precipitation at low elevations and increasing precipitation over higher elevation mountains. Monsoon-driven precipitation can occur during summer during some years. Irrigated agriculture is generally distributed in groups of development near areas having favorable soil types and access to ground-water or surface water. Figure 2 shows a closeup of irrigated fields of the study area expressed as March-October total ET during 2020.

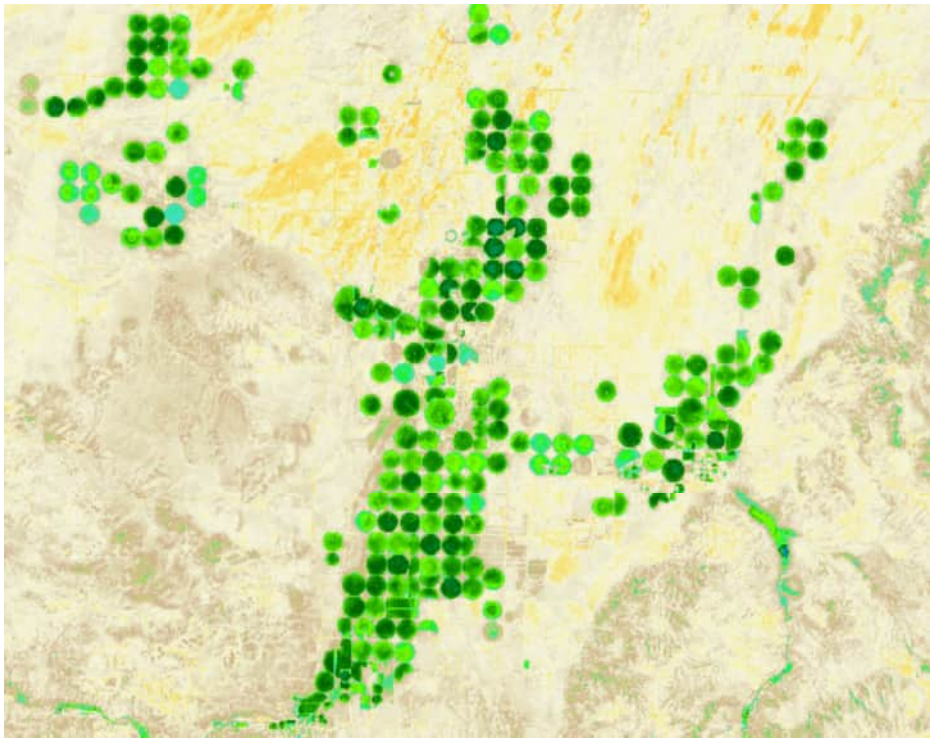

Figure 2. Irrigated fields in the Beryl Junction area showing March-October 2020 ET. Colors of fields range from light green to dark green, with highest ET shown as dark green. Beige colored areas for surrounding rangeland have low ET.

DEM and Land Use maps used for METRIC processing

Basic input files needed during METRIC processing, besides the satellite images, include a Digital Elevation Model (DEM) and Land Use (LU) images. The DEM is used during METRIC processing to adjust surface temperatures for lapse effects caused by elevation variation. In addition, maps of slope and aspect (aspect is the cardinal direction of an inclined surface) are derived from the DEM at 30 m resolution and are used to estimate solar radiation on slopes and in defining aerodynamics of heat convection in mountains.

The DEM was generated from the latest USGS 1 arc-second NED data that were downloaded from the USGS website, and resampled to a 30-meter grid using bilinear interpolation. A visual overview of elevation features in the region surrounding the study area is shown in Figure 3, where high elevations are shown as lighter shades of grey.

A land use (LU) map was used to support the estimation of aerodynamic roughness and soil heat flux during METRIC processing. For 2020 and 2021, the NLCD (National Land Cover Database, 2016) Land Use map was obtained from the USGS-seamless webpage (http://seamless.usgs.gov/) in a standard Albers Equal Area projection. That projection was reprojected to the UTM projection.

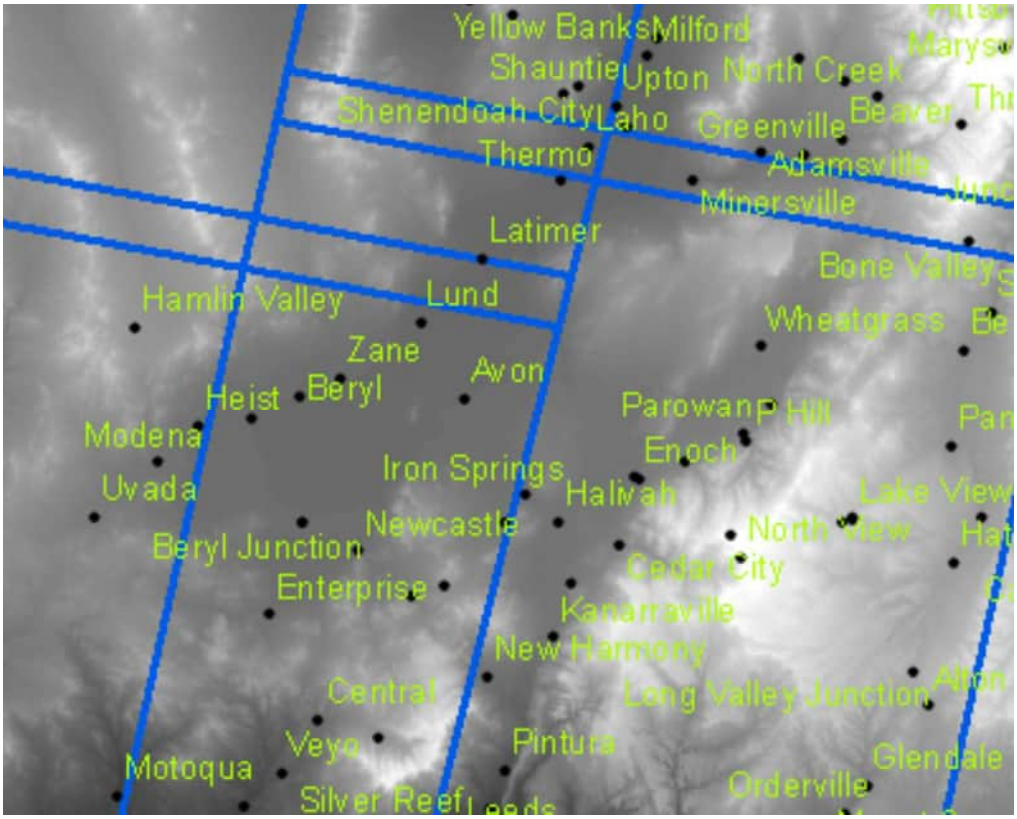

Figure 3. Elevations of the region surrounding the study area where higher elevations show as lighter shades of grey. Names of towns, including Beryl Junction and Enterprise are noted.

3. The METRIC Model

METRIC™ (Mapping Evapotranspiration with high Resolution and Internalized Calibration) bases the ET estimate on the evaluation of the energy balance at the earth's surface. METRIC™ processes instantaneous remotely-sensed digital and weather data and estimates the partitioning of energy into net incoming radiation (R_n), heat flux into the ground (G), sensible heat flux to the air (H), and latent heat flux (LE). The latent heat flux is computed as a residual in the energy balance, represents the energy consumed by ET:

$$LE = R_n - G - H \quad (1)$$

where LE = latent energy consumed by ET; R_n = net radiation; G = sensible heat flux conducted into the ground; and H = sensible heat flux convected to the air. Determining LE by energy balance keys off the large energy required to transform liquid water to vapor. The main advantage of using an energy balance is that actual ET is computed, rather than a potential ET that is based on amount of vegetation, so that any reductions in ET caused by shortage of soil moisture are captured in the ET estimate. In traditional applications of energy balance, the computation of LE is only as accurate as the summed estimates for R_n, G, and H. However, METRIC employs a calibration

strategy to overcome this limitation by focusing the internal calibration on producing accurate LE, with H used to assimilate intermediate estimation errors and biases.

METRIC™ utilizes spectral raster images from the visible, near infrared, and thermal infrared energy spectrum to compute the energy balance on a pixel-by-pixel basis. In METRIC, R_n is computed from the satellite-measured narrow-band reflectance and radiometric surface temperature; G is estimated from R_n, radiometric surface temperature, sensible heat flux and vegetation indices; and H is estimated from surface temperature ranges, surface roughness, and wind speed using buoyancy corrections. Figure 4 shows a general schematic of the METRIC process.

METRIC is calibrated uniquely for each image date due to the unique surface temperature conditions occurring on each image date and changing weather conditions including wind speed and air humidity. The main objective of calibration is the production of accurate estimates of ET from lands having agricultural production. This is done because of the generally high importance of ET from agricultural areas. Calibration settings also focus on agricultural areas because of their more uniform and predictable behavior which improves the accuracy of the calibration of the sensible heat flux function of METRIC. The calibration of METRIC automatically transfers to other land use types in an image, including forest and rangeland.

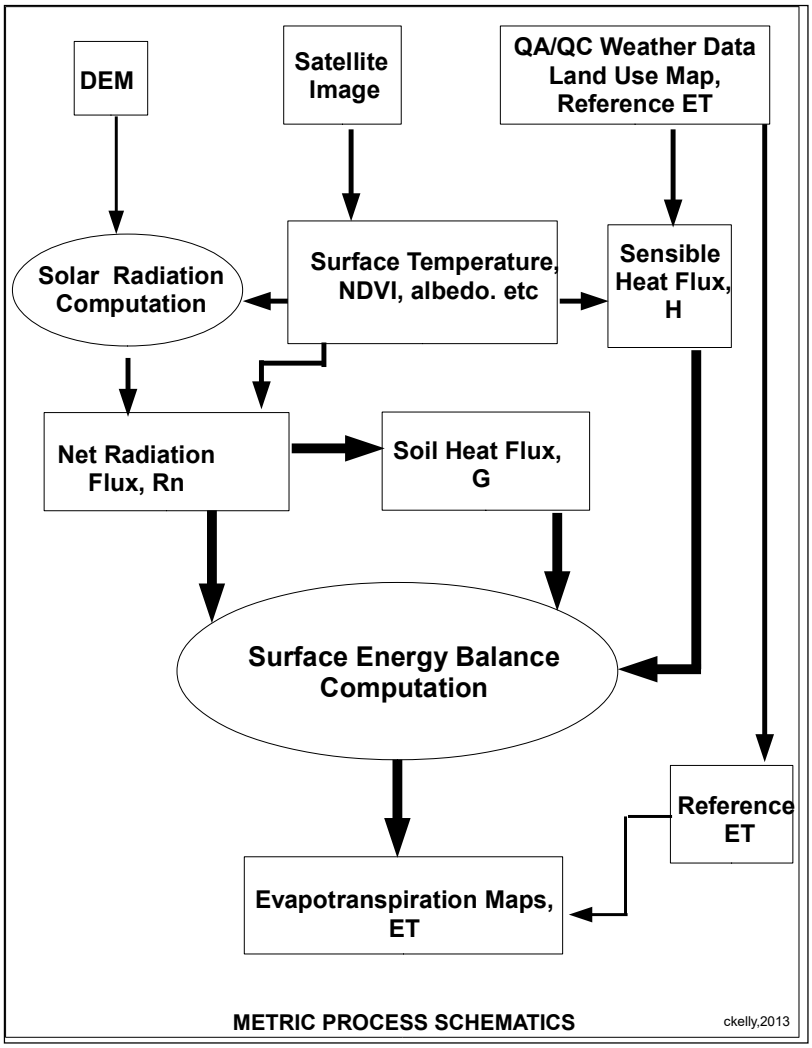

Figure 4. General schematic of the METRIC and EEFlux processes.

Calibration of METRIC

METRIC uses a vertical near surface-to-air temperature difference, dT, to estimate sensible heat flux. Sensible heat flux (H) is the amount of heat that is convected from a surface into the air, thereby reducing the amount of available energy for evaporation. H is estimated in METRIC using a one-dimensional, blended aerodynamic, temperature gradient based method:

$$H = \frac{\rho c_p dT}{r_{ah}} \qquad (2)$$

where ρ is air density (kg m^{-3}), c_p is air specific heat (J kg^{-1} K^{-1}), dT (K) is the temperature difference between two heights (z_1 and z_2) in a near surface blended layer, and r_{ah} is the aerodynamic resistance to heat transport (s m^{-1}) between z_1 and z_2.

The dT function is modeled as linearly proportional to surface temperature and is defined using the properties of two user selected anchor pixels, the "cold" and the "hot" pixels, that represent the near extreme conditions encountered within the image. The cold condition represents a condition having nearly complete conversion of available energy into evapotranspiration and the hot condition represents a condition having nearly zero conversion of available energy into evapotranspiration. During METRIC operation, surface temperature of a pixel is used to determine dT using a linear equation.

The cold anchor pixel generally represents a fully vegetated and actively transpiring vegetation, while the hot anchor pixel represents a bare and dry or nearly dry agricultural soil with little or no vegetation. The selection of cold and hot anchor pixels by the user is described by Allen et al., (2007b) and Allen (2008). These pixels are generally selected from agricultural fields for consistency and to conform with conditions surrounding the development of soil heat flux algorithms, for example, where those algorithms were developed for agricultural soils (Allen et al. 2007b). The linear dT vs. surface temperature function is determined by solving the surface energy balance for sensible heat flux at the two assigned ET conditions and then solving the sensible heat flux equation for dT. The two values for dT are associated with the values for surface temperature as sensed by the satellite. The surface temperature used to estimate dT is 'delapsed' prior to its use in the dT equation using assigned temperature lapse rates to account for differences in surface temperature occurring as a result of cooling of the land surface due to changes in altitude rather than due to changes in evaporation.

During the internal calibration of sensible heat flux in METRIC, a fraction of ET_r, ET_rF, is assigned to the hot and cold conditions within the image. ET_rF is equivalent to the crop coefficient (K_c) based on full-cover alfalfa as the reference crop. ET_rF at the cold pixel is generally assigned a value of 1.05 (Allen et al., 2007a, b) unless vegetation cover is insufficient to support this assignment (for example, early in spring and during winter when full, robust vegetation cover is rare). The 1.05 assignment to ET_rF accounts for the variation in ET inherent within a large population of fully vegetated fields. Previous applications of METRIC and comparisons against lysimeter measurements of ET at Kimberly, Idaho show that the "nearly coldest", or wettest, agricultural fields having full vegetation cover tend have ET rates that are typically 5% higher than that of the alfalfa reference ET_r. This is because, for a large population of fields, some fields may have a wet soil surface beneath the canopy, or the canopy may be wet from recent (sprinkler) irrigation or precipitation, that tend to increase the total ET rate to about 5% above ET_r. In addition, when viewing a large population of fields containing full cover alfalfa, a specific subpopulation of fields will have somewhat wetter conditions and therefore slightly higher ET and slightly cooler temperature than the "mean" full cover condition represented by the alfalfa reference. When the METRIC image is calibrated using an ET_rF of 1.05 at the cold pixel, sampling of ET_rF over a large population of full cover, irrigated fields tends to produce, on average, an ET_rF value of 1.0. See for example, Figure 5, below, for randomly sampled agricultural pixels on the April 25, 2020 image date, showing a general increase in ET_rF with increasing NDVI, with a clustering of ET_rF for (at-surface) at NDVI above 0.85 that averages about 1.0. The figure also shows a clustering of ET_rF for NDVI below about 0.15, representing bare or near bare pixels that have ET_rF that averages about 0.05. The average of ET_rF at low NDVI is about 0.2, which represents average residual evaporation from bare soil due to antecedent precipitation.

The cold pixel is selected from a population of fields having full cover and relatively cold temperatures, and from field interiors, away from boundary effects. Ideally, an alfalfa field is preferred for calibration, since the ASCE Penman-Monteith equation is calibrated to an alfalfa reference. However, Wright (1982) has shown that most agricultural crops, when at full cover, transpire at levels very similar to those of alfalfa. Therefore, even though crop type is generally unknown when selecting the cold pixel in METRIC, as long as the cold pixel is from an agricultural area and has a normalized difference vegetation index (NDVI) > 0.70 as outlined in the METRIC manual and in a number of journal papers, for example, Allen et al., (2007a), the cooler portion of agricultural fields tend to exhibit similar temperatures and can function as the cold condition.

If NDVI is less than about 0.7 for nearly all candidate cold pixels, which can occur during early spring or late fall, this indicates that vegetation cover is insufficient to support the assumption of full ET and ET_rF of 1.0 or 1.05 and the value for ET_rF is adjusted downward according to general crop coefficient estimation practice and following guidelines in Allen et al., (2013a).

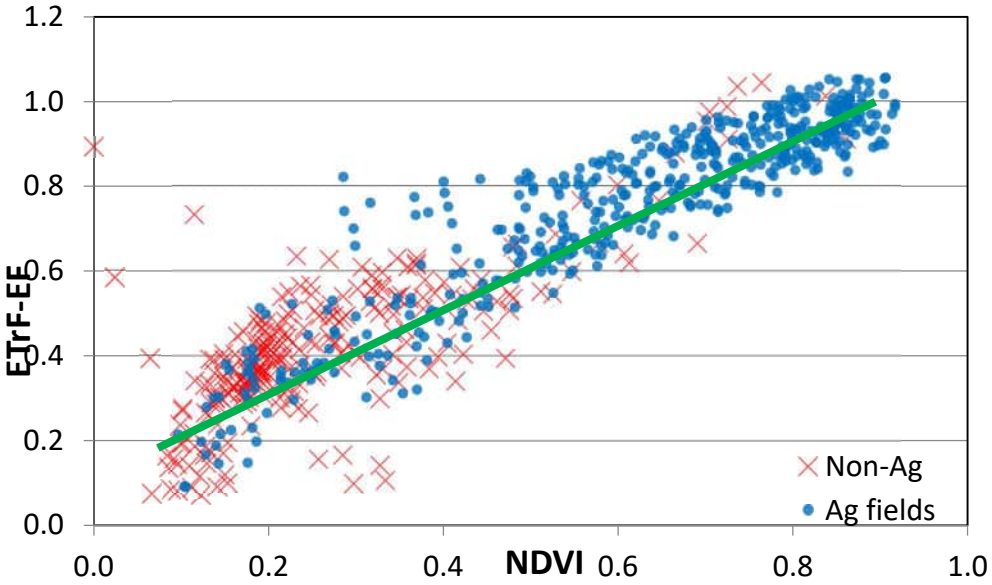

Figure 5. Plot of ET_rF vs. NDVI for sampled pixels (one per field) from agricultural areas of the study area in path 38 on April 25, 2020 showing a general increase in ET_rF with increasing NDVI, with a clustering of ET_rF at NDVI above 0.8 that averages about 1.0 and a clustering of ET_rF for NDVI below about 0.15 that averages about 0.1 to 0.2. Blue symbols represent samples from agricultural fields.

NDVI is a standard measure of vegetation cover on the ground and is calculated as the relative difference in reflectance between the shortest near infrared band (band 4 of Landsat 7 or band 5 of Landsat 8) and the red band (band 3 of Landsat 7 or band 4 of Landsat 8), respectively:

$$NDVI = \frac{\rho_{NIR} - \rho_{red}}{\rho_{NIR} + \rho_{red}} \quad (3)$$

where ρ_{NIR} and ρ_{red} are surface reflectances in the near infrared and red bands, respectively, corrected for atmospheric effects. NDVI is slightly sensitive to the color of the soil, spectral

bandwidth, and whether the reflectances used are at-satellite (no accounting for atmospheric attenuation) or are at-surface (with accounting for atmospheric attenuation). In version 3.0 of METRIC, NDVI can be computed using both at-satellite and at-surface reflectances, with at-surface NDVI used during land/water differentiation and estimation of vegetation properties such as aerodynamic roughness. Typically, NDVI varies between 0.1 and 0.8, with the higher value indicating dense vegetation and values less than about 0.2 associated with soil/rocks. Negative NDVI values typically indicate water bodies and snow, which reflect more energy in the red spectrum than in the near infrared.

4. Weather data processing

METRIC utilizes alfalfa reference ET (i.e., ET_r) as calculated by the ASCE standardized Penman-Monteith equation (ASCE-EWRI 2005; Jensen and Allen 2016). ET_r is used to represent near maximum ET based on energy available for ET and is employed in the calibration of the energy balance process and to establish a daily soil water balance to estimate residual soil evaporation from bare soil following precipitation events (Allen et al. 2007a). Hourly ET_r is used as a means to 'anchor' the surface energy balance by representing the ET from locations having high levels of vegetation and cooler radiometric surface temperatures.

The soil water balance is based on the two-stage daily soil evaporation model of the United Nations Food and Agriculture Organization's Irrigation and Drainage Paper 56 (Allen et al 1998). The procedure employs the skin evaporation enhancement of Allen (2011) that increases the magnitude of evaporation spikes following light precipitation events. Estimated soil evaporation is used during calibration of Landsat images to account for any residual evaporation stemming from antecedent rainfall events.

Hourly data from five agricultural weather stations operated by Utah State University were used to conduct a daily soil water balance to estimate background evaporation at overpass time and to provide a spatially interpolated ET_r surface used during time integration of overpass ET into monthly ET estimates. In addition, ET_r calculated for the Beryl Junction weather station was used during image calibration. The Beryl Junction station is central to the study area and is representative of evaporative demand conditions for irrigated fields in the study area. Evaporation estimates were used during ET_rF image review to assess expected ET_rF for low vegetation conditions.

The five weather stations are listed in Table 3. Hourly data were obtained from the Utah Climate Center - Utah State University (usu.edu) web site. The hourly data were QAQC'd using the University of Idaho REF-ET software and QAQC system. The data were found to be of high quality and representative of irrigated agricultural environments. Hourly ET_r calculated using the ASCE Penman-Monteith equation compared very well with ET_r provided on the USU web site, as shown in Figure 6 for Beryl Junction during 2020. The USU ET_r tended to be about 3% lower than the REF-ET computed ET_r. That was most likely caused by specific methods used to calculate clear sky solar radiation used to estimate impacts of cloudiness on long wave radiation.

Table 3. Locations of USU weather stations useds to establish daily reference ET layers for years 2020 and 2021. Beryl Junction was used for METRIC calibration.

Station	Latitude	Longitude	Elevation, ft
Beryl Junction	37.71960	-113.70200	5187
Milford Flat	38.29828	-113.00527	5065
Buckhorn	38.03990	-112.71150	5820
Parowan	37.86230	-112.88110	5770
Cedar City	37.67300	-113.13720	5529

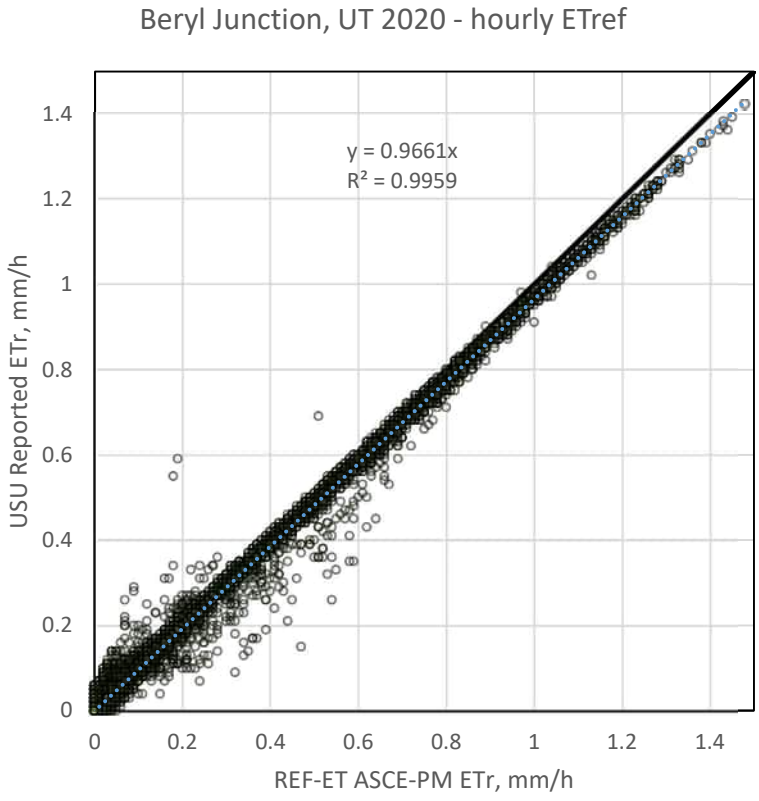

Figure 6. Plot of ET_r distributed from the USU weather site vs. ET_r computed by REF-ET using downloaded hourly weather data for Beryl Junction during 2020.

Precipitation at Beryl Junction was compared with an independent data set obtained from the NRCS Soil Climate Analysis Network (SCAN) site located near Enterprise. This was done to verify the integrity of the Beryl Junction data. Trends in precipitation were similar, although amounts recorded per wetting event differed at times, for example, during a January 2021 event, as illustrated in Figure 7. The relatively close comparisons confirmed the integrity of the Beryl Junction data and its use to estimate daily evaporation from bare soil that is used during calibration of METRIC to establish expected minimum ET.

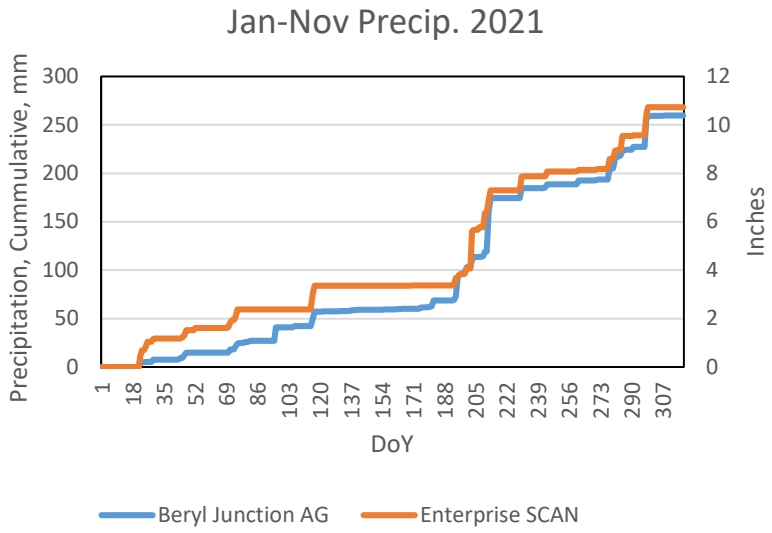

Figure 7. Cummulative plot of precipitation reported for the Beryl Junction weather site and reported by the Enterprise SCAN weather station.

5. METRIC™ processing and results

EEFlux produces 30x30 m spatial resolution maps of both ET_rF (Fraction of Reference Evapotranspiration) and actual ET. The main products produced are:

- Daily ET_rF and ET maps, for every image date.
- Monthly ET, ET_rF and ET_r maps.
- Summary (multi month) ET, ET_rF and ET_r maps.

Treatment of SLC-Off Gaps for Landsat 7 images

Landsat 7 images acquired after May 2003 have information gaps caused by the malfunction of the scan line corrector (SLC). As a result, Landsat 7 images were "SLC-off" images where wedge shaped gaps exist in the images, extending from the edges of the image and stretching towards the centers, as shown in Figure 8. Full description of the SLC-off malfunction is provided at USGS web sites (http://landsat.usgs.gov/products_slcoffbackground.php).

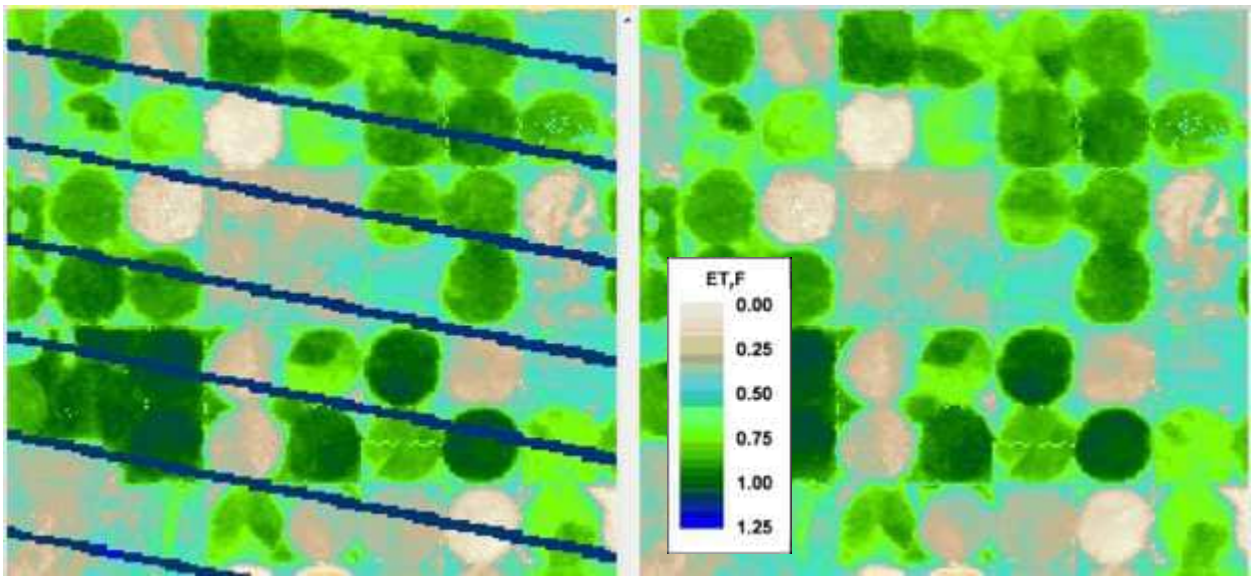

Figure 8. Left: Close-up of a typical ET_rF image produced from a Landsat 7 image in southern Idaho, showing gaps (stripes) originated from the Landsat 7 image. Right: The same ET_rF map, after gaps were filled using natural neighbor interpolation.

As indicated previously only one Landsat 7 image was required during time integration for year 2021 to produce monthly ET. Only one Landsat 7 image was needed due to a sufficient number and time distribution of clear Landsat 8 images. The SLC-off gaps in that ET_rF image were 'filled' using a natural neighbor gap-filling approach in ArcMAP software. That process bases ET_rF material placed into gaps on ET_rF values along the edges of the gaps, as shown in Figure 8. The gap filling normally tends to reduce most visual evidence of the gaps in the final monthly and growing season ET products. However, in the case of the August 8, 2022 Landsat 7 image processed here, there were substantial artifacts produced in gap areas. Therefore, the Landsat 7 image was processed during time integration with unfilled gaps, where the gaps were treated as clouds and therefore not included during the time integration. However, this did cause some striping artifacts during the production of monthly ET for August.

Dealing with clouded parts of images

Satellite images often have clouds in portions of the images. ET_rF cannot be directly estimated for clouded areas using surface energy balance because cloud temperature masks surface temperature and cloud albedo masks surface albedo.

Clouds and shadows were identified using the FMASK computer application developed at Boston University. FMASK is a precursor of the USGS EROS application used to produce the Landsat BQA product that accompanies each Landsat image that contains cloud and shadow identification. The cloud plus shadow mask produced by FMASK was despeckled using a focal minimum function on a 3x3 pixel kernel. That function removed clusters of masked pixels having sizes of three pixels or less. Those small clusters are often false identifications of clouds. The cloud/shadow mask was then dilated using a 15 x 15 pixel focal maximum function followed by a 15 x 15 pixel focal mode function. The focal maximum function expanded and smoothed edges of masked regions and the focal mode further expanded and merged masked regions.

The buffering worked relatively well in expanding the original cloud/shadow mask and to reduce the occurrence of small clear pixel inclusions within larger clouded areas. The buffering expanded cloud/shadow masks outward to cover areas adjacent to originally marked clouds and shadows that may have exhibited cool thermal artifacts from recent cloud movement, or due to the FMASK product missing these impacted areas. Masking these areas reduced error in the ET estimates caused by a false cool thermal signal. Figure 9 shows an example of a close up of a FMASK cloud/shadow mask and the same result following buffering for an image in eastern Utah during 2017.

ET_rF of cloud/shadow masked areas associated with an image were not used in the linear interpolation of daily ET_rF but were instead replaced by ET_rF values interpolated from earlier and later images when the area was cloud free. For example if an area was cloudy on April 12, the ET_rF for the area was based on linear interpolation between March 19th and April 20th provided the area was cloud free for those image dates.

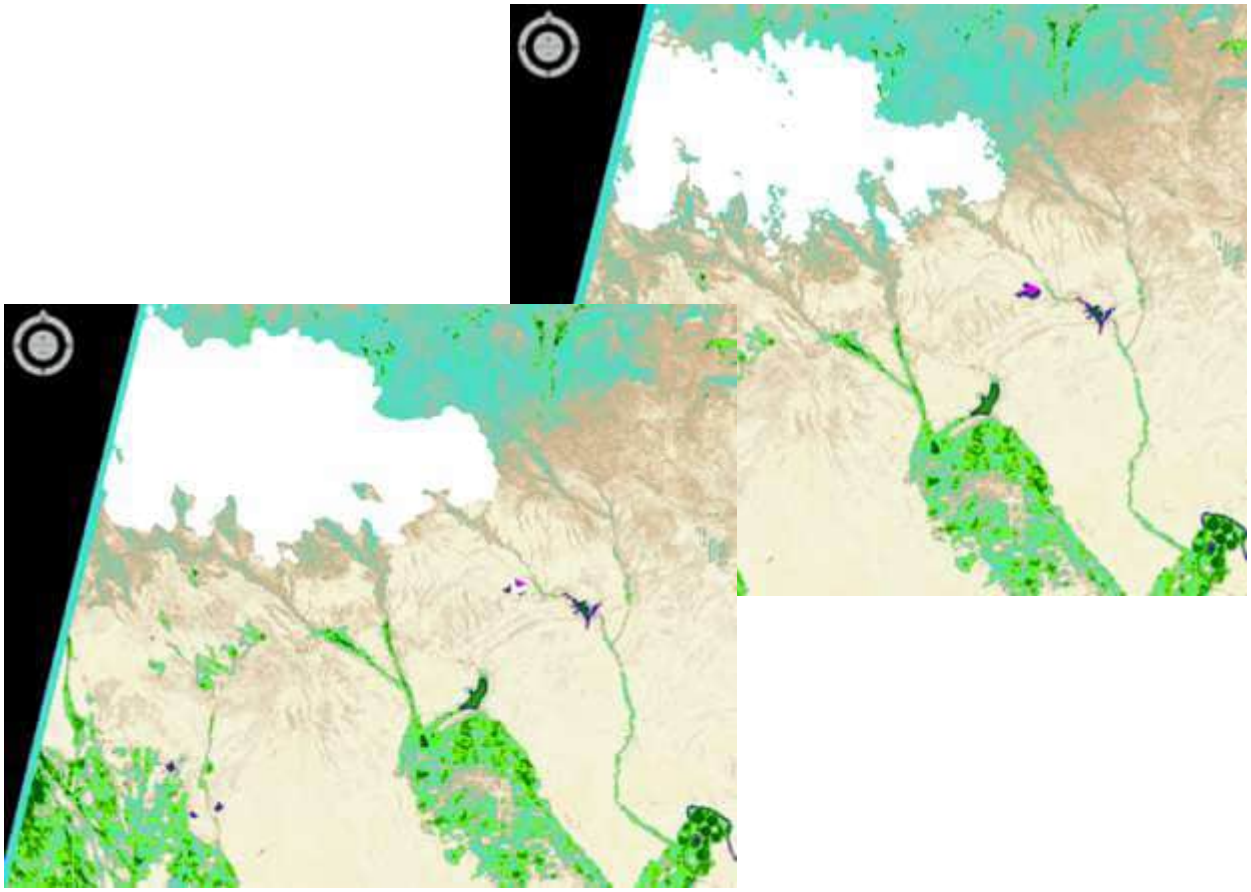

Figure 9. Left: Close-up of an ET_rF image for 6/22/2017 (P36) near the Pelican Lake, UT area, showing cloud masked areas (white areas) overlying a colorized ET image. Right: the original cloud/shadow masked area from the FMASK (an EROS BQA equivalent) product in white. The left image shows the same area following buffering.

Calibration Review and Adjustment

The ET_rF images produced by the ERDAS-based METRIC were each manually reviewed to evaluate the populations of ET_rF. If deemed necessary, the calibrations were adjusted by selecting new hot and cold pixels as discussed later. Review of the ET_rF spectrum was based on review of plots of ET_rF vs. NDVI as shown in Figure 5 and the following Figure 10, and by visual inspection of spatial ET_rF, surface temperature and NDVI images. The objective of the adjustments was to produce ET_rF images that had an upper distribution of ET_rF lying near values of 1.0 and a lower distribution of ET_rF lying close to the estimated ET_rF resulting from residual evaporation from any recent precipitation. Adjustments to initial calibrations of images averaged about 0.0 to 0.1 ET_rF.

As an example of a review step, Figure 10 shows a plot of ET_rF vs. NDVI for an April 25, 2020 image over the study area. Each blue point in the figure represents a sampled pixel from a field in the study area. Red symbols represent ET_rF from adjacent rangeland. Locations of sampled points are shown in Figure 11.

The colored lines were placed to describe general trends in the ET_rF data, with ET_rF increasing with increasing NDVI. The upper, orange line in the example represents ET_rF characteristic of fields that exhibited some impacts of wet soil within the vegetation canopy. The evaporation from wet soil added to total ET and pushed ET_rF towards a value of about 1.0. The lower, green line represents characteristic ET_rF for fields that likely had dry soil within or beneath the crop canopies.

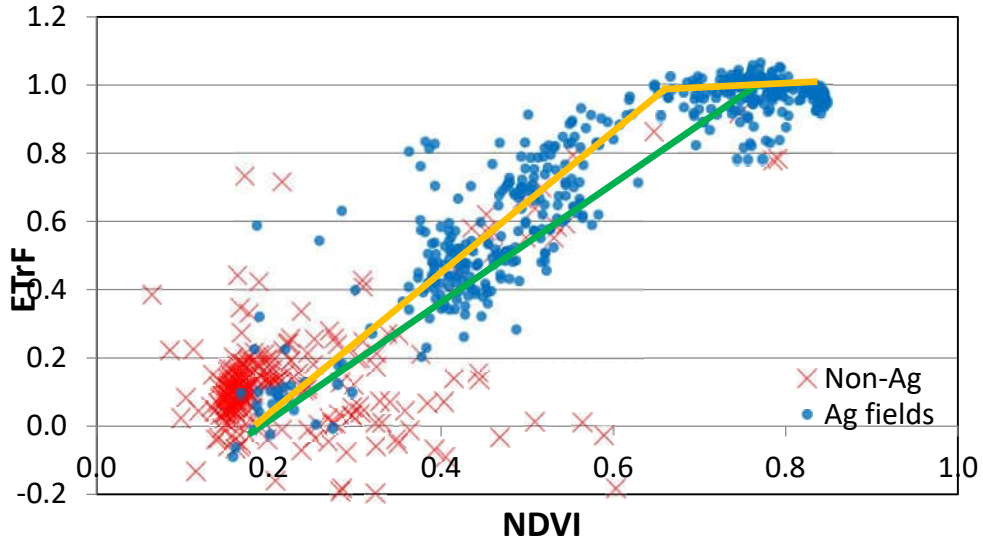

Figure 10. Plot of ET_rF vs. NDVI for sampled pixels from about 200 locations mostly in irrigated fields of the study area (blue points). Red points were sampled from adjacent rangeland.

The ET_rF at the upper end has a 'plateau' of values near 1.0 over a range of NDVI from about 0.65 to 0.85. This occurrence is relatively common where NDVI > 0.65 can represent crops having mostly full ground cover and therefore having similar maximum ET_rF. That maximum ET_rF represents an upper limit on conversion of available energy (net solar radiation and sensible

heat flux) into evapotranspiration. That upper limit is generally well represented by the ET_r estimated by the ASCE standardized Penman-Monteith equation. The colored lines were placed to describe general trends in the ET_rF data, with ET_rF increase with increasing NDVI.

Appendices 1 and 2 contain ET review summaries for each image processed for years 2020 and 2021. The summaries characterize special conditions occurring for images (high reference ET, high wind, recent rain, etc.) as well as contain comments on the initial calibration results and recommended adjustments to the calibrations. The summaries also contain figures for each image date similar to that of Figure 10.

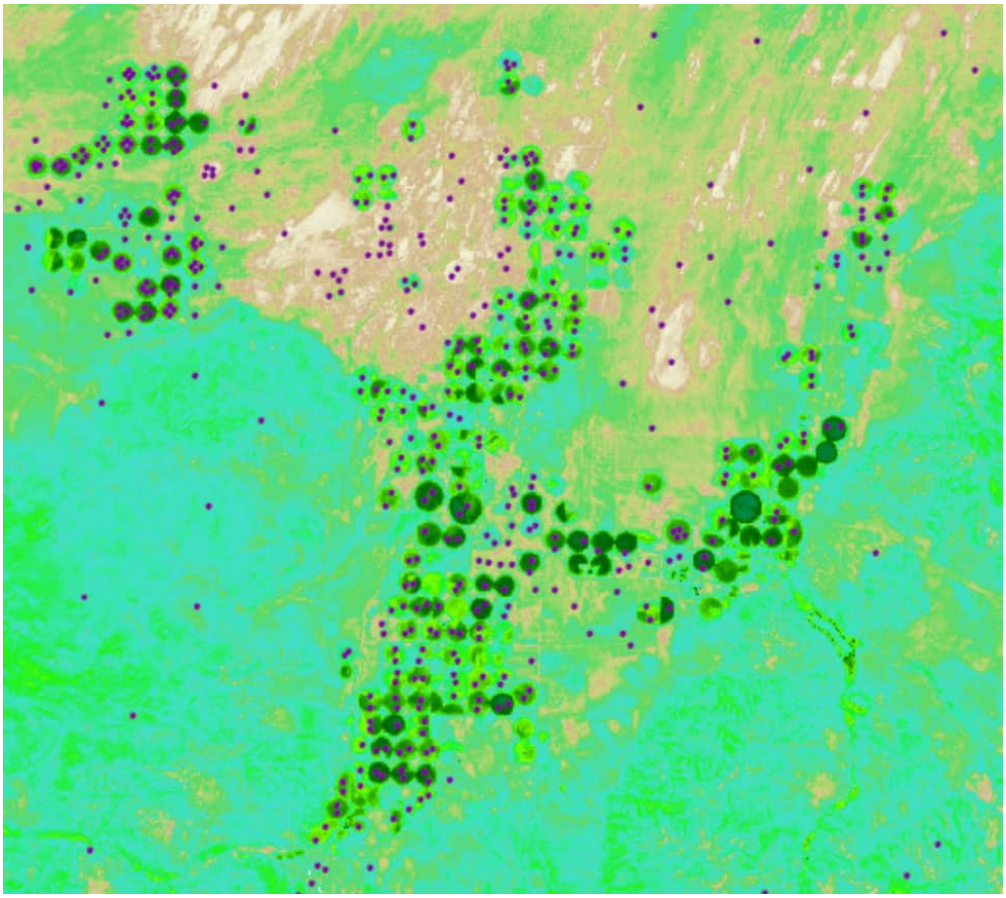

Figure 11. Locations of sampled pixels (in purple) from about 200 locations, mostly in irrigated fields of the study area, that were used during review of METRIC calibrations.

Monthly ET and ET_rF for the months of March-October 2020 and 2021

Individual satellite images processed using METRIC (Tables 1 and 2) were used to establish daily maps of ET_rF for the days of the Landsat images.

The March, April, May, June, July, August, September and October monthy ET images were produced using two interpolation methods: spline and linear. Each method produced daily ET_rF estimates for periods in between individual satellite image dates. Images from Paths 38 and 39

were combined, with focus on the path overlap area containing the study area. The daily ET_rF images tend to follow trends in daily ET caused by vegetation development and tend to reflect evaporation from precipitation events occurring on days immediately before image acquisitions. Following their production, the daily ET_rF images were multiplied by the daily reference ET (ET_r) images created by spatial interpolation of daily ETr from the five weather stations listed in Table 3. The product was a series of daily ET images. The daily ET were then summed over each month to produce monthly ET. The reference ET_r images account for impacts of weather on daily potential ET demand. Only clear-sky pixels were used for the interpolation of daily ET_rF. A python process was used to perform the interpolation. Figure 12 illustrates a typical time series of interpolated ET_rF for a pixel sampled from a field identified as corn by the Cropland Data Layer (CDL). That field appears to have had an early grain crop, such as triticale, cultivated prior to planting of corn. Red symbols represent ET_rF produced from METRIC for Landsat image dates.

The spline interpolation (blue line) tends to follow expected gradual trends in ET_rF over time, as opposed to linear interpolation (dashed line) and was selected for use in this study. Figure 13 shows a similar graph for a field identified by the CDL as alfalfa. The ET_rF trends show impacts of cuttings during the growing season. Due to the relatively large (8 to 16 or more) days between Landsat revisits, the Landsat image series may miss some alfalfa cutting events and/or their regrowth periods. This can introduce some error into the monthly and growing season ET estimates. However, one can expect that impacts of missing cutting events or, conversely, picking up very low ET_rF immediately following a cutting will tend to average out over a growing season. In addition, these impacts tend to average out even more when ET from more than one alfalfa field is aggregated.

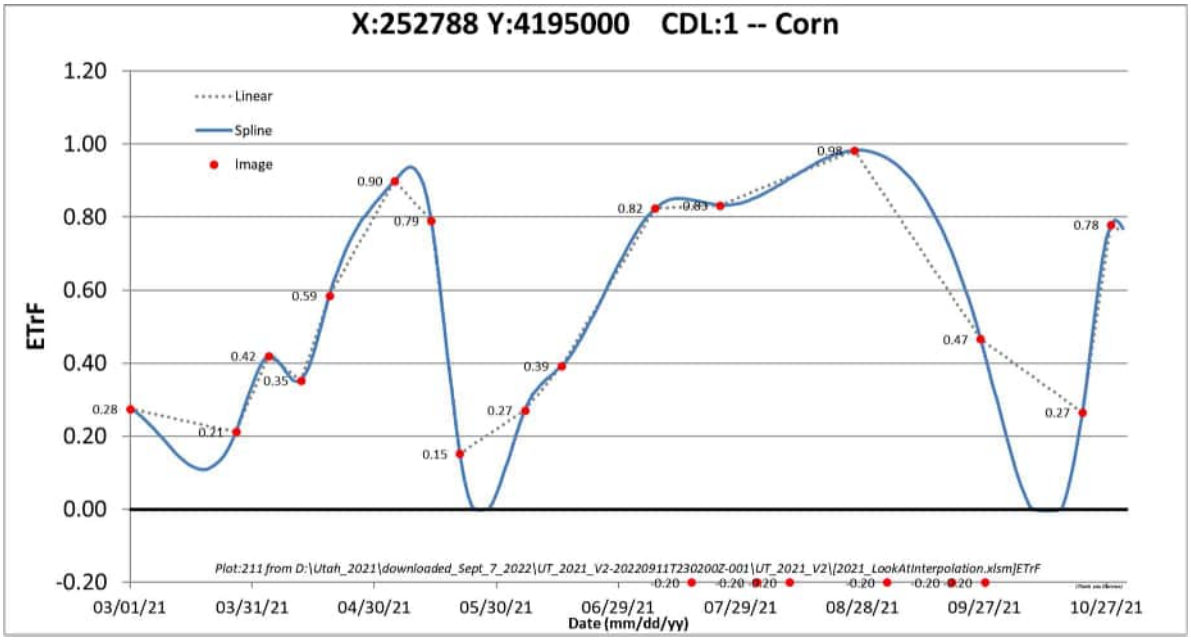

Figure 12. Daily ET_rF produced by the temporal interpolation of ET_rF between image dates for a field identified by the USDA CDL as corn. The blue curve shows results of a cubic spline interpolation method and the dashed line shows results of a purely linear interpolation. Red symbols represent ET_rF for Landsat image dates.

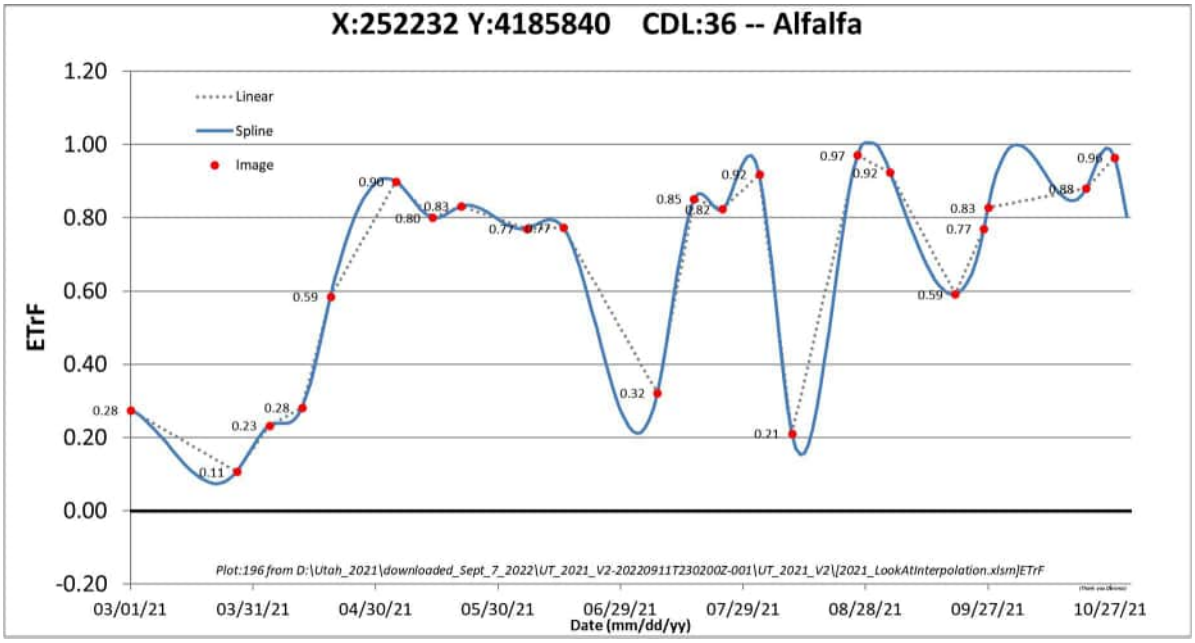

Figure 13. Daily ET_rF produced by the temporal interpolation of ET_rF between image dates for a field identified by the USDA CDL as alfalfa. The blue curve shows results of a cubic spline interpolation method and the dashed line shows results of a purely linear interpolation. Red symbols represent ET_rF for Landsat image dates.

Description of METRIC Monthly Products

The 2020 and 2021 ET products consist of individual month image data sets. The monthly ET image data sets have three layers. The first layer is the monthly ET in mm, the second layer is the monthly ET_rF, and the third layer is monthly ET_r in mm. The images were produced in the ERDAS Imagine *img* format.

Year 2020. Figures 14-21 show monthly ET_rF and ET for months of March to October 2020 for the study area. ET_rF tended to become progressively higher from March through August as irrigated crops developed. ET_rF from irrigated areas tended to dominate the landscape, with some ET from rangeland areas in early spring and during summer precipitation events.

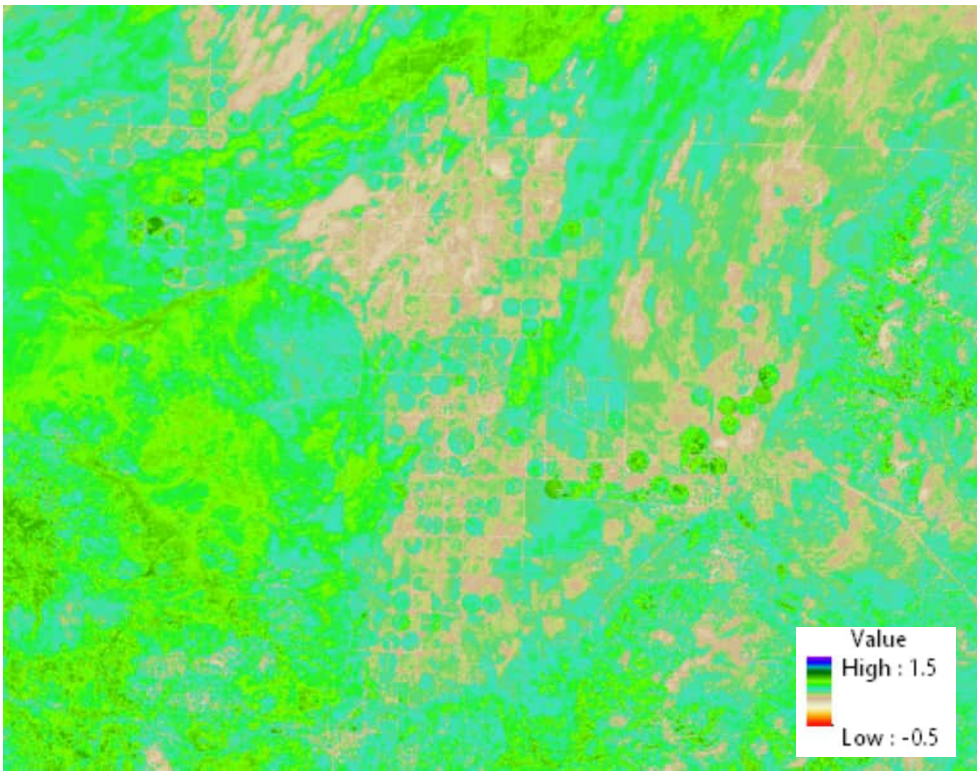

Figure 14a. ET_rF for the month of March 2020 for the Beryl Junction / Enterprise study area. Rangeland areas exhibit ET_rF from recent wetting events.

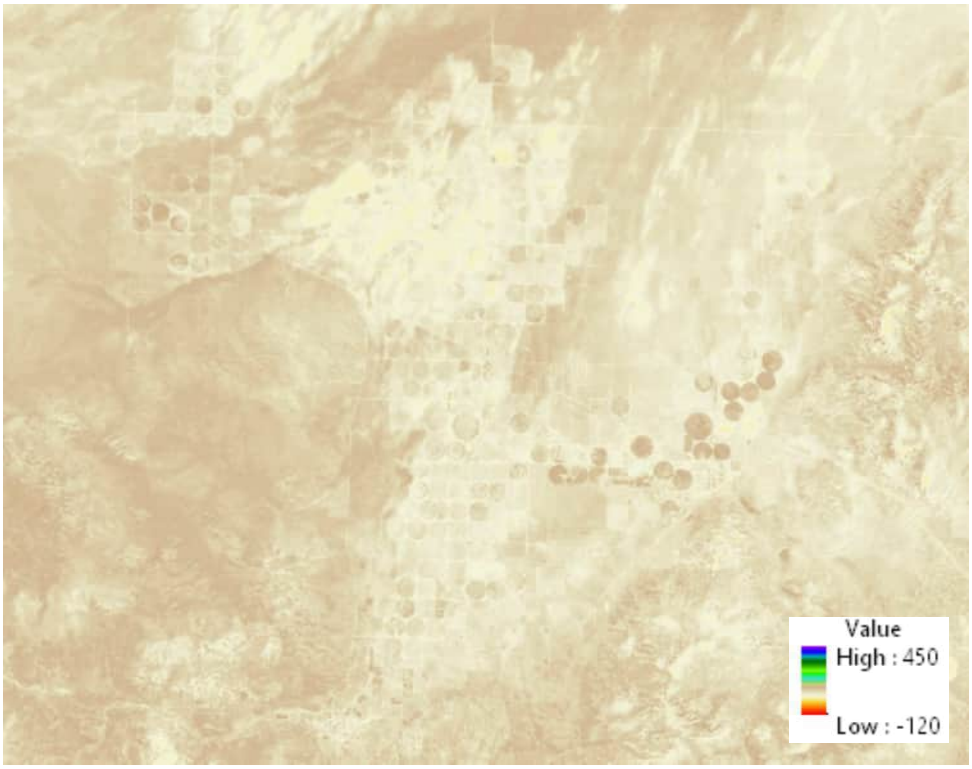

Figure 14b. ET, millimeters, for the month of March 2020 for the Beryl Junction / Enterprise study area.

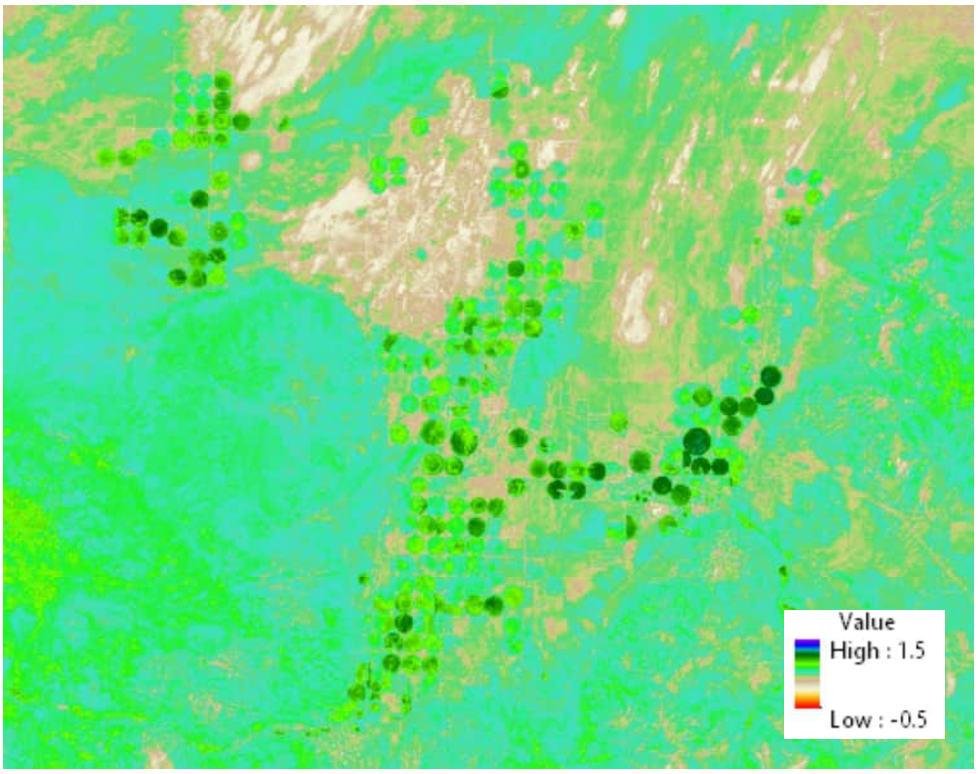

Figure 15a. ET_rF for the month of April 2020 for the Beryl Junction / Enterprise study area. Rangeland areas exhibit ET_{rF} from recent wetting events.

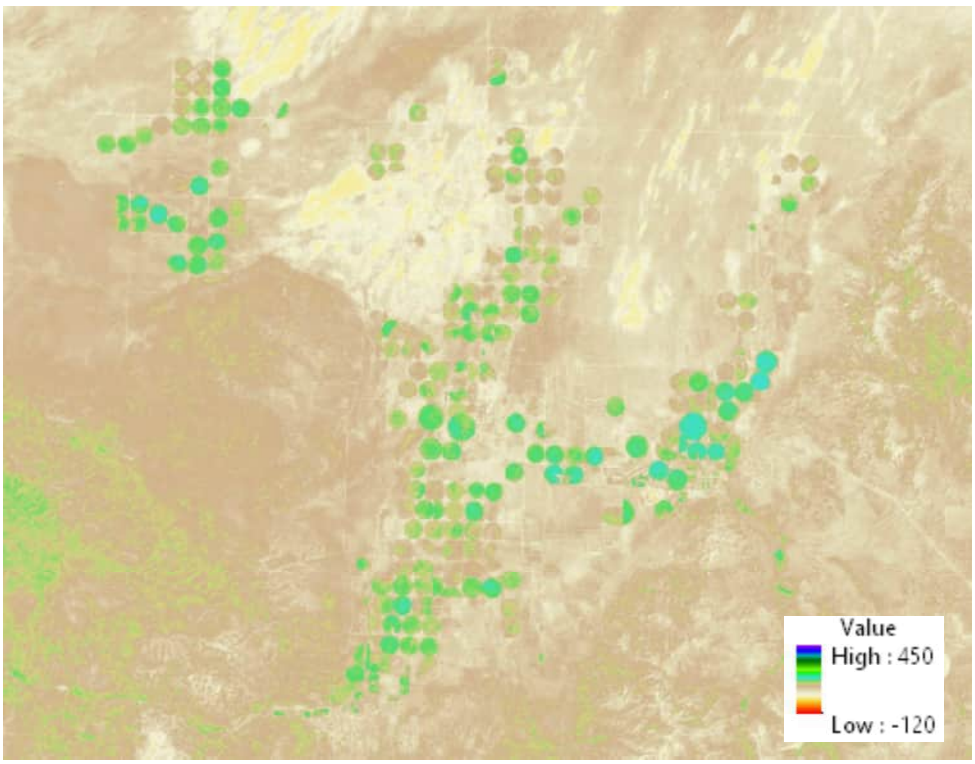

Figure 15b. ET, millimeters, for the month of April 2020 for the Beryl Junction / Enterprise study area.

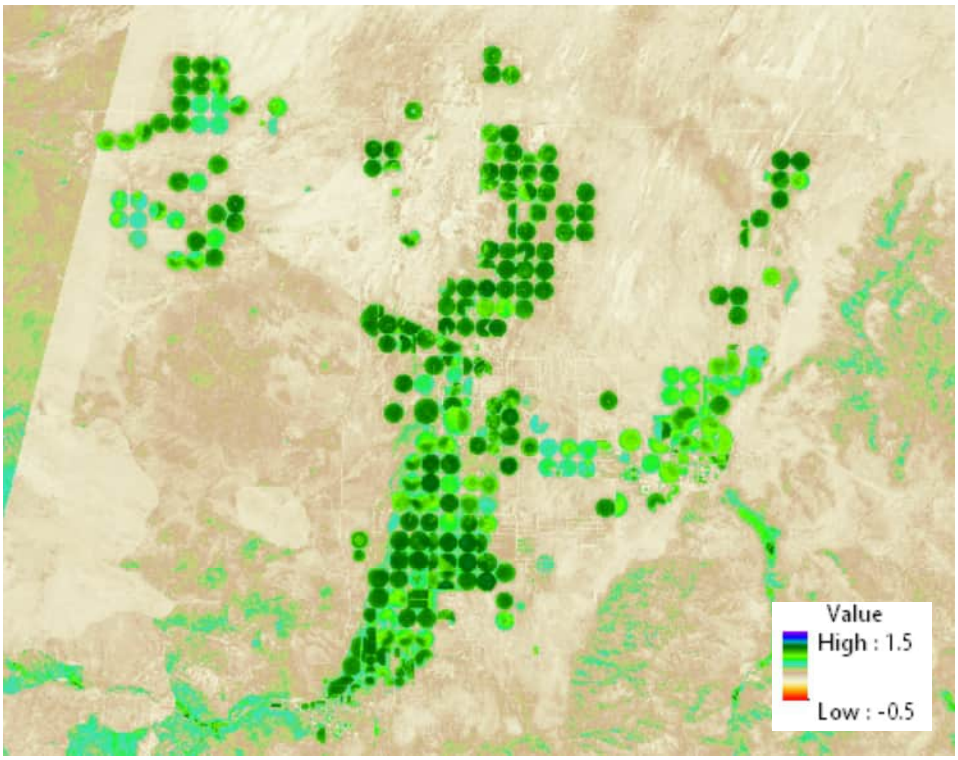

Figure 16a. ET_rF for the month of May 2020 for the Beryl Junction / Enterprise study area.

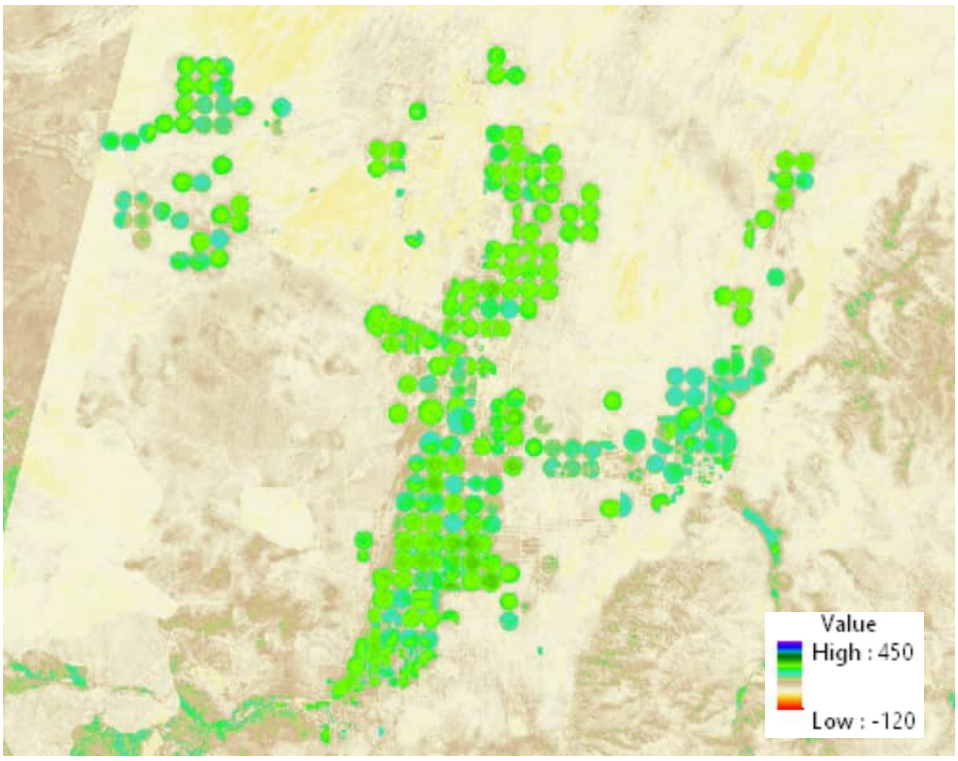

Figure 16b. ET, mm, for the month of May 2020 for the Beryl Junction / Enterprise study area.

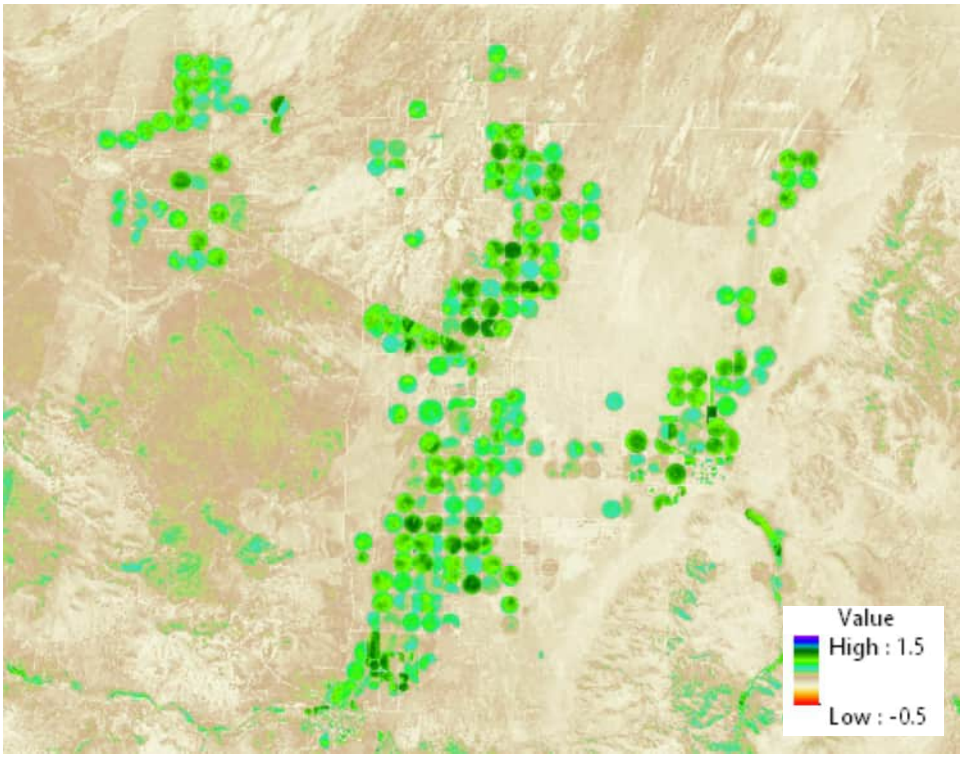

Figure 17a. ET_rF for the month of June 2020 for the Beryl Junction / Enterprise study area.

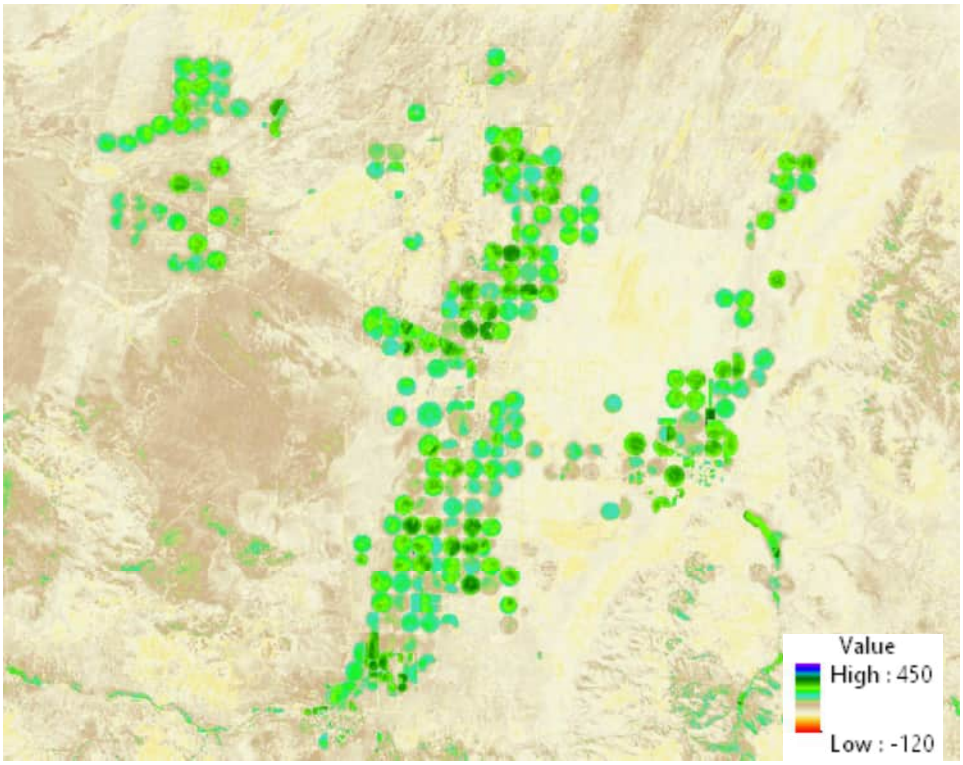

Figure 17b. ET, mm, for the month of June 2020 for the Beryl Junction / Enterprise study area

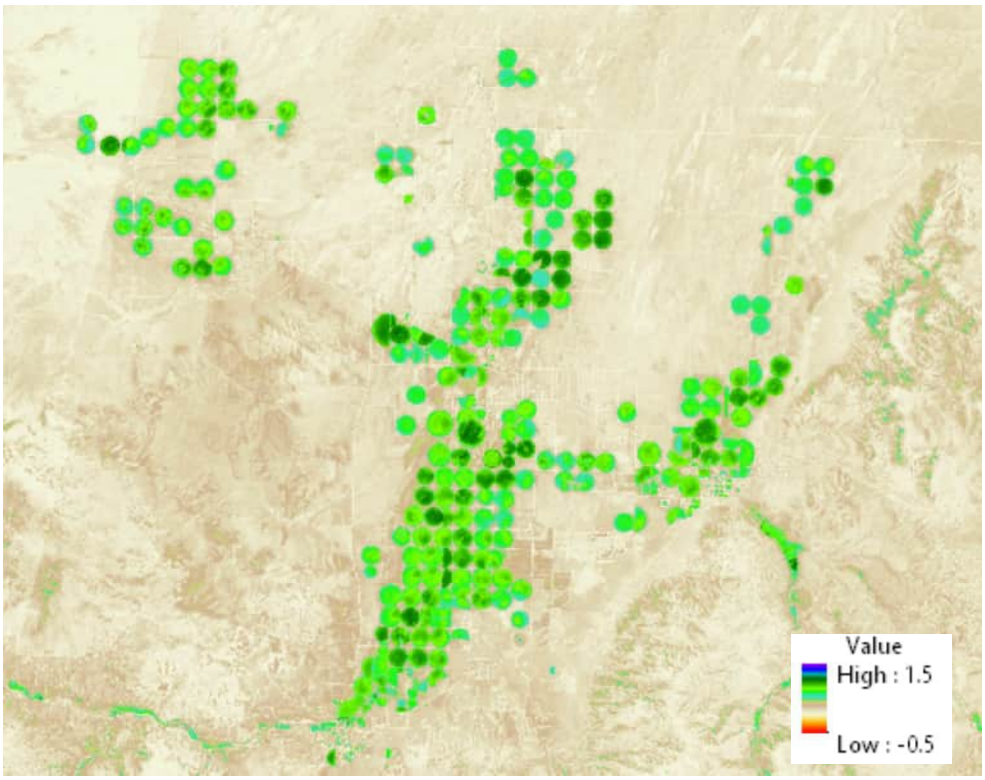

Figure 18a. ET_rF for the month of July 2020 for the Beryl Junction / Enterprise study area.

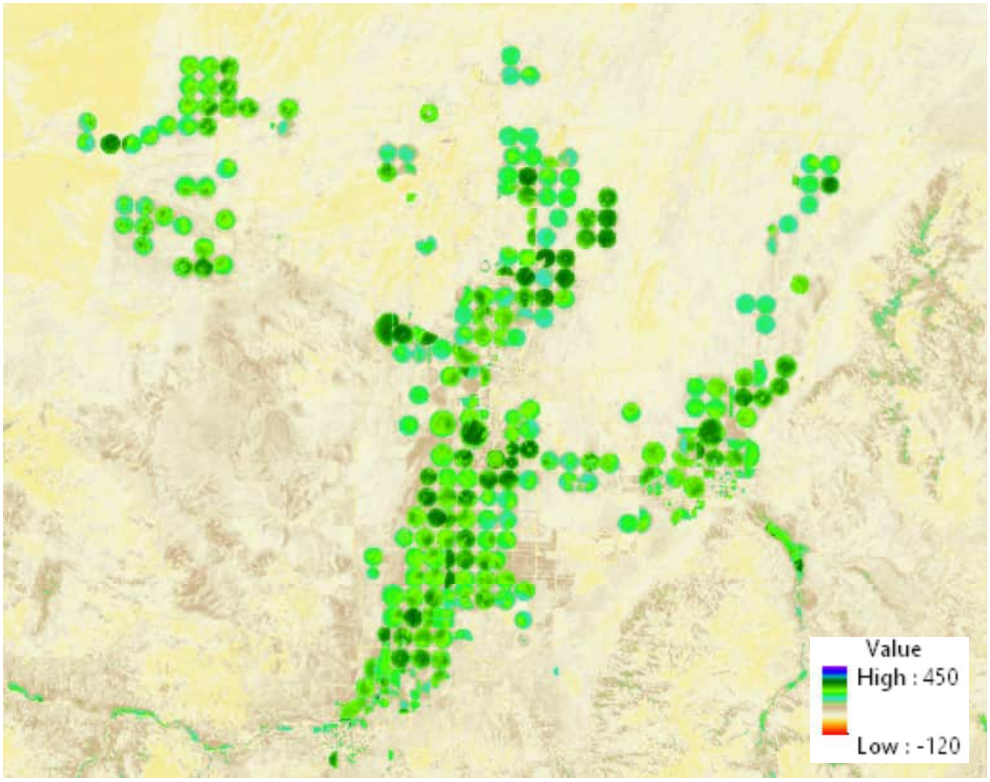

Figure 18b. ET, mm, for the month of July 2020 for the Beryl Junction / Enterprise study area.

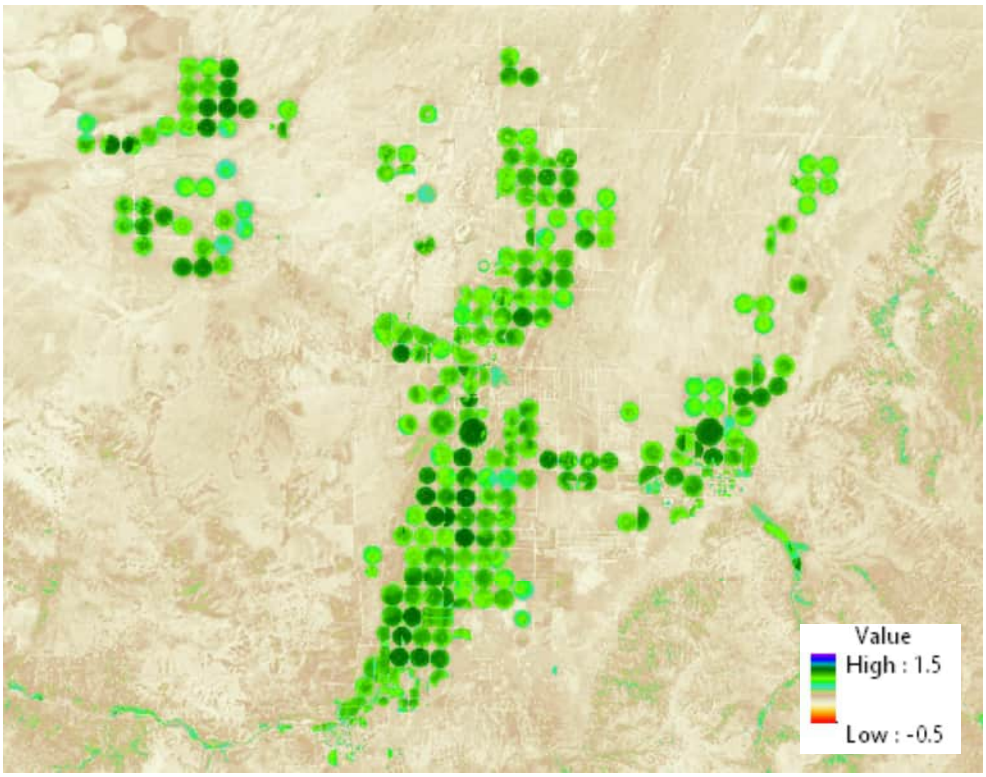

Figure 19a. ET_rF for the month of August 2020 for the Beryl Junction / Enterprise study area.

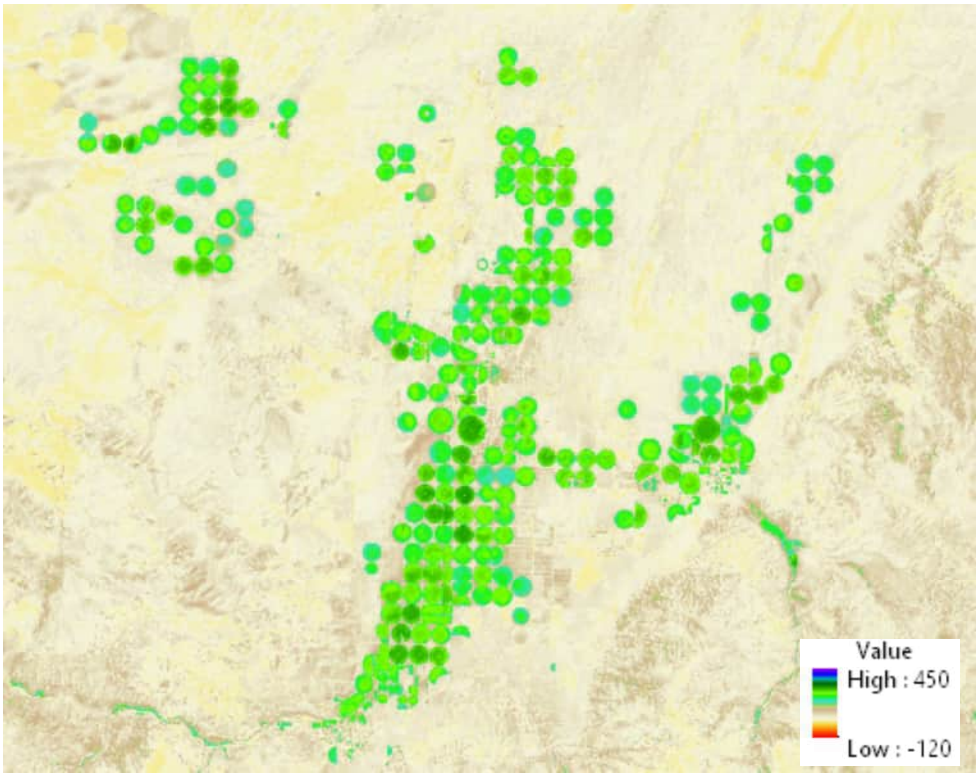

Figure 19b. ET, mm, for the month of August 2020 for the Beryl Junction / Enterprise study area.

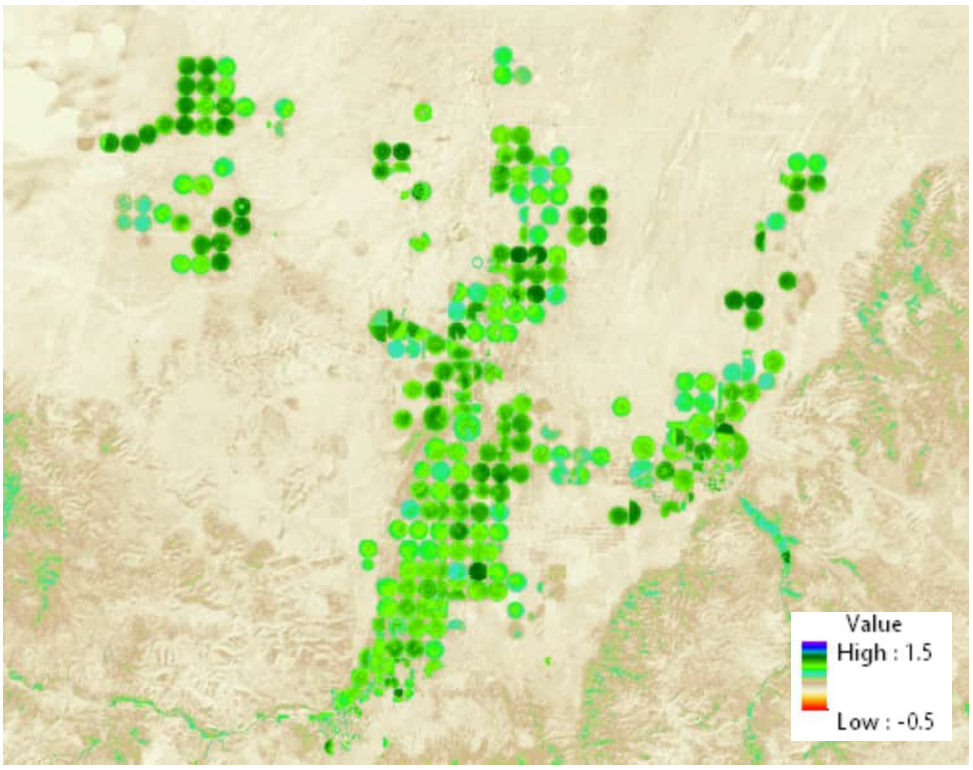

Figure 20a. ET_rF for the month of September 2020 for the Beryl Junction / Enterprise study area.

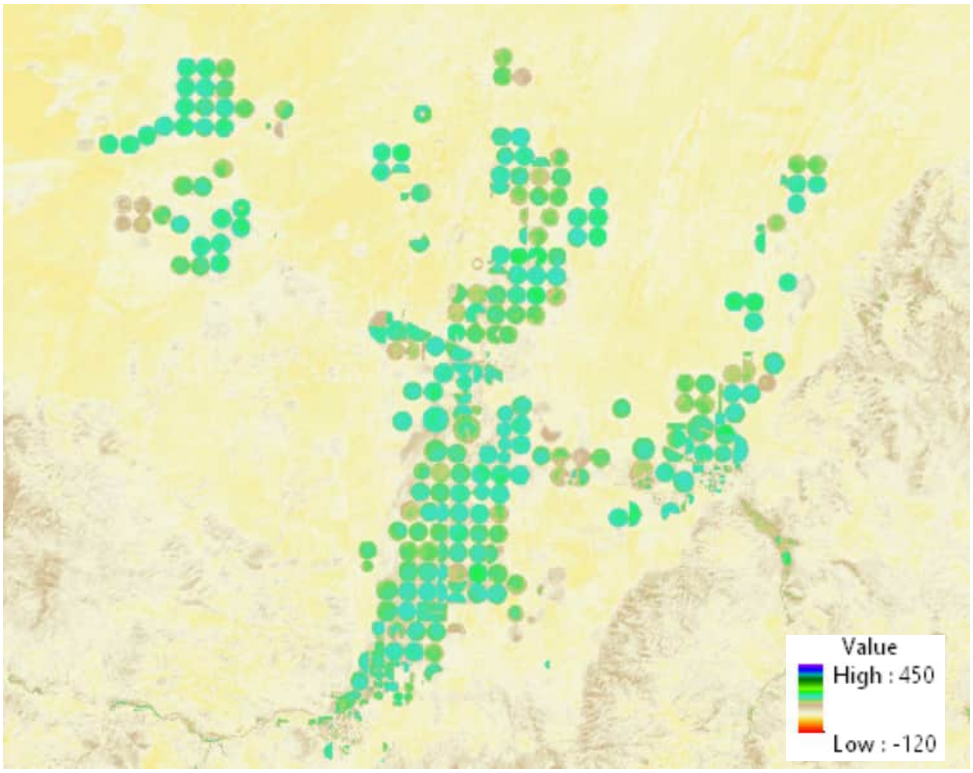

Figure 20b. ET, mm, for the month of September 2020 for the Beryl Junction / Enterprise study area.

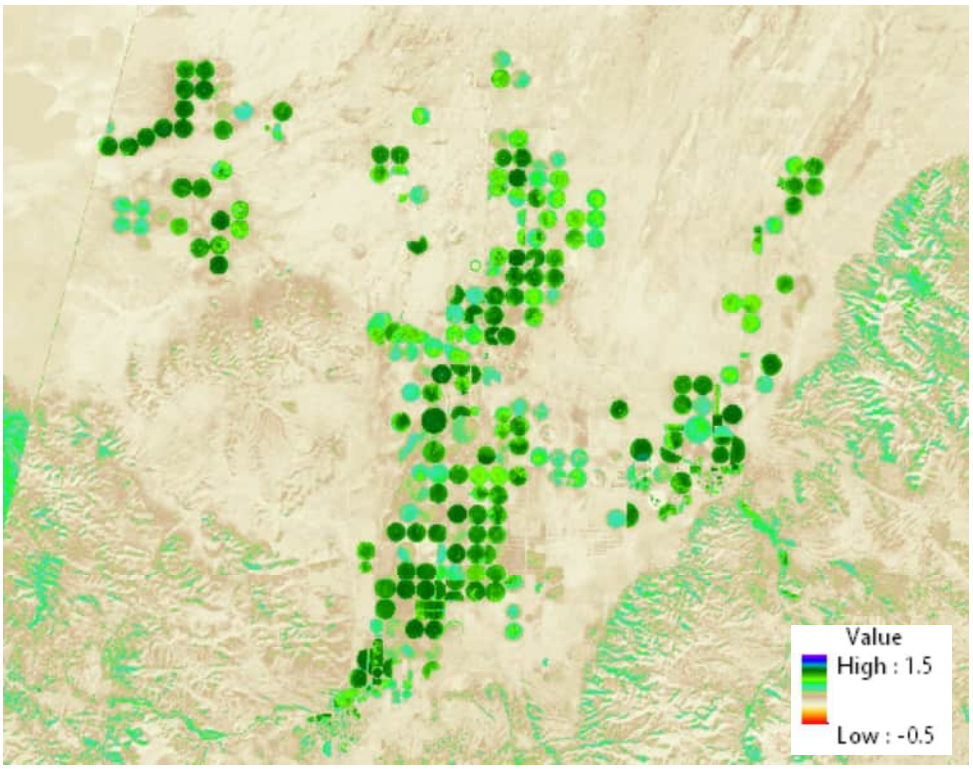

Figure 21a. ET_rF for the month of October 2020 for the Beryl Junction / Enterprise study area.

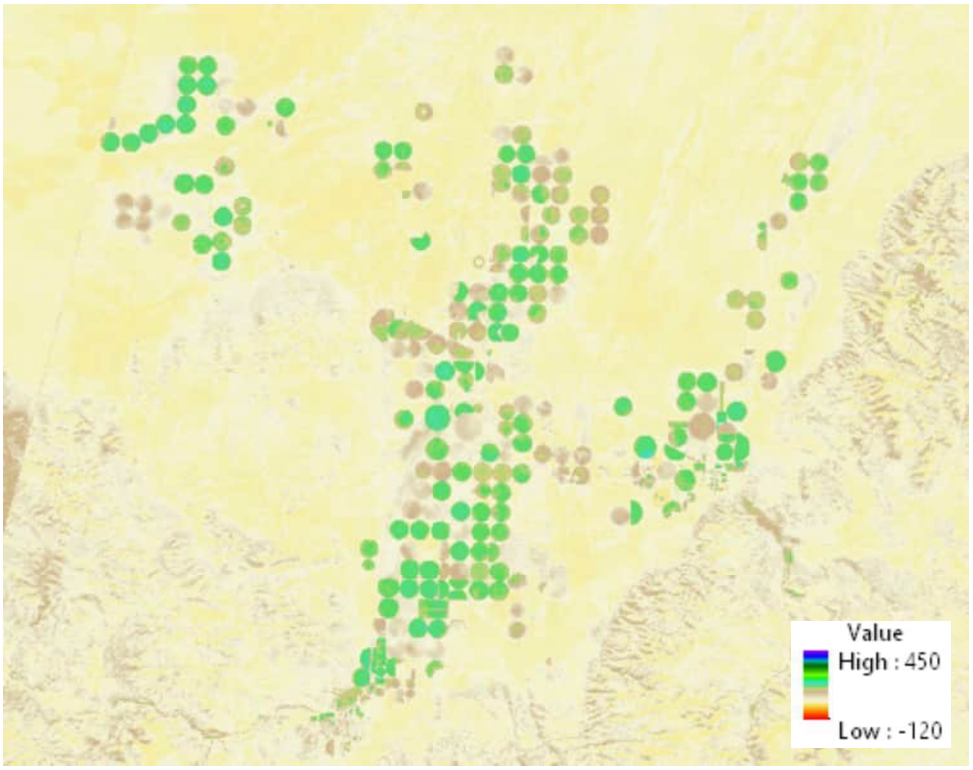

Figure 21b. ET, mm, for the month of October 2020 for the Beryl Junction / Enterprise study area.

Year 2021. Figures 22-29 show monthly ET_rF and ET for months of March to October 2021 for the study area. ET_rF tended to become progressively higher from March through August as irrigated crops developed. ET_rF from irrigated areas tended to dominate the landscape, with some ET from rangeland areas in early spring and during summer precipitation events.

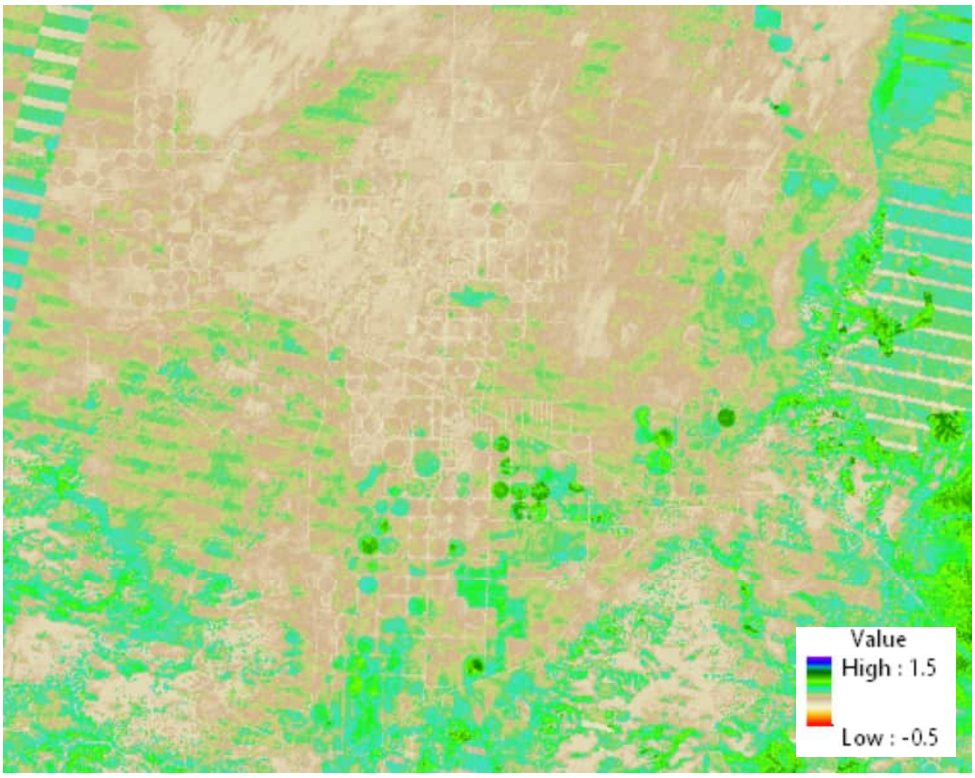

Figure 22a. ET_rF for the month of March 2021 for the Beryl Junction / Enterprise study area. Rangeland areas exhibit ET_rF from recent wetting events.

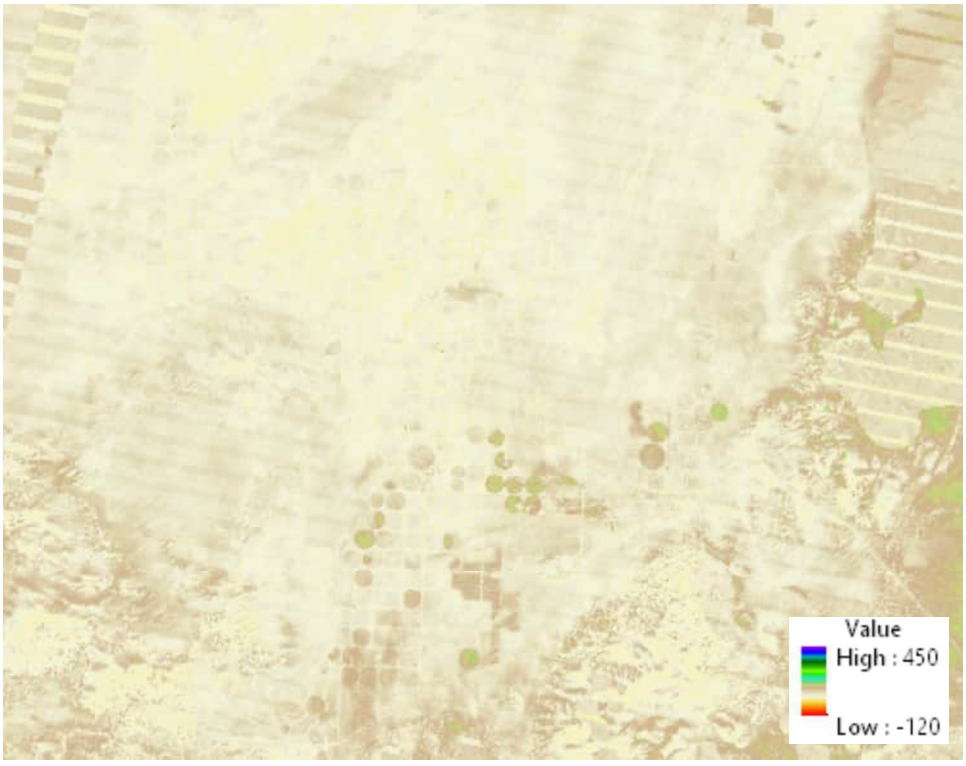

Figure 22b. ET, millimeters, for the month of March 2021 for the Beryl Junction / Enterprise study area.

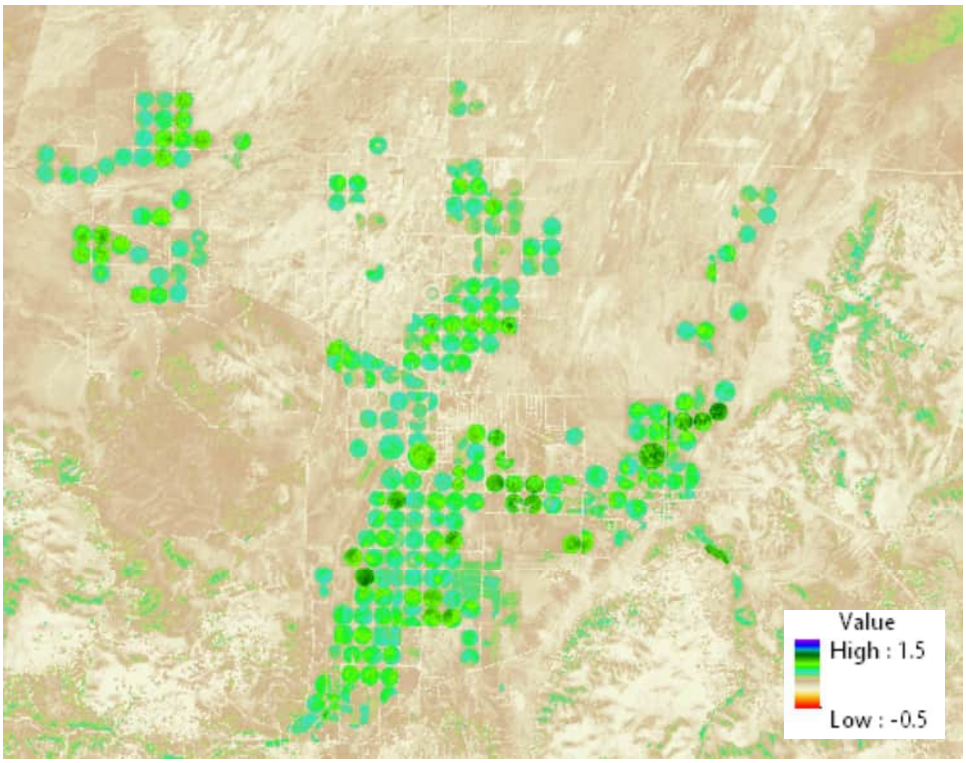

Figure 23a. ET_rF for the month of April 2021 for the Beryl Junction / Enterprise study area. Rangeland areas exhibit ET_{rF} from recent wetting events.

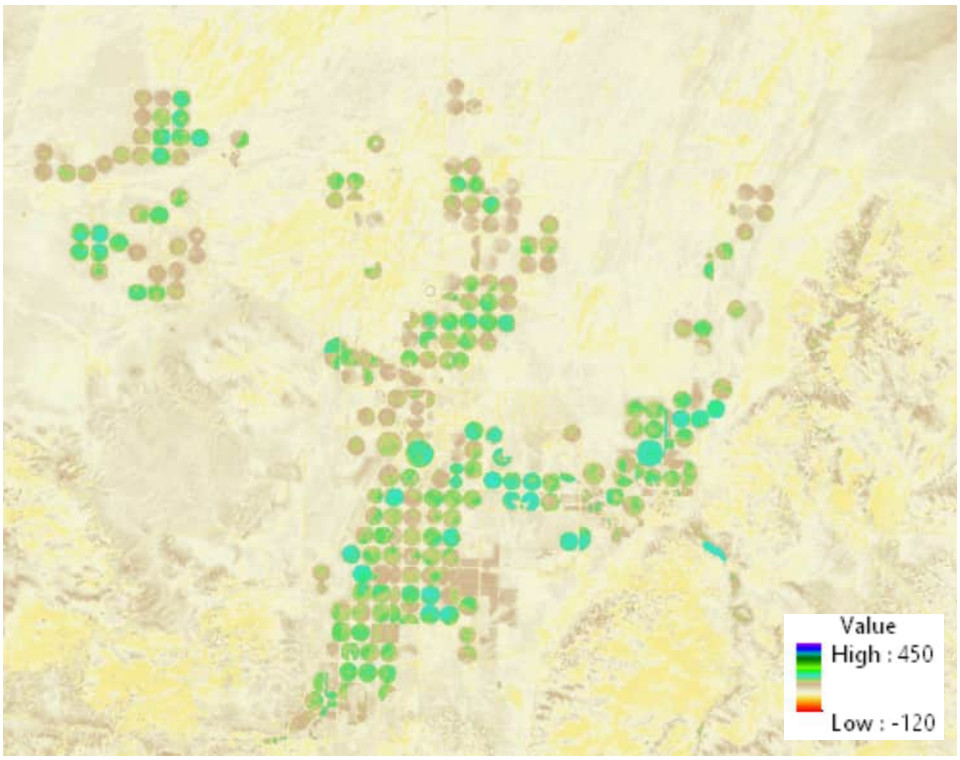

Figure 23b. ET, millimeters, for the month of April 2021 for the Beryl Junction / Enterprise study area.

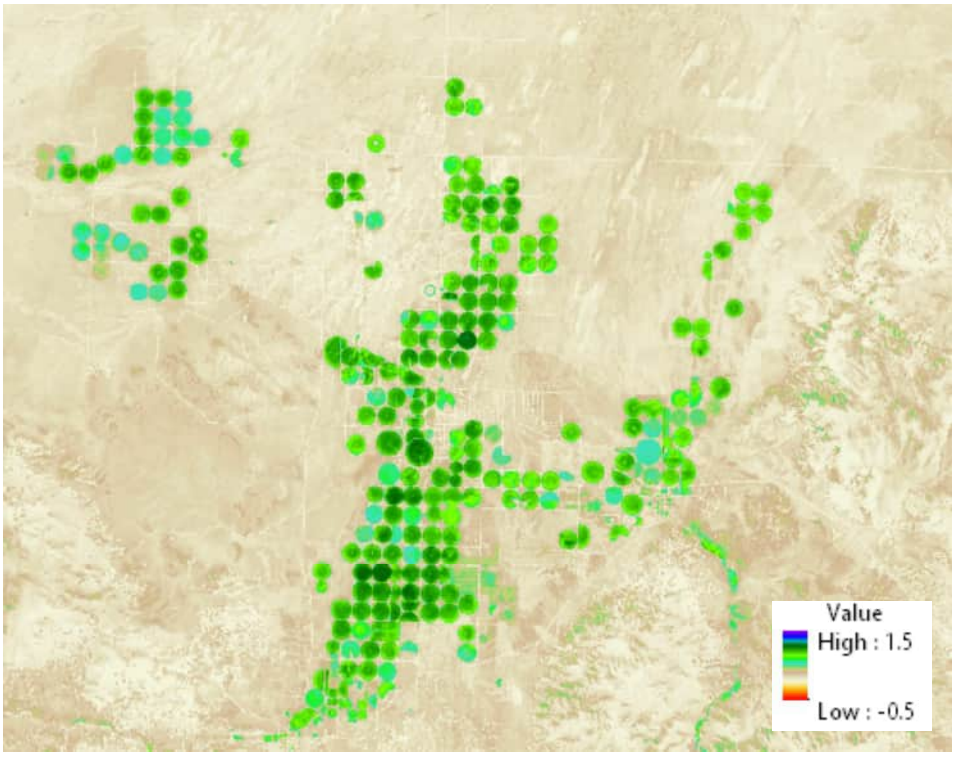

Figure 24a. ET_rF for the month of May 2021 for the Beryl Junction / Enterprise study area.

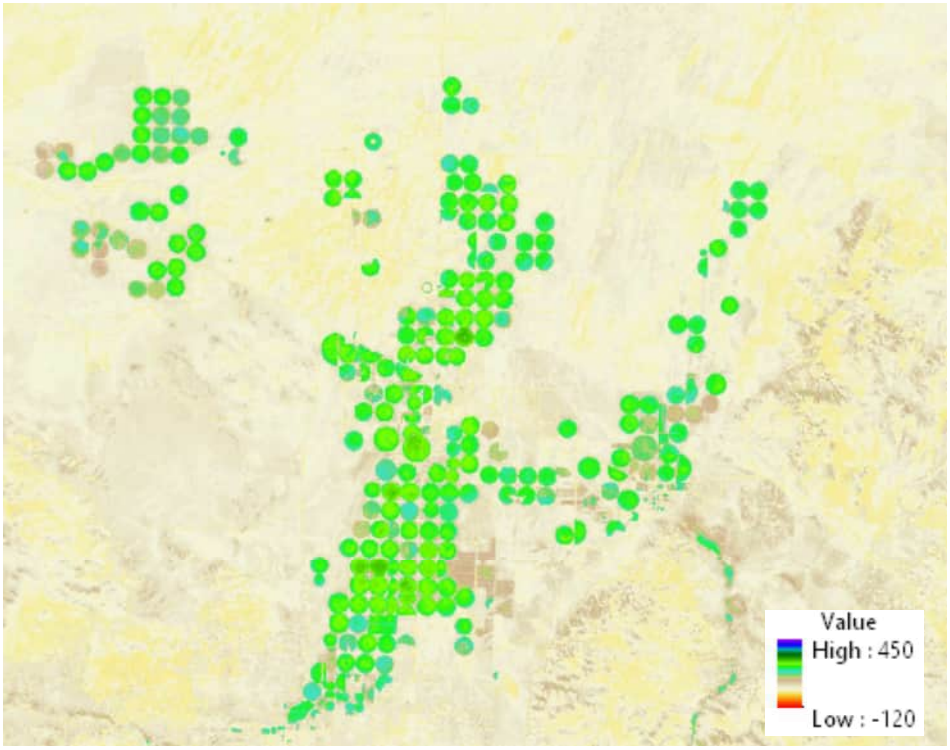

Figure 24b. ET, mm, for the month of May 2021 for the Beryl Junction / Enterprise study area.

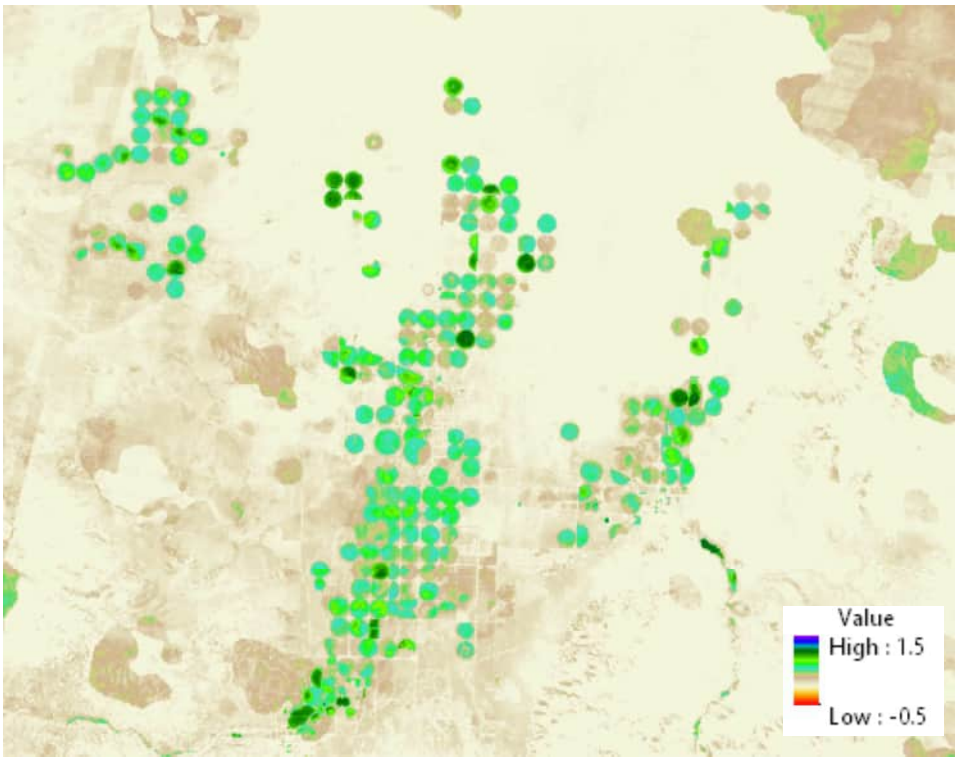

Figure 25a. ET_rF for the month of June 2021 for the Beryl Junction / Enterprise study area.

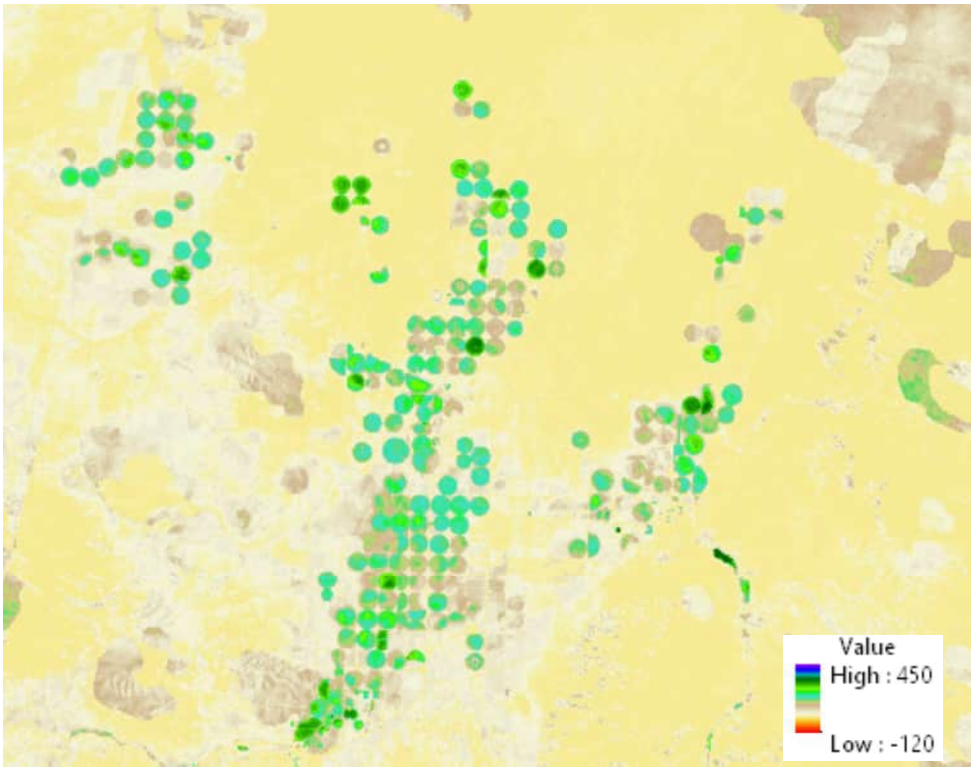

Figure 25b. ET, mm, for the month of June 2021 for the Beryl Junction / Enterprise study area

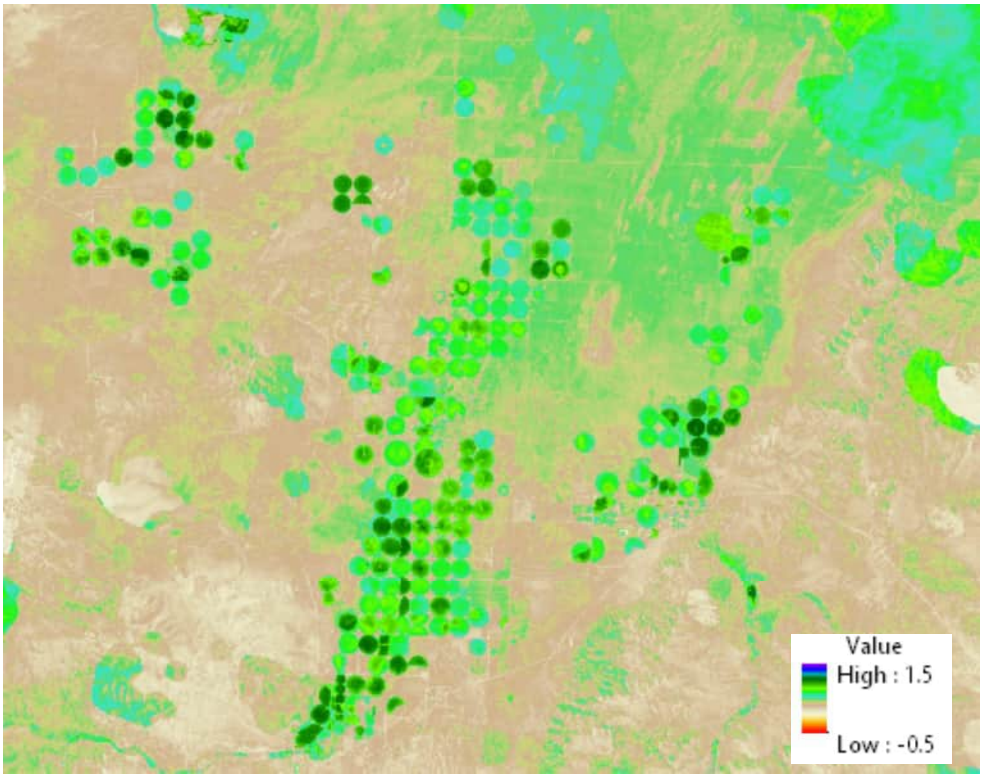

Figure 26a. ET_rF for the month of July 2021 for the Beryl Junction / Enterprise study area.

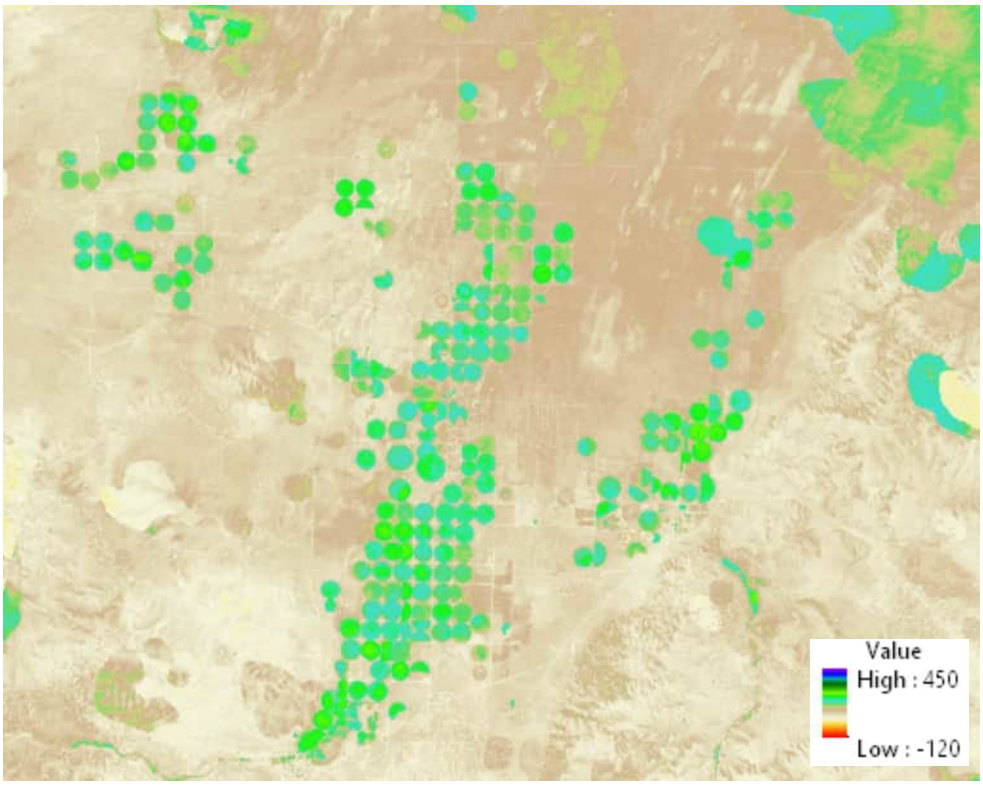

Figure 26b. ET, mm, for the month of July 2021 for the Beryl Junction / Enterprise study area.

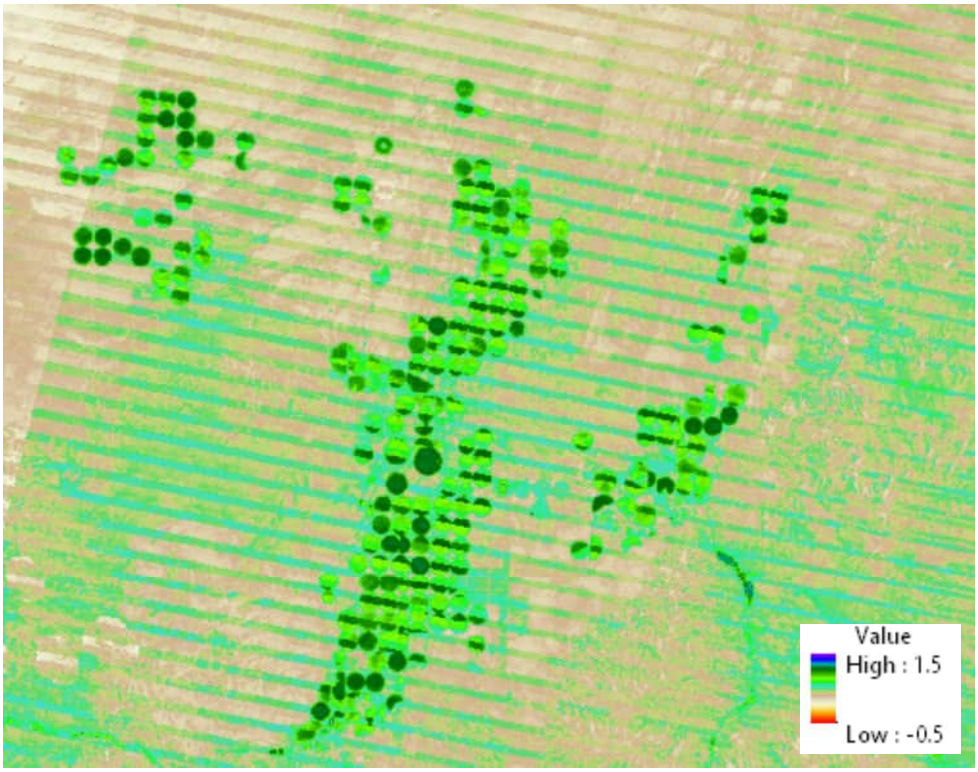

Figure 27a. ET_rF for the month of August 2021 for the Beryl Junction / Enterprise study area.

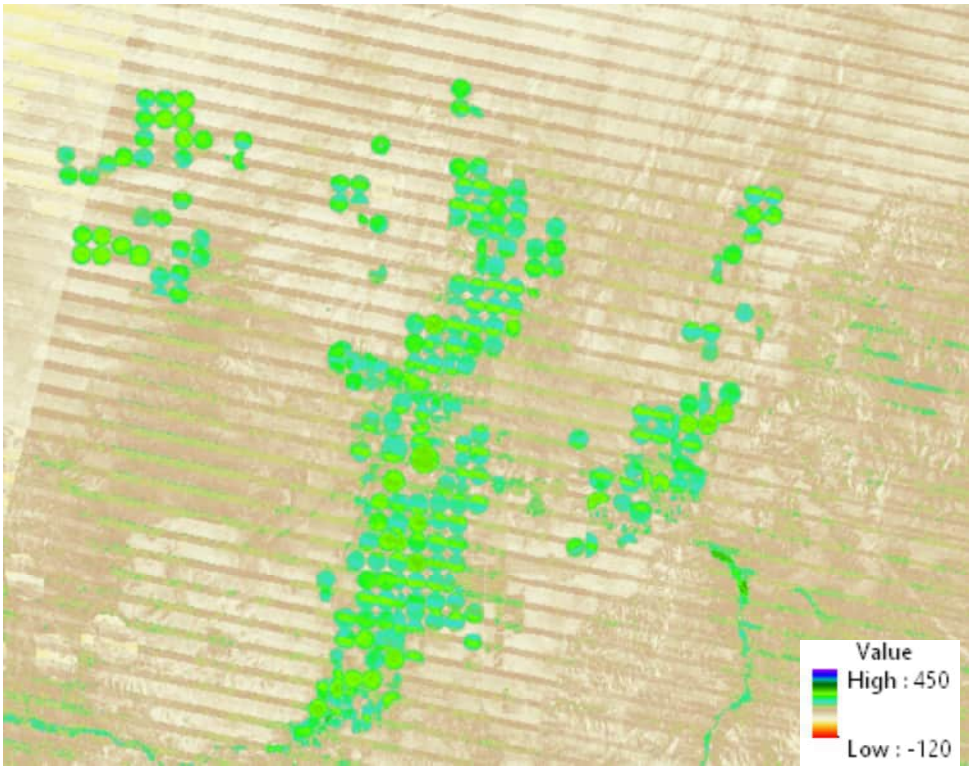

Figure 27b. ET, mm, for the month of August 2021 for the Beryl Junction / Enterprise study area.

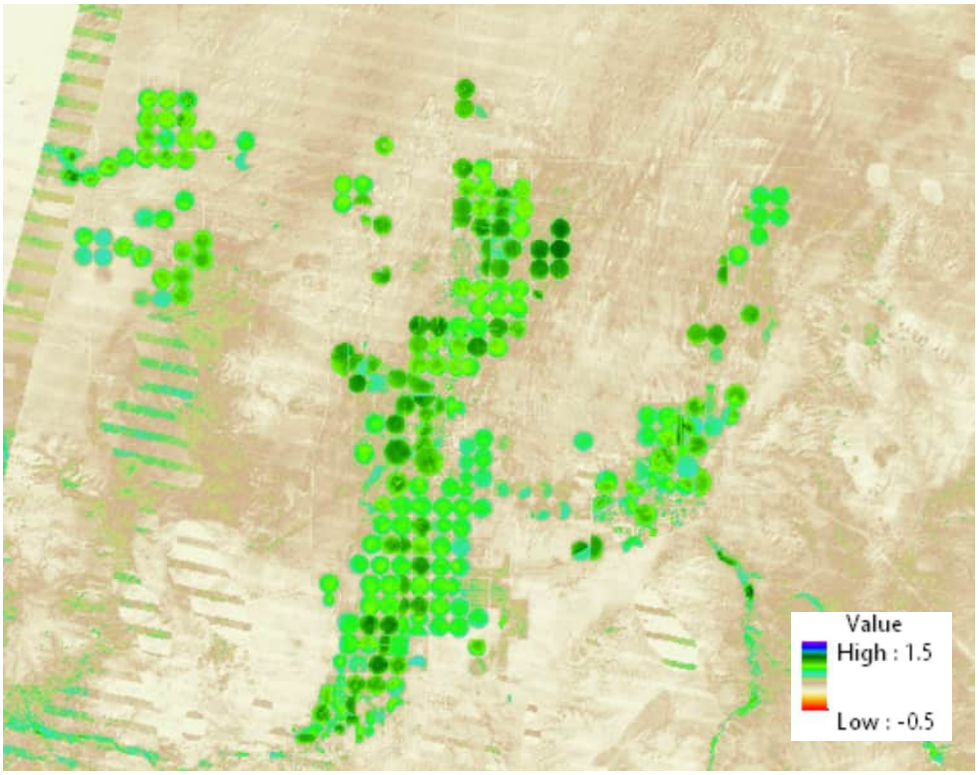

Figure 28a. ET_rF for the month of September 2021 for the Beryl Junction / Enterprise study area.

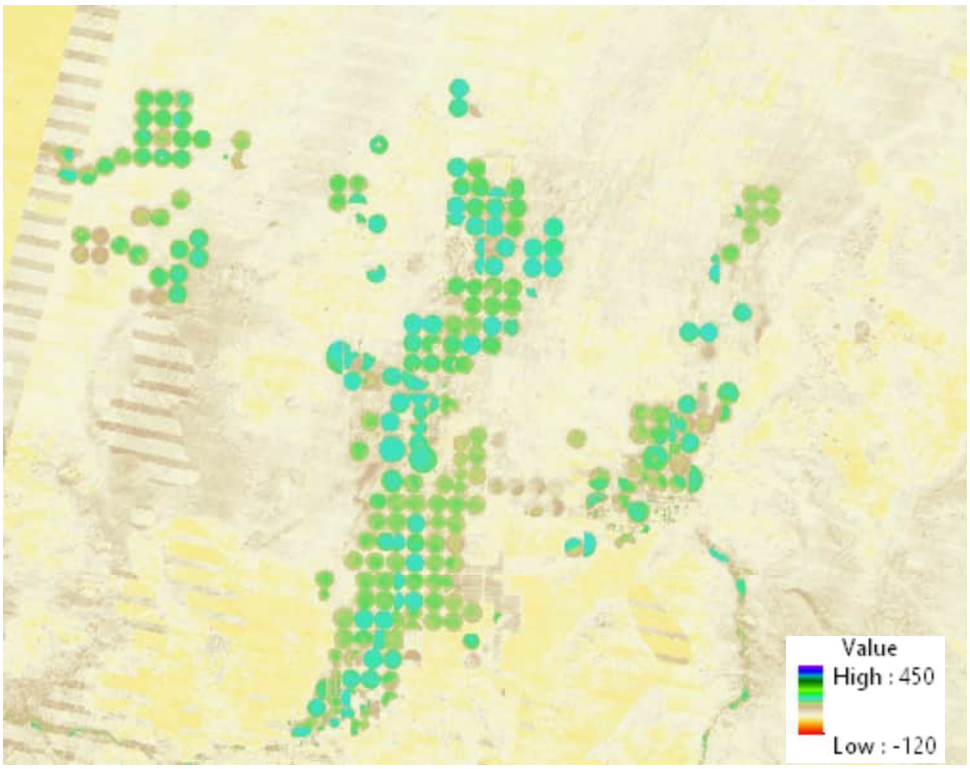

Figure 28b. ET, mm, for the month of September 2021 for the Beryl Junction / Enterprise study area.

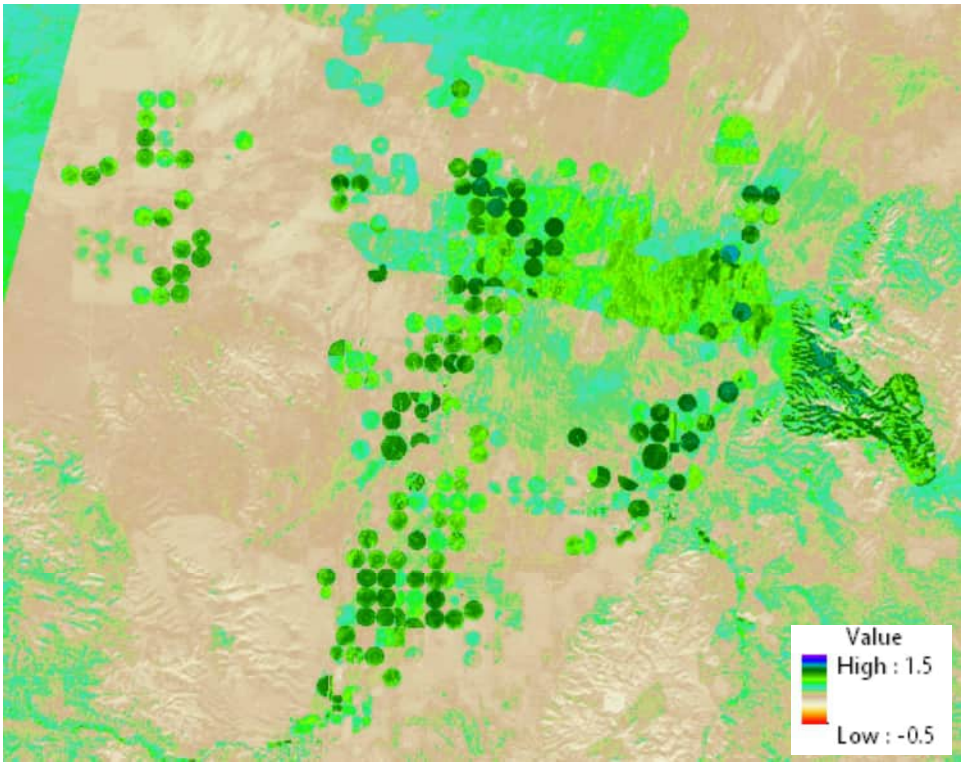

Figure 29a. ET_rF for the month of October 2021 for the Beryl Junction / Enterprise study area.

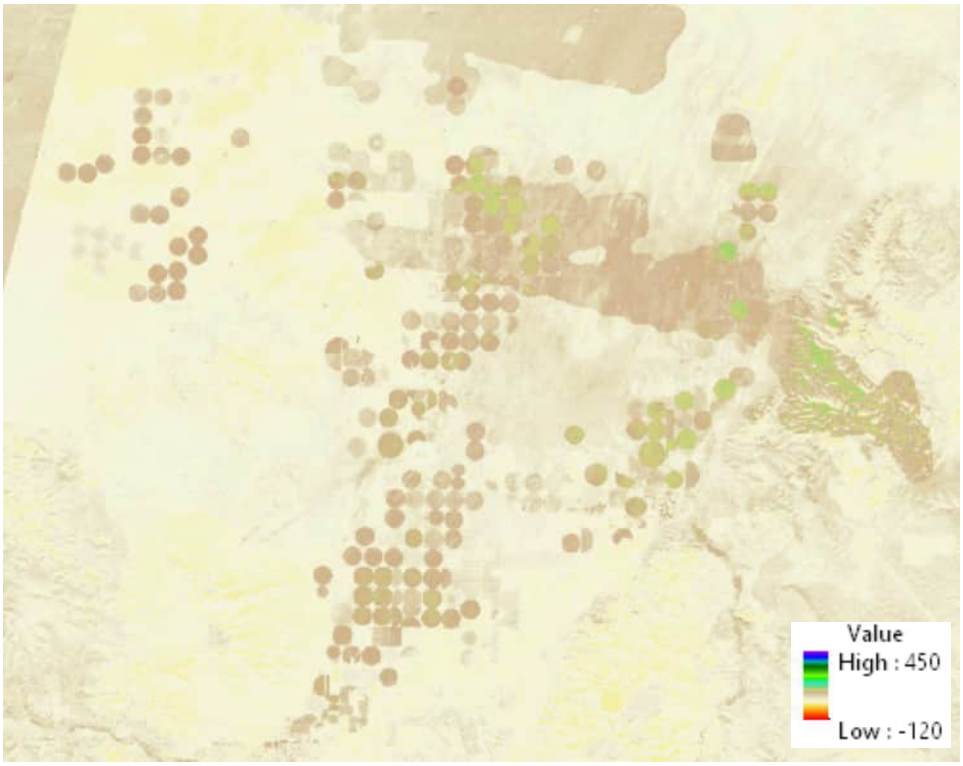

Figure 29b. ET, mm, for the month of October 2021 for the Beryl Junction / Enterprise study area.

Summary ET_rF and ET for March through October

Growing season summary products were produced for season-average ET_rF and for total actual evapotransiration in millimeters (25.4 mm = 1.0 inch) as shown in Figures 30 for 2020 and 31 for 2021.

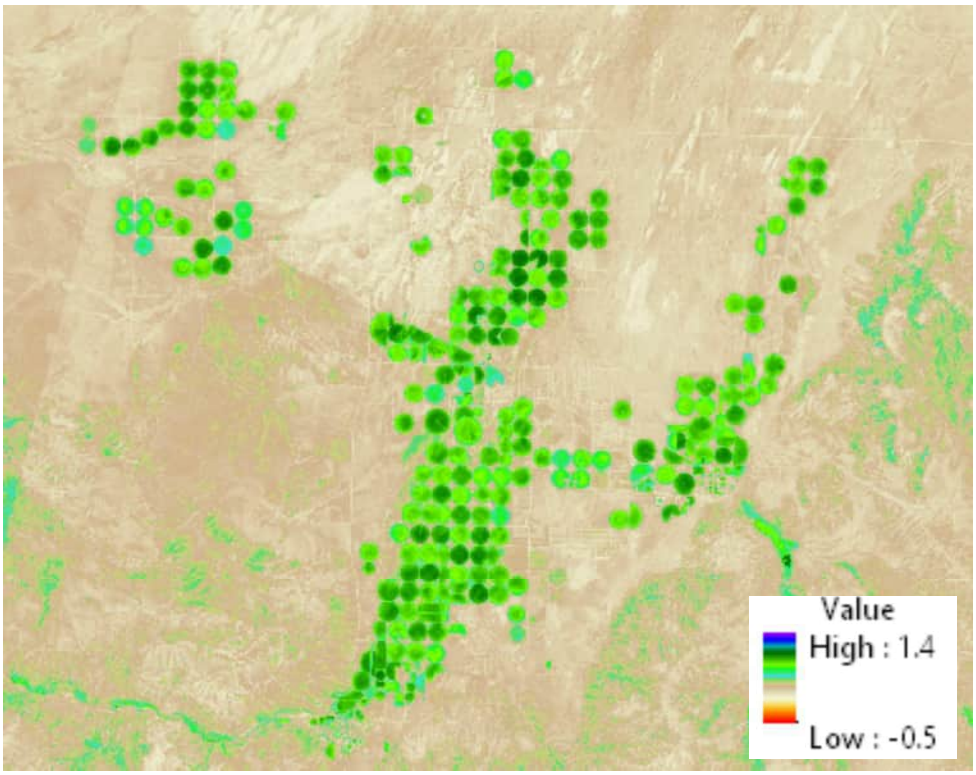

Figure 30a. Average ET_rF for the growing period March - October 2020 for the Beryl Junction / Enterprise study area.

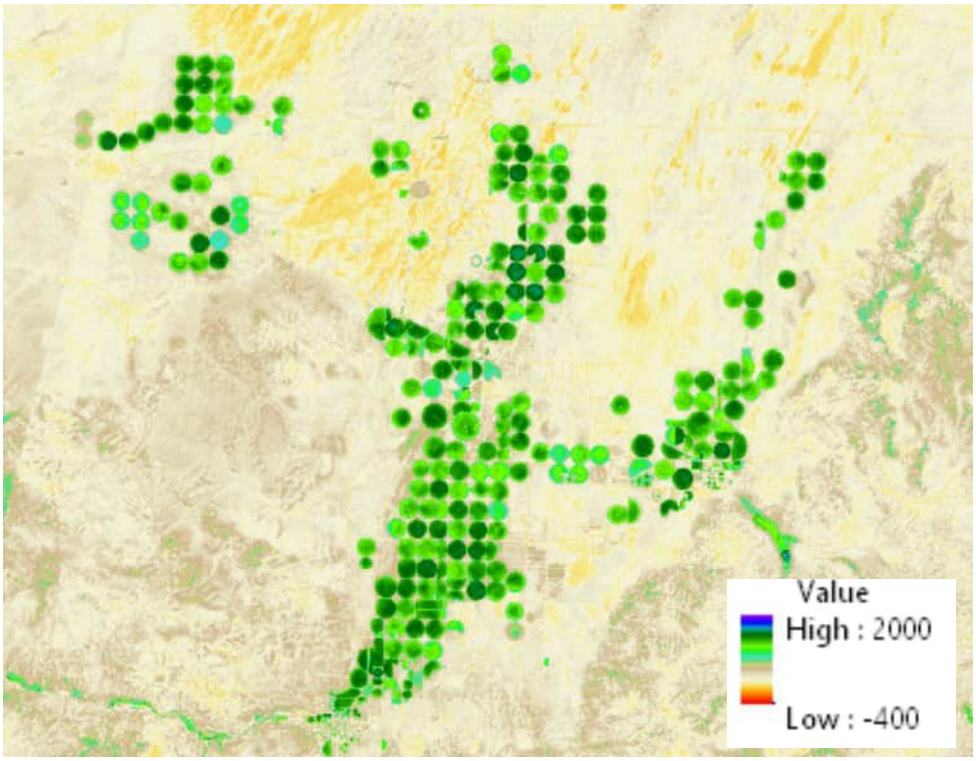

Figure 30b. Total ET, millimeters, for the growing period of March - October 2020 for the Beryl Junction / Enterprise study area.

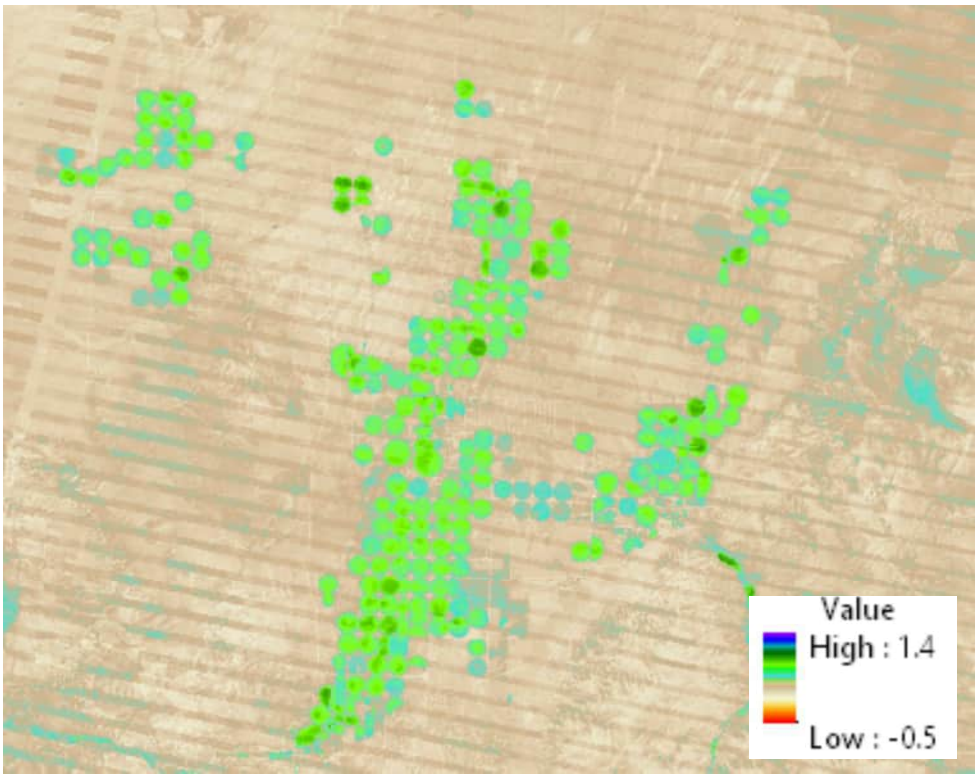

Figure 31a. Average ET_rF for the growing period March - October 2021 for the Beryl Junction / Enterprise study area.

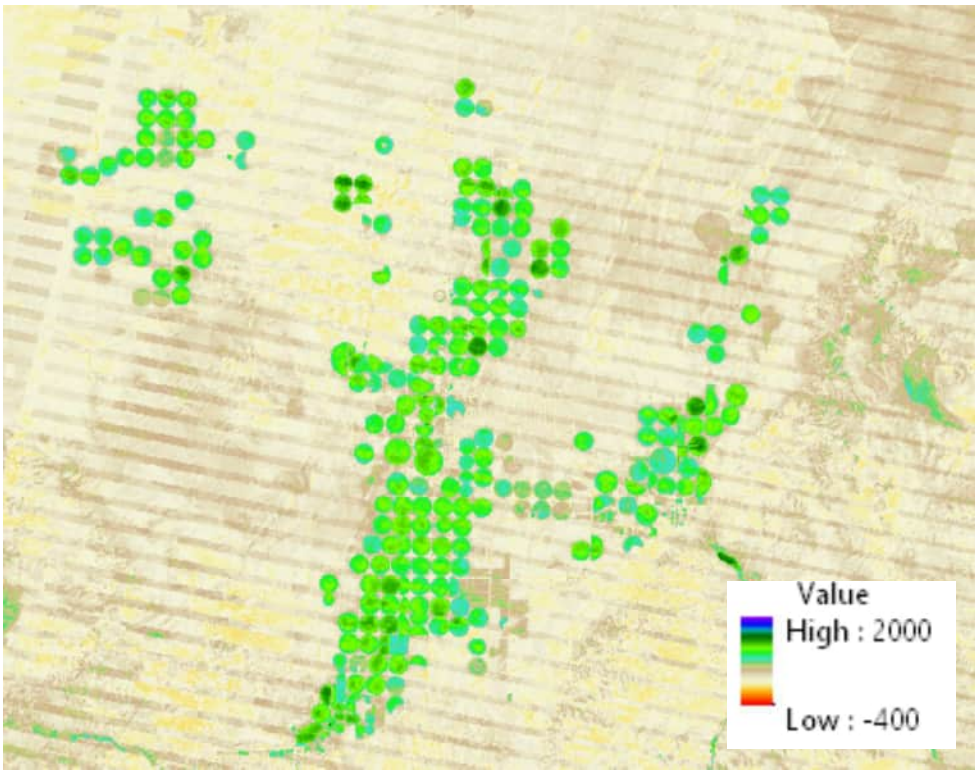

Figure 31b. Total ET, millimeters, for the growing period of March - October 2021 for the Beryl Junction / Enterprise study area.

Comparison of ET between Years 2020 and 2021

Comparing Figures 14 through 21 for year 2020 with Figures 22 through 29 for year 2021 indicates that the month of March had very low ET for irrigated areas and was similar between the two years. ET of most fields during April was similar for both years, with year 2020 having higher ET from range areas due to precipitation. ET during May was also similar between the two years.

June 2020 had more fields showing high or moderately high ET than for June 2021. This may have been due to cropping patterns. ET during July 2021 was substantially lower than ET during July 2020 for irrigated fields, even though ET was higher in July 2021 for rangeland due to higher precipitation. Alfalfa reference ET was 30% lower during July 2021 than during June 2020, mostly due to higher cloudiness, where July 2021 solar radiation was 21% less, and humidity was higher. Monthly alfalfa reference ET is shown in Table 4 for the two years.

August 2020 ET was a little higher, on average than during August 2021, with a larger number of fields exhibiting ET that was greater than the average ET across fields. This pattern was not exhibited for August 2021. The impact of using a Landsat 7 image for August 2021 is noticeable, where impacts of missing scan lines brought in ET information from a more distant image in time during the time integration step.

Monthly ET during September was similar between the two years. Monthly ET during October 2020 was greater than during October 2021, where ET for October 2021 was quite low. ET for October 2020 was moderately high. Comparison of ET_rF between the two Octobers shows a similar magnitude between the years. This suggests that the higher ET for October 2020 was caused by the 21% higher ET_r for 2020.

Comparison of Figures 30 and 31 suggests that the season average ET_rF for March through October was lower for fields having highest ET_rF during 2021 (less dark green color in Figure 31a than in Figure 30a). This may have been caused by a difference in cropping patterns or cutting behavior between years. This caused March – October ET to be noticeably lower during 2021 than during 2020. The reference ET_r was 6% lower during March – October 2021 than during 2020.

Table 4. Monthly alfalfa reference ETr from the Bery Junction weather station and the percentage change from year 2020 to year 2021. December 2021 data were not processed.

Month	2020 mm	2020 inches	2021 mm	2021 inches	Percent Change
1	54	2.1	45	1.8	-16%
2	76	3.0	80	3.1	4%
3	106	4.2	126	5.0	19%
4	164	6.4	194	7.7	19%
5	248	9.8	260	10.2	5%
6	295	11.6	291	11.5	-1%
7	317	12.5	220	8.7	-31%
8	267	10.5	239	9.4	-11%
9	196	7.7	188	7.4	-4%
10	133	5.3	105	4.1	-21%
11	79	3.1	42	1.7	-47%
12	50	2.0	--	--	--
Mar-Oct	1726	68.0	1623	63.9	-6%

6. Summary

Monthly evapotranspiration (ET) maps were produced for March, April, May, June, July, August, September and October for years 2020 and 2021 for the region surrounding Enterprise, Utah where irrigation is practiced. The ET products have 30 m spatial resolution and cover the path overlap area of Landsat WRS paths 38 and 38 and residing in row 34. ET was produced using the ERDAS Imagine Level 3 version of the METRIC model (Mapping Evapotranspiration at high Resolution using Internalized Calibration) developed by the University of Idaho. The METRIC procedure utilizes visible, near-infrared and thermal infrared energy spectral bands from Landsat satellite images and weather data to calculate ET on a pixel by pixel basis. Surface energy is partitioned into net incoming radiation (both solar and thermal), ground heat flux, sensible heat flux to the air and latent heat flux. The latent heat flux is calculated as the residual of the energy balance and represents the energy consumed by ET. Alfalfa reference ET, computed hourly, is used to account for day to day impacts of weather on ET demands, with information on individual pixel behavior, relative to the reference ET, provided for the individual Landsat image dates.

7. References

Allen, R.G. 2011. Skin layer evaporation to account for small precipitation events—An enhancement to the FAO-56 evaporation model. Agricultural Water Management. 99(1):8-18.

Allen, R.G., 2012. REF-ET: Reference Evapotranspiration Calculation Software for FAO and ASCE Standardized Equations. University of Idaho, 82 pp. [http://www.kimberly.uidaho.edu/ref-et/index.html]. Contact author for updates.

Allen, R.G., Pereira, L.S., Raes, D., Smith, M., 1998. Crop Evapotranspiration. Guidelines for computing crop water requirements. FAO Irrig. and Drain. Paper 56. FAO, Rome, 300 pp.

Allen, R.G., Tasumi, M., Trezza, R., 2007a. Satellite-Based Energy Balance for Mapping Evapotranspiration with Internalized Calibration (METRIC) – Model. J. Irrig. Drain Engr., 133(4), 380-394.

Allen, R.G., Tasumi, M., Morse, A., Trezza, R., Wright, J.L., Bastiaanssen, W., Kramber, W., Lorite, I., Robison, C.W., 2007b. Satellite-Based Energy Balance for Mapping Evapotranspiration with Internalized Calibration (METRIC) – Applications. J. Irrig. Drain Engr., 133(4), 395-406.

Allen, R.G., Trezza, R., Tasumi, M., Kjaersgaard, J.H., 2016. METRIC. Mapping Evapotranspiration at High Resolution. Applic. Manual, V 3.0. University of Idaho. 279 pp.

Allen, R.G., J.H. Kjaersgaard, R. Trezza, A. Oliveira, C. Robison, I. Lorite-torres. 2011. Refining components of a satellite based surface energy balance model to complex-land use systems. Proceedings of Remote Sensing and Hydrology 2011 Symposium held at Jackson Hole, Wyoming, USA, September 2011, IAHS Publ. 3XX, 2011. 3 p.

Allen, R.G., B. Burnett, W. Kramber, J. Huntington, J. Kjaersgaard, A. Kilic, C. Kelly, R. Trezza. 2013. Automated calibration of the metric-landsat evapotranspiration process. JAWRA J. Am. Water Resour. Assoc., 49 (3) (2013), pp. 563-576.

ASCE-EWRI, 2005. The ASCE Standardized Reference Evapotranspiration Equation. ASCE, Reston, Virginia.

Jensen, M.E. and R.G. Allen (ed.). 2016. Evaporation, Evapotranspiration and Irrigation Water Requirements. ASCE Manual of Practice no. 70, revised. 744 pages.

NLCD (2011): Homer, C.G., Dewitz, J.A., Yang, L., Jin, S., Danielson, P., Xian, G., Coulston, J., Herold, N.D., Wickham, J.D., and Megown, K., 2015, Completion of the 2011 National Land Cover Database for the conterminous United States-Representing a decade of land cover change information. Photogrammetric Engineering and Remote Sensing, v. 81, no. 5, p. 345-354

Wright, J.L., 1982. New evapotranspiration crop coefficients. J. Irrig. Drain. Engr., 108(1), 57-74.

Appendix A.

METRIC Processing of Path 38 Path 39, Row 34, Year 2020 images

All are L8 images

Dr. Wenguang Zhao, Dr. Richard Allen and Dr. Ayse Kilic

General Information:
The agricultural (AG) area of focus is located within the overlapping area of two Landsat paths. With the 16 day revisit time of Landsat 8 (L8), the overlapping of the two paths provides for acquisition of images over the overlapped area that are 7 and 9 days apart. This provided for a relatively dense time series of L8 dates over the 2020 season and avoided the need to process Landsat 7 images that have missing image gaps due to the SLC-off malfunction. The Path 38, Row 34 image is primarily located in the southwest of Utah, with the lower part extending into northwest Arizona. The Path 39, Row 34 image is primarily located in the lower eastern part of Nevada, with the eastern part extending into Utah and a corner in Nevada overlapping with the Path 38 Row 34 image.
The primary area of interest is in the overlap area of Path 38 and Path 39 and includes center pivot irrigated fields near Beryl Junction, UT and towards Enterprise, UT. A mid summer snapshot of evapotranspiration (ET) shown as the ratio of ET to an alfalfa reference ET (ETr) is shown below, taken from Path 38:

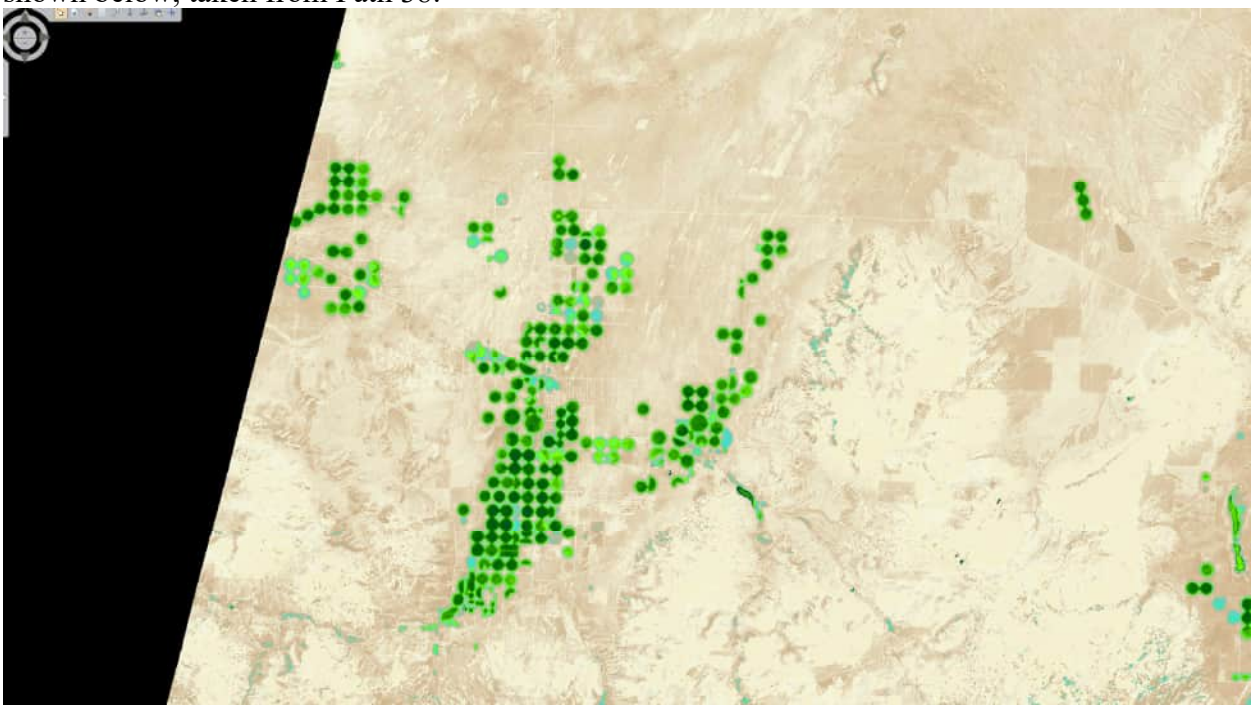

The list of twenty Landsat 8 images processed for the study area for year 2020 are listed in Table 1. These images were selected for processing based on clearness of each image near the study area for each image date.

Table 1. Landsat 8 images processed for year 2020.

Image No.	Year	MoDa	Sat.	Path
1	2020	0331	L8	P39
2	2020	0425	L8	P38
3	2020	0502	L8	P39
4	2020	0511	L8	P38
5	2020	0527	L8	P38
6	2020	0612	L8	P38
7	2020	0619	L8	P39
8	2020	0628	L8	P38
9	2020	0705	L8	P39
10	2020	0714	L8	P38
11	2020	0730	L8	P38
12	2020	0806	L8	P39
13	2020	0815	L8	P38
14	2020	0822	L8	P39
15	2020	0831	L8	P38
16	2020	0916	L8	P38
17	2020	0923	L8	P39
18	2020	1002	L8	P38
19	2020	1018	L8	P38
20	2020	1119	L8	P38

The ET from individual fields in the study area tend to vary substantially in time during the growing season due to alfalfa cuttings, rapid development of annual crops and rain events. Therefore, a high frequency of image processing is valuable for defining time-based changes in ET rates.

The geometric projection for the Path 38 images is UTM zone 12 and the projection for the Path 39 image is UTM zone 11. Therefore the Path 39 image was reprojected to zone 12 prior to processing with METRIC to produce a common projection for later mosaicking of ET data.

The calibration weather station used is the Beryl Junction weather station located at 37.7196°N and 113.702°W in Iron County, Utah. The soil type of the area is **very fine sandy loam** according to the NRCS soil survey (Please consult the following link at Page 40 and Page 41): https://www.nrcs.usda.gov/Internet/FSE_MANUSCRIPTS/utah/berylenterpriseUT1960/berylenterpriseUT1960.pdf

The field capacity of the soil was set to 0.2 m^3 m^{-3} representing a value between that for a sandy loam of 0.14 and a loam of 0.25—0.32, because of its "very fine" denotation. The wilting point of the soil was set to 0.07 m^3 m^{-3} representing a value between that for a sandy loam of 0.05 and a loam of 0.09—0.15. Lapse rates used by METRIC to delapse surface temperature were set at the standard values of 0.6 and 10 K km^{-1} for "flat" areas and "mountainous" areas, respectively, and elevation threshold was set at 1650 m for transitioning between the two lapse rates.

The selection of sampling points for producing plots of surface temperature and ETrF (fraction of alfalfa reference ET) for review was done by manually selecting locations in interiors of agricultural fields within and near the study area. In order to have a general review for the whole

image, we also sampled agricultural fields in other locations of the scenes, for instance, in the P38 image we sampled areas near Cedar City, Parowan, Milford, Beaver, Circleville and Panguitch, etc.; and in the P39 image we sampled areas near Lake Valley Produce, Panaca, Bunkerville and Amber etc. For non-Agricultural areas, we collected samples throughout the image scenes, so that we could have a general view of the ET behavior throughout the images. Figure 1 shows the locations of sampling points near the study area.

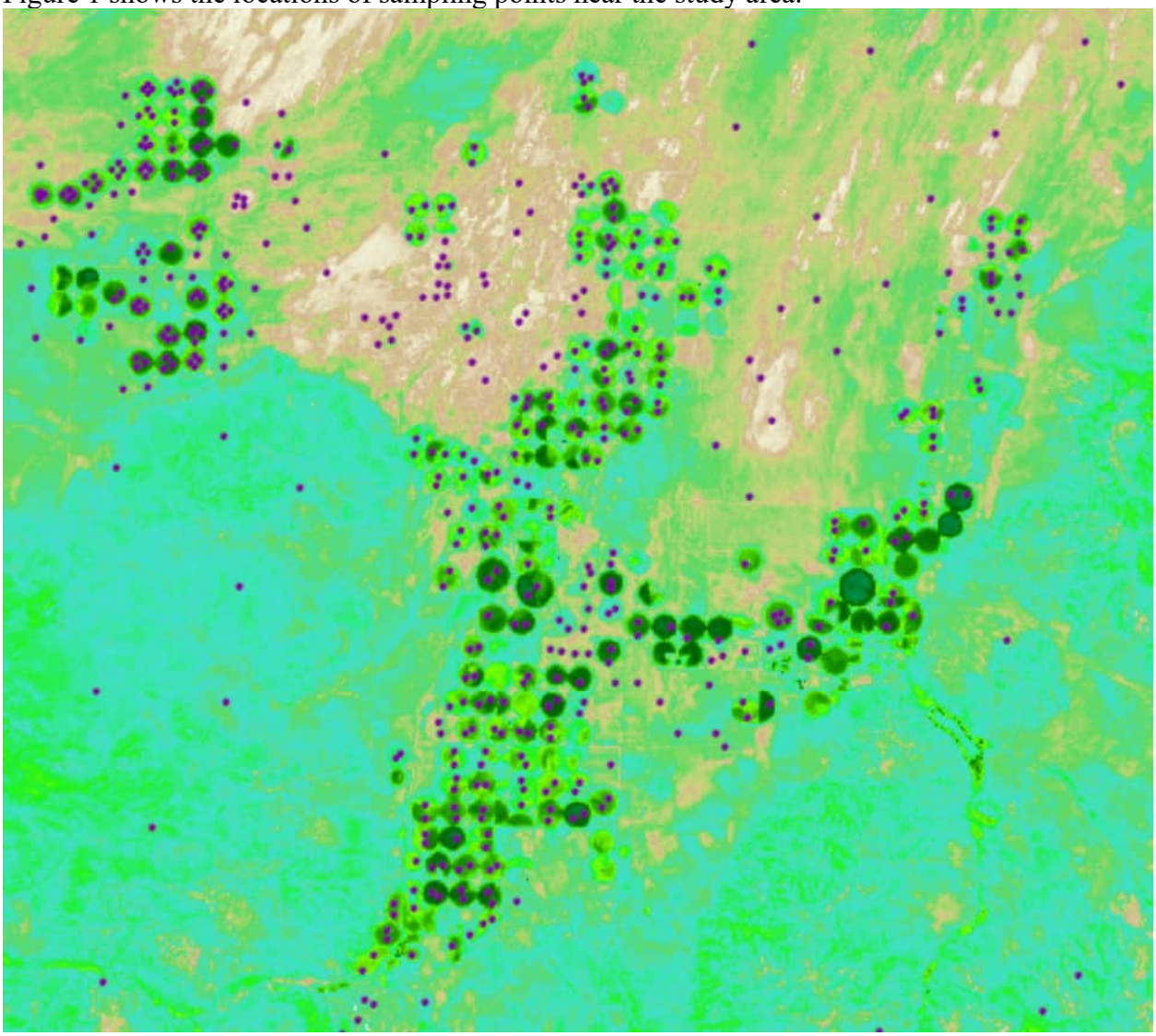

Figure 1. Locations of sampling points near and within the study area.

Path 38 Images:

April 25, 2020

This image is mostly clear with substantial snow in mountains. There are a few small clouds in the north and northeastern area. However, the Ag areas that we are most interested in are clear. Wind speed is 1.5 m/s and ETr is 0.7 mm/h. There was 12.2 mm rain between April 19 and April 20. Also, there was 8.6 mm of rain on April 18.

Estimated Ke is 0.19 for the satellite overpass time and 0.27 for the previous day. due to 1 mm of rain the previous day. ETrFcold is set at 1.05 and ETrFhot is 0.20. Hcold (sensible heat flux at the cold pixel) is 61 W/m^2 and Hhot (sensible heat flux at the hot pixel) is 248 W/m^2.

The graph for de-lapsed surface temperature vs. NDVI is as follows (where the blue points are from agricultural fields, and the red crosses are from Non-Agricultural areas):

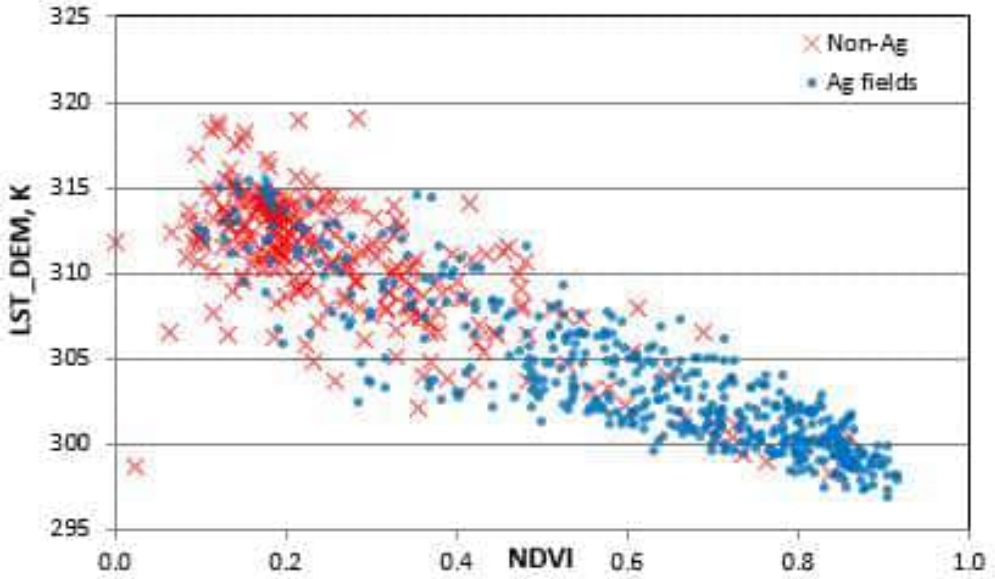

NDVI stands for normalized difference vegetation index. Its value ranges from about 0.1 to 0.15 for bare soils having little to no green vegetation to about 0.7 to 0.9 for fields (or pixels) having nearly full ground cover by green vegetation. NDVI is computed in METRIC using surface reflectances in the near-infrared band and the red band. NDVI is a common parameter to express vegetation amount.

The graph for ETrF-EF vs. NDVI is as follows (where the blue points are from agricultural fields, and the red crosses are from Non-Agricultural areas):

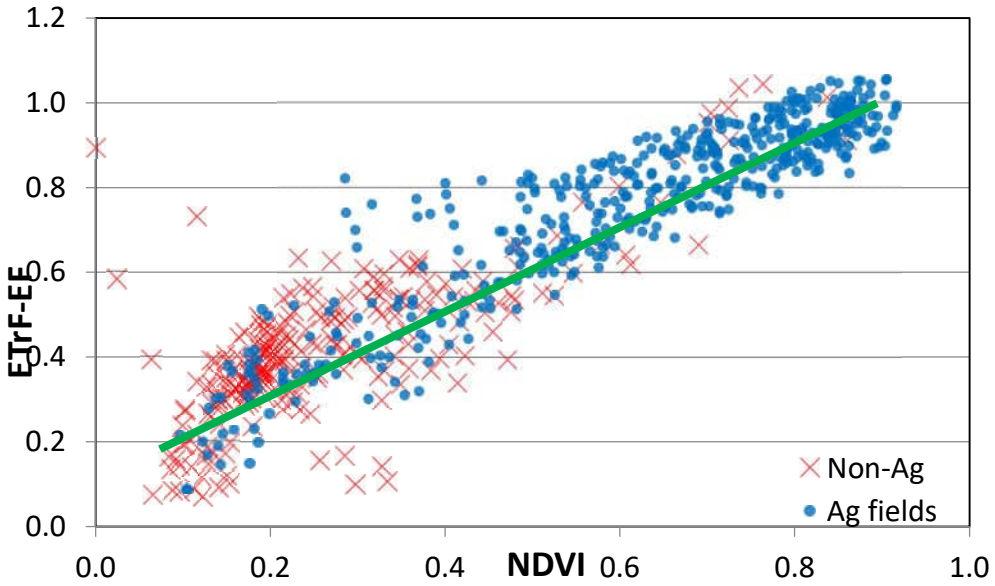

ETrF represents ET expressed as a fraction of the alfalfa reference ET. A value of 1.0 indicates that the sampled ET is the same as that for the alfalfa reference. The alfalfa reference ET represents a near upper limit on ET, limited by environmental energy (photons from the sun and any heat convected from the air) to convert liquid water to vapor. The "EF" label added to ETrF indicates that an evaporative fraction function was used for nonagricultural land uses to transform instantaneous ETrF to a 24-hour ETrF. Agricultural land uses assume that 24-hour ETrF is the same as the ETrF produced at satellite overpass time.
There are a few ag points between NDVI = 0.25 and 0.45 that have a higher ETrF compared to other points. These may be because of irrigation or local rain (the samples include some ag fields in the north and the north east portion of the image).

May 11, 2020
This image is quite cloudy. Clouds occupied 2/3 of the east side of the image. Fortunately, the Agricultural areas that we are most interested in are clear. Therefore we included this image for METRIC processing.
Wind speed is high at 7.7 m/s and ETr is 0.95 mm/h. There was no rain since April 29 and the soil should be dry. Estimated Ke for both the satellite overpass date and for the previous day are 0.00. ETrFcold is set to 1.05 and ETrFhot is set to 0.10. Hhot is 263 W/m^2 and Hcold is -115 W/m^2. The negative H for the cold pixel condition indicates substantial advection of heat energy from upwind range areas to the irrigated agriculture. Because our agricultural area is surrounded by dry, hot rangeland, Rn-G is not enough to support ET from the well-watered ag fields, so that a downward H flux of 115 W/m2 (originating (advected) from the surrounding hot dry land) occurs. This seems reasonable, especially under high wind speed situations like on this day.
The graph for de-lapsed surface temperature vs. NDVI is as follows (where the blue points are from agricultural fields, and the red crosses are from non-agricultural areas):

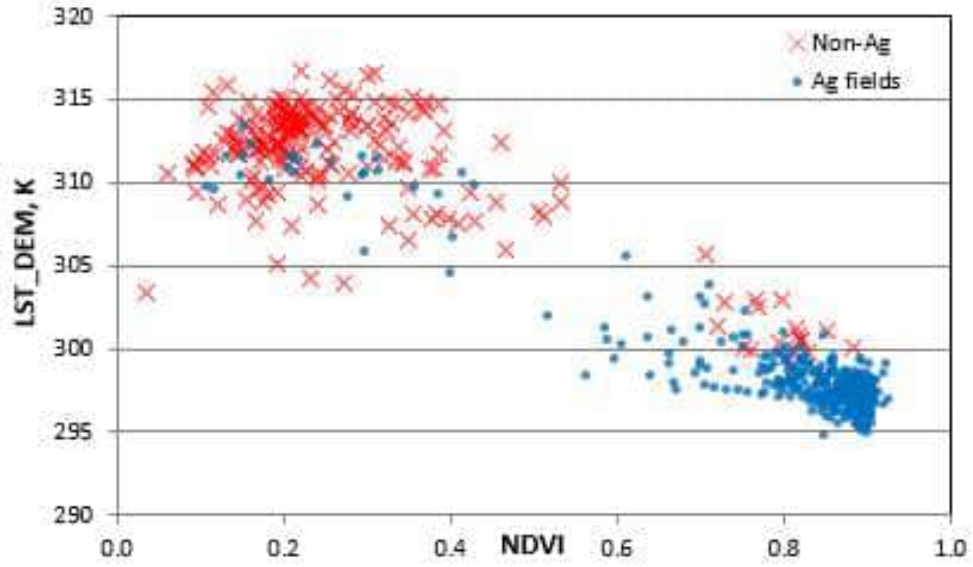

The graph for ETrF-EF vs. NDVI is as follows (where the blue points are from agricultural fields, and the red crosses are from Non-agricultural areas):

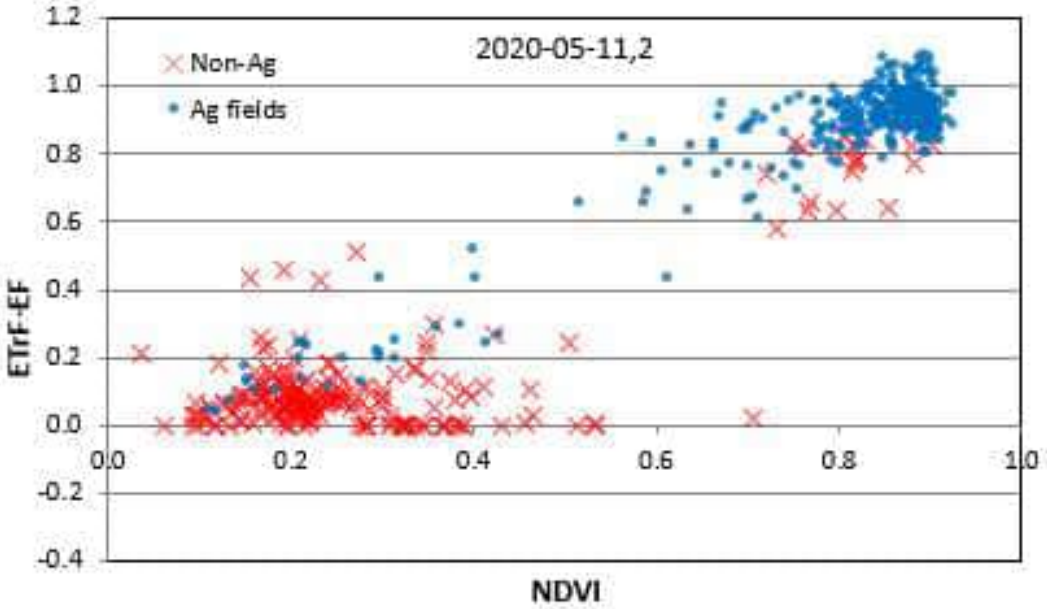

The final calibration is judged to be good.

May 27, 2020

This image also has quite a lot of clouds. However, the Ag areas that we are most interested in are clear. Wind speed is 2.0 m/s and ETr is 0.76 mm/h. There was no rain since April 29, almost a month ago. The bare soil should be quite dry without irrigation.

Estimated Ke is 0.00 for the satellite overpass date and for the previous day. ETrFcold is set to 1.00 (we tried to set it 1.05 for quite a few different cold pixels, but always got higher ETrF at the high end than desired. This is an advantage of calibration by an experienced METRIC operator compared to complete automatic operation) and ETrFhot for an agricultural pixel is 0.10. Hcold is 15.9 W/m^2 and Hhot is 282.5 W/m^2.

The graph for de-lapsed surface temperature vs. NDVI is as follows (where the blue points are from agriculture fields, and the red crosses are from non-Agriculture areas):

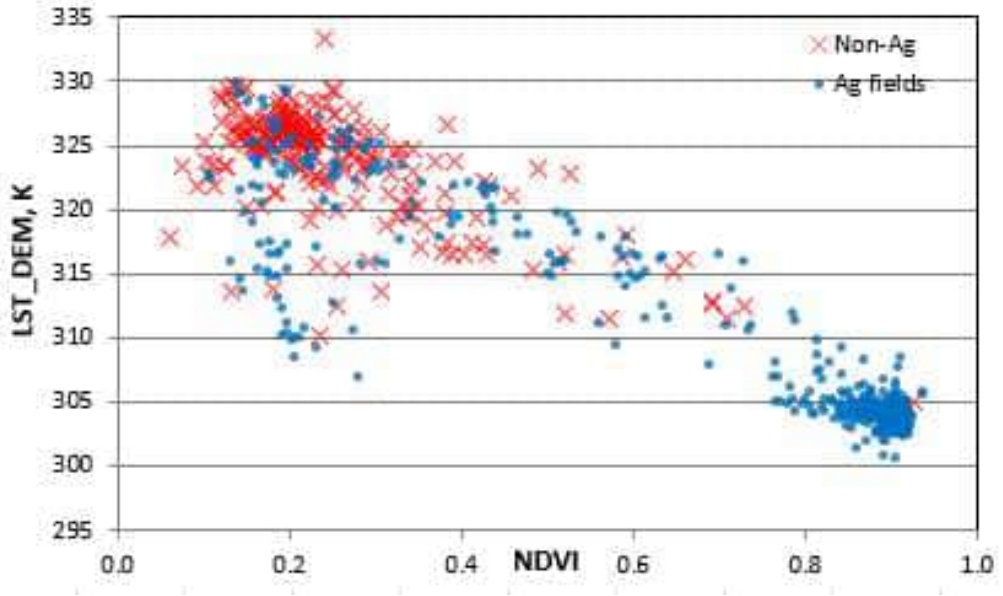

The graph for ETrF-EF vs. NDVI is as follows (where the blue points are from agriculture fields, and the red crosses are from Non-Agriculture areas):

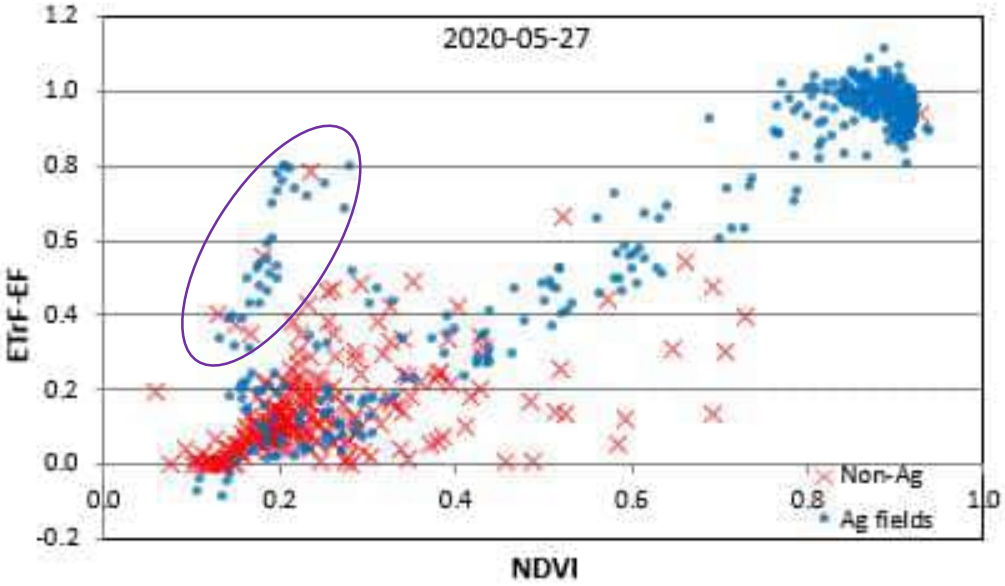

There are quite a few ag points between NDVI = 0.15 and 0.30 that have higher ETrFs (inside the purple circle) compared to other points close to the clustered trend line. This is most likely because of irrigation or a local rain (we also sampled some of the ag fields at the north and the northeast parts of the image).

June 12, 2020

This image has only a few clouds at the west side. Unfortunately, Part of the Ag areas that we are most interested in are covered by clouds. Still, we have some ag fields that are clear. There is

strong wind speed at 8.1 m/s and high ETr at 1.35 mm/h. There was no rain since April 29, more than 40 days ago. The soil should be quite dry without irrigation.
Estimated Ke is 0.00 for the satellite overpass date and for the previous day. ETrFcold is set to 1.05 and ETrFhot is 0.10. Hhot is 257 W/m^2 and Hcold is -145 W/m^2. The -145 value is quite negative, indicating an estimation of very strong advection from upwind rangeland and stable near-surface boundary layer. The value of ETr of 1.35 mm/h, which is quite high due to the strong wind speed, was limited to 1.0 mm/h during processing to reduce the magnitude at Hcold from -248 W/m^2 to -145 W/m^2. This limiting does not impact the calibration at the endpoints.
The graph for de-lapsed surface temperature vs. NDVI is as follows (where the blue points are agricultural fields, and the red crosses are non-Agricultural fields):

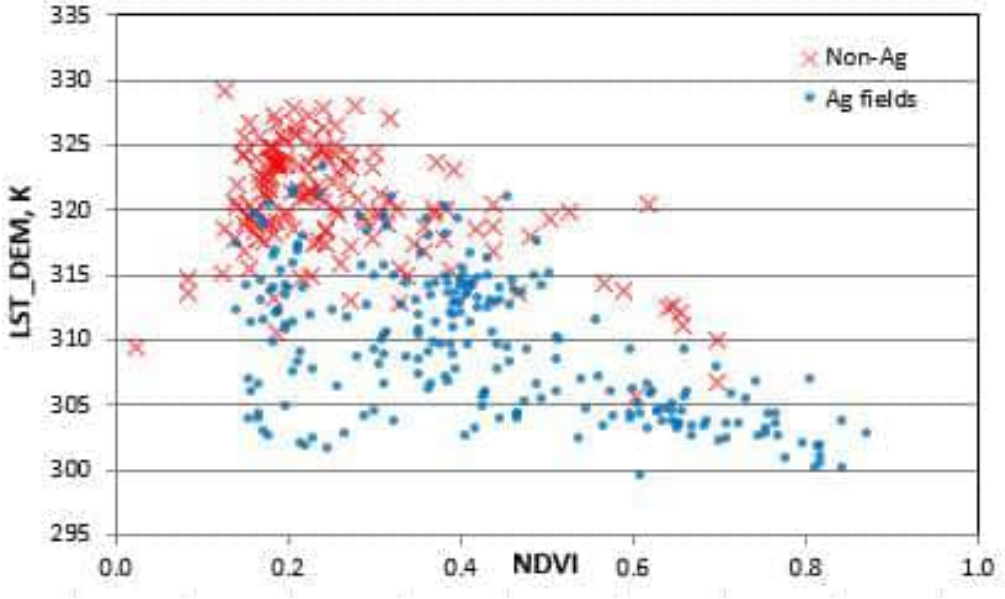

The graph for ETrF-EF vs. NDVI is as follows (where the blue points are from agricultural fields, and the red crosses are from Non-Agricultural areas):

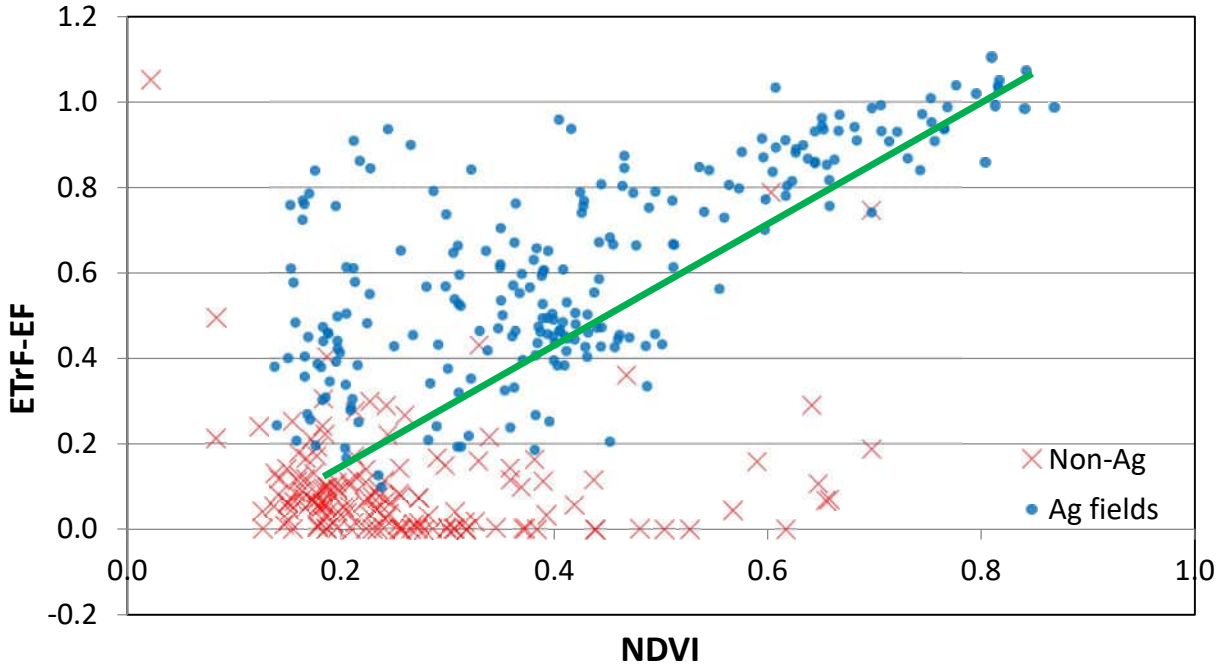

A number of the nonagricultural areas had negative ETrF, most likely due to their soils having thermal characteristics that are different from the agricultural fields. This occurred even though the excess resistance toggle in METRIC was set on (1.0) and the parameter to reduce soil heat flux, G, when organic residue is detected was set on (1.0). These two toggles increase aerodynamic resistance in rangeland areas and reduce G if organic matter is detected on the surface. Both of these toggles work to keep ETrF in rangeland from being calculated as negative. The negative ETrF values are set to 0.0 during the time-integration step.

For the final calibration (not shown), the high end of ETrF was reduced by 0.10 and the low end was reduced by 0.15.

June 28, 2020

This image has a lot of clouds almost all over the image. In the Ag areas that we are most interested in, about 1/3 of fields are covered by clouds (according to the Fmask plus the buffer). We will process this image any way. Later we will decide if we want to use this image for the final spline. There is very strong wind speed at 12 m/s and relatively high ETr at 1.29 mm/h. There was no rain since April 29. The soil should be quite dry without irrigation.
Estimated Ke is 0.00 for the satellite overpass date and for the previous day. ETrF at the cold pixel is set to 1.05 and at the hot pixel is set to 0.10. H at the hot pixel is 260 W/m^2 and H at the cold pixel is -344 W/m^2. The -344 W/m^2 indicates very strong advection. The net radiation amounts at the hot and cold pixels are often 150 to 200 W/m^2 different from one another for many of the image dates (cold Rn is higher) due to the larger outgoing long wave radiation at the hot pixel that is often 100 W/m^2 greater than for the cold pixel due to the higher surface temperature. In addition, the albedo for the bare agricultural soils is typically 0.35, which is higher than for many soils in other areas that often range from 0.20 to 0.28. The higher albedo also reduces the Rn for the bare soil condition.

The graph for de-lapsed surface temperature vs. NDVI is as follows (where the blue points are from agricultural fields, and the red crosses are from Non-Agricultural areas):

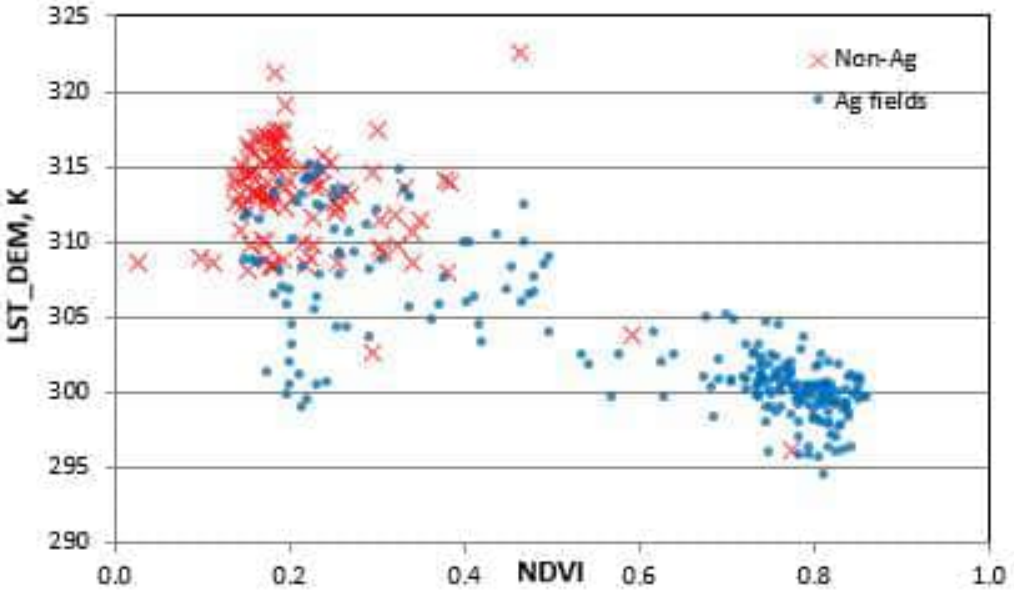

The graph for ETrF-EF vs. NDVI is as follows (where the blue points are from agricultural fields, and the red crosses are from Non-Agricultural areas):

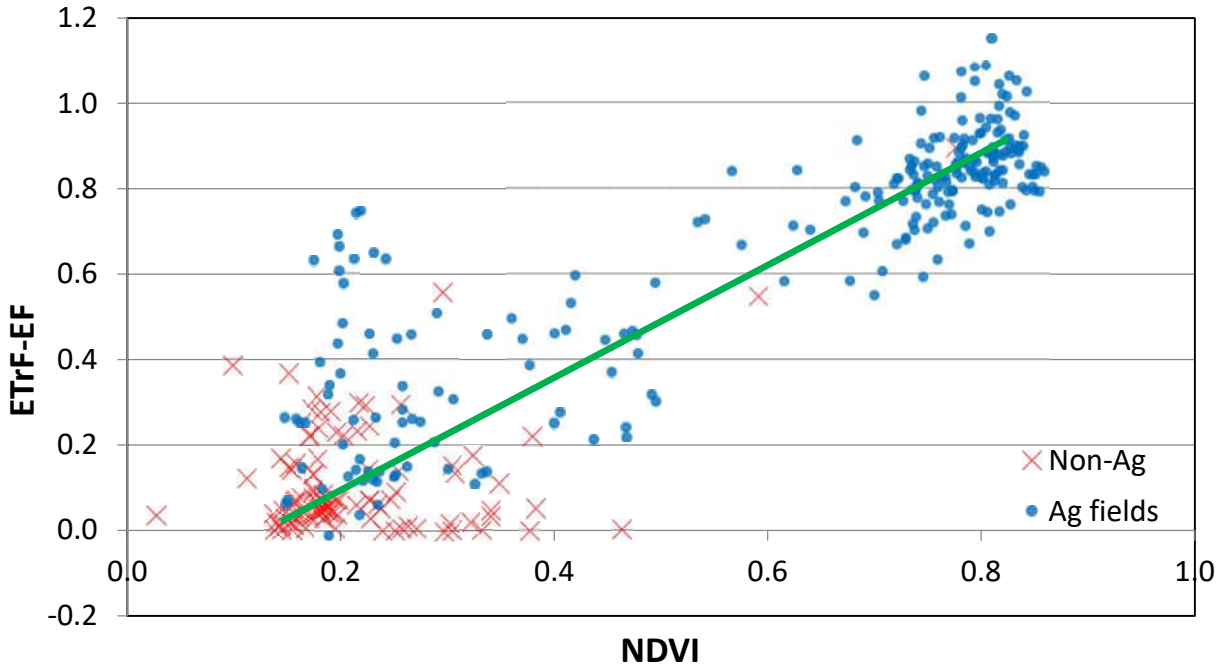

The H at the cold pixel is -344 W/m^2, and means a downward sensible heat flux of greater than 300 W/m^2 is absorbed by the vegetation at the cold pixel and used for evapotranspiration. If we decide to use this image in the final spline, we will refine this image, for example, decrease the ETr to lower the negative H, and/or decrease the lower end by 0.05 . We will increase the ETrF at the upper end by 0.10.

July 14, 2020

This is a good image that has only a few small clouds located at the northeast quarter of the image. The ag areas that we interested in are clear. There was a range burning near the Red Cliffs National Conservation Area north of St. George/ Washington. It seems that Fmask was only able to mask a small portion of the smoke (the smoke tails) and left a large portion of the uncooled smoke not masked.

Relatively strong wind speed at 4.7 m/s and higher ETr at 1.06 mm/h. There was no rain since April 29. The soil should be quite dry without irrigation. Estimated Ke is 0.00 for the satellite overpass date and for the previous day. ETrF at the cold pixel is set to 1.05 and at the hot pixel is set to 0.10. Hhot is 209 W/m^2 and Hcold is -225 W/m^2.

The graph for de-lapsed surface temperature vs. NDVI is as follows (where the blue points are from agricultural fields, and the red crosses are from Non-Agricultural areas):

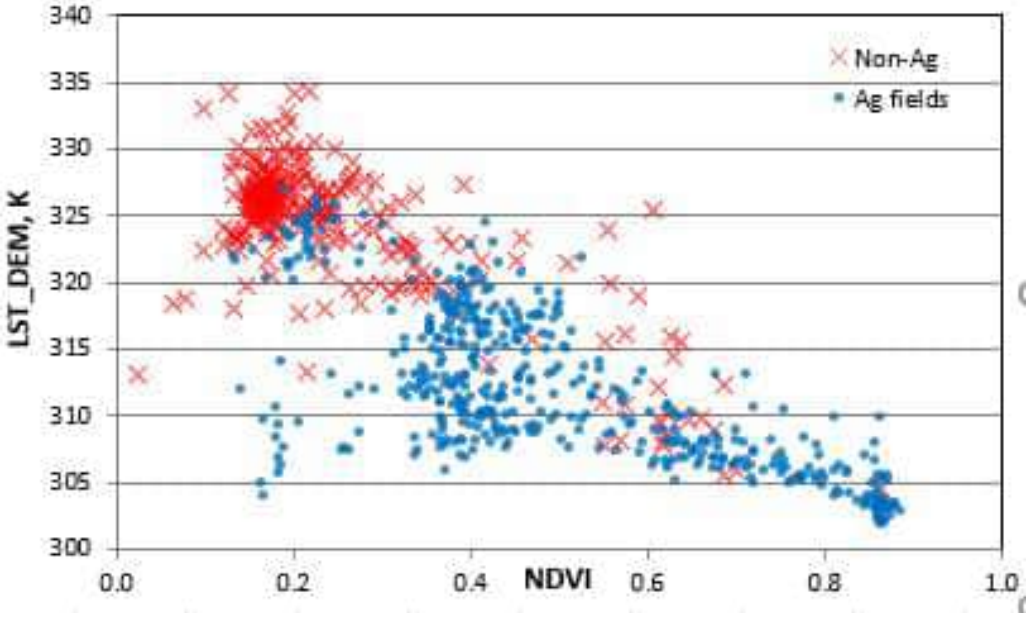

The graph for ETrF-EF vs. NDVI is as follows (where the blue points are from agricultural fields, and the red crosses are from Non-Agricultural areas):

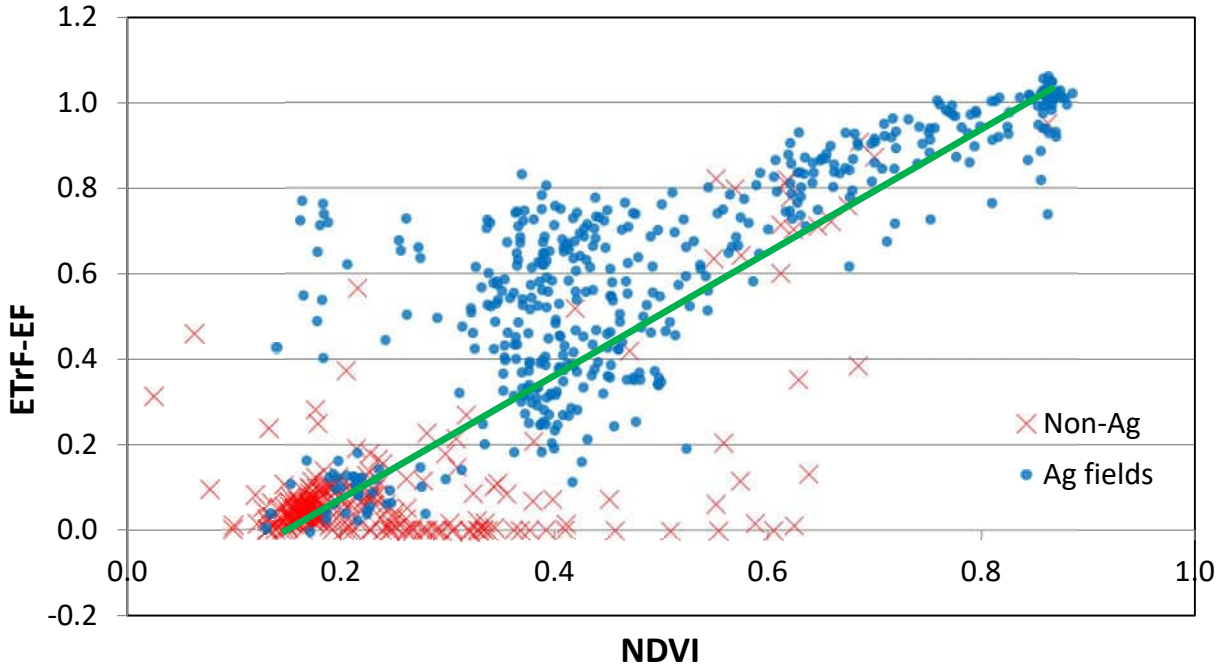

The H at the cold pixel, -225 W/m^2, means a downward sensible heat flux that is absorbed by the vegetation at the cold pixel and used for evapotranspiration. We decreased the ETr from 1.16 mm/h to 1.0 mm/h and get an H at cold pixel at -182 W/m^2. So that the equilibrium boundary layer did not have so much stability in the boundary layer correction functions. We adjusted calibration pixel selection so that the ETrF at the upper end reduced by 0.05.

July 30, 2020

This is a good image that has only a few clouds located at the east side of the image. The ag areas that we are interested in are clear. By comparing the Landsat images between July 14 and July 30, it seems that there was a fire near the north side of the Kaibab National Forest, east of the Le Fevre Overlook and Rest Area in Arizona. This smoke was not masked by the Fmask software (It was only able to mask a small portion of the smoke).

Wind speed is 2.2 m/s and ETr is 0.85 mm/h. There was 0.25 mm of rain (probably just one tip by the tipping bucket rain gauge) on July 27. This amount of rain would evaporate quickly under the late July hot weather. Soil still should be dry without irrigation. Estimated Ke is 0.00 for the satellite overpass date and for the previous day. ETrF at the cold pixel is set to 1.05 and at the hot pixel is set to 0.10. H at the hot pixel is 217 W/m^2 and at the cold pixel is -31 W/m^2. Therefore, advection is lower for this image than for previous image dates.

The graph for de-lapsed surface temperature vs. NDVI is as follows (where the blue points are from agricultural fields, and the red crosses are from Non-Agricultural areas):

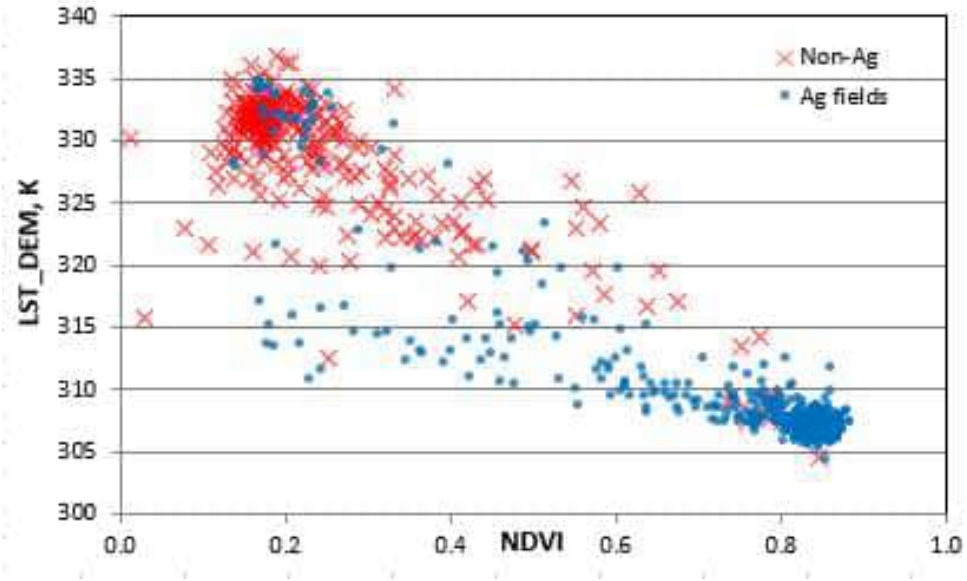

The graph for ETrF-EF vs. NDVI is as follows (where the blue points are from agricultural fields, and the red crosses are from Non-Agricultural areas):

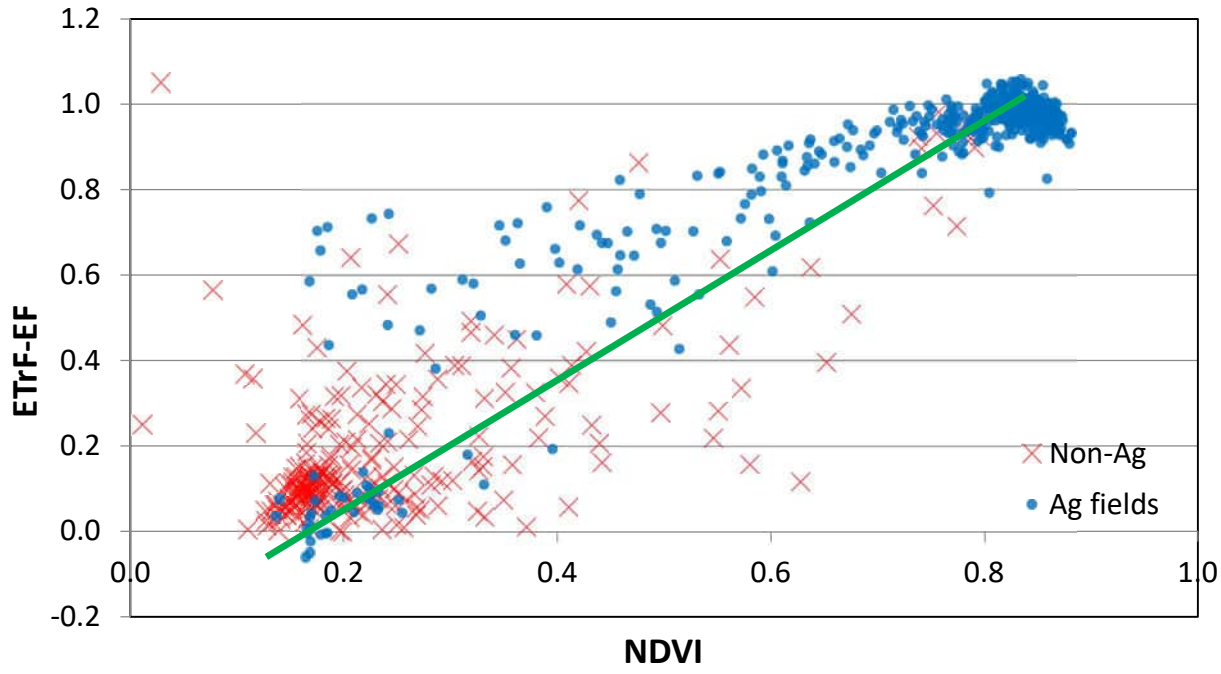

We reduced the ETrF at the upper end by 0.05 for the final calibration (not shown). The lower end was OK.

August 15, 2020

This is a relatively good image that has clouds in the Northeast quarter of the image. The ag areas that we are interested in are clear. Wind speed is is very low at **0.8 m/s** and ETr is 0.73 mm/h. There was no rain since the 0.25 mm on July 27 and 20.3 mm on April 29. The soil should be very dry without irrigation. Estimated Ke is 0.00 for the satellite overpass date and for the previous day. ETrF at the cold pixel is set to 1.05 and at the hot pixel is set to 0.10. H at the hot pixel is 178 W/m^2 and at the cold pixel is +39 W/m^2. The positive H at the cold pixel is due to the very low wind speed that reduces advection, along with the relatively low ETr.

The graph for de-lapsed surface temperature vs. NDVI is as follows (where the blue points are from agricultural fields, and the red crosses are from Non-Agricultural areas):

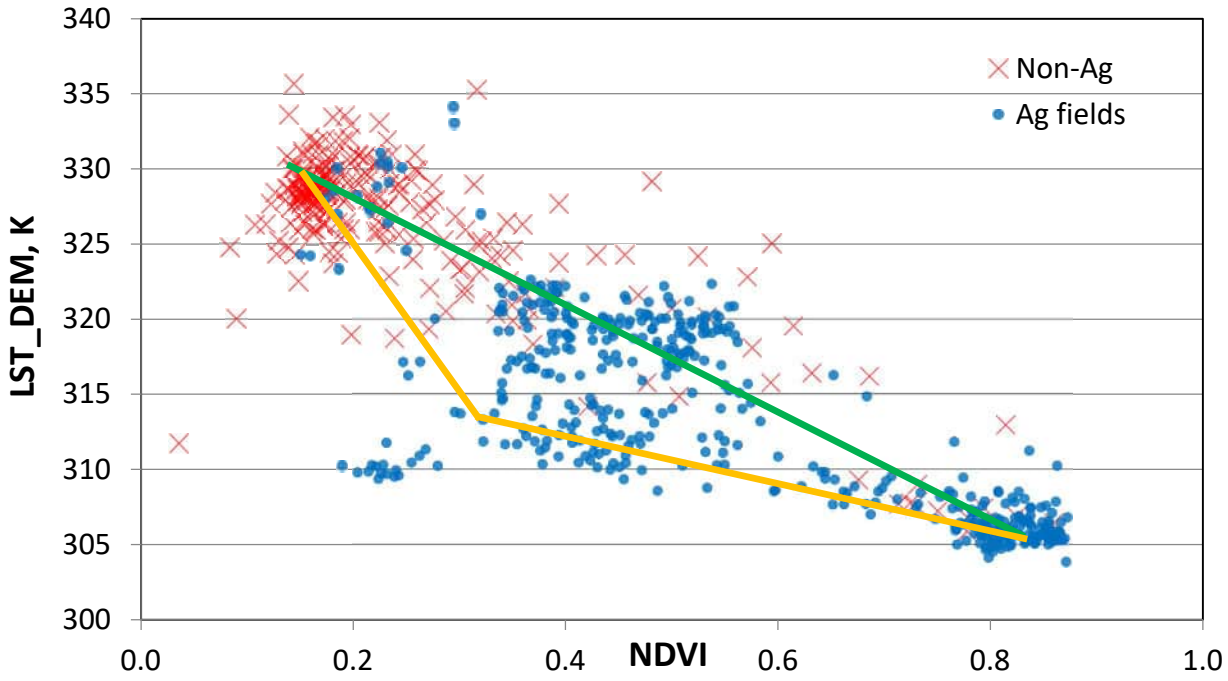

The graph for ETrF-EF vs. NDVI is as follows (where the blue points are from agricultural fields, and the red crosses are from Non-Agricultural areas):

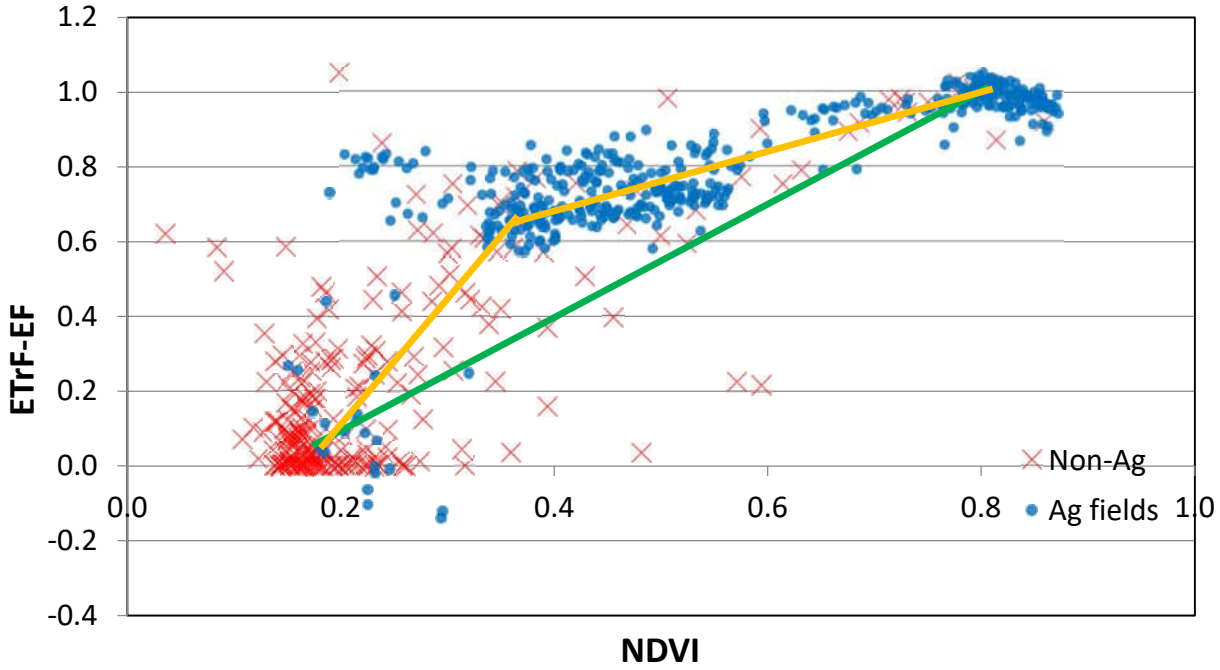

The ETrF vs. NDVI image for this date has a relatively uncharacteristic upward trend in ETrF for midrange NDVI values. This is attributed to irrigation of essentially all sampled pixels (fields) in the sampled area. The plot of land surface temperature (LST) vs. NDVI shows two groups of mid-NDVI temperatures, with one group cooler than the linear line between coldest LST and hottest LST. This group is expected to plot ETrF above a linear trend in ETrF vs. NDVI due to the evaporative cooling. The other group, however, tends to lie along a linear line between hottest and coolest LST, and would be expected to produce ETrF that is also along a linear line between lowest ETrF and highest ETrF (highest NDVI). That group, however, also produced ETrF that lays above the linear relationship. This is apparently due to the low wind speed that reduced convective transfer of H to the boundary layer and therefore retained more energy for ET. We will explore this phenomenon and outcome in more detail.

The following slides show distributions of albedo, estimated leaf area (LAI) and a soil heat flux adjustment multiplier that are produced by METRIC. These are shown for the same sample points used for LST and ETrF. The plots were separated, symbol-wise, into groups where LST (land surface temperature), adjusted for elevation and termed Ts_DEM, was greater than or less than 315 Kelvin temperature (equivalent to 45 Celsius or 113 F). The 315 K value was selected from the plot of LST_DEM vs. NDVI above to represent a general cutoff of those fields (sampled pixels) displaying LST more in line with a dry surface condition (> 315) and those displaying additional evaporative cooling from wetting of soil (< 315). This separation is arbitrary and is used only for analysis. The LST values are high since this is the surface temperature and not the air temperature that tends to run cooler.

We find that the albedo is lowest at highest NDVI, and with very little differences between the two LST groups in the midrange NDVI.

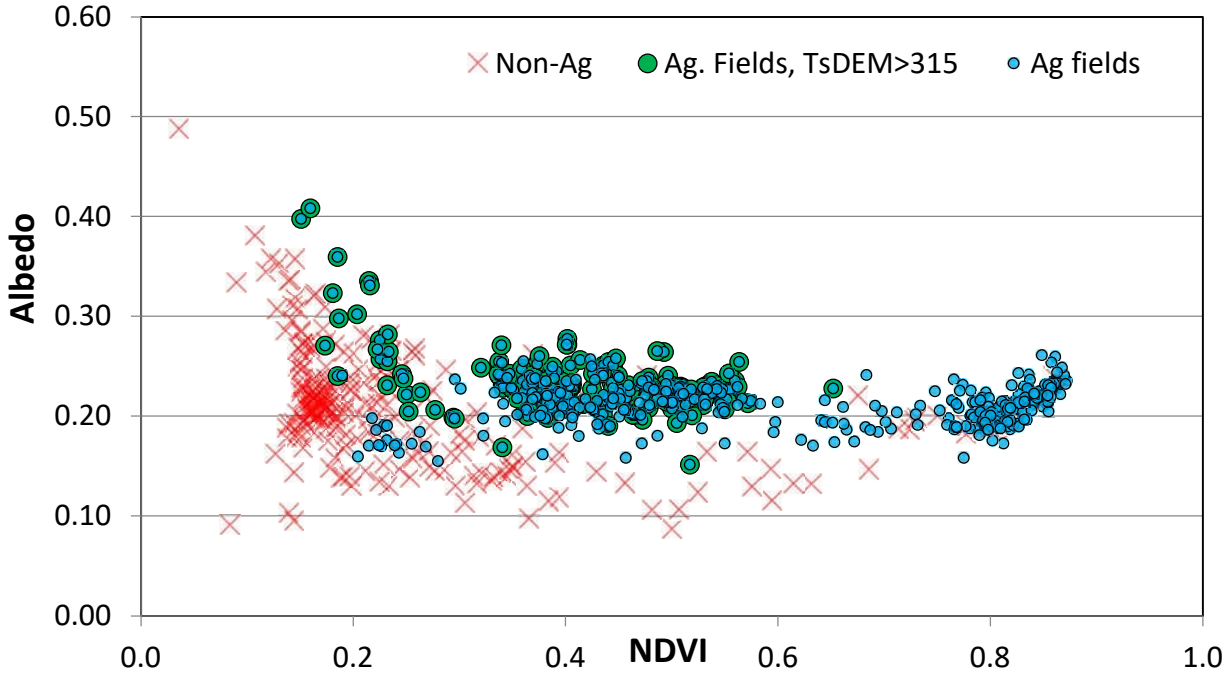

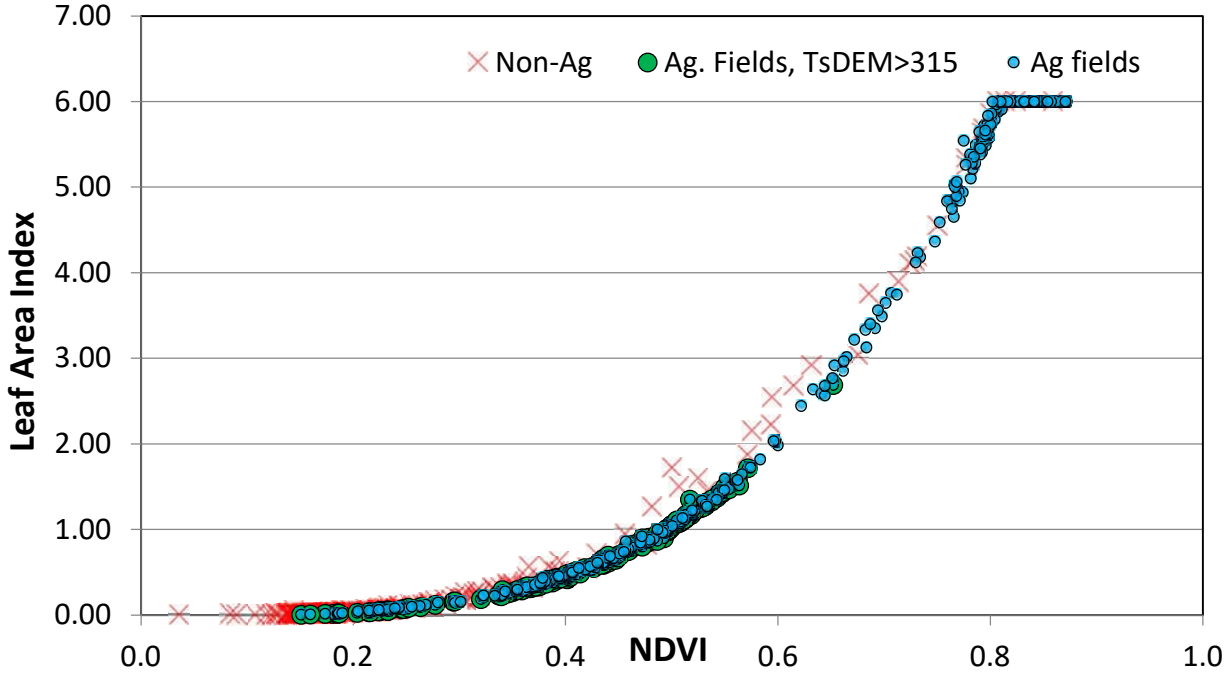

The LAI vs. NDVI confirms consistent estimation of LAI from a singular function of NDVI.

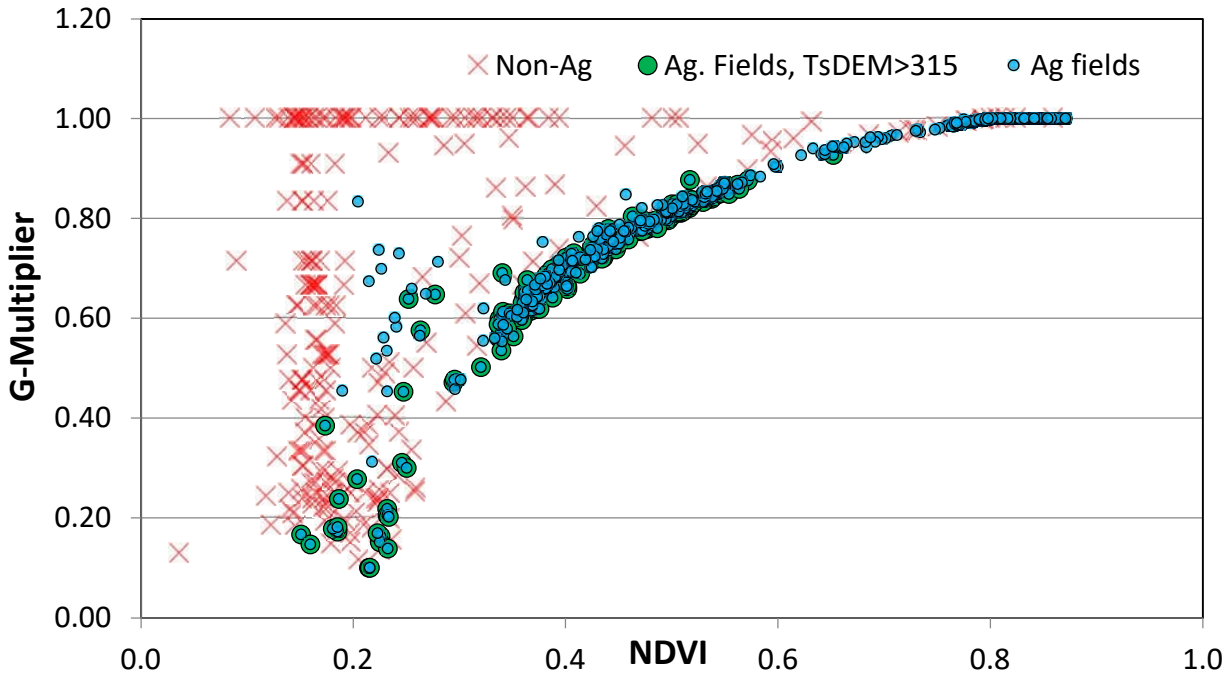

The G-Multiplier is a reducer on the initial estimate for soil heat flux. It is invoked as a function of estimated (dead) organic mulch present on the surface that functions as an insulator. The multiplier approaches 1.0 (meaning no adjustment) as NDVI increases, representing more ground surface shaded by green vegetation and less exposure of any surface covered by an organic mulch. There were no differences detected between the > 315 K and < 315 K LST groups.

As a check on the influence of weather, we downloaded the weather data from weather stations close to the Beryl Junction weather station. These weather stations include: Enterprise (USCAN), Cedar City (USRN), Cedar City (AGWX) and Parowan (AGWX). We were not able to download precipitition data from the weather stations Modena (AGWX) and Leeds (FGNET). The results did not show any rain events large enough to affect the ETrF on the August 15 image date:

A	B	C	D	E	F
	Beryl Junction	Enterprise (USCAN)	Cedar City (USRN)	Cedar City (AGWX)	Parowan (AGWX)
date_time	precip (mm)	precip (mm)	precip (mm)	precip (mm)	precip (mm)
01/01/2020	1.02	0.25	1.32	0.76	0.00
07/14/2020	0.00	0.00	0.00	0.00	0.00
07/15/2020	0.00	0.00	0.00	0.00	0.00
07/16/2020	0.00	0.00	0.00	0.00	0.00
07/17/2020	0.00	0.00	0.00	0.00	0.00
07/18/2020	0.00	0.00	0.00	0.00	0.00
07/19/2020	0.00	0.00	0.00	0.00	0.00
07/20/2020	0.00	0.00	0.00	0.00	0.51
07/21/2020	0.00	0.00	0.05	0.00	0.00
07/22/2020	0.00	0.00	0.00	0.00	14.48
07/23/2020	0.00	0.00	0.00	0.00	0.51
07/24/2020	0.00	0.00	0.00	0.00	0.00
07/25/2020	0.00	0.00	0.00	0.00	0.00
07/26/2020	0.00	0.00	0.00	0.00	0.00
07/27/2020	0.25	0.00	0.41	0.00	0.00
07/28/2020	0.00	0.00	0.00	0.00	0.00
07/29/2020	0.00	0.00	0.00	0.00	0.00
07/30/2020	0.00	0.00	0.00	0.00	0.00
07/31/2020	0.00	0.00	0.00	0.00	0.00
08/01/2020	0.00	0.00	0.00	0.00	0.00
08/02/2020	0.00	0.00	0.00	0.00	0.00
08/03/2020	0.00	0.00	0.00	0.00	0.00
08/04/2020	0.00	0.00	0.00	0.00	0.00
08/05/2020	0.00	0.00	0.00	0.00	0.00
08/06/2020	0.00	0.00	0.00	0.00	0.00
08/07/2020	0.00	0.00	0.00	0.00	0.00
08/08/2020	0.00	0.00	0.00	0.00	0.00
08/09/2020	0.00	0.00	0.00	0.00	0.00
08/10/2020	0.00	0.00	0.00	0.00	0.00
08/11/2020	0.00	0.00	0.00	0.00	0.00
08/12/2020	0.00	0.00	0.00	0.00	0.00
08/13/2020	0.00	0.00	0.00	0.00	0.00
08/14/2020	0.00	0.00	0.00	0.00	0.00
08/15/2020	0.00	0.00	0.00	0.00	0.00
08/16/2020	0.00	0.00	0.00	0.00	0.00

We decided to use the following result as final. We will explore causes of the increase in ETrF for mid-range NDVI in more depth over the next month.

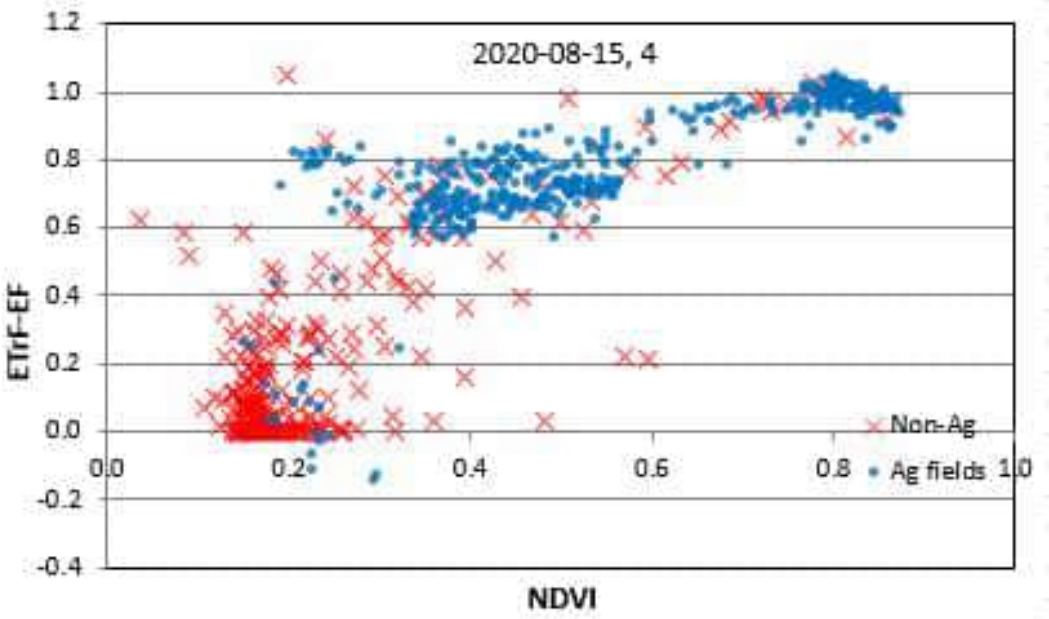

August 31, 2020

This image has only a few clouds at the northern portion of the image and occasionally a few small clouds distributed here and there. However, the ag areas that we interested in are clear. Wind speed is 3.8 m/s and ETr is 0.835 mm/h. There was no rain since July 27 according to the Beryl Junction weather station. However, there was 4.83 mm rain recorded by the Enterprise Weather station and 25 mm rain recorded by Cedar City USRN weather station on August 23, and 2.0 mm rain recorded by the Cedar City AGWX weather station. Estimated Ke is 0.00 for the satellite overpass date and for the previous day for the Beryl Junction station. ETrF at the cold pixel is set to 1.05 and at the hot pixel is set to 0.03. H at the hot pixel is 220 W/m^2 and at the cold pixel is **-94** W/m^2.

The graph for de-lapsed surface temperature vs. NDVI is as follows (where the blue points are from agricultural fields, and the red crosses are from Non-Agricultural areas):

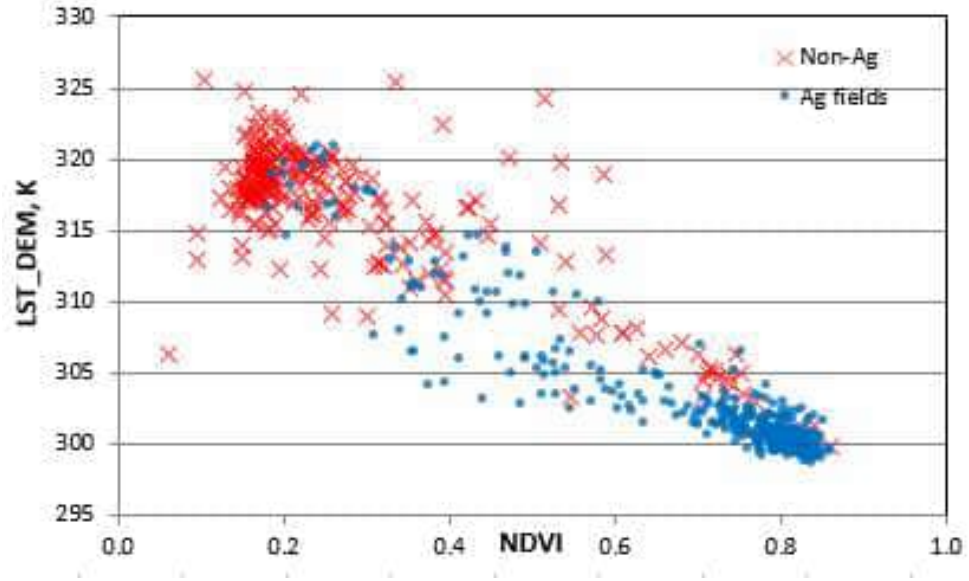

The graph for ETrF-EF vs. NDVI is as follows (where the blue points are from agricultural fields, and the red crosses are from Non-Agricultural areas):

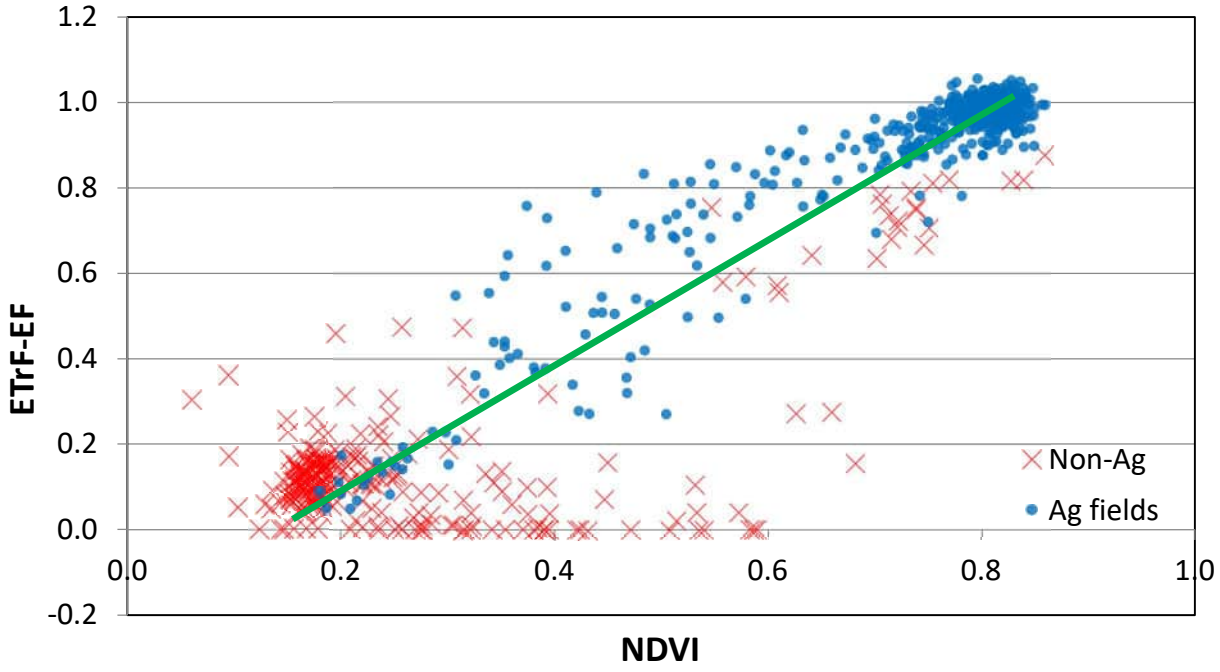

September 16, 2020

This is a good image that has only a few clouds located mainly at the northeast part of the image. The ag areas that we interested in are clear. Wind speed is only 1.0 m/s and ETr is 0.61 mm/h. There was no rain since July 27 according to the Beryl Junction weather station. However, there was 4.83 mm rain recorded by the Enterprise Weather station and 25 mm rain recorded by the Cedar City USRN weather station on August 23, and 2 mm recorded by the Cedar City AGWX weather station. Estimated Ke is 0.00 for the satellite overpass date and for the previous day. ETrF at the cold pixel is set to 1.05 and at the hot pixel is set to 0.10. H at the hot pixel is 239 W/m^2 and at the cold pixel is 25.1 W/m^2 Indicating no advection due to the low wind speed. The graph for de-lapsed surface temperature vs. NDVI is as follows (where the blue points are from agricultural fields, and the red crosses are from Non-Agricultural areas):

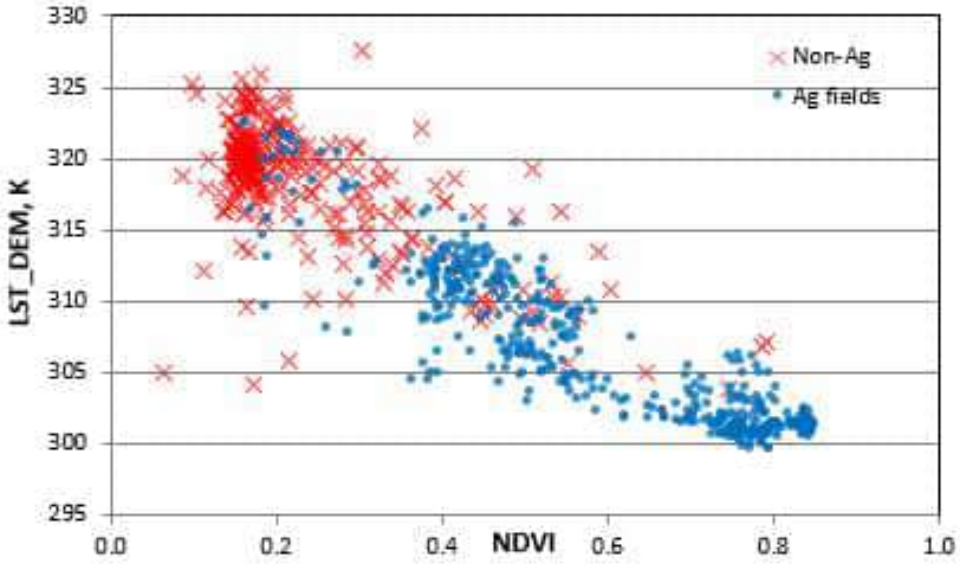

The graph for ETrF-EF vs. NDVI is as follows (where the blue points are from agricultural fields, and the red crosses are from Non-Agricultural areas):

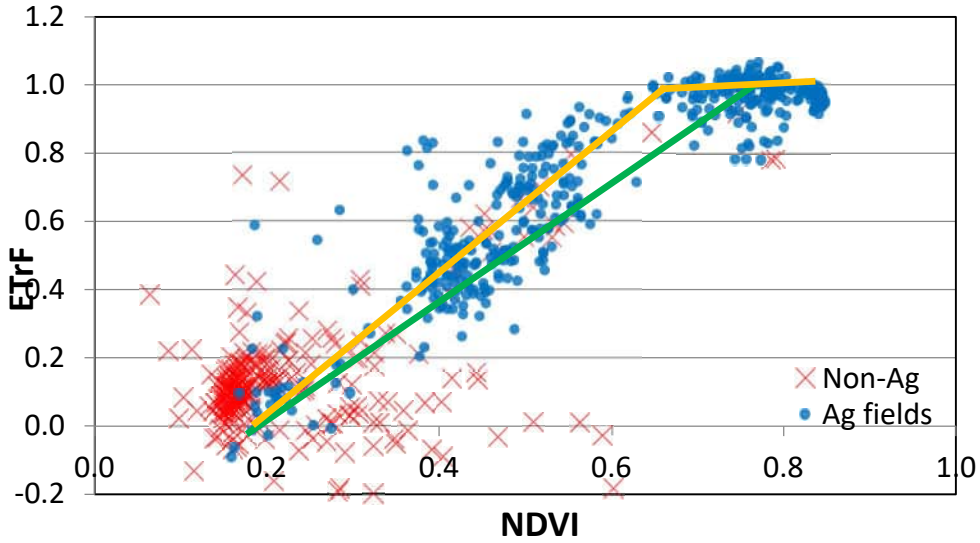

The ETrF at the upper end has a long 'plateau' of values near 1.0 over a range of NDVI from about 0.65 to 0.85. This occurrence is relatively common where NDVI > 0.65 can represent crops with full ground cover and therefore having similar ETrF representing an upper limit on conversion of available energy into evapotranspiration.

October 2, 2020

This is a nice, clear image. Although the Fmask indicated some clouds in the northeast quarter of the image, however, we do not visually detect any clouds. There may be a little snow in the mountains. The ag areas that we are interested in are clear. Wind speed is, again, very low at 0.78 m/s and ETr is 0.53 mm/h. There was no rain since July 27 according to the Beryl Junction weather station. However, there was 4.83 mm rain recorded by the Enterprise Weather station and 25 mm rain recorded by the Cedar City USRN weather station on August 23, and 2 mm recorded by Cedar City AGWX weather station on August 24 and 25. The soils near Beryl

Junction should be very dry if without irrigation. Estimated Ke is 0.00 for the satellite overpass date and for the previous day. ETrF at the cold pixel is set to 1.03 and at the hot pixel is set to 0.10. H at the hot pixel is 243 W/m^2 and at the cold pixel is 67 W/m^2 indicating a positive convection of heat from full-cover fields.
The graph for de-lapsed surface temperature vs. NDVI is as follows (where the blue points are from agricultural fields, and the red crosses are from Non-Agricultural areas):

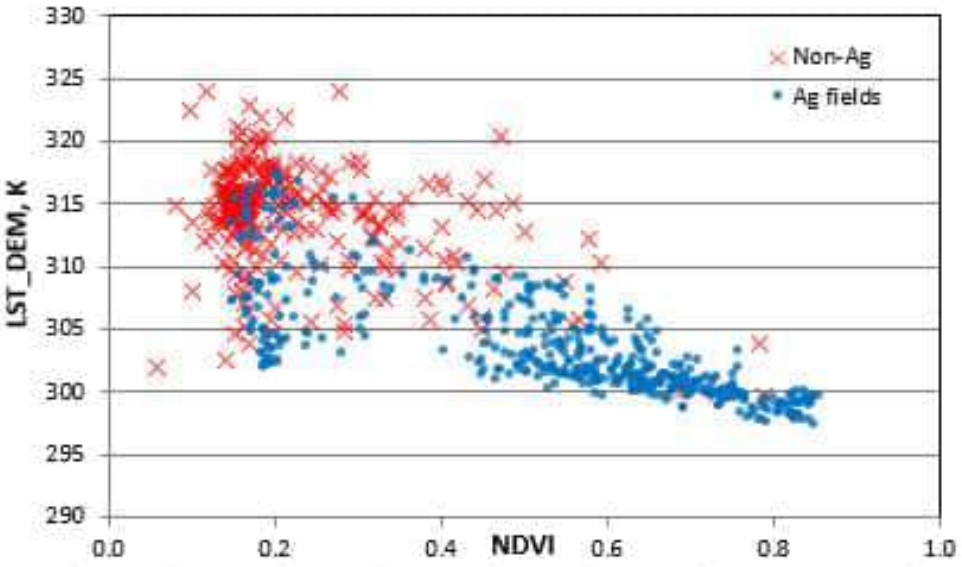

The graph for ETrF-EF vs. NDVI is as follows (where the blue points are from agricultural fields, and the red crosses are from Non-Agricultural areas):

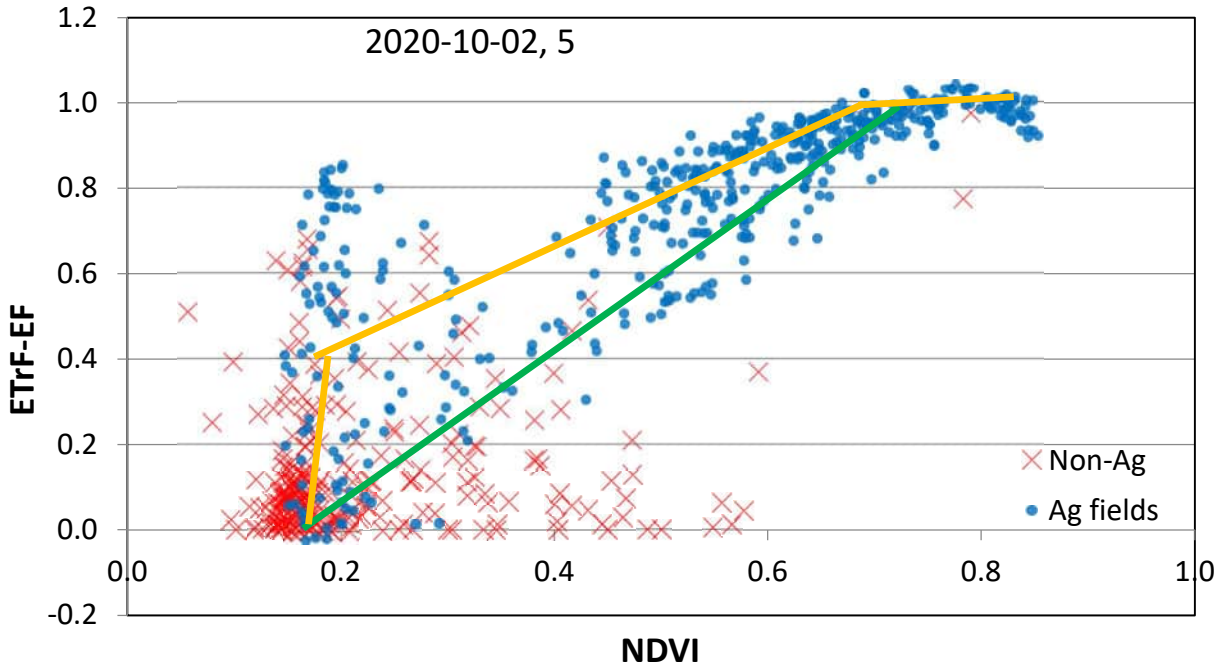

Similar to 9/16/2020, the ETrF at the upper end has a long 'plateau' of values near 1.0 over a range of NDVI from about 0.65 to 0.85. This occurrence is relatively common where NDVI >

0.65 can represent crops having full ground cover and therefore having similar ETrF representing an upper limit on conversion of available energy into evapotranspiration. There is a characteristic decrease in ETrF for the very highest NDVI. This is caused by crops at the highest NDVI having complete full cover and that have a more horizontal leaf orientation in the upper canopy. The horizontal orientation causes the NDVI signal to increase above 0.8 and causes the albedo to increase slightly due to more effective reflectance by the horiziontal leaves and fewer shadows within the canopy as viewed by the nadir-looking Landsat. This slight reduction in ETrF for very high NDVI is probably real. Crops in the mix that have slightly lower NDVI of about 0.7 still have sufficient ground cover and leaf area to produce ET near the maximum. Those crops, for example corn, tend to show more shadowing to the nadir-looking Landsat (i.e., Landsat views the surface from directly overhead). The shadowing indicates more absorption of photons from the sun and effective conversion of those photons into ET. The shadowing also tends to reduce the NDVI signal.

The upper yellow line on the plot above shows a trend for many fields (i.e., sampled pixels) where ETrF for mid-range NDVI was elevated over the green 'basal' line that represents ET from fields having a relatively dry soil surface. In other words, the green line represents largely the transpiration components. The yellow line indicates additional evaporation occurring from some fields due to recent wetting by irrigation. Similarly, high values for ETrF when NDVI is low (< 0.25) indicate fields (i.e., sampled pixels) that are mostly bare of green vegetation, but that are wet from irrigation.

October 18, 2020

This is a nice, clear image. Although the Fmask indicated that there were small, isolated clouds in the northeast quarter of the image, we do not visually detect any clouds within the whole image. Wind speed is very mild at 0.9 m/s for the satellite pass time and 1.1 m/s for the 3-hour average. ETr is 0.46 mm/h. There has been no rain since July 27 according to the Beryl Junction weather station. There were about 0.5 mm at Cedar City weather stations and Parowan weather station on September 21 to 23, which is trivial. The soils should be very dry without irrigation. Estimated Ke is 0.00 for the satellite overpass date and for the previous day. ETrF at the cold pixel is set to 1.05 and at the hot pixel is set to 0.10. H at the hot pixel is 219 W/m^2 and at the cold pixel is 46 W/m^2.

The graph for de-lapsed surface temperature vs. NDVI is as follows (where the blue points are from agricultural fields, and the red crosses are from Non-Agricultural areas):

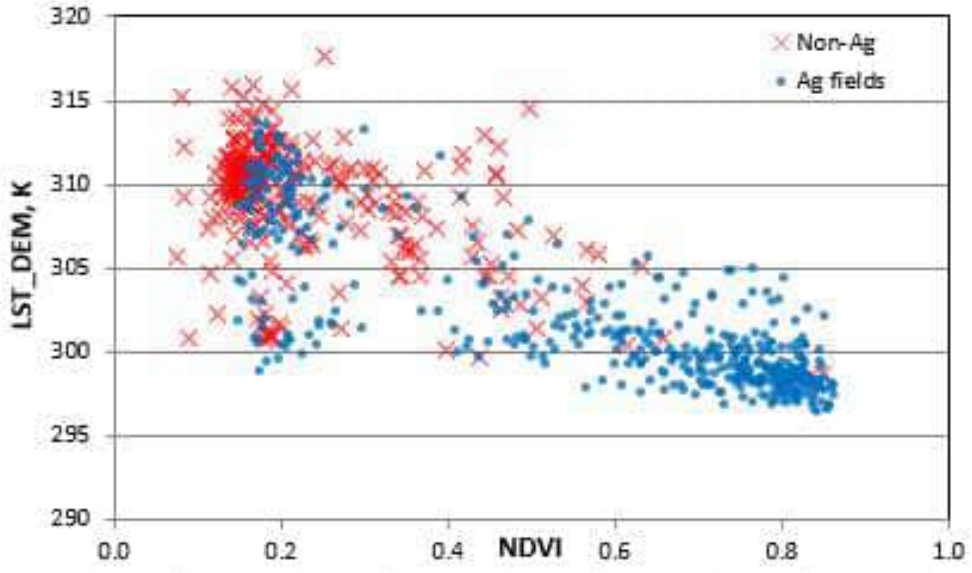

The graph for ETrF-EF vs. NDVI is as follows (where the blue points are from agricultural fields, and the red crosses are from Non-Agricultural areas):

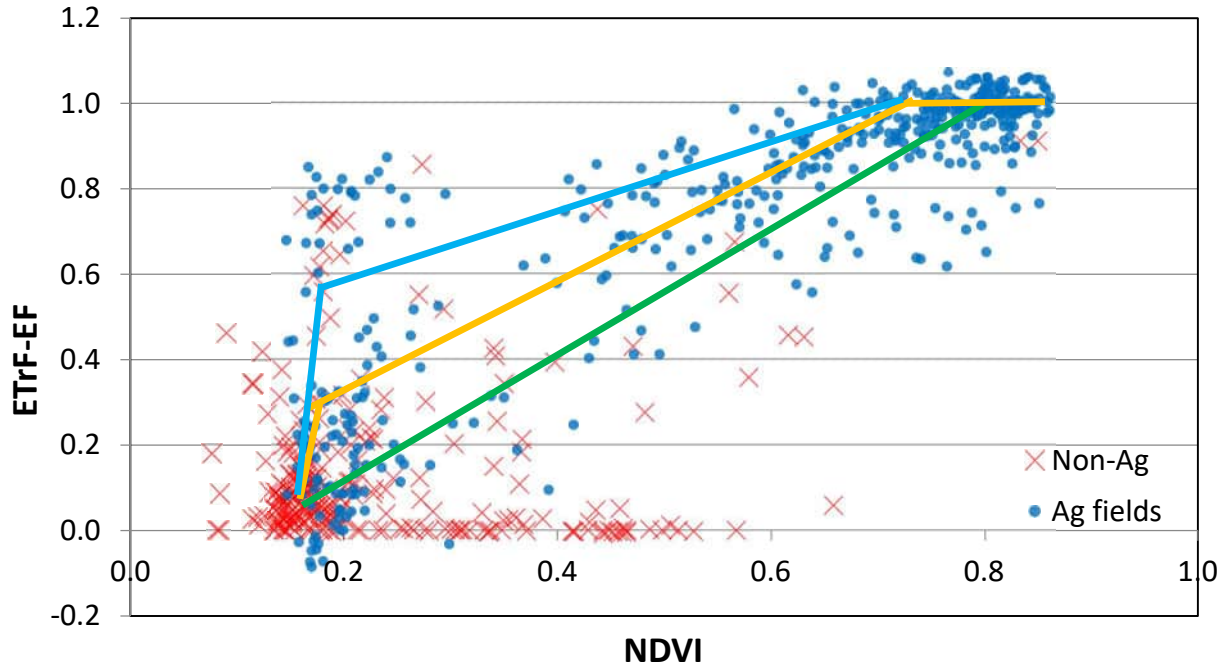

Similar to 9/16/2020 and 10/2/2020 dates, the ETrF at the upper end of NDVI has a long 'plateau' of values near 1.0 over a range of NDVI from about 0.65 to 0.85. Reasons for this are explained under the 9/16 and 10/2 sections.

The upper yellow line on the plot above shows a trend for many fields (i.e., sampled pixels) where ETrF for mid-range NDVI was elevated over the green 'basal' line that represents ET from fields having a relatively dry soil surface. In other words, the green line represents largely the transpiration components. The blue line indicates additional evaporation occurring from some fields due to recent wetting by irrigation. Similarly, high values for ETrF when NDVI is

low (< 0.25) indicate fields (i.e., sampled pixels) that are mostly bare of green vegetation, but that are wet from irrigation. The yellow line is drawn to represent a central trend in ETrF vs. NDVI across all fields (represented by sampled pixels).

November 19, 2020

This is also a nice, clear image. Because of the late date, the solar elevation is low. Although the Fmask indicated that there were some isolated clouds here and there, we do not visually detect any clouds within the whole image. As with previous fall months, wind speed is low at 1.1 m/s and ETr is 0.36 mm/h. There were very low amounts of 0.25 mm and 0.51 mm of precipitation respectively on Nov. 8 and Nov 9 according to the Beryl Junction weather station. However, there was 4.6 mm precipitation recorded by the Enterprise Weather station, which is close to Beryl Junction weather station from Nov 7 to Nov 9. A relatively further weather station, the Cedar City USRN weather station, recorded 26 mm precipitation during the same time period. Estimated Ke is still 0.00 for the satellite overpass date and for the previous day for areas near Beryl Junction. ETrF at the cold pixel is set to 1.05 and at the hot pixel is set to 0.10. H at the hot pixel is 168 W/m^2 and at the cold pixel is 28 W/m^2. Ts at the hot pixel is 297.6 K and at the cold pixel is 291.0 K, indicating only 6.6 K difference. The smaller difference is due to the lower sun angle on this date and later sunrise and therefore less opportunity for surface heating. For this late November that should be normal.

The graph for de-lapsed surface temperature vs. NDVI is as follows (where the blue points are from agricultural fields, and the red crosses are from Non-Agricultural areas):

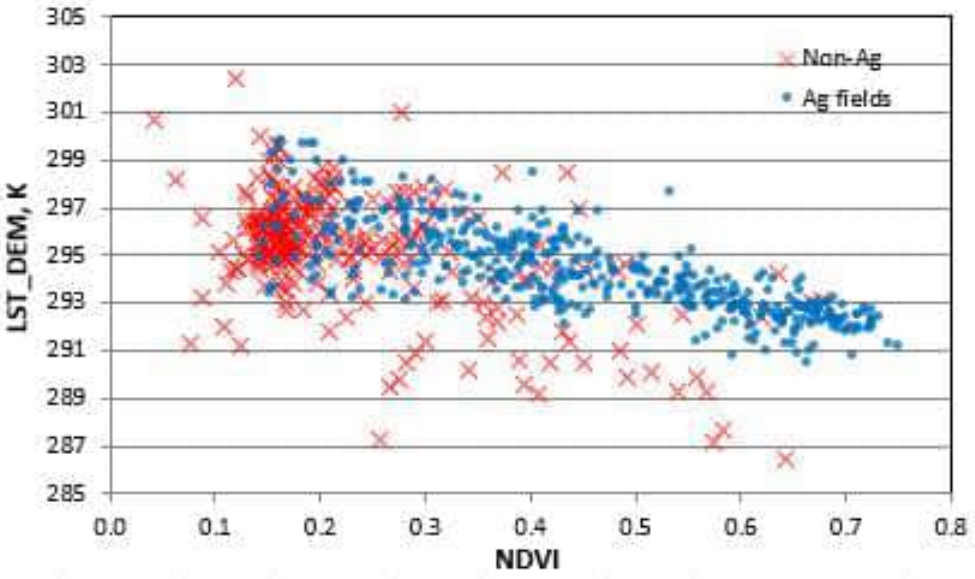

The graph for ETrF-EF vs. NDVI is as follows (where the blue points are from agricultural fields, and the red crosses are from Non-Agricultural areas):

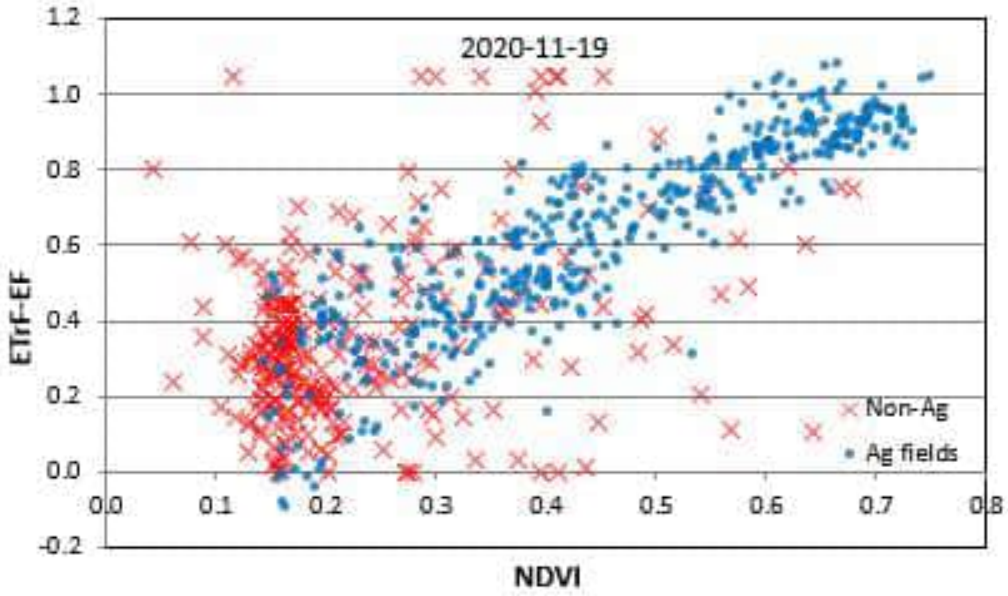

The plot of ETrF vs. NDVI follows a more characteristic linear relationship for this date. This likely indicates that irrigation had prevously ceased and therefore most soils in fields were in a relatively dry state. For the final calibration (not shown), we lowered the lower end of ETrF by 0.10.

Path 39 Images:

March 31, 2020

This was a difficult image to process because of its wetness from recent precipitation and the lower solar elevation.

It seems that there were cirrus clouds towards the south part of the image. The Fmask seems to have successfully masked them out. However, the Fmask also masked clouds in other places that we could not see visually, except areas where some snow cover was present and was inadvertently masked as clouds. The agricultural areas that we are interested in are clear. Wind speed is 2.8 m/s and ETr is 0.64 mm/h. There was 27 mm precipitation from March 11 to March 14, 14.2 mm from March 17 to March 20 and 1 mm on March 23 and 5.6 mm from March 26 to March 27, which was only four days prior to this image. Estimated Ke is 0.23 for the satellite overpass date and 0.33 for the previous day indicating drying of the soil surface, but still some residual evaporation. This is also apparent in the viewing of the ETrF for the area (see below). This area is the same area as shown in the first graphic of this document and shows large areas of evaporation from recently wetted soils. Some areas having sandy soil show more drying than other areas.

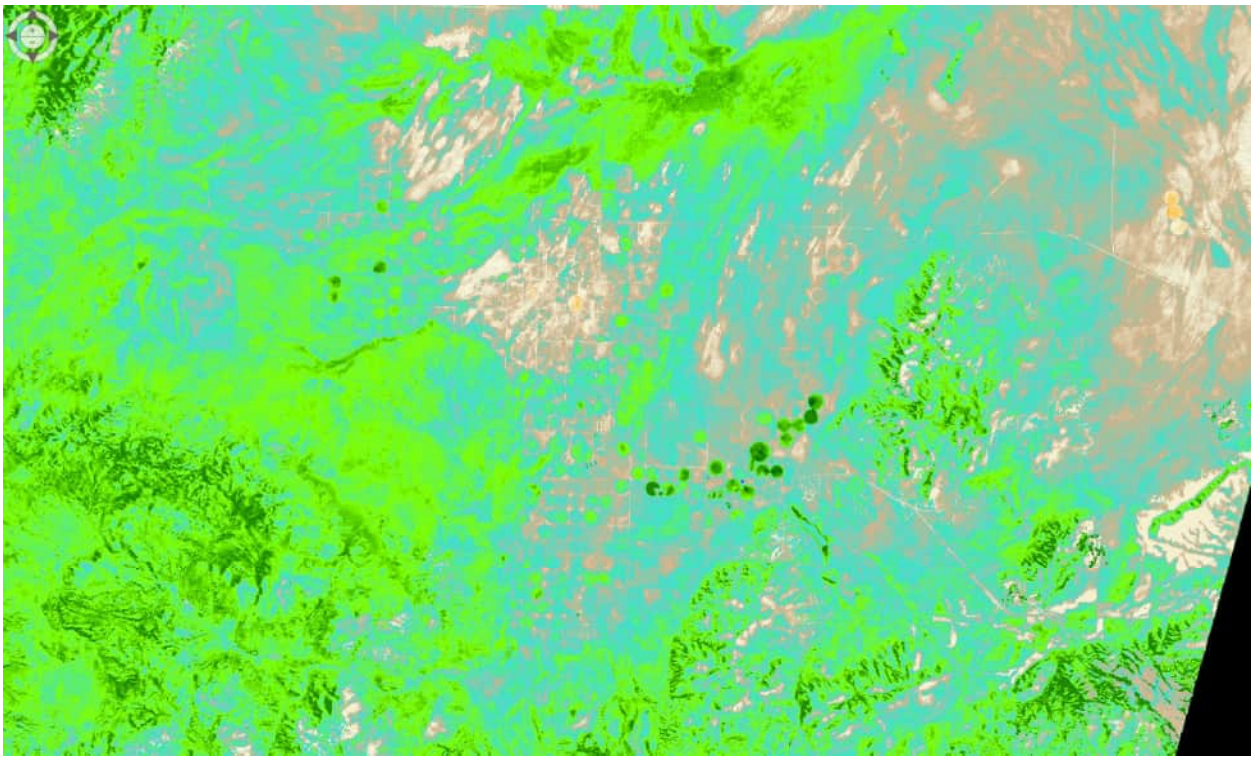

ETrF at the cold pixel is set to 0.95 (with a cold pixel NDVI value of 0.68), due to the somewhat lower NDVI found than for midsummer periods, and at the hot pixel is set to 0.23 (this is the Ke value suggested by the METIRC soil water balance). H at the hot pixel is 316 W/m^2 and at the cold pixel is 97 W/m^2.

The graph for de-lapsed surface temperature vs. NDVI is as follows (where the blue points are from agricultural fields, and the red crosses are from Non-Agricultural areas):

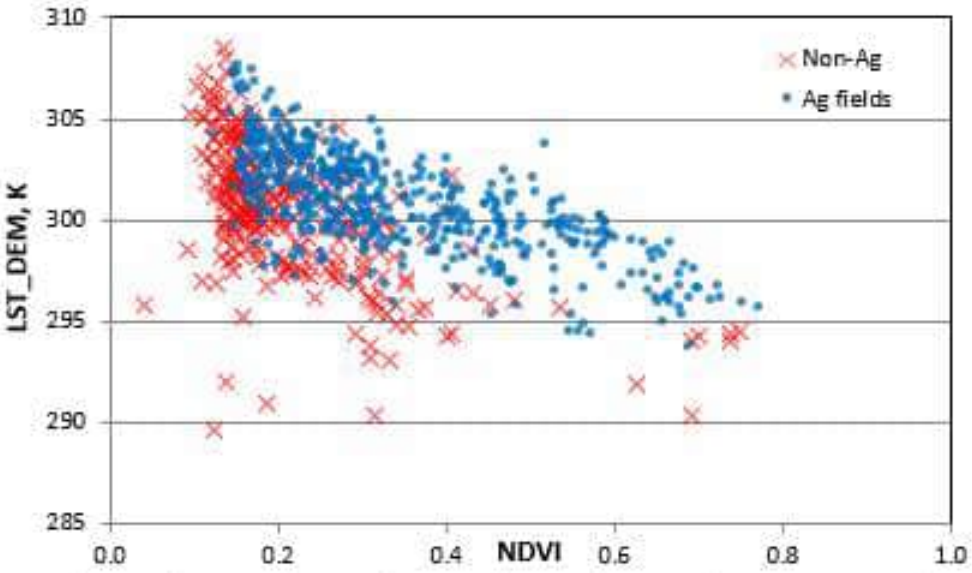

The graph for ETrF-EF vs. NDVI is as follows (where the blue points are from agricultural fields, and the red crosses are from Non-Agricultural areas):

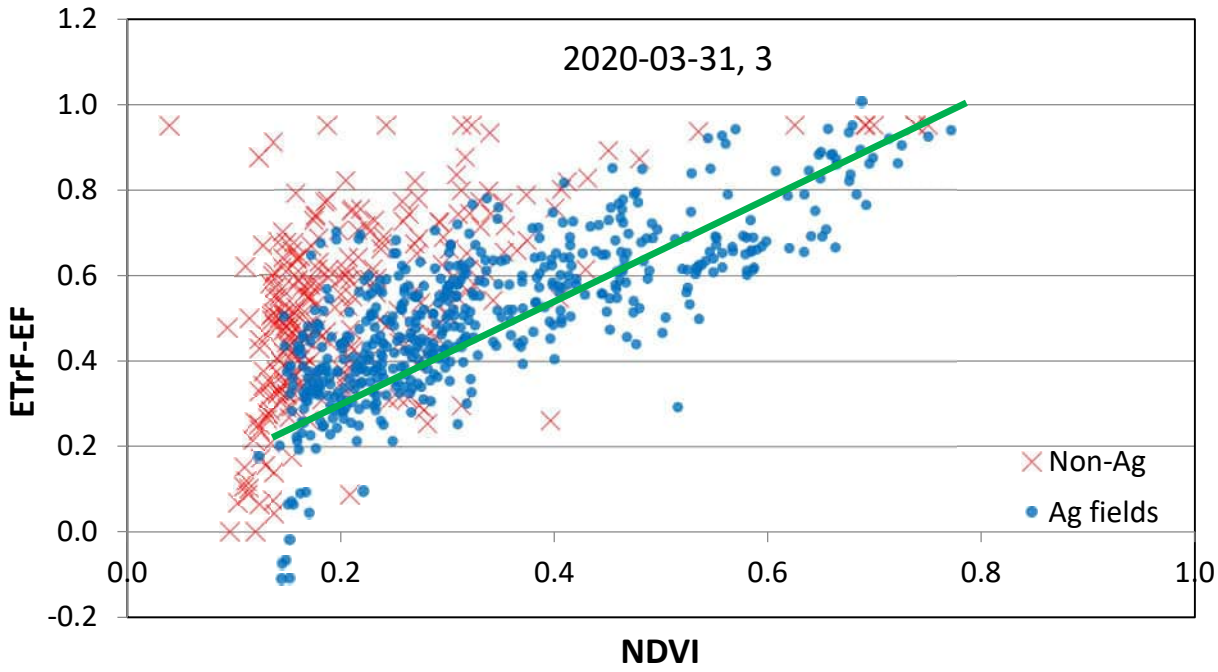

Although there were a few sample points that have lower ETrF values, even with a few negative estimated values, the majority group were located around a trend line which passes 0.23 at NDVI of about 0.15 (representing bare soil). Negative values may be due to some organic mulch on the surface that causes an elevation of LST and an overestimation of H.

May 02, 2020

There were altocumulus and altostratus clouds distributed toward the north part of the image. The Fmask cloud detection successfully masked the clouds out. Fortunately, the agricultural areas that we are interested in are clear. Wind speed is 2.8 m/s and ETr is 0.64 mm/h.
There was 13 mm rain from April 8 to April 9, 25.7 mm from April 17 to April 20 and 20.32 mm on April 29, just three days prior to the overpass. Year 2020 is noted to have been a wet spring. Estimated Ke is 0.14 for the satellite overpass date and 0.30 for the previous day, indicating relatively rapid drying for the most common soil of the local area. The following snapshot of ETrF for the local area shows substantial evaporation from rangeland areas.

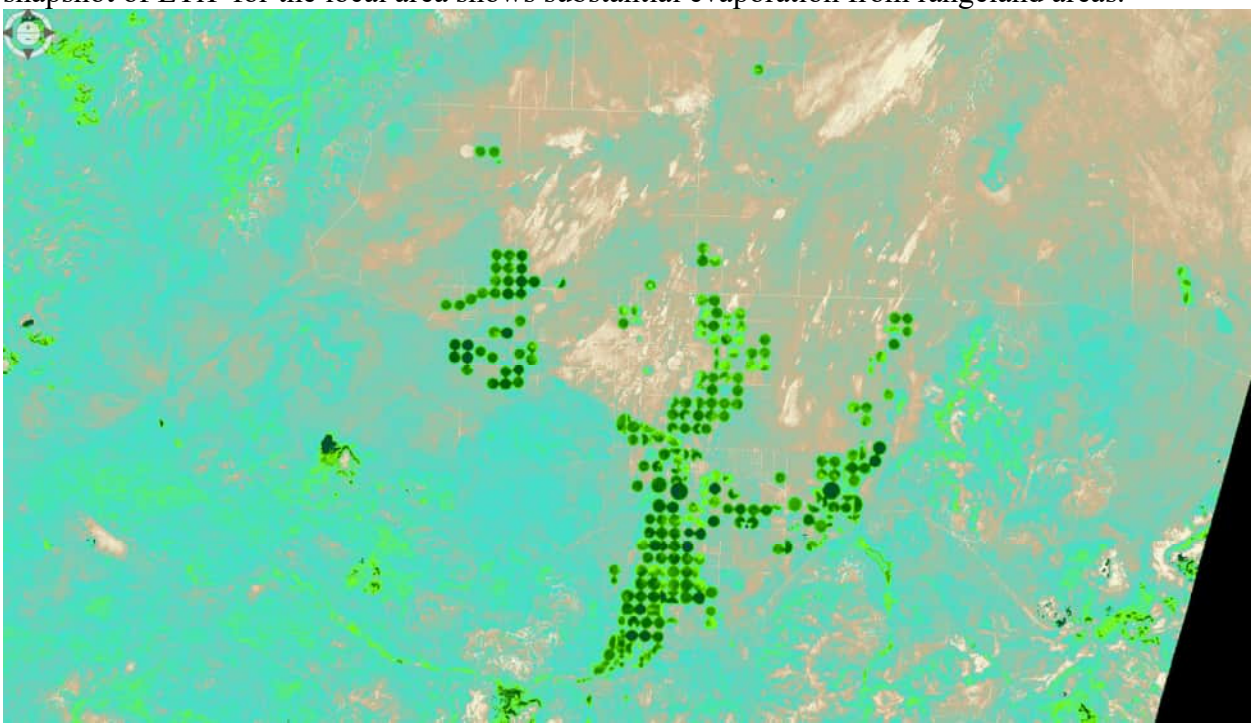

ETrF at the cold pixel is set to 1.05 and at the hot pixel is set to 0.14 (Ke value suggested by the METIRC). H at the hot pixel is 311 W/m^2 and at the cold pixel is 61 W/m^2.
The graph for de-lapsed surface temperature vs. NDVI is as follows (where the blue points are from agricultural fields, and the red crosses are from Non-Agricultural areas):

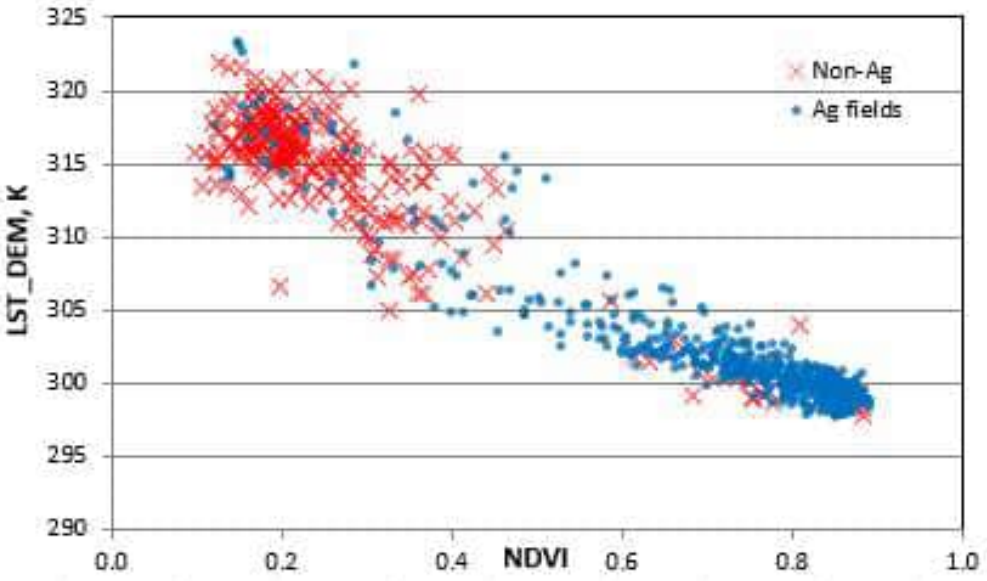

The graph for ETrF-EF vs. NDVI is as follows (where the blue points are from agricultural fields, and the red crosses are from Non-Agricultural areas):

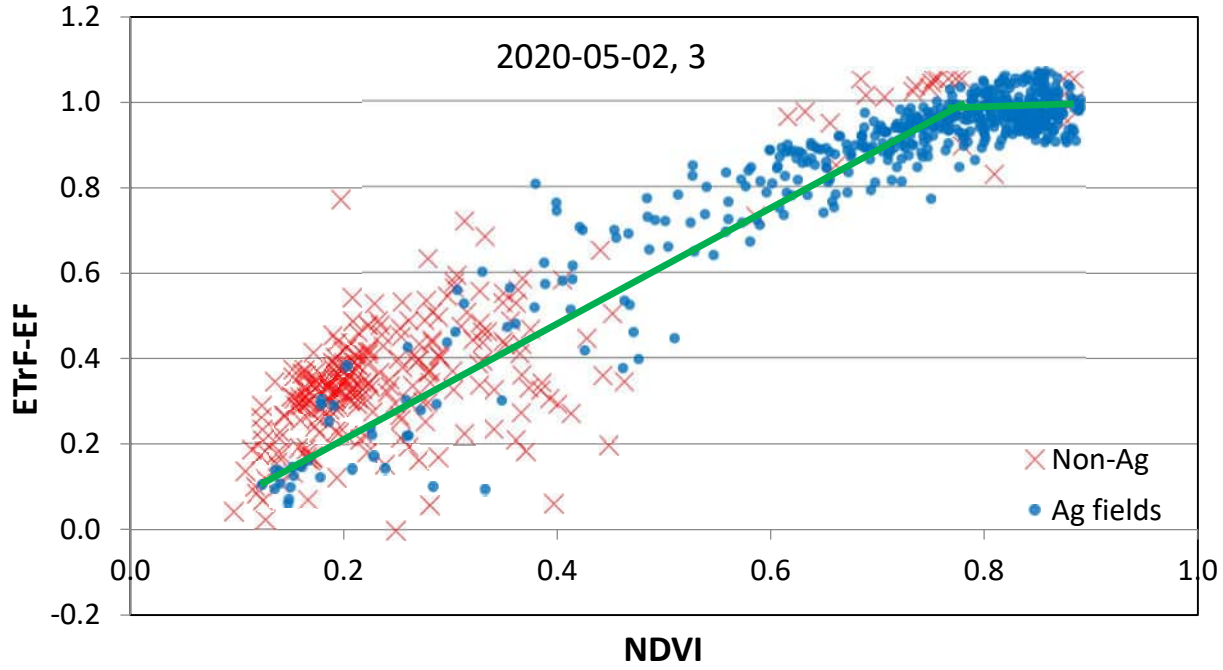

For the final calibration (not shown), we reduced ETrF at the high end by 0.05. Bottom end is OK.

June 19, 2020

There is nice, clear image with only a few small clouds. The agricultural areas that we are interested in are clear. Wind speed is 2.7 m/s and ETr is 0.85 mm/h.

There has been no reported rain for Beryl Junction since the 20.3 mm precipitation on April 29, about 51 days ago. Estimated Ke is 0.00 for both the satellite overpass date and the previous day.

ETrF at the cold pixel is set to 1.05 and at the hot pixel is set to 0.10. H at the hot pixel is 277 W/m^2 and at the cold pixel is -9 W/m^2.
The graph for de-lapsed surface temperature vs. NDVI is as follows (where the blue points are from agricultural fields, and the red crosses are from Non-Agricultural areas):

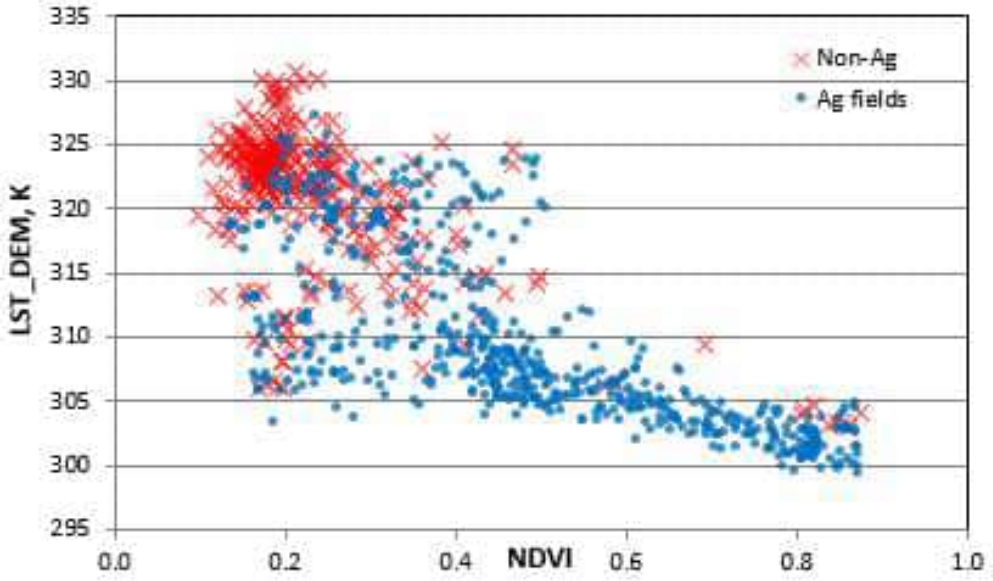

The graph for ETrF-EF vs. NDVI is as follows (where the blue points are from agricultural fields, and the red crosses are from Non-Agricultural areas):

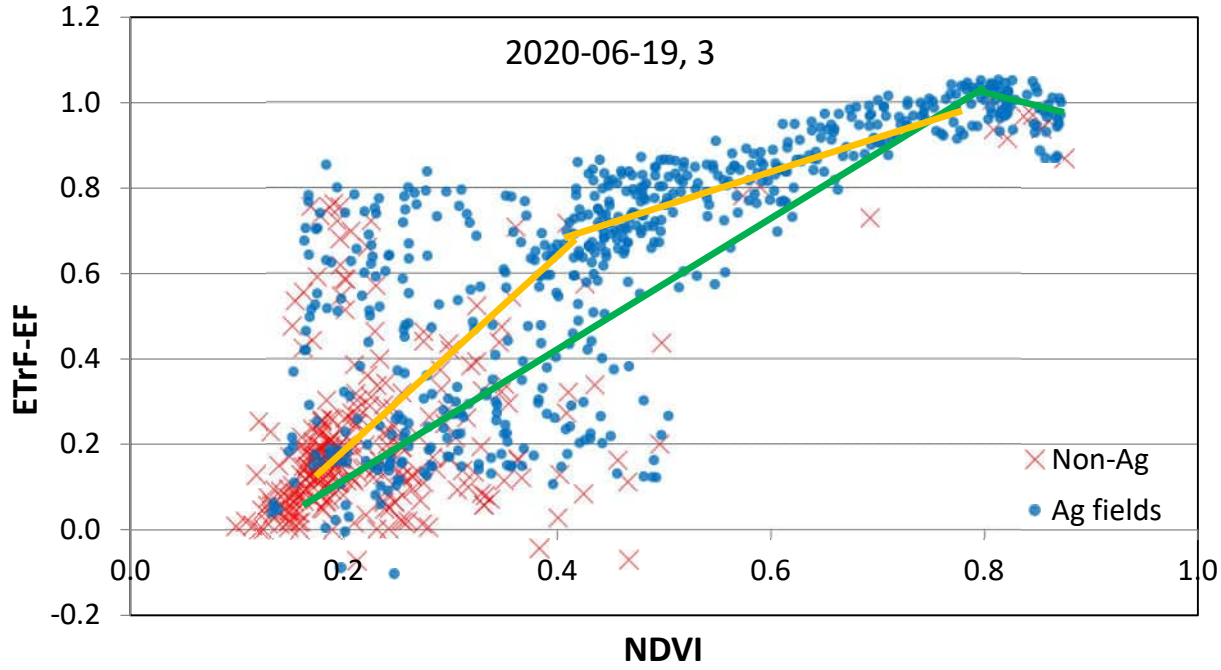

For the final calibration (results not shown), we decreased the top end and the bottom end of ETrF by 0.05.

July 05, 2020

There is a nice, clear image with only a few small clouds. The agricultural areas that we are interested in are clear. Wind speed is 3.2 m/s and ETr is 1.01 mm/h.
There has been no rain at Beryl Junction since April 29. The soil should be quite dry without irrigation. Estimated Ke is 0.00 for the satellite overpass date and for the previous day. ETrF at the cold pixel is set to 1.05 and at the hot pixel is set to 0.10. H at the hot pixel is 236 W/m^2 and at the cold pixel is -153 W/m^2. The large negative H for the cold pixel condition indicates substantial advection of heat energy from upwind range areas to the irrigated agriculture.
The graph for de-lapsed surface temperature vs. NDVI is as follows (where the blue points are from agricultural fields, and the red crosses are from Non-Agricultural areas):

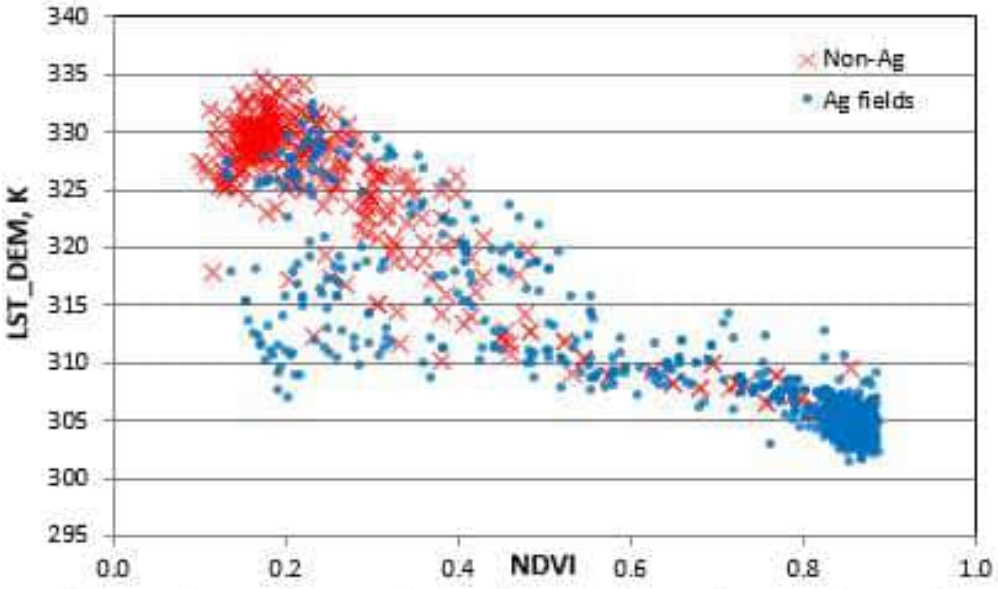

The graph for ETrF-EF vs. NDVI is as follows (where the blue points are from agricultural fields, and the red crosses are from Non-Agricultural areas):

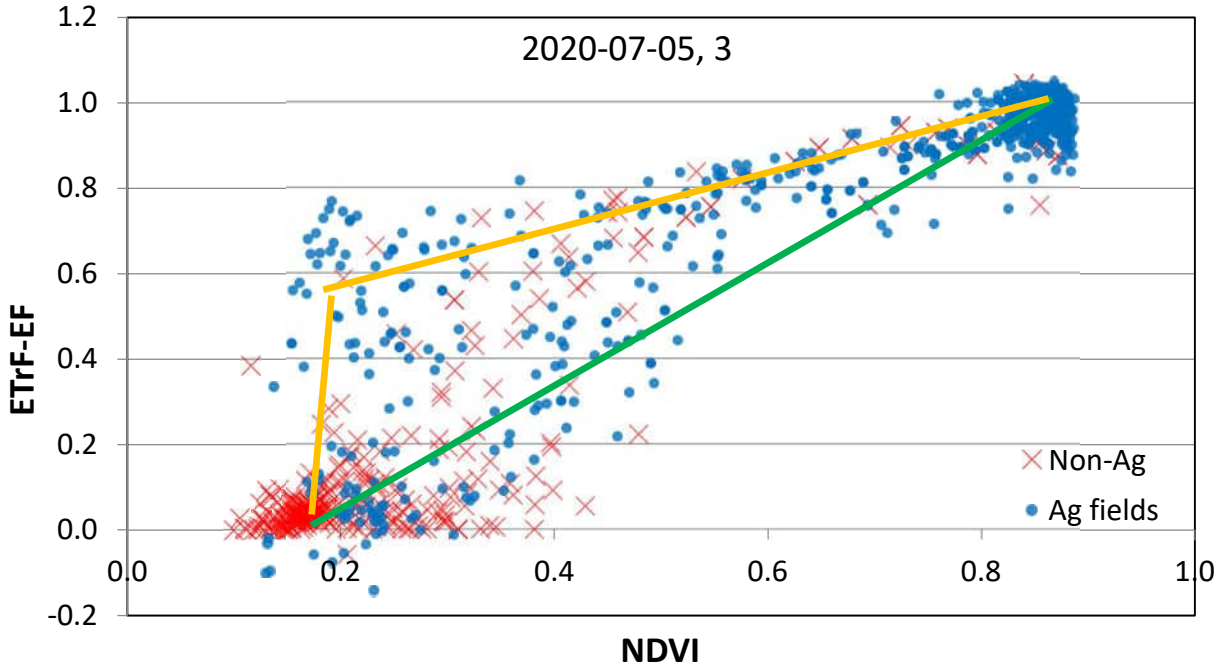

The green trend line represents ETrF for fields that have relatively dry exposed soil surfaces. The upper orange trend line represents fields that have been recently irrigated and where exposed soil is wet and evaporating. For the final calibration (results not shown), we reduced the upper end of ETrF by 0.03.

August 06, 2020

There is also a very clear image. Although Fmask estimated that there were a few tiny clouds near the east side of the image, they were not visible when viewing, even the view was magnified. The agricultural areas that we are interested in are clear. Wind speed is 4.9 m/s and ETr is 1.05 mm/h.

There was only 0.25 mm rain on July 27. Before that, there was not rain for almost 3 months, according to the Beryl Junction Weather Station record. The soil should be quite dry without irrigation. Estimated Ke is 0.00 for the satellite overpass date and for the previous day. ETrF at the cold pixel is set to 1.05 and at the hot pixel is set to 0.10. H at the hot pixel is 268 W/m^2 and at the cold pixel is -228 W/m^2. The -228 represents substantial advection of sensible heat from upwind range areas and is required to match total evaporable energy with the energy required to sustain the reference ET estimated from weather data at satellite overpass time.

The graph for de-lapsed surface temperature vs. NDVI is as follows (where the blue points are from agricultural fields, and the red crosses are from Non-Agricultural areas):

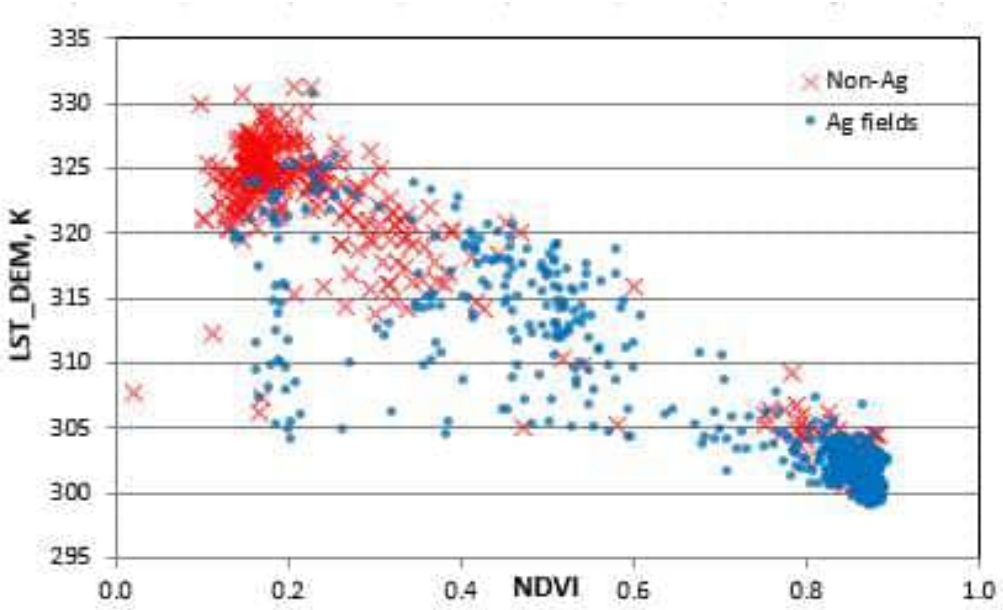

The graph for ETrF-EF vs. NDVI is as follows (where the blue points are from agricultural fields, and the red crosses are from Non-Agricultural areas):

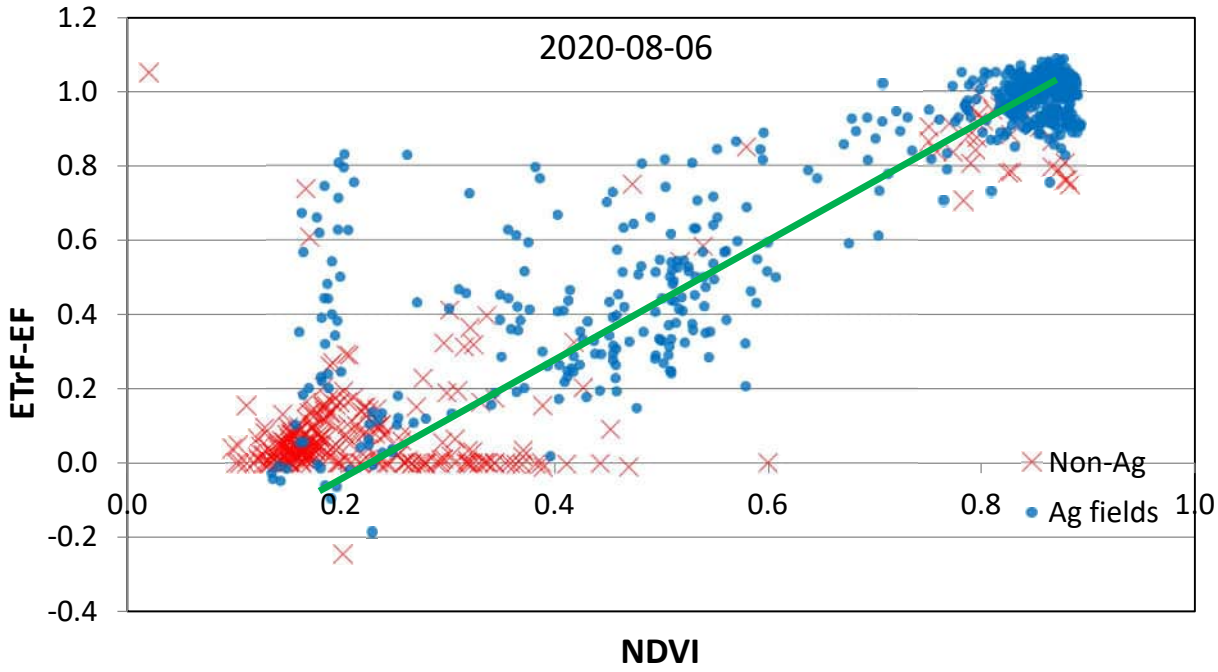

For the final calibration (results not shown), we decreased the upper end of ETrF by 0.07 and increased the lower end by 0.05.

August 22, 2020

The weather data for the August 22 were missing from 0900 to midnight on August 22, 2020 in the USU climate record.

To produce weather data for August 22, we downloaded weather data from the Enterprise Weather station (USCAN) and, following QA/QC of data, used them to replace the August 22 data at the Beryl Junction. The Modena weather station was not yet on line in August of 2020. The following is a screenshot of the weather data after we replaced the Beryl Junction data with the Enterprise data:

	A	B	C	D	E	F
2	**The user needs to supply information on image time and wind, humidity (ir**					
3		*Spreadsheet created by R.Allen, Univ. Idaho, Kimberl*				
4		*The authors accept no liability for errors in this sprea*				
5	**Input appropriate values in the orange boxes**					
6						
7	**Weather station name**		Entrprise			
8	**Weather station latitude, decimal**		37.720	degrees **North**		
9	**Weather station longitude, decimal**		113.702	degrees **West**		
10	**Abbreviated name of project**		UT	(use no spaces in name)		
11	**Abbreviated name of satellite (L5 or L7**		L8	*(linked to Start Here page)*		
12	**Satellite path**		39	*(linked to Start Here page)*		
13	**Satellite row/rows**		34	*(linked to Start Here page)*		
14						
15	**Image date**		Year	Month	Day	
16	yyyy/mm/dd		2020	08	22	
17			*(linked to Start Here page)*			
18	**Image Time**		Hour	Minute	Second	
19	Greenwich Time (GMT)		18	15	15.41	
20						
21	**Longitude of Center of Time Zone**			105	degrees **West**	
22						
23	**Length of Weather Time Period**			1.00	hours	
24						
25	**Flag for Weather Reporting Time**			1.0		
26						
27						
28	**Flag for Daylight Savings Time in Weather**			1		
29						
30	**Minutes after the hour for data reporting**			0	(normally 0) This	
31						
32						
33	**For Computing the 'Instantaneous' Weather at Satellite Overpass:**					
34	**Time "label" for the first Weather Period:**			11.00	Local Time in **dec**	
35	**Time "label" for the second Weather Period:**			12.00	Local Time in **dec**	
36		*These data are read from the REF-ET hourly sheet*				
37	Data Period (Hr:Min):	11:00	12:00	13:00	**This is Daylight**	
38	Wind Speed, m/s	2.500	2.590	3.000	Wind speed is at t	
39	Dew Point Temp, °C	16.200	14.000		*Note that the third*	
40	Air Temp, °C	31.500	33.000			
41	ETr, mm/hour	0.660	0.860	ETr is the alfalfa reference E		
42	Wind Direction (Deg. From N)	0				
43	**Results**	**Instantan.**	**3-hour ave.**			
44	Wind Speed, m/s	2.57	2.70		**DoY**	
45	Dew Point Temp, °C	14.55			235	
46	Air Temp, °C	32.63				
47	ETr, mm/hour	0.810				
48						

There were quite a few clouds over the image. There was also a cloud edge that touched the northwest edge of the agricultural areas that we are interested in. Estimated wind speed is 2.6 m/s and ETr is 0.81 mm/h. There was only 0.25 mm rain on July 27. Before that, there was no rain for almost 3 months, according to the Beryl Junction Weather Station record. The soil should be quite dry without irrigation. Estimated Ke is 0.00 for the satellite overpass date and for the previous day. ETrF at the cold pixel is set to 1.05 and at the hot pixel is set to 0.10. H at the hot pixel is 256 W/m^2 and at the cold pixel is -55 W/m^2 when using the Enterprise data.
The graph for de-lapsed surface temperature vs. NDVI is as follows (where the blue points are from agricultural fields, and the red crosses are from Non-Agricultural areas):

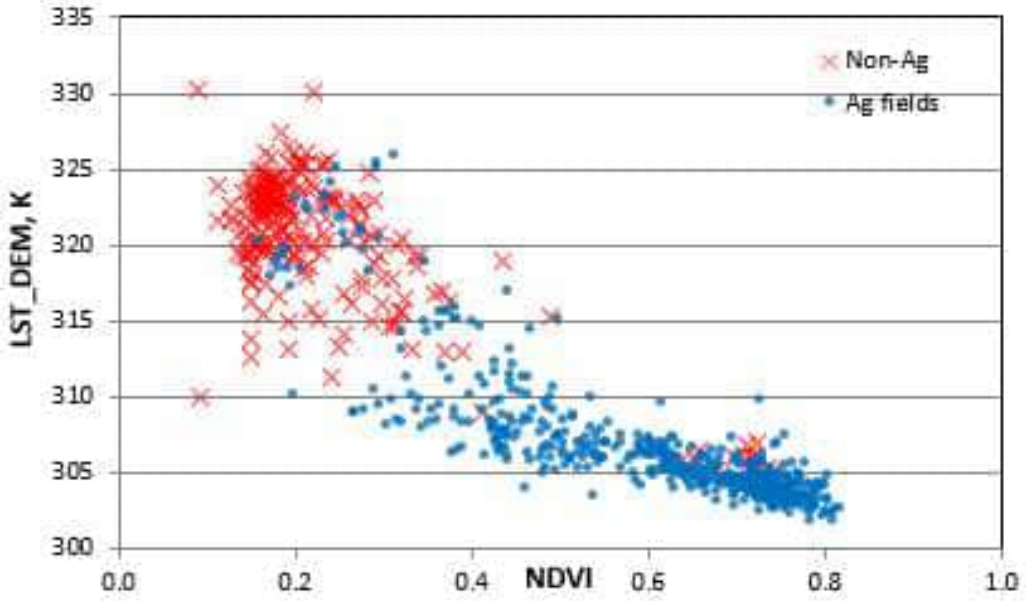

The graph for ETrF-EF vs. NDVI is as follows (where the blue points are from agricultural fields, and the red crosses are from Non-Agricultural areas):

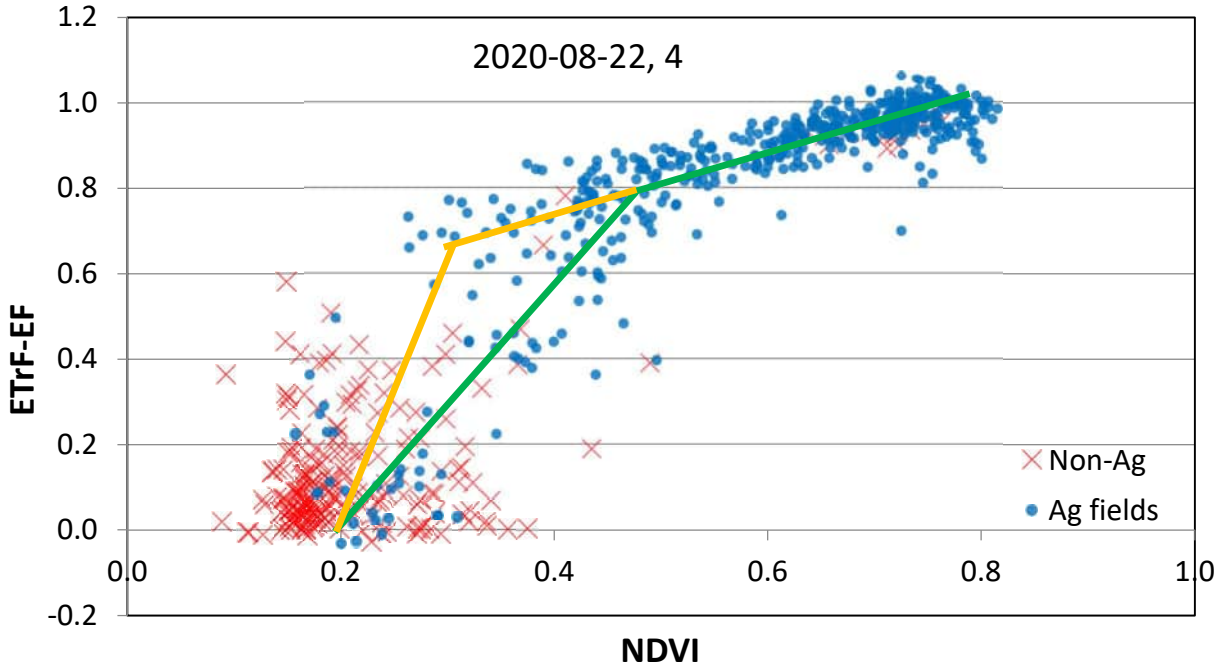

September 23, 2020

It seems that there is a fire burning near the Virgin Peak Ridge Camping Ground in Nevada on this date. From left to right, the following images are: ETrF showing highly negative ET over the fire due to the very high temperature directing METRIC to estimate very high sensible heat flux, H, and therefore, negative ET from the surface energy balance. This negative error is due to the lack of energy input from the fire, which is beyond METRIC's scope of computations. The other three screenshots show ETrF after setting negative ET to zero, the Landsat false color image and clouds determined from FMask after buffering. The FMask routine distinguished tails of the smokes as clouds (in the right side of the image). This may be appropriate if the smoke intercepts some solar radiation from reaching the surface and sends a cooler temperature signal to the satellite, thereby impacting the true estimate for ET.

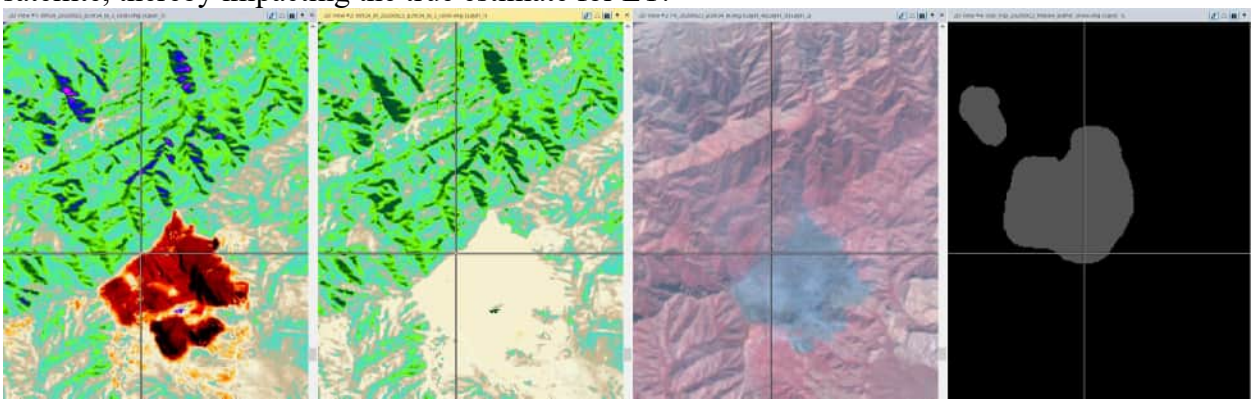

Wind speed is 1.6 m/s and ETr is 0.72 mm/h. There was no rain since July 27 according to the Beryl Junction weather station. The soil should be quite dry without irrigation. Estimated Ke is 0.00 for the satellite overpass date and for the previous day. ETrF at the cold pixel is set to 1.02.

ETrF at the hot pixel is set to 0.10. H at the hot pixel is 266 W/m^2 and at the cold pixel is -43 W/m^2.
The graph for de-lapsed surface temperature vs. NDVI is as follows (where the blue points are from agricultural fields, and the red crosses are from Non-Agricultural areas):

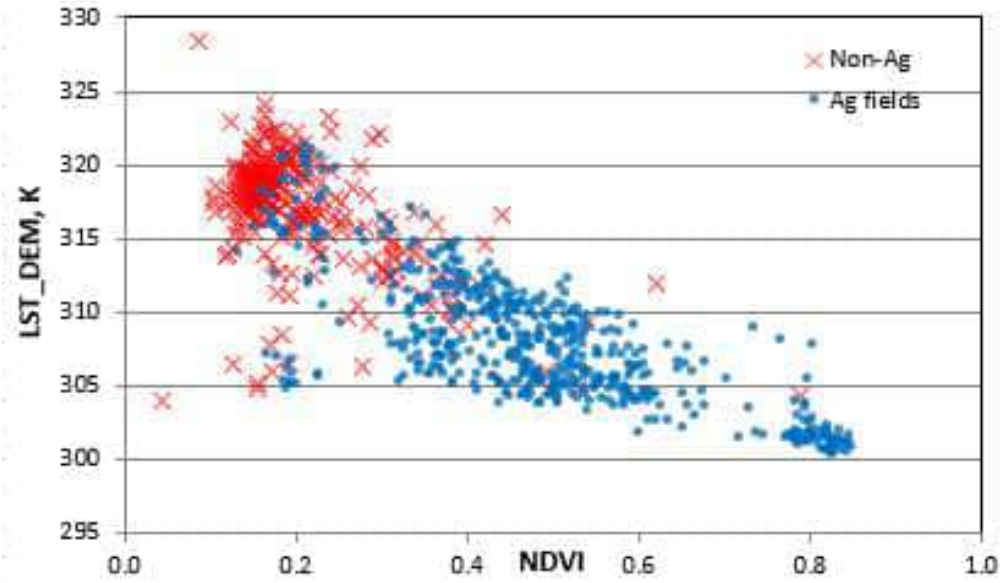

The graph for ETrF-EF vs. NDVI is as follows (where the blue points are from agricultural fields, and the red crosses are from Non-Agricultural areas):

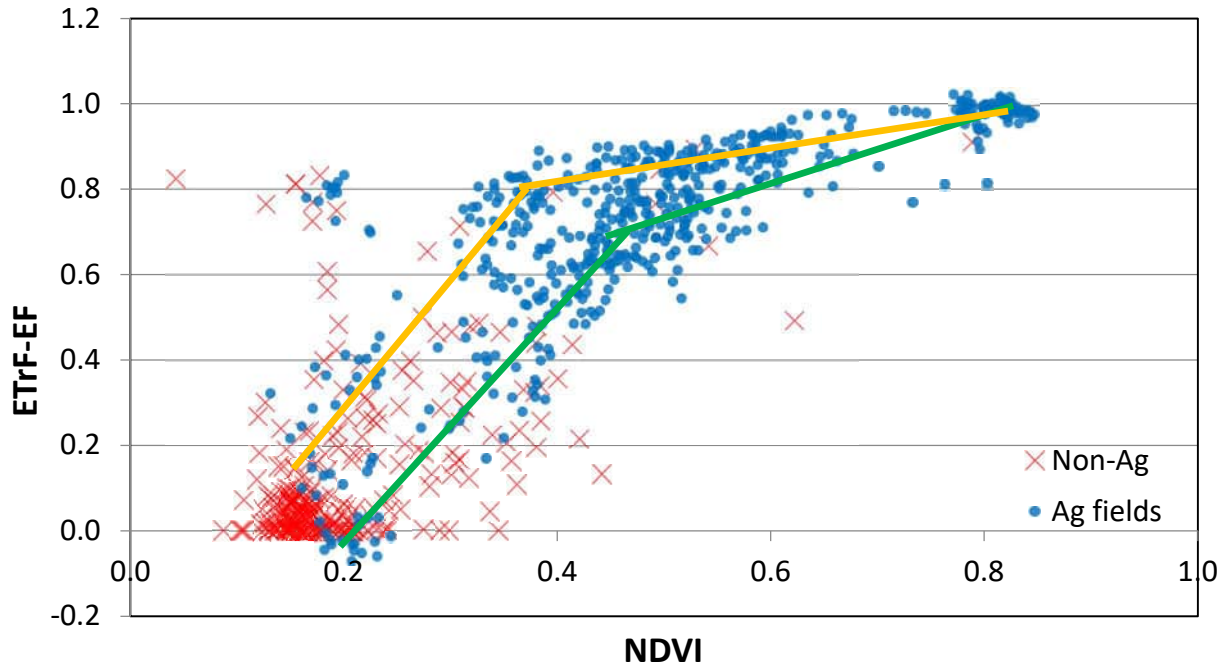

The high ETrF at mid-range NDVI is probably due to a combination of soil evaporation from irrigated fields plus the impact of transitioning from a stable boundary layer with low sensible heat flux (H) at NDVI > 0.4 to a more buoyant boundary layer when NDVI was < 0.4 and LST was higher. The latter created a larger positive H and reduced estimates for ET at lower NDVI.

This transition was more pronounced than for other image dates due to the relatively calm wind which reduced turbulent mixing of the boundary layer and caused the sensible heat flux to instead rely on buoyancy that occurs under larger H experienced with low amounts of vegetation and low ET.

Appendix B.

METRIC Processing of Path 38 Path 39, Row 34, Year 2021 images

Dr. Wenguang Zhao, Dr. Richard Allen and Dr. Ayse Kilic

General Information:

The agricultural (AG) area of focus is located within the overlapping area of the two Landsat paths 38 and 39. With the 16 day revisit time of Landsat 8 (L8), the overlapped area of the two paths receives acquisition of images that are 7 and 9 days apart. However, there were many L8 images during the 2021 growing season that had substantial cloudiness. Therefore, four Landsat 7 images were processed for 2021 in order to reduce time gaps between clear Lansat 8 images. Unfortunately, Landsat 7 images have missing gaps in their images due to the scan line corrector (SLC)-off malfunction that occurred in 2003. Those gaps were filled in during the time-integration phase of the computation process using the natural neighbor gap-filling tool of ArcGIS.

The primary area of interest is in the overlap area of Path 38 and Path 39 and includes center pivot irrigated fields near Beryl Junction, UT and towards Enterprise, UT. A mid summer snapshot of evapotranspiration (ET) shown as the ratio of ET to an alfalfa reference ET (ETr) is shown below, taken from Path 38 during 2020:

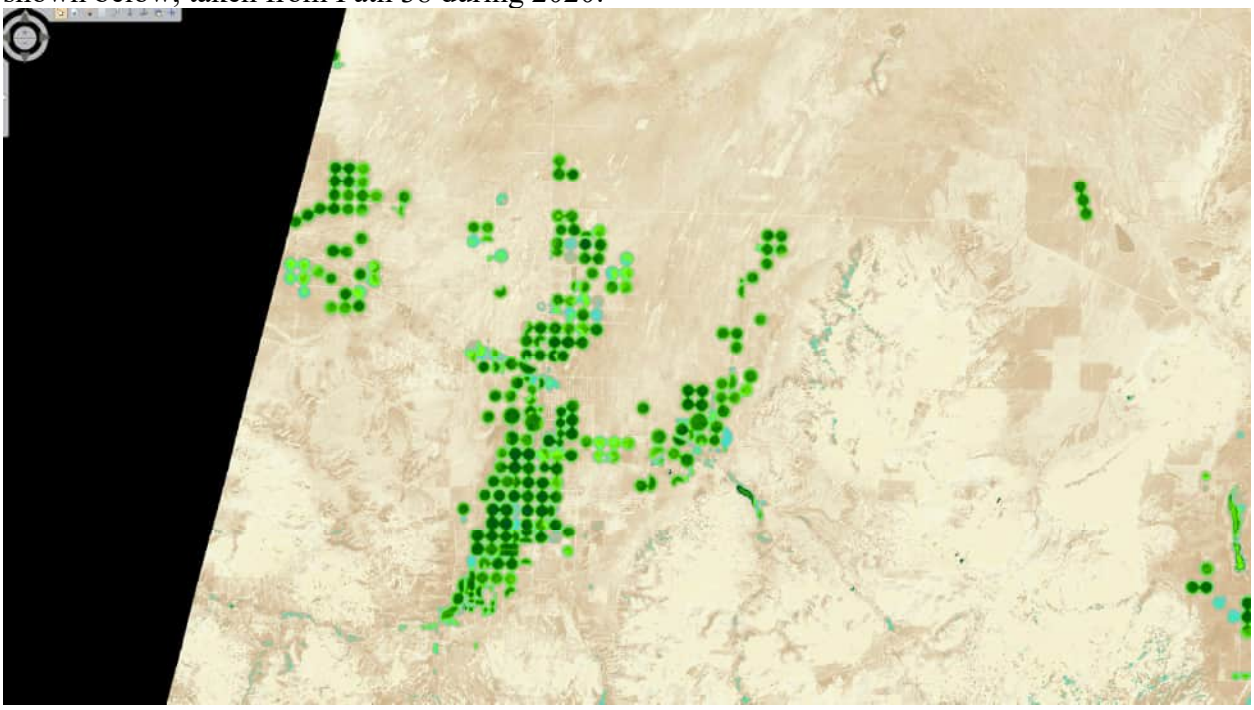

The list of Seventeen Landsat 8 images and four Landsat 7 images processed for the study area for year 2021 are listed in Table 1. These images were selected for processing based on clearness of each image near the study area for each image date.

Table 1. Landsat images processed for year 2021.

Image No.	Year	MoDa	Sat.	Path
1	2021	0327	L8	P38
2	2021	0404	L7	P38
3	2021	0412	L8	P38
4	2021	0419	L8	P39
5	2021	0505	L8	P39
6	2021	0514	L8	P38
7	2021	0521	L8	P39
8	2021	0606	L8	P39
9	2021	0615	L8	P38
10	2021	0708	L8	P39
11	2021	0717	L8	P38
12	2021	0724	L8	P39
13	2021	0802	L8	P38
14	2021	0810	L7	P38
15	2021	0826	L7	P38
16	2021	0903	L8	P38
17	2021	0919	L8	P38
18	2021	0926	L8	P39
19	2021	0927	L7	P38
20	2021	1021	L8	P38
21	2021	1028	L8	P39

The ET from individual fields in the study area tended to vary substantially in time during the growing season due to alfalfa cuttings, rapid development of annual crops and rain events. Therefore, a high frequency of image processing was valuable for defining time-based changes in ET rates.

The geometric projection for the Path 38 images is UTM zone 12 and the projection for the Path 39 image is UTM zone 11. Therefore the Path 39 image was reprojected to zone 12 prior to processing with METRIC to produce a common projection for later mosaicking of ET data.

The calibration weather station used is the Beryl Junction weather station located at 37.7196°N and 113.702°W in Iron County, Utah. The soil type of the area is **very fine sandy loam** according to the NRCS soil survey (Please consult the following link at Page 40 and Page 41): https://www.nrcs.usda.gov/Internet/FSE_MANUSCRIPTS/utah/berylenterpriseUT1960/berylenterpriseUT1960.pdf

The field capacity of the soil was set to 0.2 m^3 m^{-3} in the daily soil evaporation model of METRIC that is used to estimate any residual evaporation occurring after rainfall events. The 0.2 value represents a value between that for a sandy loam of 0.14 and a loam of 0.25—0.32, because of its “very fine” denotation. The wilting point of the soil was set to 0.07 m^3 m^{-3} representing a value between that for a sandy loam of 0.05 and a loam of 0.09—0.15.

Lapse rates used by METRIC to delapse surface temperature with change in elevation were set at the standard values of 0.6 and 10 K km^{-1} for "flat" areas and "mountainous" areas, respectively, and elevation threshold was set at 1650 m for transitioning between the two lapse rates.
The selection of sampling points for producing plots of surface temperature and ETrF (fraction of alfalfa reference ET) for review was done by manually selecting locations in interiors of agricultural fields within and near the study area. In order to have a general review for the whole image, we also sampled agricultural fields in other locations of the scenes, for instance, in the P38 image we sampled areas near Cedar City, Parowan, Milford, Beaver, Circleville and Panguitch, etc.; and in the P39 image we sampled areas near Lake Valley Produce, Panaca, Bunkerville and Amber etc. For non-Agricultural areas, we collected samples throughout the image scenes, so that we could have a general view of the ET behavior throughout the images. Figure 1 shows the locations of sampling points near the study area.

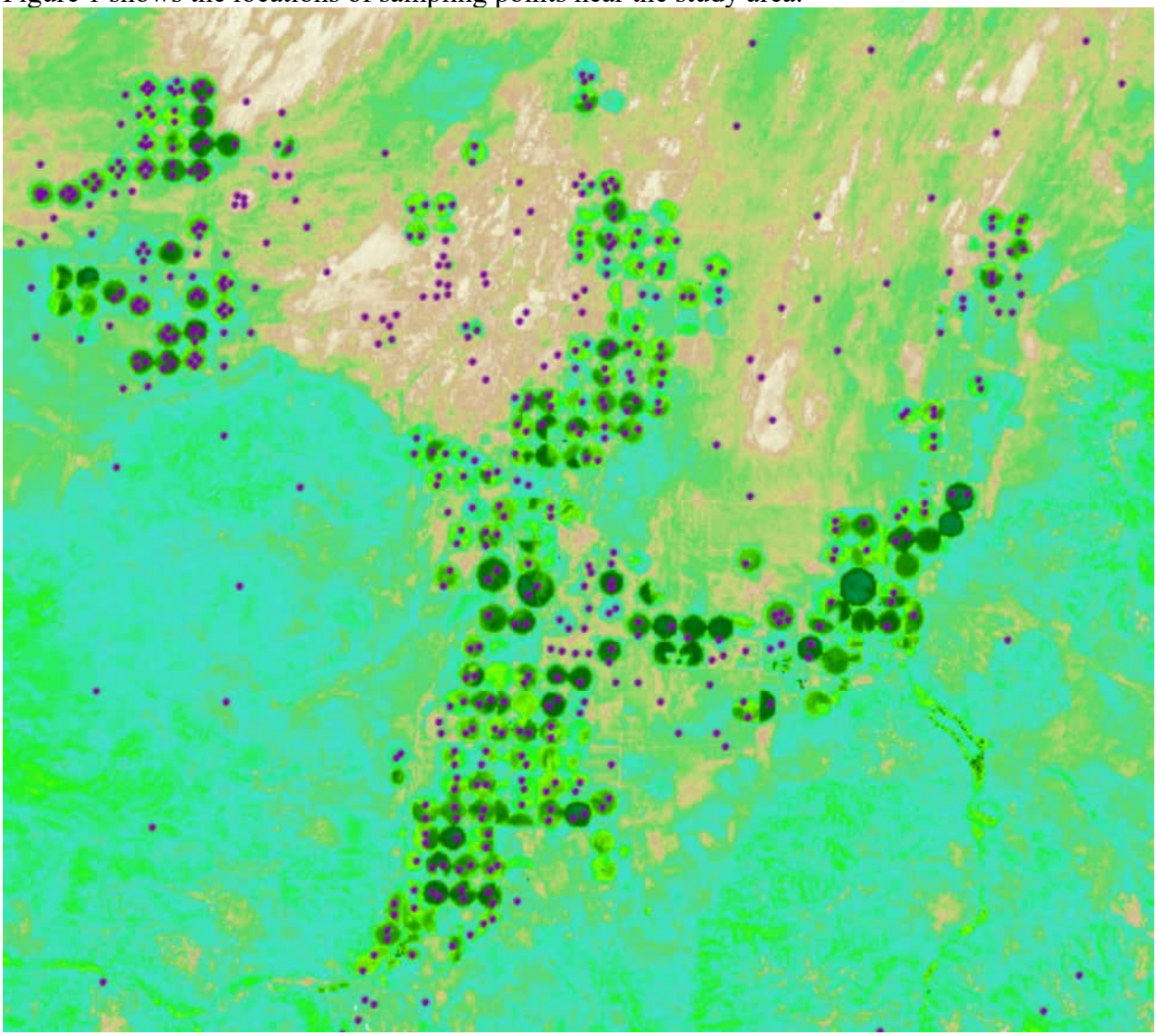

Figure 1. Locations of sampling points near and within the study area.

Path 38 Landsat 8 Images:

June 15, 2021

This image is mostly cloudy on the 3 quarters of the image (mainly south and east sides). From the USGS Earth Explorer site, it seemed that the Ag areas in the path overlap area that we are most interested inwere clear. However, after downloading and cloudmasking using FMask, it seems apparent that there were some thin cirrus clouds over parts of the Ag areas that we are most interested in. The FMask algorithm caught these clouds. The influence on reducing estimated LST and thereby elevating estimated ETrF is apparent. We process this image anyway; we will decide whether to use it in the final splining for monthly ET. Wind speed was 4.2 m/s and ETr was 1.06 mm/h. There was 0.5 mm rain on June 14 and 0.25 mm rain on June 11 and June 4. Those small rain amounts should evaporate fairly quickly. The most effective/evident rain was the 15 mm rain on April 26 and April 27. It would not affect conditions on June 15. Estimated Ke is 0.0 for the satellite overpass time and 0.04 for the previous day. The period Ke is 0.01. Due to a relatively lower NDVI at the cold pixel, ETrFcold is set at 1.03 (recommended) and ETrFhot is set to 0.10. Hcold is -188 W/m^2 and Hhot is 166 W/m^2.
The graph for de-lapsed surface temperature vs. NDVI is as follows (where the blue points are agricultural fields, and the red crosses are non-Agricultural fields):

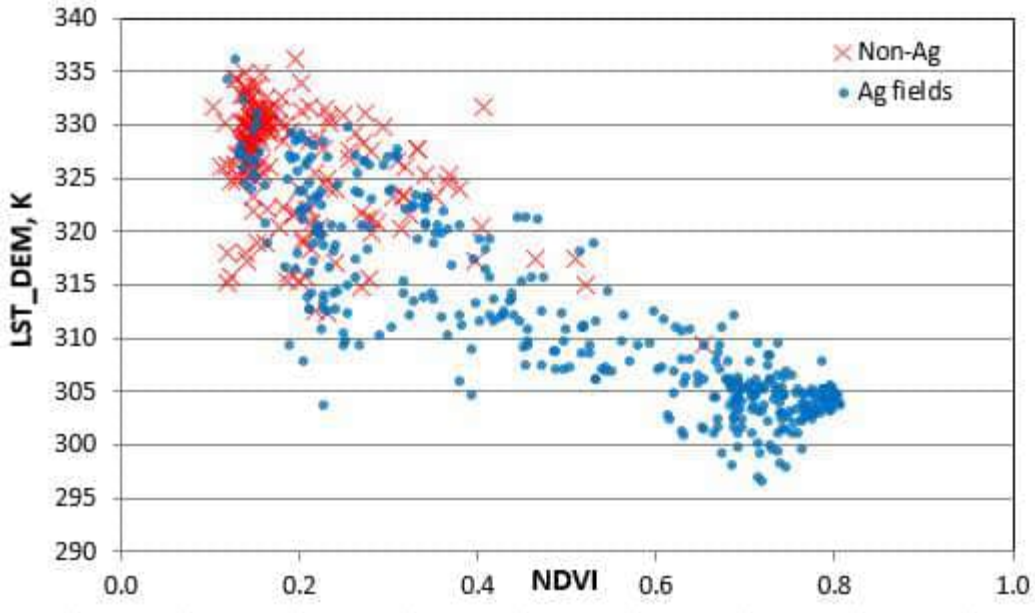

The graph for ETrF-EF vs. NDVI is as follows (where the blue points are agricultural fields, and the red crosses are Non-Agricultural fields):

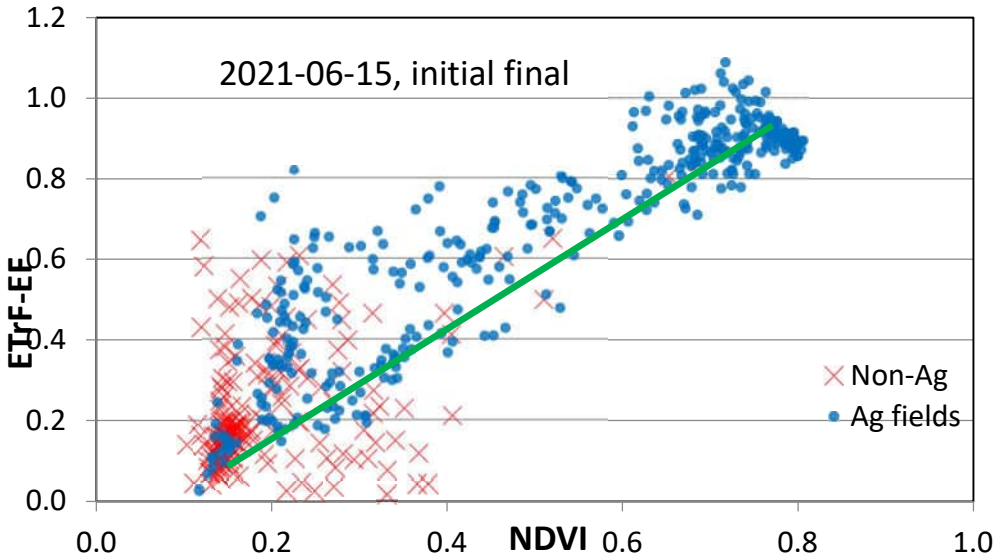

Based on the ETrF vs. NDVI plot and a review of the ETrF image, one can observe that ETrF is elevated in the cloud-masked areas. In the clear parts of the image, ETrF at the upper end appears to be understated by about 0.10 and should be increased by that amount. The lower end of ETrF looks OK.

July 17, 2021

It is quite cloudy at the Northeast quarter of the image. Also the image has a little cloudiness at the southeast side and at the center of the image. Fortunately, the Agricultural areas that we are most interested are clear.

Wind speed is low at 1.3 m/s and ETr is 0.73 mm/h. There was 20.1 mm of rain on July 14, 2.5 mm on July 15 and 1.8 mm on July 16. Estimated Ke for the satellite overpass time is 0.46 and for the previous day is 0.79. Therefore, this is a 'wet' image with significant background evaporation. Period average (for the time period half-way between adjacent images in time) Ke is 0.57 and both Ke from the water balance and the Ke that METRIC recommended for the hot pixel is 0.17. ETrFcold is set to 1.05 and ETrFhot is set to 0.17. Hhot is 270 W/m^2 and Hcold is 22 W/m^2.

The graph for de-lapsed surface temperature vs. NDVI is as follows (where the blue points are agricultural fields, and the red crosses are non-Agricultural fields):

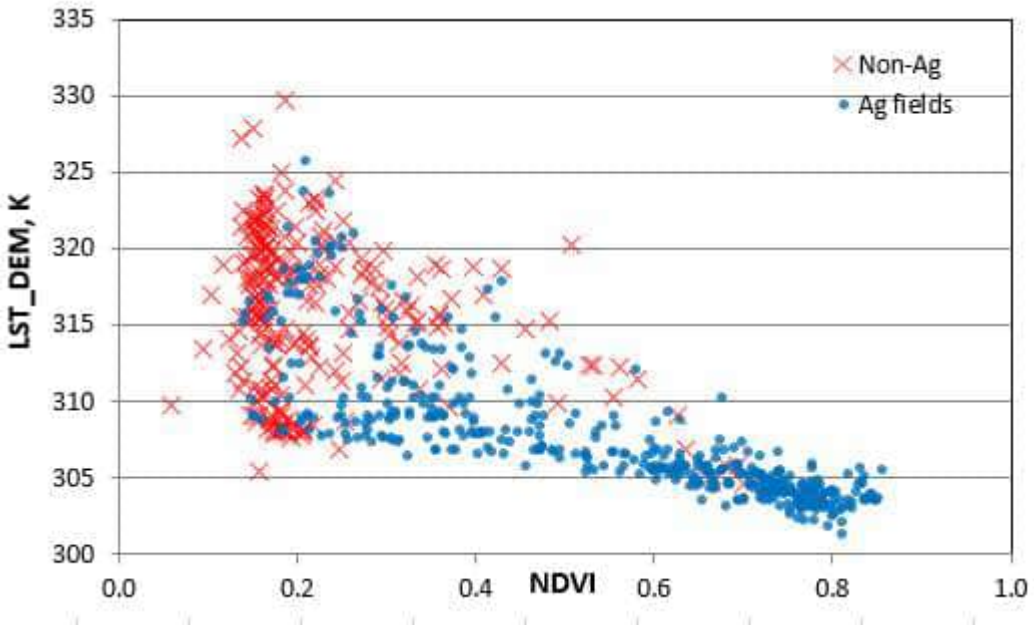

The graph for ETrF-EF vs. NDVI is as follows (where the blue points are agricultural fields, and the red crosses are Non-Agricultural fields):

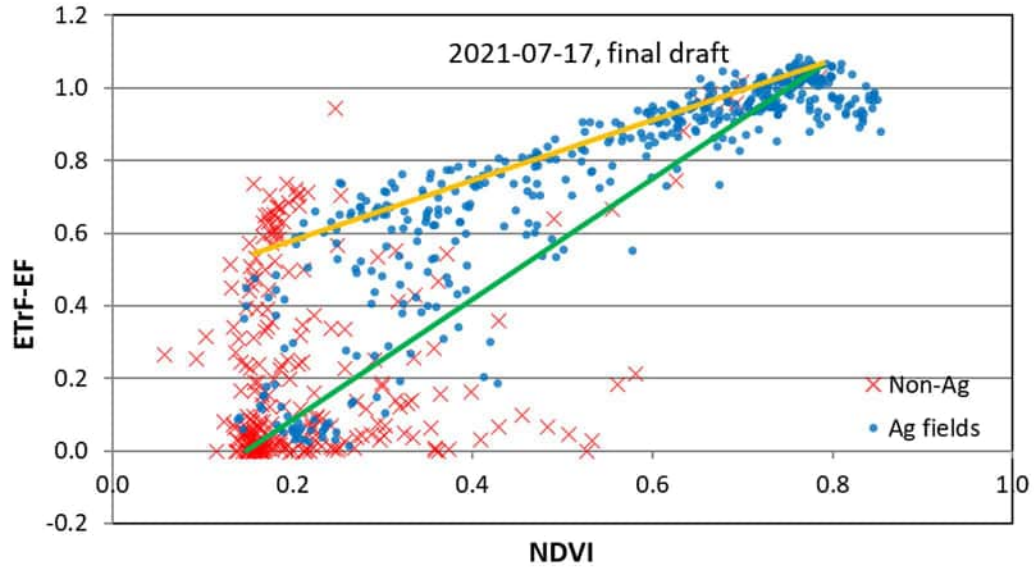

Based on the above ETrF-EF vs. NDVI figure and viewing the ETrF image, where the orange trend line follows an upper trend for fields that are experiencing evaporation from exposed soil due to the large rain on July 14 and light rain on July 15 and 16. The green trend line follows a drier trend for ETrF and may represent areas where rains were lighter or where soils are sandier and therefore dried more quickly prior to the satellite overpass. In addition, a view of the ETrF image for the Enterprise area shows low ETrF in the SW of the area and higher ETrF NE of Enterprise where greater rain depths apparently occurred.

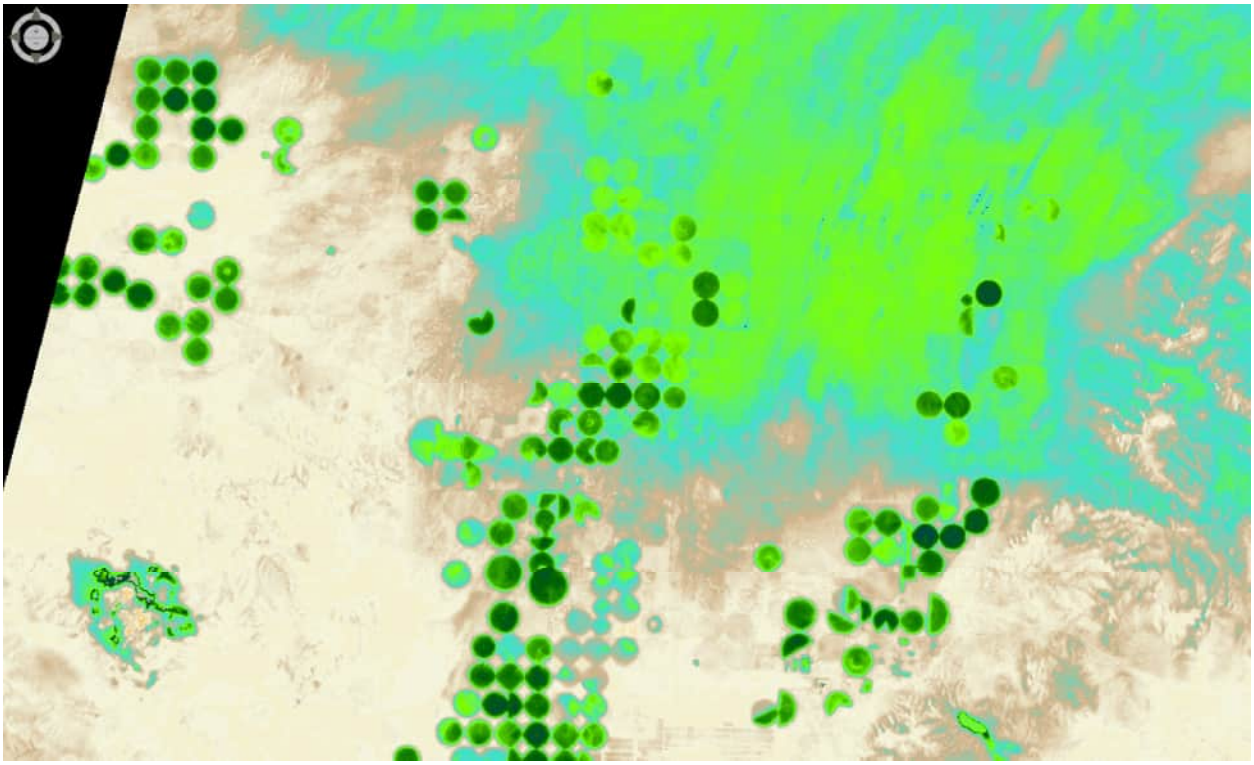

In reviewing the initial calibration, we will adjust the upper end down by 0.10. The lower end of ETrF appears to be OK. However, the lower end could be increased by about 0.20 if we thought that all low NDVI pixels that were sampled had some residual wetness.

August 02, 2021

There were quite a few clouds (probably Cs or As clouds) distributed all over the image. Fortunately, the agricultural areas that we are most interested are clear.

Wind speed is low at 1.0 m/s and ETr is 0.64 mm/h. There was 41.7 mm of rain on July 31 and 13.7 mm on August 1. The soil should be wet. Both the estimated Ke for the satellite overpass time and for the previous day are 1.0. Period average Ke is 0.28. ETrFcold is set to 1.05 and ETrFhot is set to 0.70 (this value may be too low. However we may also want to consider the period average Ke). Hhot is 109 W/m^2 and Hcold is 89 W/m^2 indicating little separation between cool and warm conditions. The following is a screenshot of ETrF for the study area showing relatively high residual evaporation from both rangeland and agricultural areas.

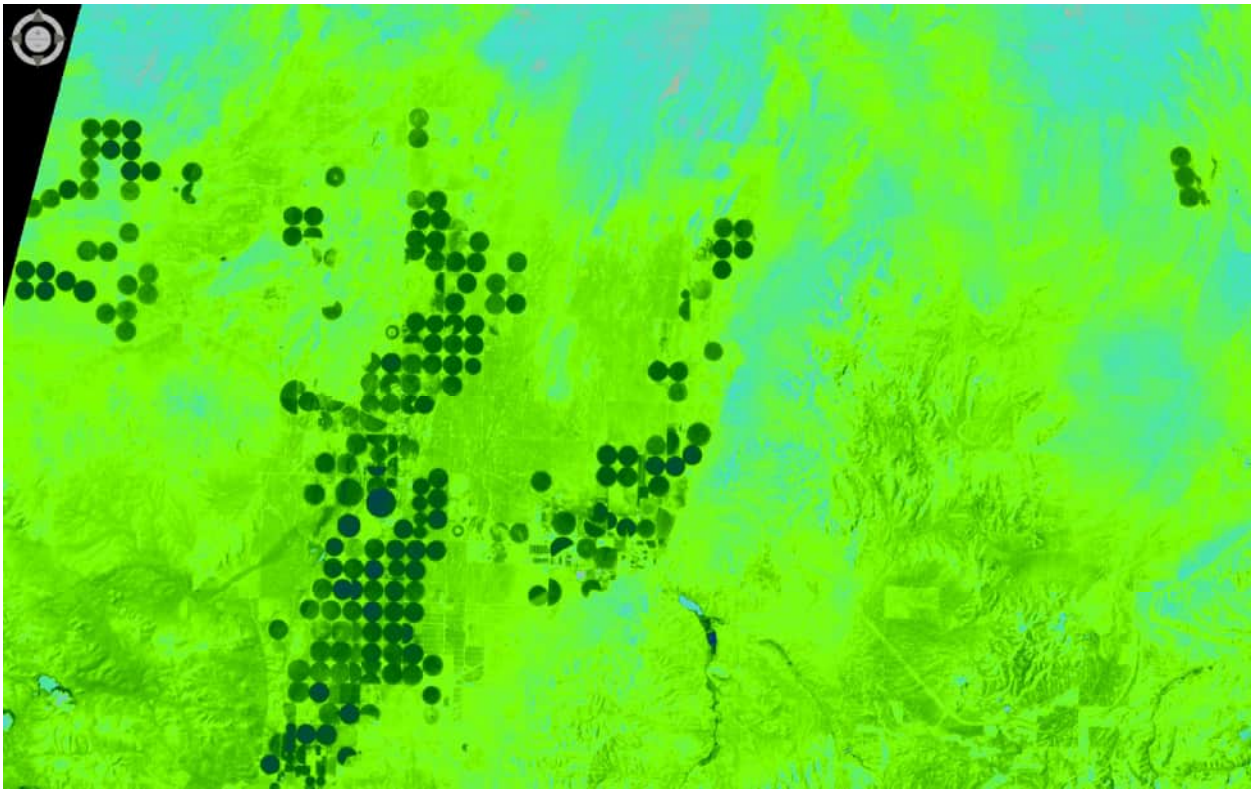

The graph for de-lapsed surface temperature vs. NDVI is as follows (where the blue points are agricultural fields, and the red crosses are non-Agricultural fields):

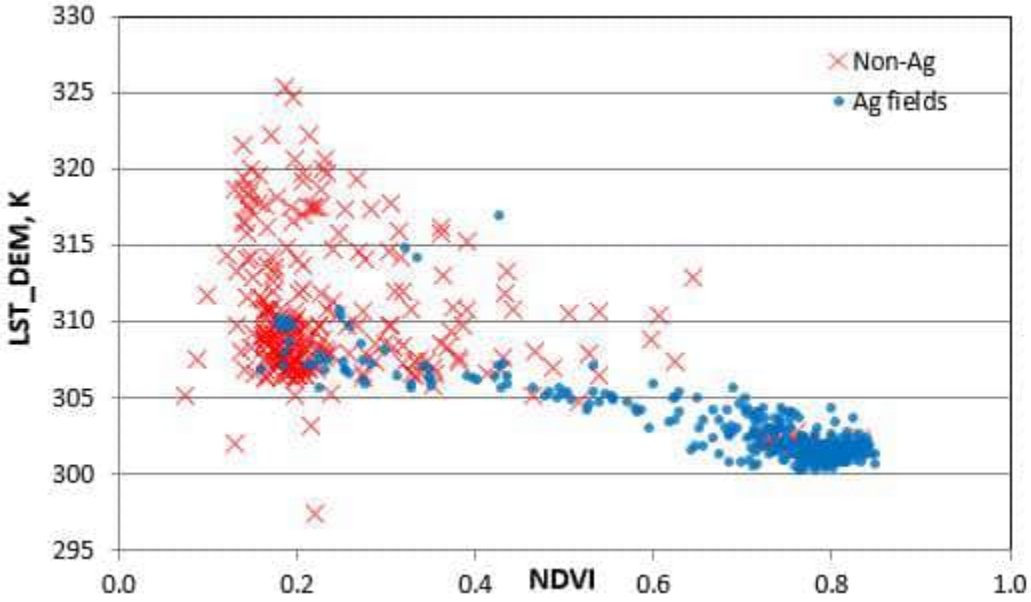

The graph for ETrF-EF vs. NDVI is as follows (where the blue points are agricultural fields, and the red crosses are Non-Agricultural fields):

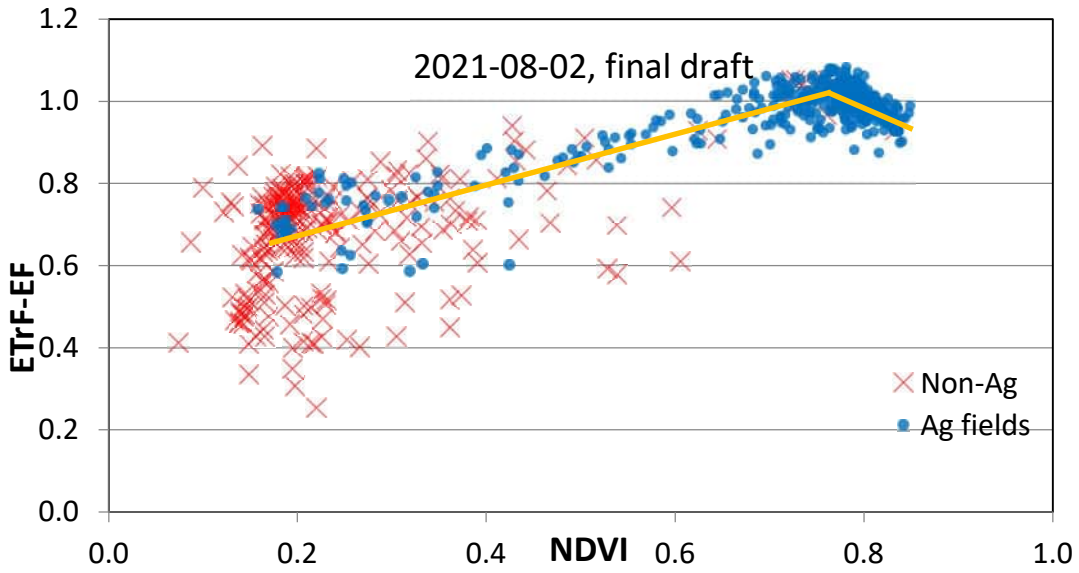

Based on the ETrF vs NDVI plot and ETrF in the image viewer, the ETrF at the upper end could be reduced by 0.05. However, it is probably OK as is since crop canopies may have still been wet. The ETrF at the lower end and the orange trend line look reasonable, given the recent rain events, and where ET from bare soil would tend to be some amount less than from highly vegetated surfaces due to the smoother texture of the soil. The short orange trend line at high NDVI shows a common behavior of ETrF decreasing with NDVI > ~0.75. This is likely due to highest NDVI being associated with dense, horizontal leaf orientation that increases NDVI but increases albedo due to less shadows visible inside canopies.

September 03, 2021

There are isolated clouds here and there among the mountains. However, the Ag areas that we are most interested in are clear. Wind speed is 1.7 m/s and ETr is 0.67 mm/h. There was 1 mm of rain on August 31 and 3 mm of rain on September 1. Therefore there was a small amount of residual evaporation. However, the estimated evaporation at image time was small because the 4 mm would have evaporated away by overpass time. Estimated Ke is 0.03 for the satellite overpass time and 0.05 for the previous day. ETrFcold is set to 1.05 and ETrFhot is set to 0.10. Hcold is 16.7 W/m^2 and Hhot is 301.8 W/m^2.

The graph for de-lapsed surface temperature vs. NDVI is as follows (where the blue points are agricultural fields, and the red crosses are non-Agricultural fields):

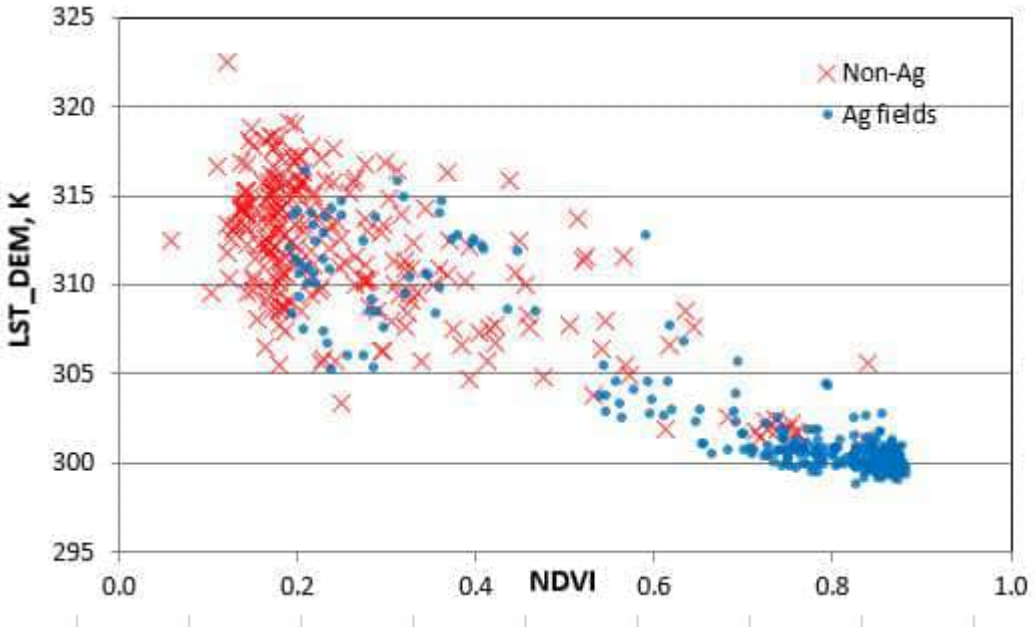

The graph for ETrF-EF vs. NDVI is as follows (where the blue points are agricultural fields, and the red crosses are Non-Agricultural fields):

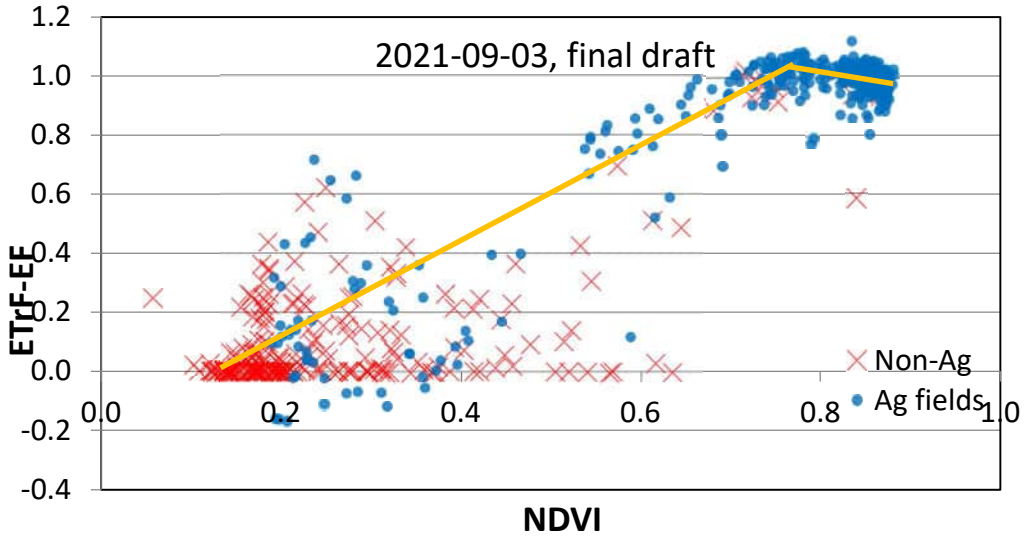

Based on the ETrF vs. NDVI plot and ETrF in the image viewer, the ETrF at the upper end can be reduced by 0.05. The ETrF at the lower end can be increased by 0.01.

September 19, 2021

There were clouds on the east side of the image. The west side of the image that includes the Ag areas that we are most interested in are clear. There was strong wind speed at 8.9 m/s. ETr was 0.9 mm/h. There was 3.8 mm rain on the previous day (September 18) and a total of 4.0 mm on August 31 and September 1. Estimated Ke is 0.25 for the satellite overpass day and 0.41 for the previous day. ETrFcold is set to 1.05 and ETrFhot is 0.25. Hhot was 143 W/m^2 and Hcold was -195 W/m^2 indicating moderate advection.

The graph for de-lapsed surface temperature vs. NDVI is as follows (where the blue points are agricultural fields, and the red crosses are non-Agricultural fields):

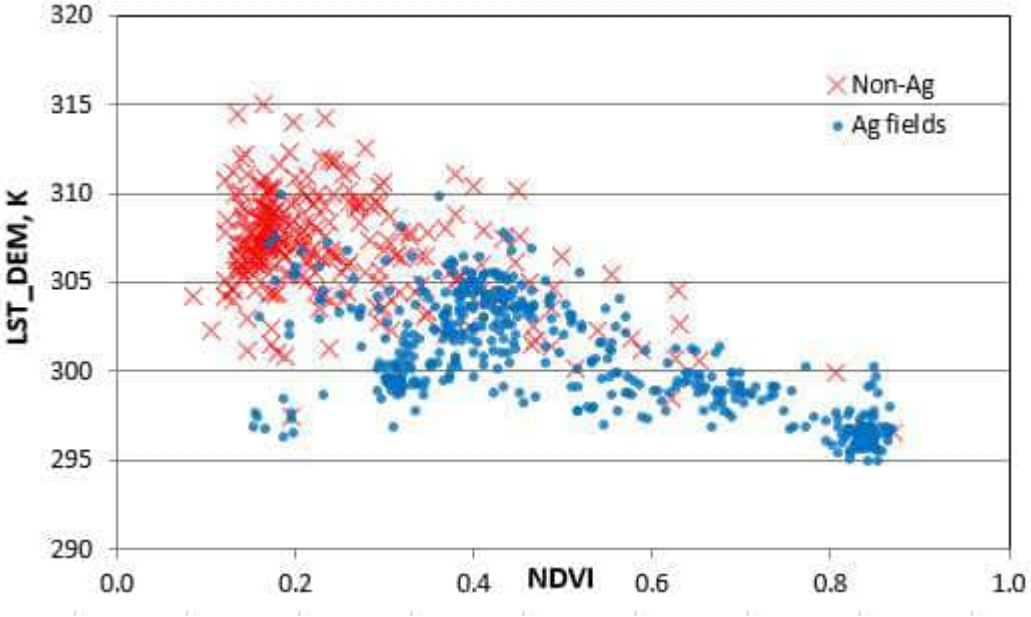

The graph for ETrF-EF vs. NDVI is as follows (where the blue points are agricultural fields, and the red crosses are Non-Agricultural fields):

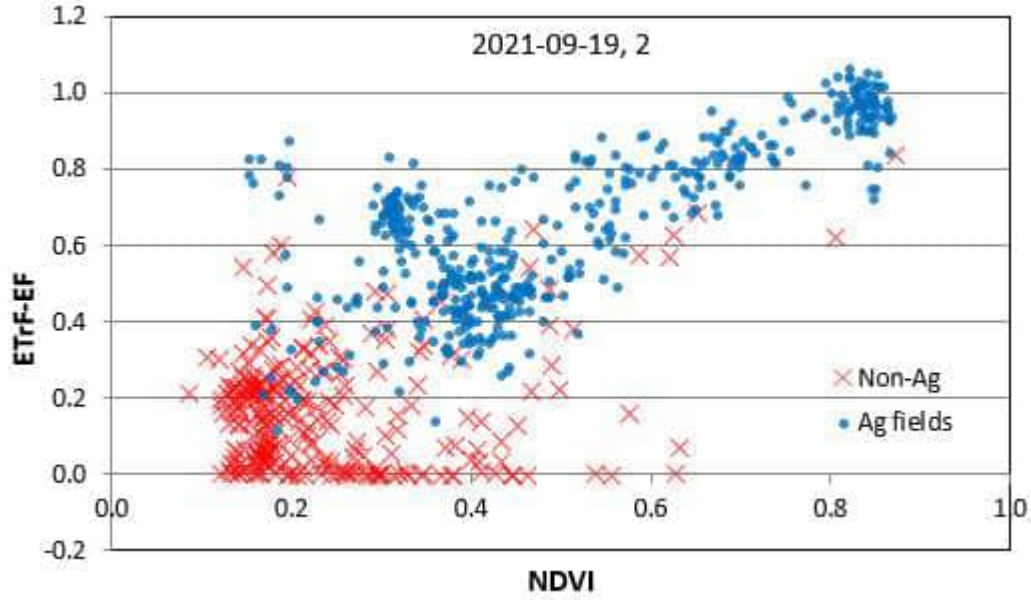

Please note that the H at the cold pixel is -195 W/m^2, which means a downward sensible heat flux of 195 W/m^2 was estimated to have been absorbed by the vegetation at the cold pixel field and used for evapotranspiration. Even with a strong wind of 8.9 m/s to promote mixing of the near-surface boundary layer and being surrounded by hot dry rangeland environment, the amount of negative H may be difficult to accomplish, at -195 W/m^2.
Therefore, we exploratorily decreased the ETr from 0.90 mm/h to 0.75 mm/h and reran the models. For this situation, Hhot became 168 W/m^2 and Hcold became -85 W/m^2. The graph for ETrF-EF vs. NDVI is as follows (where the blue points are agricultural fields, while the red crosses are Non-Agricultural fields):

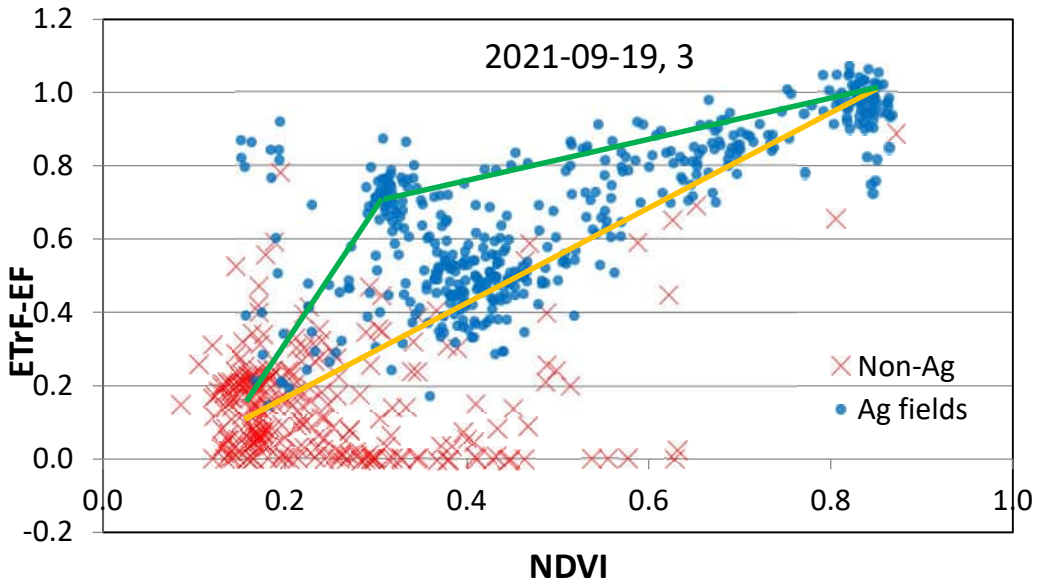

The impact of reducing ETr was to slightly lower ETrF of some sampled points and to slightly raise ETrF of other points. The calibration endpoints (ETrFcold and ETrFhot) were not changed so that the basic calibration was not impacted.
The upper green trend line in the second ETrF vs. NDVI figure shows an upper trend for irrigated fields that were wet either from irrigation or residual rain. It also appears, from viewing spatial ETrF that a number of fields may have been harvested (corn sileage or alfalfa) prior to the overpass date and thereby had low NDVI but higher residual ETrF from newly exposed wet soil. The lower yellow trend line shows a more basal trend where exposed soil among plants has a relatively dry surface and most ET is via transpiration.
Based on the ETrF vs. NDVI plot and review of ETrF in the image viewer, the calibration is judged to be good.

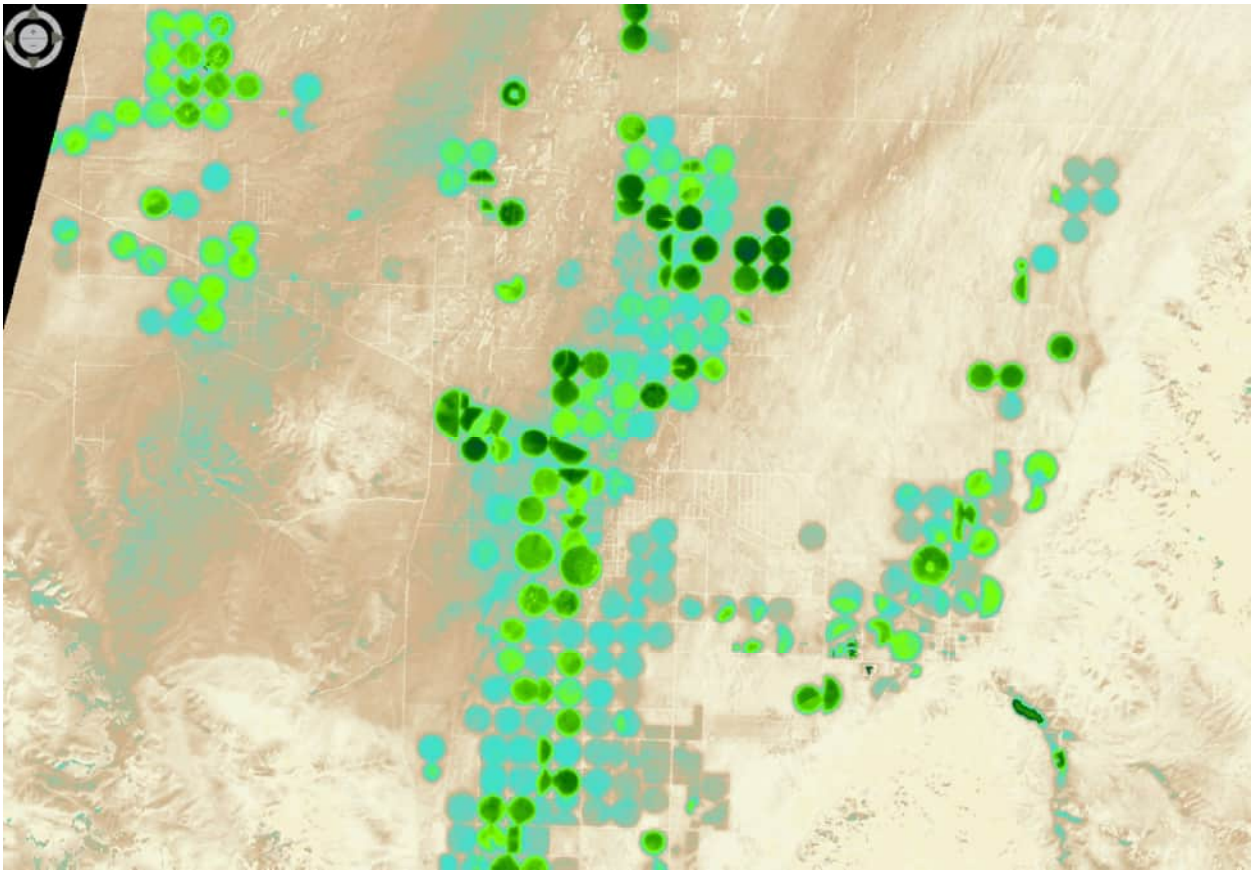

October 21, 2021

There were clouds mainly in the south and southwest parts of the image. In the Ag areas that we are most interested in, conditions seemed to be clear from the USGS Earth Explorer web site. However, after the image was downloaded, FMasked and stacked and viewed, it seems that there was some cloudiness (possibly expanded jet contrails) near the northern portion of the Ag areas that we are most interested in. We processed the image anyway, as it has a significant portion of the image that is clear and can be used. Wind speed was very low at 0.8 m/s. ETr was also low at 0.4 mm/h. There was 3.3 mm rain on October 18, three days ago. There was also 30.7 mm rain from October 5 to October 14 (mainly on October 5 (10.9 mm) and October 8 (10.7 mm)). Estimated Ke is 0.11 for the satellite overpass date and 0.14 for the previous day indicating some residual drying. ETrF at the cold pixel is set to 1.05 and at the hot pixel is set to 0.11. H at the hot pixel is 243 W/m^2 and H at the cold pixel is 86 W/m^2.

The graph for de-lapsed surface temperature vs. NDVI is as follows (where the blue points are agricultural fields, and the red crosses are non-Agricultural fields):

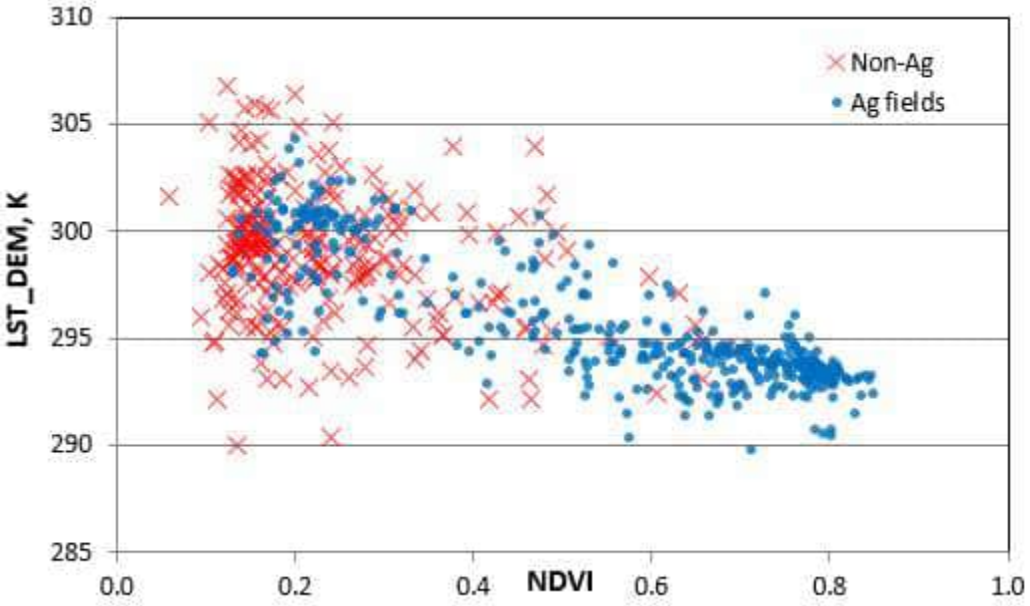

The graph for ETrF-EF vs. NDVI is as follows (where the blue points are agricultural fields, while the red crosses are Non-Agricultural fields):

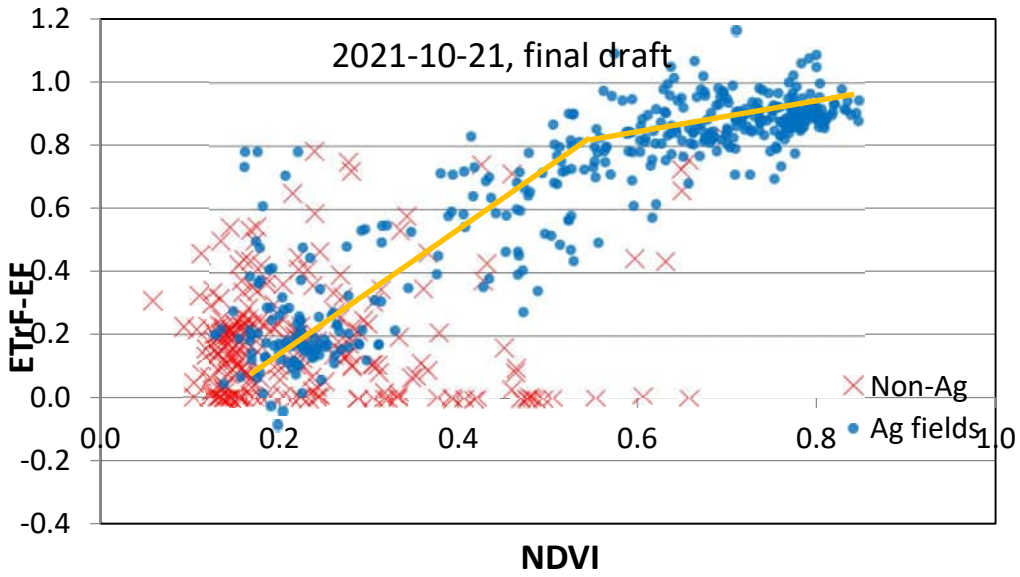

Based on the ETrF vs. NDVI plot and viewed ETrF, spatially, the draft calibration seems to be good.

May 14, 2021

There were some clouds located near the north edge of the image in the mountain areas. The ag areas that we interested in were clear. Wind speed was at 3.0 m/s and ETr was at 0.89 mm/h. There was 0.25 mm rain both on May 2 and on May 11. Before that, there was a total of 15 mm rain on April 26 and 27. The soil should be relatively dry without irrigation. Estimated Ke was 0.00 for the satellite overpass date and for the previous day. ETrF at the cold pixel is set to 1.05

and at the hot pixel is set to 0.10. Hhot is 213 W/m^2 and Hcold is -82 W/m^2 indicating some advection of sensible heat for high ET conditions.
The graph for de-lapsed surface temperature vs. NDVI is as follows (where the blue points are agricultural fields, and the red crosses are non-Agricultural fields):

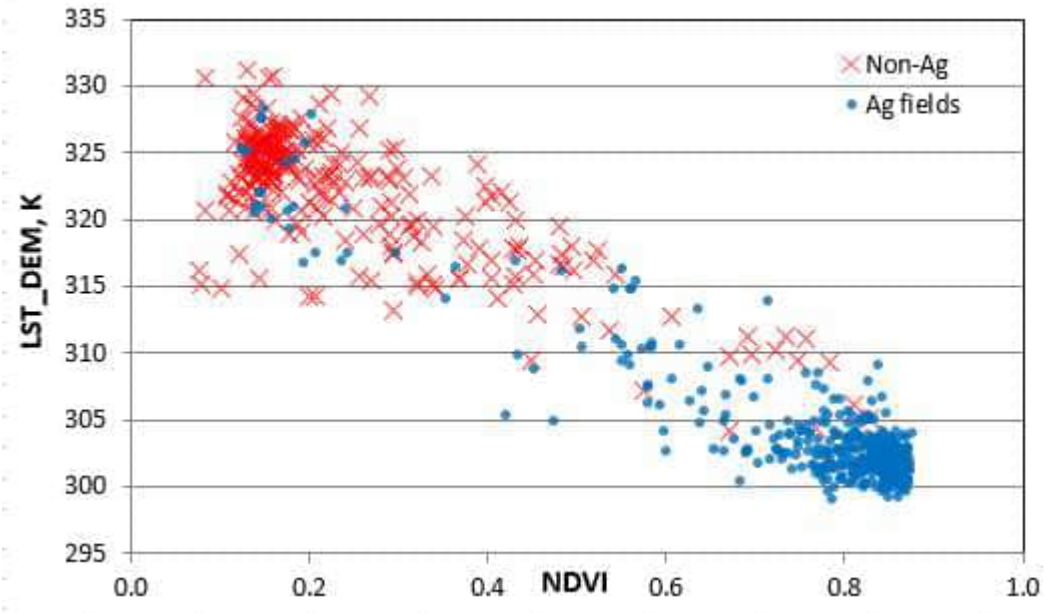

The graph for ETrF-EF vs. NDVI is as follows (where the blue points are agricultural fields, while the red crosses are Non-Agricultural fields):

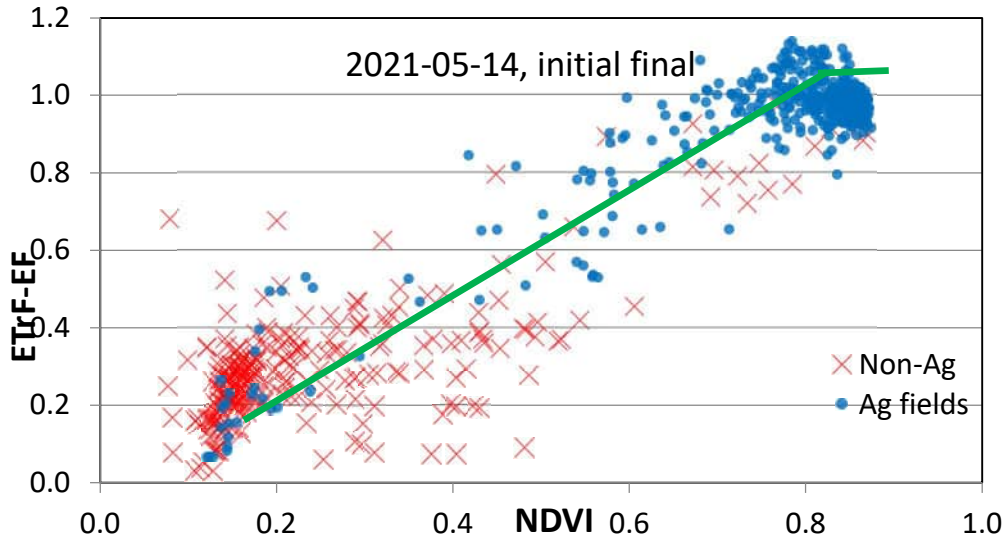

The ETrF vs. NDVI plot shows a typical behavior for high NDVI where ETrF reaches a plateau for NDVI > ~0.75. This is caused by the attainment of maximum conversion of environmental energy into ET when NDVI ~ 0.75, with no increase possible for ET above that. There is even a small reduction in ETrF at highest NDVI, likely due to a more horizontal leaf structure that causes increased reflectance in the NIR band and a small increase in calculated NDVI. That same leaf structure may reduce overall aerodynamic roughness to some degree which reduces the magnitude of negative H at high NDVI and therefore, ETrF and ET.

Based on the ETrF vs. NDVI plot, the lower end of ETrF could be reduced by 0.15. Based on the plot and viewing ETrF in the viewer, the upper end of ETrF could be reduced by about 0.10.

April 12, 2021

There are some apparent clouds in this image. However, most of them appear to be aircraft contrails. The ag areas in the path overlap area that we interested were clear, except there was one aircraft contrail that affected a tiny portion of the ag area at the east side.

Wind speed was 6.4 m/s and ETr was 0.63 mm/h. There was 13.7 mm of rain on April 6, 6 days before the image date. Although it is early to middle April, most of the precipitation was consumed by evaporation and the bare soil should be relatively dry. Estimated Ke is 0.01 for the satellite overpass date and 0.02 for the previous day. ETrF at the cold pixel is set to 1.05 and at the hot pixel is set to 0.10. H at the hot pixel is 280 W/m^2 and at the cold pixel is 104 W/m^2.

The graph for de-lapsed surface temperature vs. NDVI is as follows (where the blue points are agricultural fields, and the red crosses are non-Agricultural fields). There is relatively large vertical variation in LST for any given NDVI:

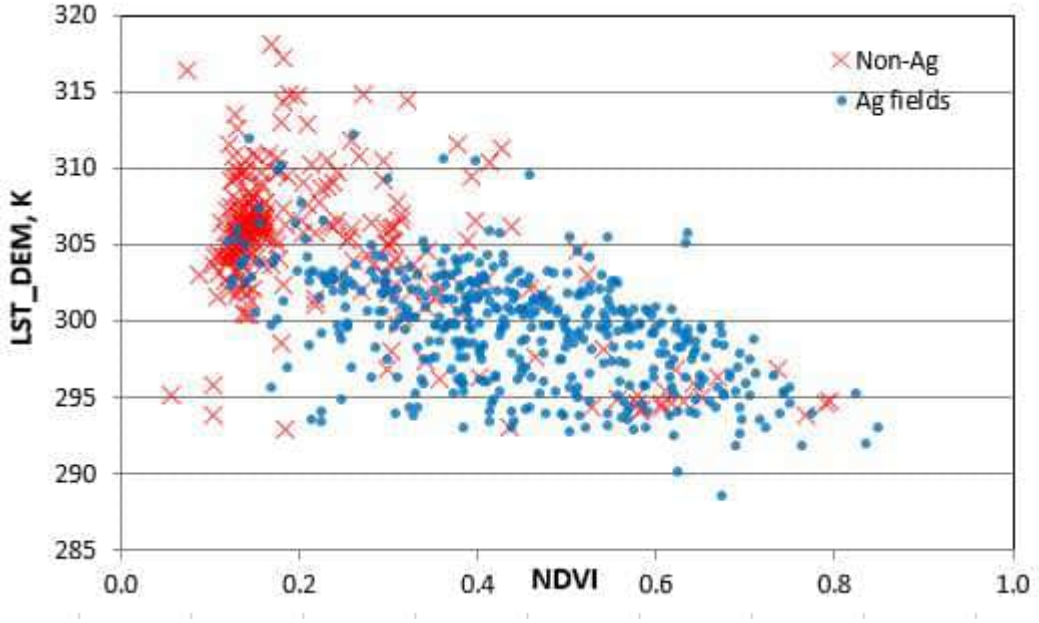

The graph for ETrF-EF vs. NDVI is as follows (where the blue points are agricultural fields, while the red crosses are Non-Agricultural fields):

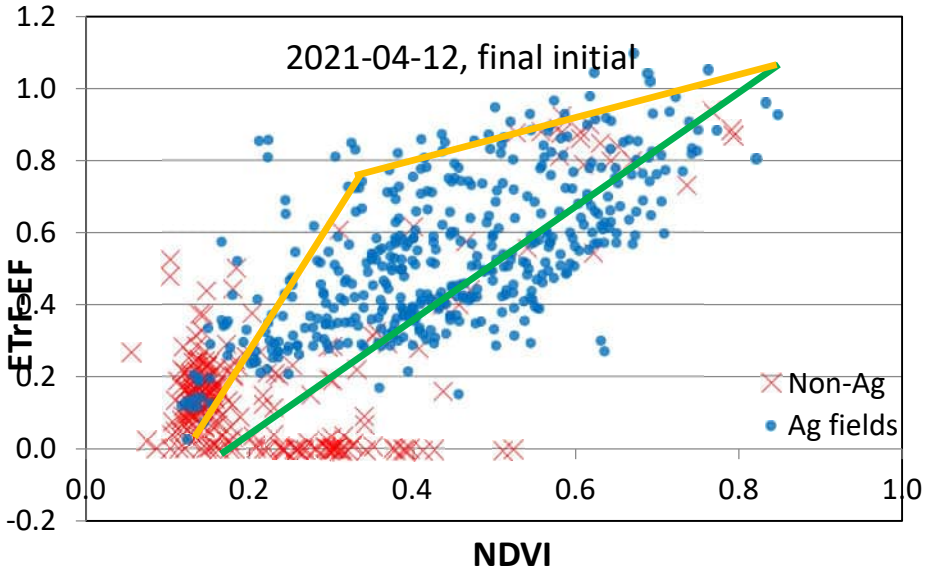

Based on the above figure and viewing of the ETrF image, the lower end of ETrF looks well calibrated, given the recent dry down of soil from rain and the large amount of low ETrF values near mid-NDVI. The upper end of ETrF can be reduced by about 0.05.

March 27, 2021

This image has a lot of clouds. However, the ag areas in the path overlap area that we interested in are clear. This was a difficult image to process because of the lower solar elevation. However, It is an important image to quantify the ETrF at the beginning of the growing season. Wind speed at overpass time was 5.4 m/s and ETr was 0.48 mm/h. There were 3.3 mm precipitation on March 12, 6.8 mm precipitation from March 15 to March 17, 0.8 mm on March 20 and 1.5 mm on March 22 and 23. The soil should be relatively dry without irrigation. Estimated Ke is 0.04 for the satellite overpass date and 0.05 for the previous day. ETrF at the cold pixel is set to 1.05 and at the hot pixel is set to 0.10. H at the hot pixel is 334 W/m^2 and at the cold pixel is 147 W/m^2.

The graph for de-lapsed surface temperature vs. NDVI is as follows (where the blue points are agricultural fields, and the red crosses are non-Agricultural fields):

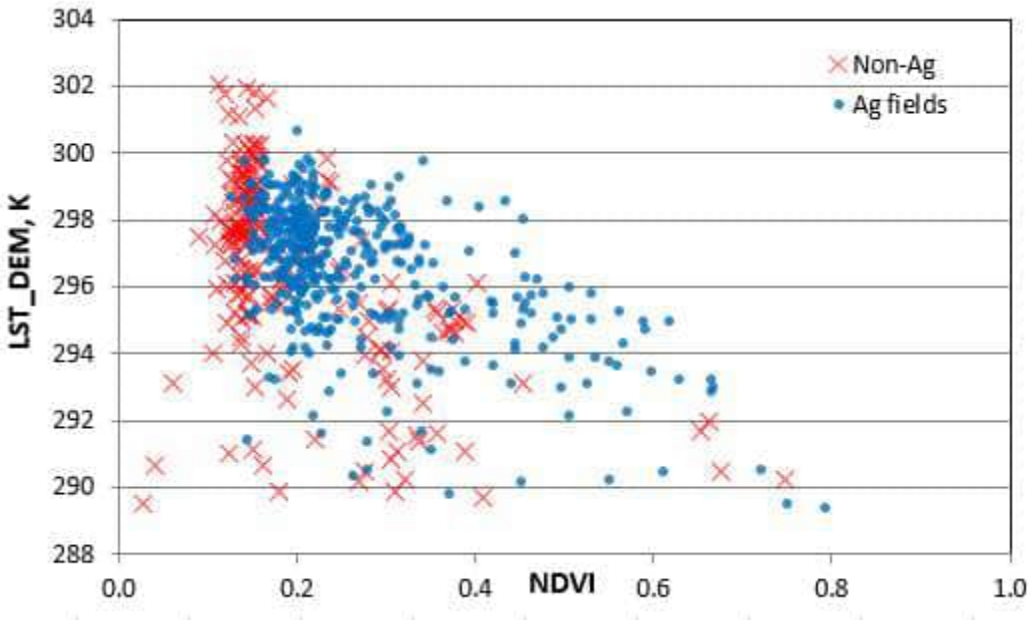

The graph for ETrF-EF vs. NDVI is as follows (where the blue points are agricultural fields, while the red crosses are Non-Agricultural fields):

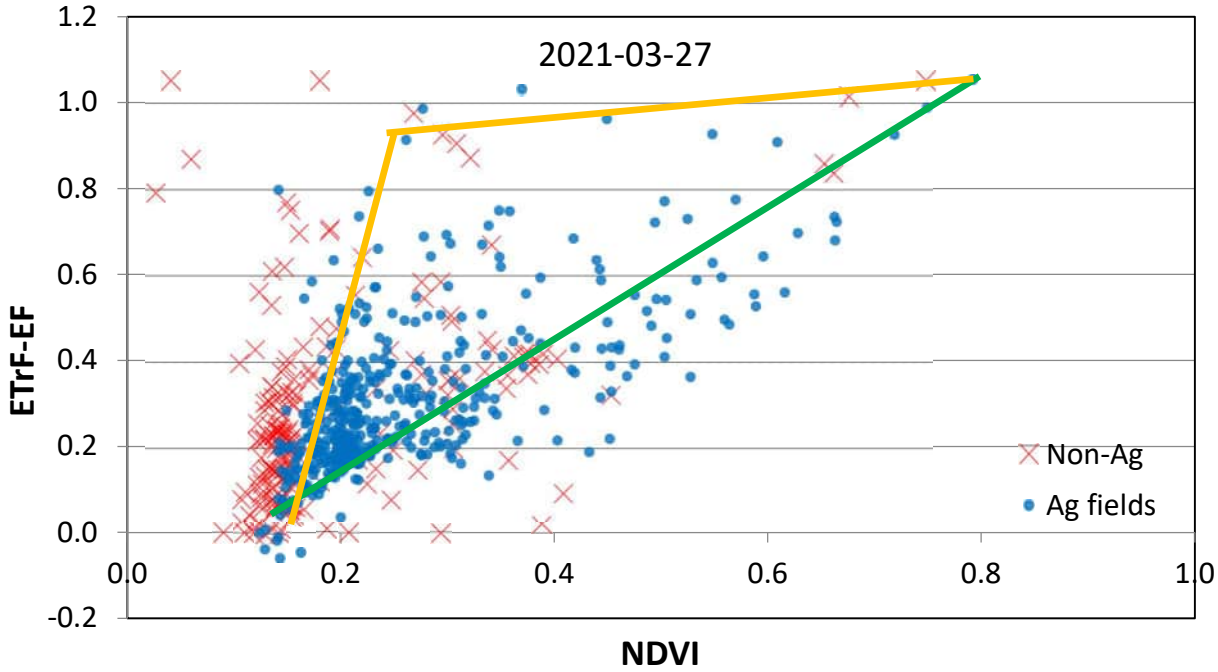

The calibration for ETrF at the lower end looks good. ETrF at the upper end can be reduced by 0.05 to 0.10 based on viewing the ETrF image.

Path 39 Landsat 8 Images:

June 6, 2021

This is a good clear Landsat 8 P39 image with almost no clouds. Wind speed was 6.8 m/s and ETr was relatively high at 1.24 mm/h. There was 0.25 mm (only one tip for the tipping bucket rain gauge) on each day for May 21, May 24 and June 4. All of that precipitation should have been consumed quickly under the June weather. Estimated Ke is 0.00 for the satellite overpass date and 0.01 for the previous day. ETrF at the cold pixel is set to 1.05 and at the hot pixel is set to 0.10.

H at the hot pixel is 214 W/m^2 and at the cold pixel is -279 W/m^2, indicating a very large amount of advected energy from the atmosphere to the irrigated fields. Even at the high wind speed of 6.8 m/s and during the summer conditions, the large negative H at the cold pixel of -279 W/m^2 seems large. We therefore decreased the ETr from 1.24 mm/h to 1.00 mm/h to reduce the advection effect As a result, H at the hot pixel becomes 230 W/m^2 and at the cold pixel is -107 W/m^2. The adjustment of ETr and Hcold does not impact the overall ETrF calibration. The calibration endpoints remain the same. The adjustment impacts the amount of atmospheric boundary layer stability and the estimated transfer of energy to the surface. This will tend to reduce some ETrF values in the middle ranges of NDVI.

The graph for de-lapsed surface temperature vs. NDVI is as follows (where the blue points are agricultural fields, and the red crosses are non-Agricultural fields):

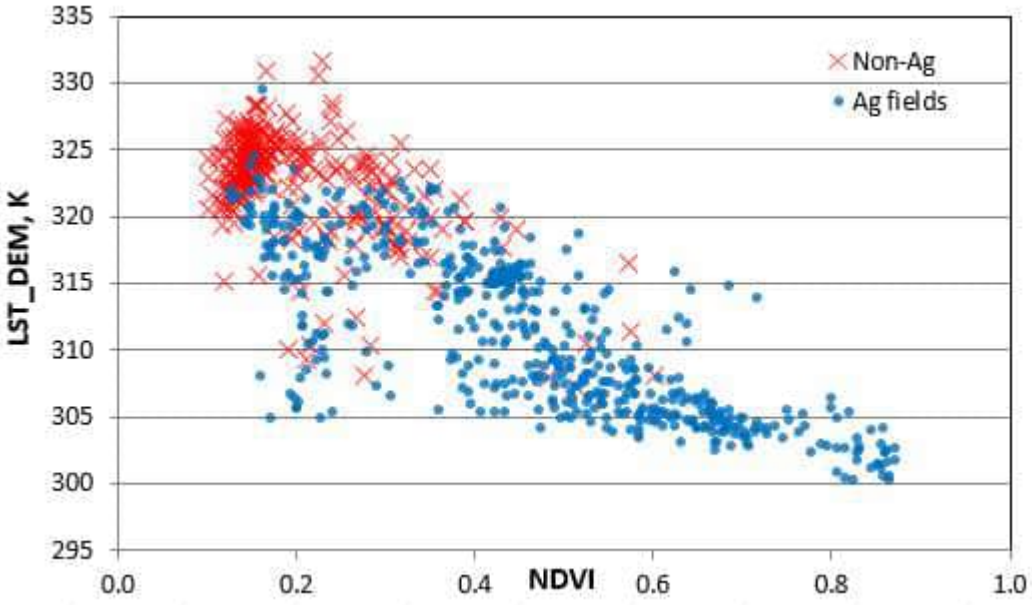

The graph for ETrF-EF vs. NDVI is as follows (where the blue points are agricultural fields, while the red crosses are Non-Agricultural fields):

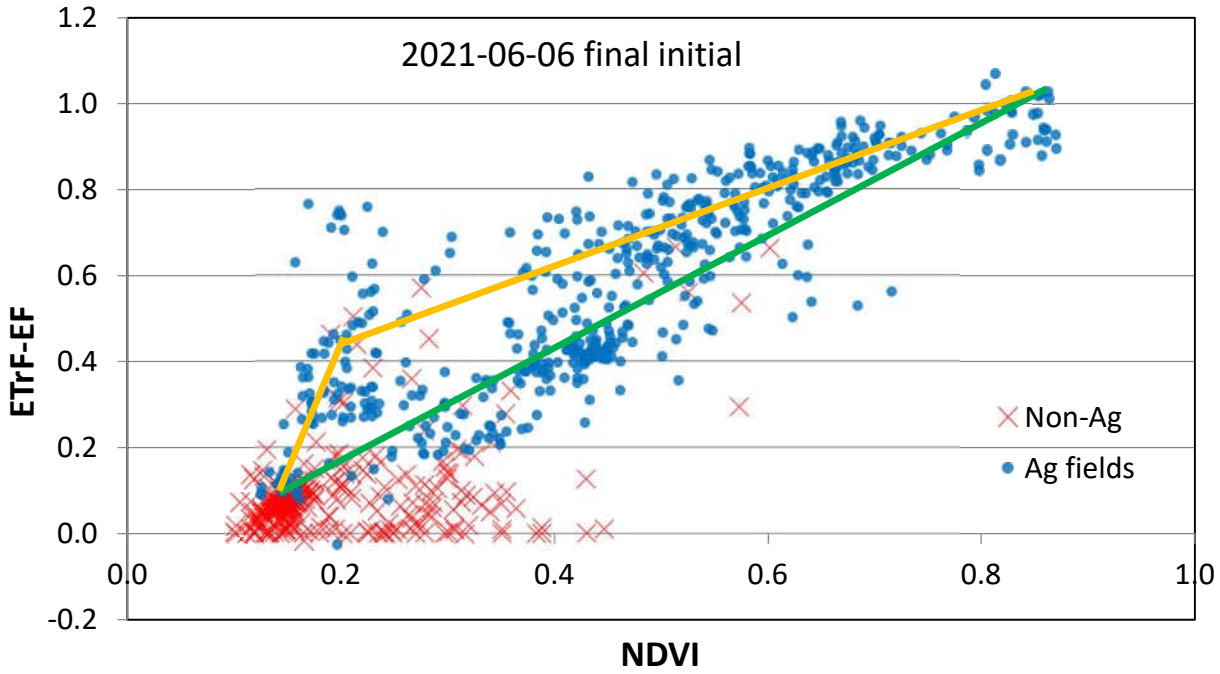

There is an upper ETrF vs. NDVI trend (orange line) for many of the sampled locations, possibly due to wetness of exposed soil from irrigation. The green line appears to represent a baseline trend between ETrF and NDVI.
Based on the ETrF vs. NDVI curve and the ETrF viewer, the ETrF at the lower end could be reduced by 0.10. The ETrF at the upper end appears to be OK.

July 8, 2021
This image has a lot of clouds. However, the ag areas that we are interested in are clear. Wind speed is 4.0 m/s and ETr is 1.26 mm/h. There was 6.8 mm rain from June 29 to July 1 according to the Beryl Junction weather station. This amount of precipitation would be consumed relatively quickly under the July weather conditions. Estimated Ke is 0.00 for the satellite overpass date and for the previous day. ETrF at the cold pixel is set to 1.05 and the hot pixel is set to 0.10. H at the hot pixel is 181 W/m^2 and at the cold pixel is -332 W/m^2. This indicates a very high amount of advection.
Even at a relatively high wind speed of 4.0 m/s and during the summer weather, it may be difficult for mixing of the near-surface boundary layer to transfer H from the boundary layer to the surface at the rate of -332 W/m^2. We therefore decreased the ETr from 1.26 mm/h to 0.95 mm/h. As a result, H at the hot pixel becomes 201 W/m^2 and at the cold pixel is -114 W/m^2. The reduction of ETr does not impact the endpoints of the calibration, which are set as ETrF. The reduction primarily impacts the calculation of boundary layer stability correction (buoyancy or lack of buoyancy).
The graph for de-lapsed surface temperature vs. NDVI is as follows (where the blue points are agricultural fields, and the red crosses are non-Agricultural fields):

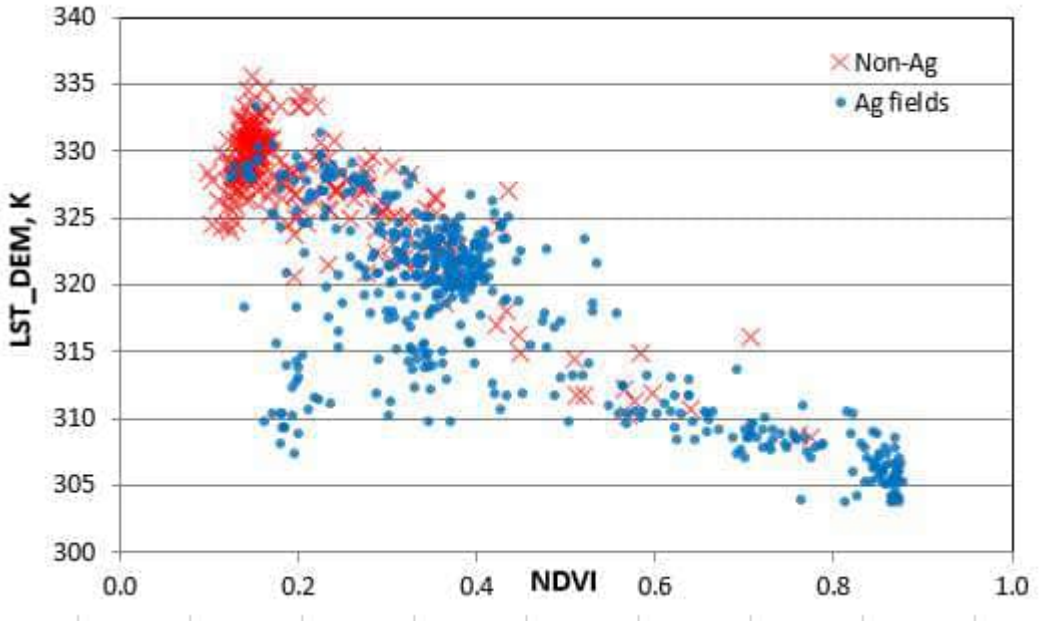

The graph for ETrF-EF vs. NDVI is as follows (where the blue points are agricultural fields, while the red crosses are Non-Agricultural fields):

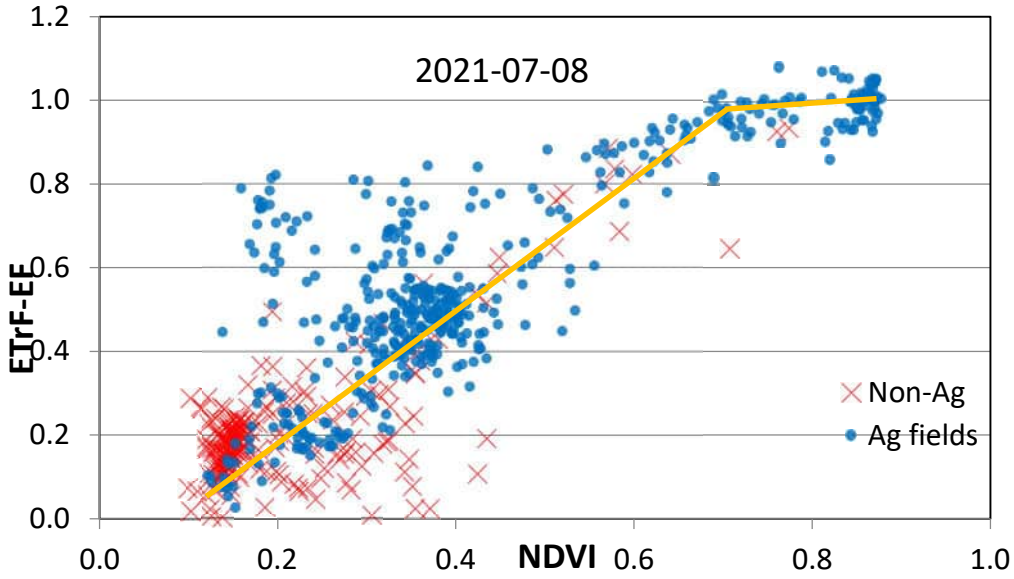

Based on the ETrF vs. NDVI graph and viewed ETrF, the upper end of ETrF is good. The lower end could be reduced by 0.07 or so, but is probably OK as is.

July 24, 2021

There were a lot of clouds distributed in the north, west and southern portions of the image. However, most of the ag areas that we are interested in were clear. Wind speed is quite low at 1.4 m/s and ETr is 0.78 mm/h. There was 27.7 mm rain from July 13 to 16, 7.6 mm rain from July 18 to 20 and 9.6 mm rain for July 22 to 23 recorded at the Beryl Junction Weather station. Estimated Ke is 0.29 for the satellite overpass date and 0.78 for the previous day, indicating rapid drying. ETrF at the cold pixel is set to 1.05 and at the hot pixel is set to 0.29. H at the hot pixel is 288.4 W/m^2 and at the cold pixel is -15.3 W/m^2.

The graph for de-lapsed surface temperature vs. NDVI is as follows (where the blue points are agricultural fields, and the red crosses are non-Agricultural fields):

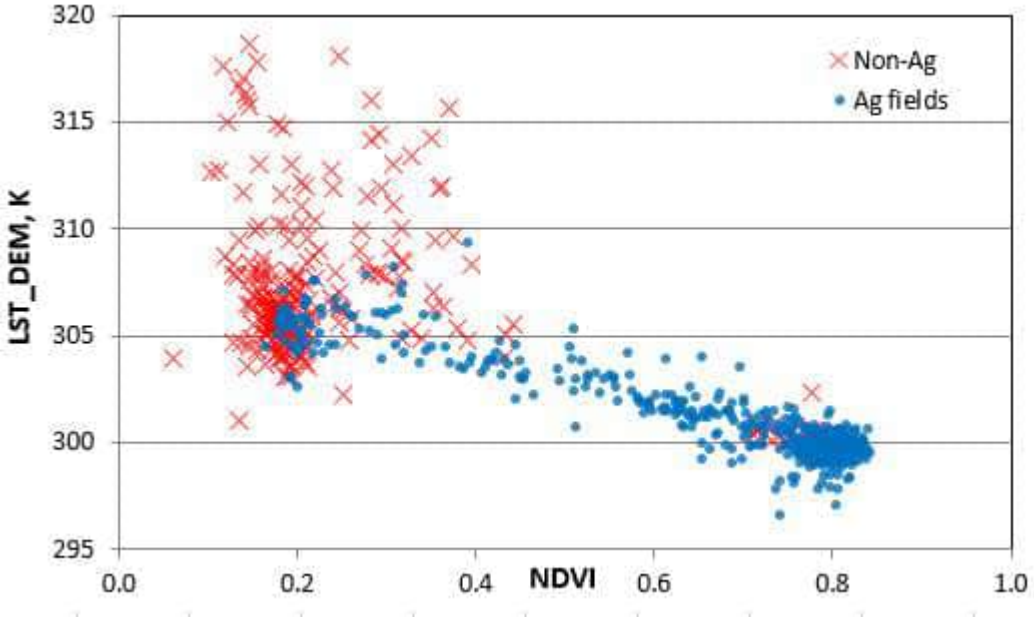

The graph for ETrF-EF vs. NDVI is as follows (where the blue points are agricultural fields, while the red crosses are Non-Agricultural fields):

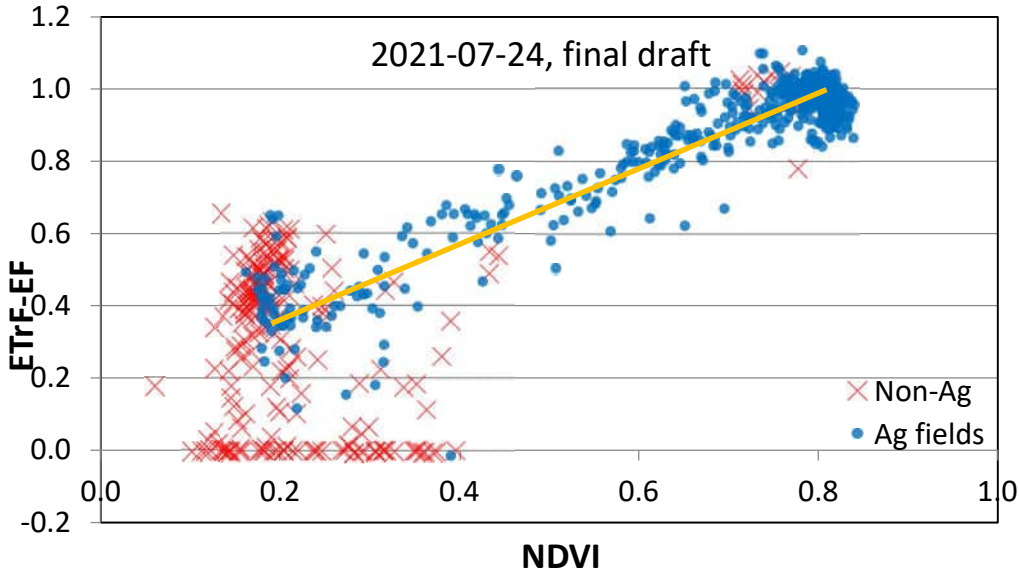

Based on the ETrF vs. NDVI plot and viewed ETrF, the ETrF at the upper end could be reduced by 0.04 or 0.05. The ETrF at the lower end appears to be good, based on the recent precipitation.

September 26, 2021

This seems to be a good image, regarding clearness, compared to most of the images during this year (year 2021). Although there were a few jet contrails near the east side and a few isolated small clouds at the north, most of the image was clear. Wind speed is low at 1.55 m/s and ETr is 0.70 mm/h. There was only 3.8 mm rain on September 18. Other than that, there was not any

other precipitation since September 2. Estimated Ke is 0.00 for the satellite overpass date and for the previous day. ETrF at the cold pixel is set to 1.03 and at the hot pixel is set to 0.10.
The resulting ETrF seemed a little bit high at the higher end (please see the following graph) when we set the ETrF at the cold pixel at 1.05 and there were not any other appropriate sample pixels that could be set to 1.05. Therefore, we stayed with the selected sampled cold pixel and decreased the assigned ETrF value from 1.05 to 1.03. With this assignment, H at the hot pixel is 226.1 W/m^2 and at the cold pixel is -29.6 W/m^2.

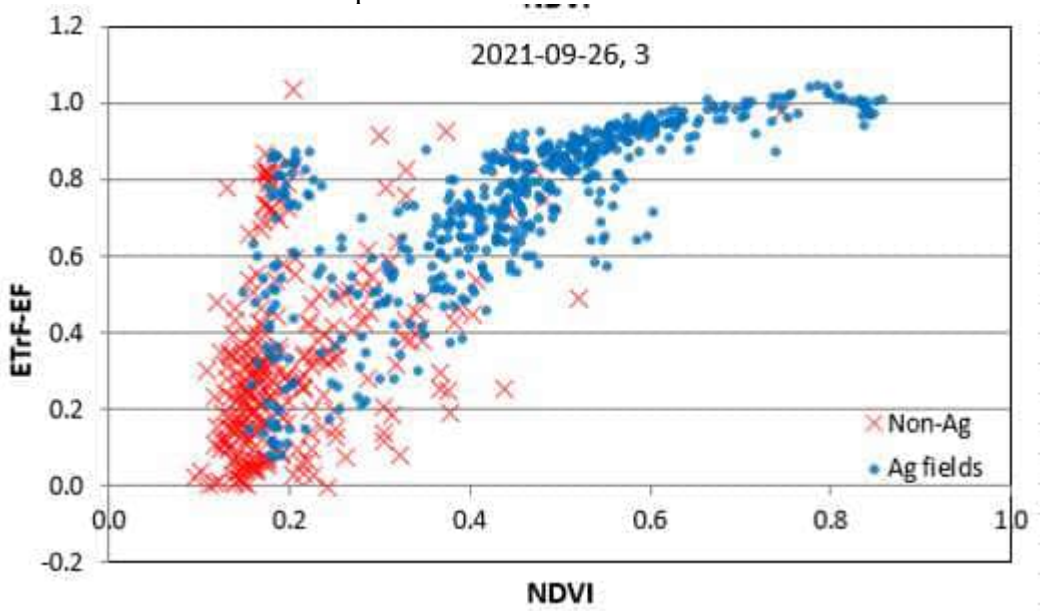

The graph for de-lapsed surface temperature vs. NDVI is as follows (where the blue points are agricultural fields, and the red crosses are non-Agricultural fields):

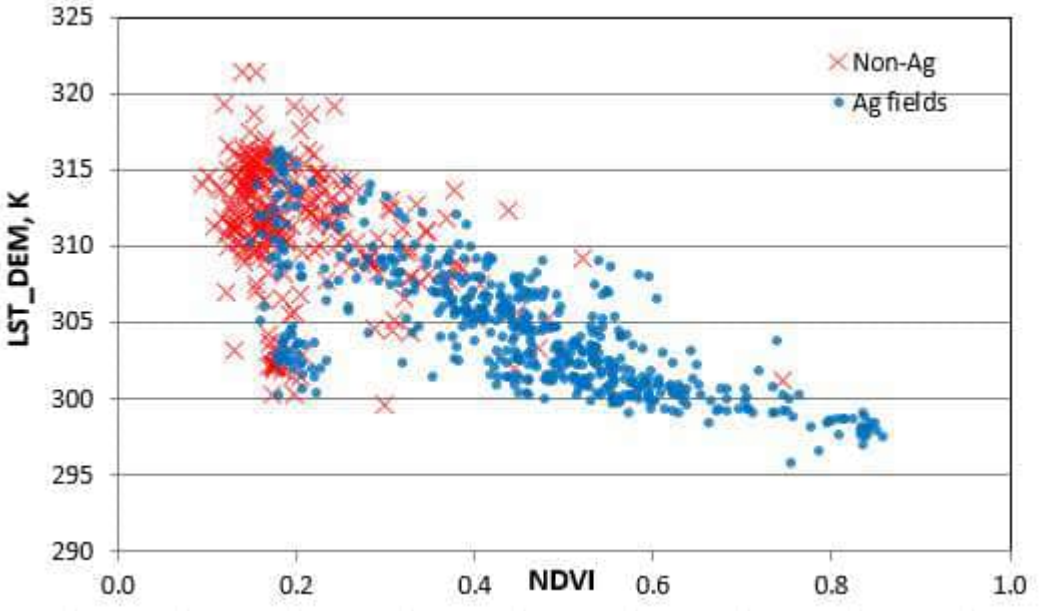

The graph for ETrF-EF vs. NDVI is as follows (where the blue points are agricultural fields, while the red crosses are Non-Agricultural fields):

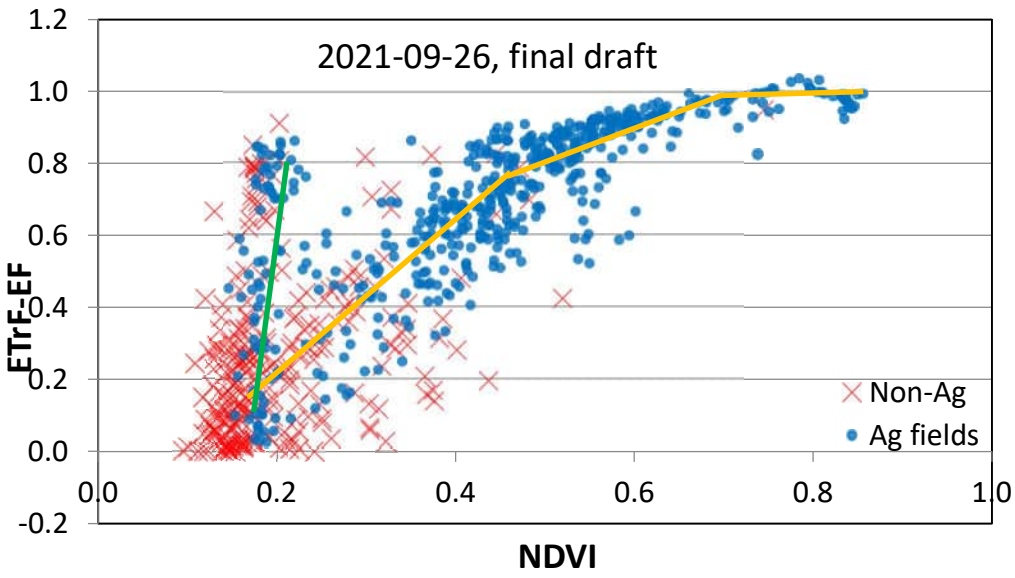

This plot of ETrF vs. NDVI shows a 3-part primary trend line (orange lines) and with a secondary (green) trend line near low NDVI where ETrF is elevated, probably due to recently harvested corn and/or alfalfa that thereby had low NDVI but high residual ET from wet soil. Based on the ETrF plot and viewed ETrF, the calibration is judged to be good. The ETrF at the lower end could be reduced by 0.10, but it is probably realistic and good as is.

October 28, 2021

This is a good image with no clouds. However, the solar elevation is low at image time due to the time of year, which makes it difficult to calibrate. Wind speed is relatively high at 6.4 m/s and ETr is 0.52 mm/h. There was 31.5 mm rain from 5:00 pm on October 25 to 1:00 am on October 26. Therefore, the soil was quite wet on the image date on October 28. Estimated Ke is 1.00 for both the satellite overpass date and for the previous day. ETrF at the cold pixel is set to 1.05 and at the hot pixel is set to 0.70. We set the ETrF at the hot pixel to 0.70 instead of 1.0 to get a significant difference between the hot and cold pixel (The average Ke in October is 0.51). H at the hot pixel is 32 W/m^2 and at the cold pixel is -10 W/m^2, indicating a relatively small spread in H and Ts. Ts at the hot pixel is 292.9 K and at the cold pixel is 288.1 K. There ws only 4.8 K difference in Ts. At the late October date and a relatively wet hot pixel, this seems to be realistic.

The graph for de-lapsed surface temperature vs. NDVI is as follows (where the blue points are agricultural fields, and the red crosses are non-Agricultural fields):

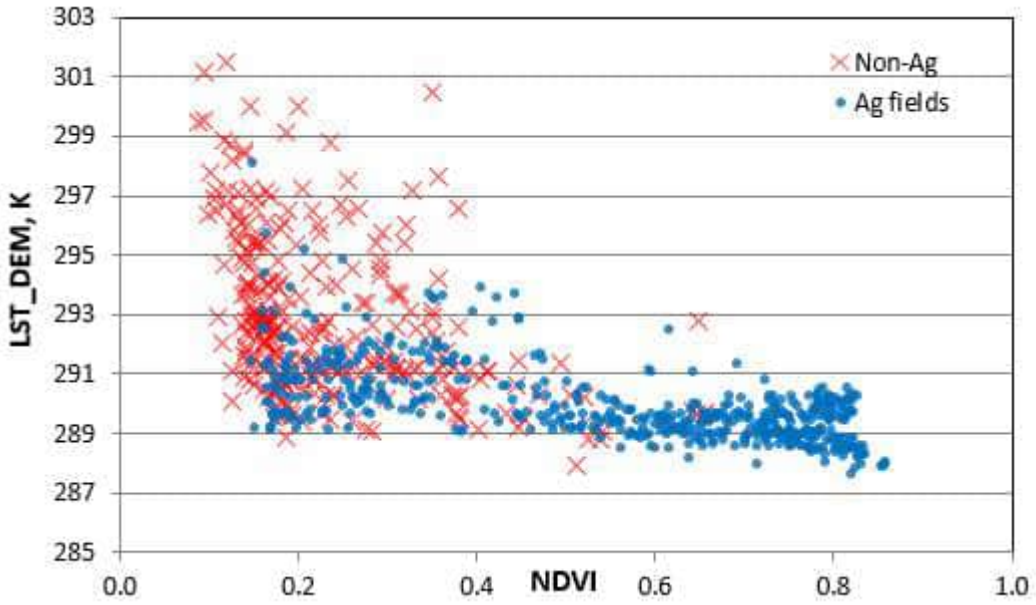

The graph for ETrF-EF vs. NDVI is as follows (where the blue points are agricultural fields, while the red crosses are non-Agricultural fields):

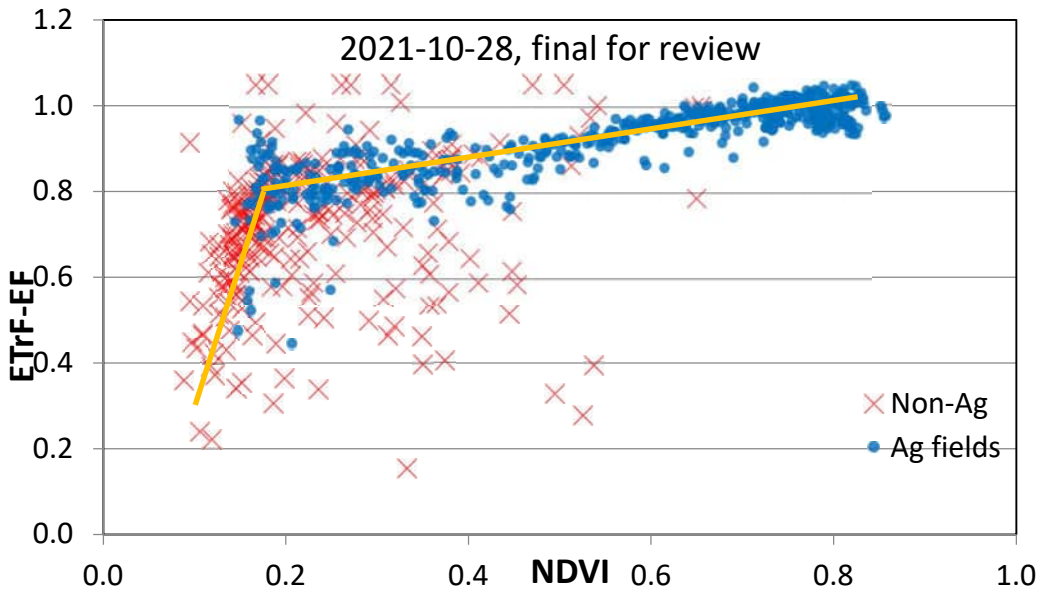

The image area was quite wet due to the recent rains as is evident in the following screenshot of ETrF for the study area. Dark greens are highest ETrF (near 1.0) and moderate greens have ETrF around 0.8. Beige colors represent lower ETrF of generally less than 0.2.

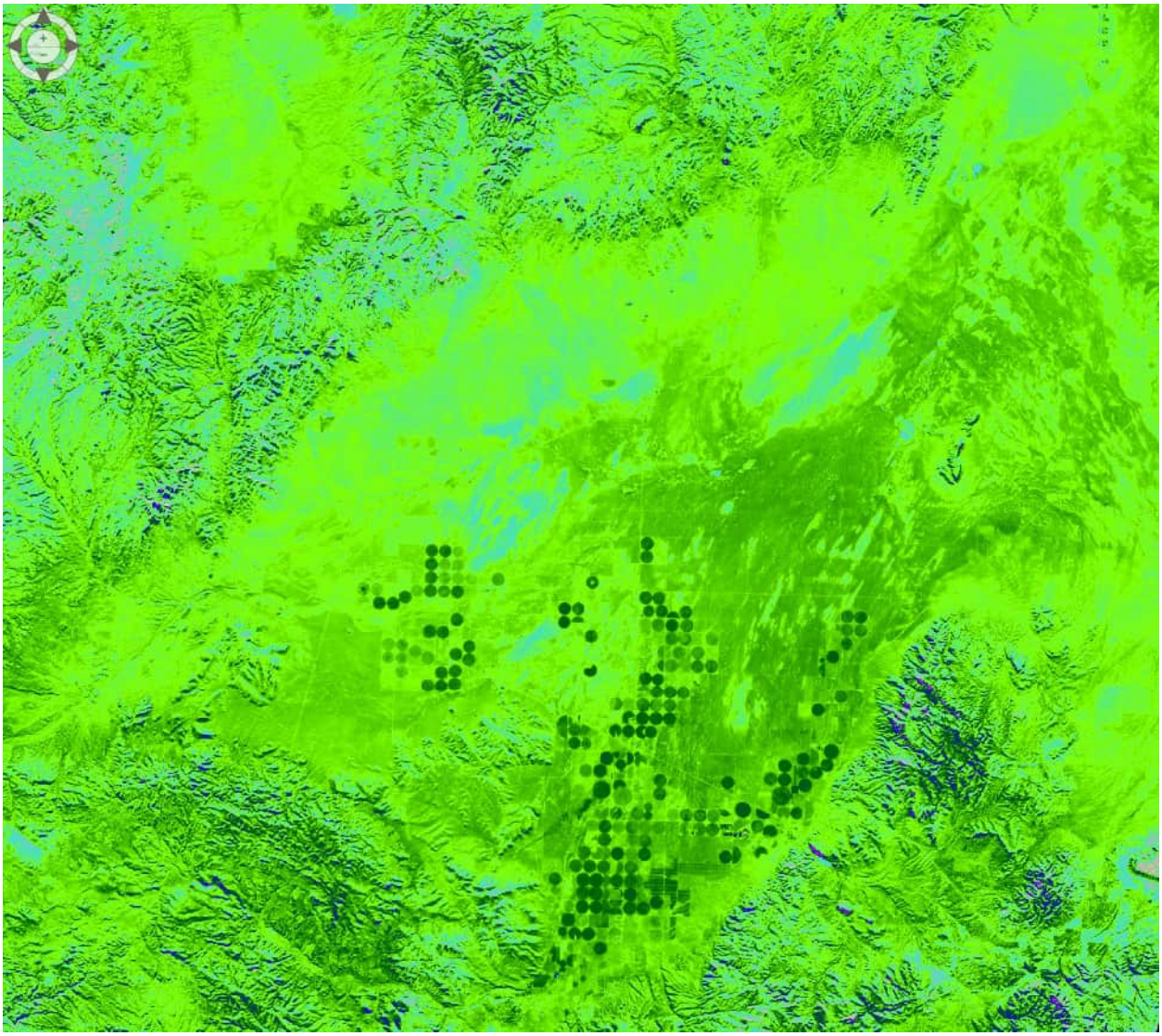

Based on the large amount of recent rains, the calibration of the image is judged to be good. However, we may or may not wish to use this image date during integration of ETrF images into monthly and growing season ET due to its wetness and possible nonrepresentativeness of the surrounding time period (month).

May 21, 2021

This were quite a few clouds on the western 1/3 of the image and a few isolated clouds on the east side of the image. However, most of the ag areas that we are interested in were clear, except there were a few clouds with coverage over the east few fields. Since it was difficult to find clear images during this period, we still processed this image for most of the ag areas and it should be useable for splining during the time integration step. Wind speed was high at 8.56 m/s and ETr was 0.81 mm/h. There was 0.25 mm precipitation each on May 16 and May 17 and 0.5 mm precipitation on May 18. The last large rain event was 15 mm on April 26-27. There was 0.25 mm (0.01 inch) of rain noted for the image date (May 21), however, this occurred at 10 pm after the satellite overpass. These little amounts of precipitation would have been evaporated

relatively quickly. Estimated Ke is 0.0 for both the satellite overpass date and for the previous day. ETrF at the cold pixel is set to 1.05 and at the hot pixel is set to 0.10. H at the hot pixel is 351.7 W/m^2 and at the cold pixel is -3.0 W/m^2.
The graph for de-lapsed surface temperature vs. NDVI is as follows (where the blue points are agricultural fields, and the red crosses are non-Agricultural fields):

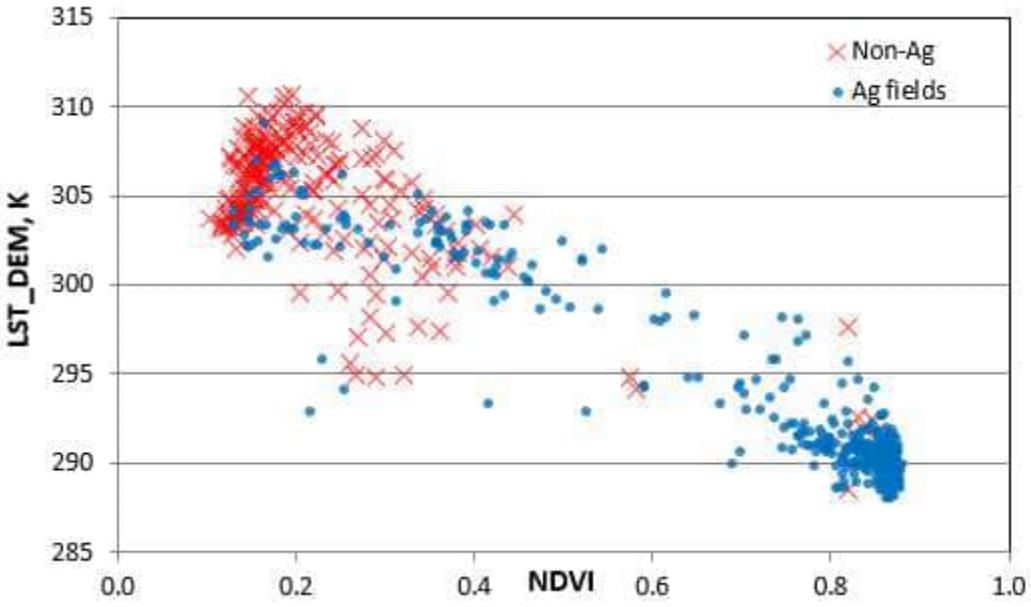

The graph for ETrF-EF vs. NDVI is as follows (where the blue points are agricultural fields, while the red crosses are non-Agricultural fields):

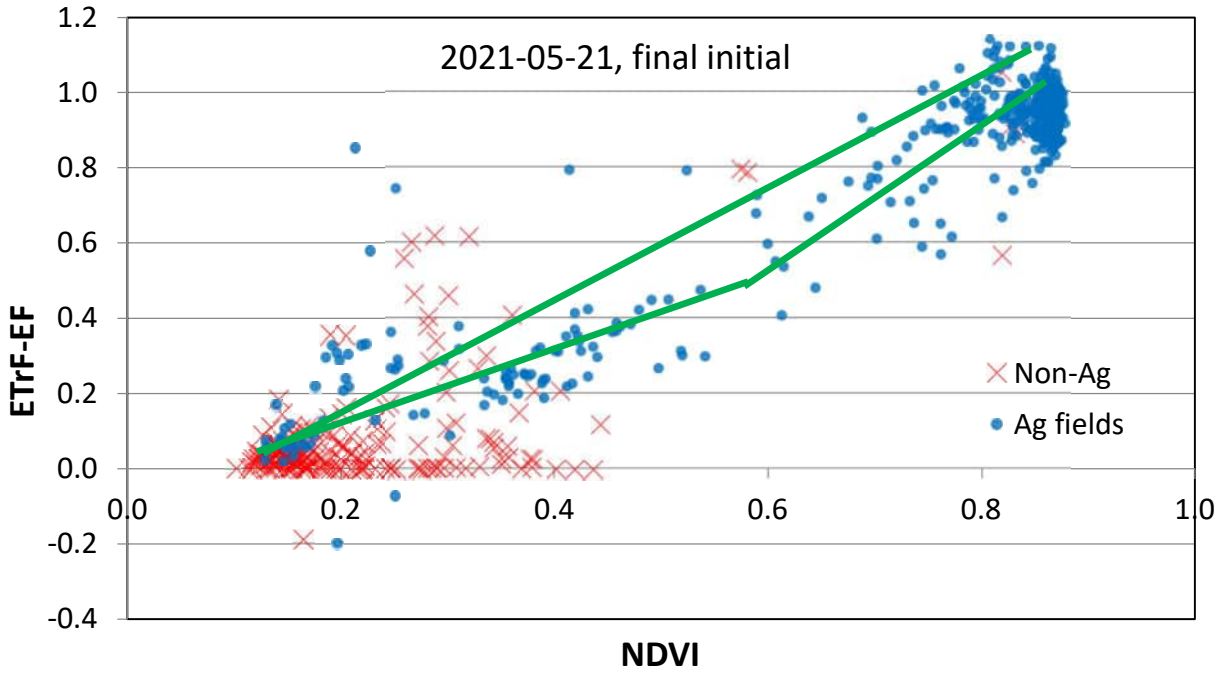

The sampled locations exhibited some elevated LST over the midrange of NDVI. These may have been some alfalfa fields during a regrowth period or developing corn plants that exhibited

some stress or very dry soil between plants. The elevated LST translated into reduced ETrF in the NDVI midrange (green broken line in the above figure). As for May 5, most sampled fields were at full ground cover.
Based on the ETrF vs. NDVI plot and ETrF viewer, the ETrF at the upper end could be reduced by 0.05 and the ETrF at the lower end could be reduced by 0.05.

May 05, 2021
This is a good, clear image with no clouds. Wind speed was 4.3 m/s and ETr was 0.84 mm/h. There was 0.25 mm rain on May 2 and 15 mm rain from April 26 to April 27 (one week prior) based on the Beryl Junction weather station. Estimated Ke is 0.01 for both the satellite overpass date and the previous day. However, some fields may have more residual evaporation. ETrF at the cold pixel is set to 1.05 and at the hot pixel is set to 0.10. H at the hot pixel is 256.5 W/m^2 and at the cold pixel is -6.0 W/m^2.
The graph for de-lapsed surface temperature vs. NDVI is as follows (where the blue points are agricultural fields, and the red crosses are non-Agricultural fields):

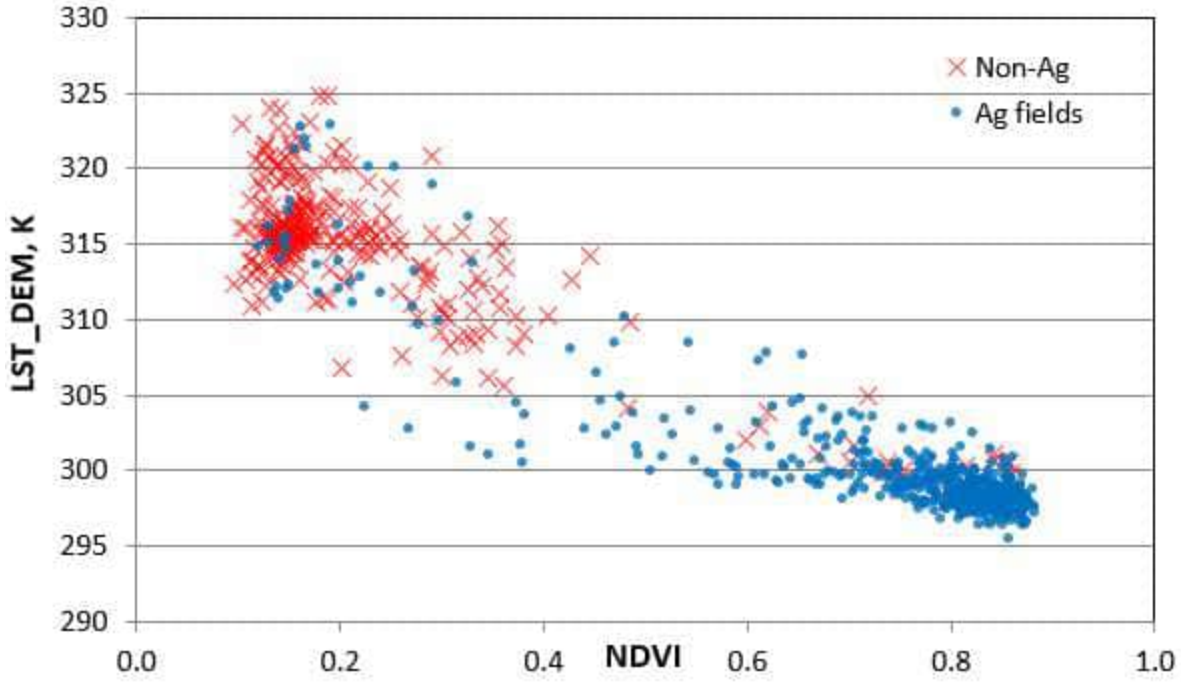

The graph for ETrF-EF vs. NDVI is as follows (where the blue points are agricultural fields, while the red crosses are non-Agricultural fields):

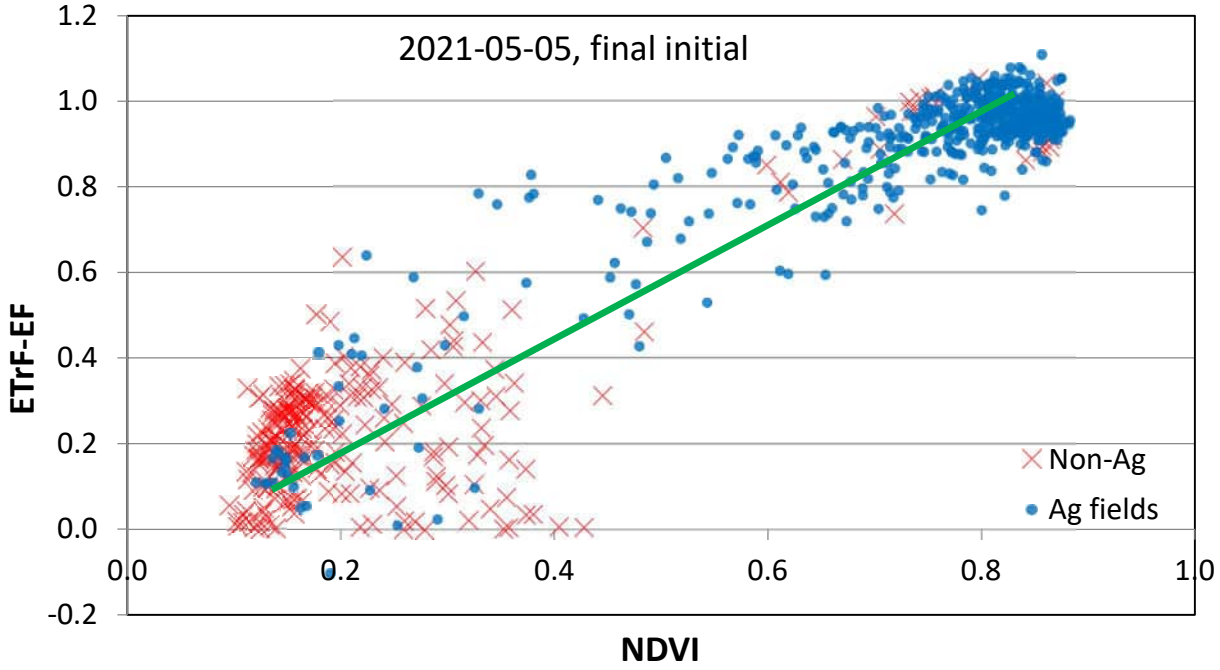

Near all fields are at full cover, probably due to the large presence of alfalfa and possibly winter grain. Based on the ETrF vs. NDVI plot and the ETrF viewer, the lower end of ETrF could be reduced by 0.08 or so. The upper end is OK as is, but could be reduced by about 0.03 (minor adjustment).

April 19, 2021

This is a good, clear image. The solar elevation is low, so that the range in LST is small, making calibration somewhat more challenging. The Fmask cloud masking indicated that there were some isolated clouds here and there inside the image, however, we could not find any visible clouds within the whole image. Wind speed was relatively high at 4.9 m/s and ETr was 0.86 mm/h. There were 13.7 mm of precipitation received on April 6 and 1.5 mm of precipitation on April 16 according to the Beryl Junction weather station. Estimated Ke is both 0.01 for the satellite overpass date and for the previous day. ETrF at the cold pixel is set to 1.05 and at the hot pixel is set to 0.10. H at the hot pixel is 273 W/m^2 and at the cold pixel is -66 W/m^2.
The graph for de-lapsed surface temperature vs. NDVI is as follows (where the blue points are agricultural fields, and the red crosses are non-Agricultural fields):

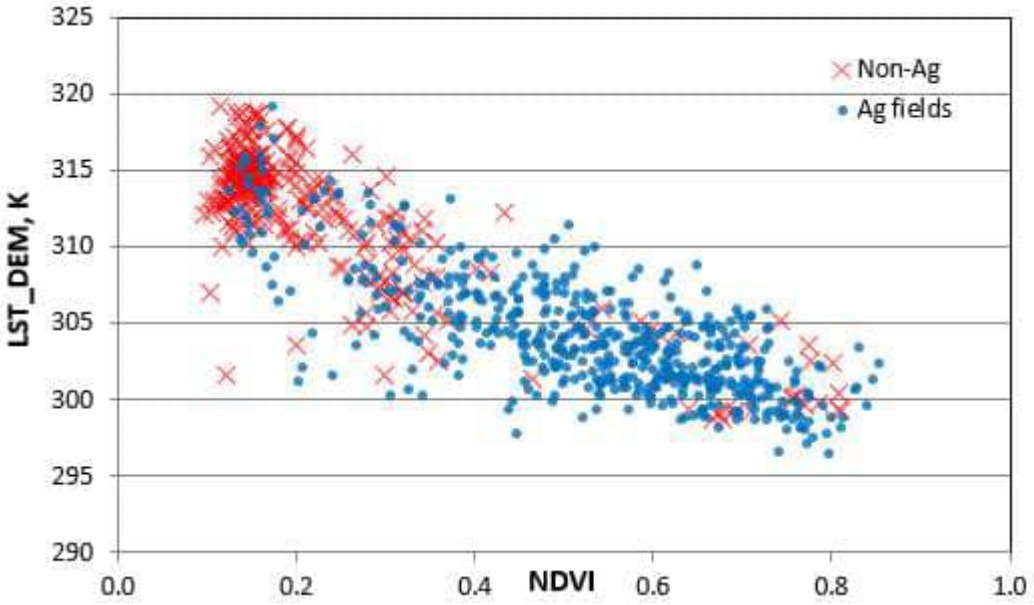

The graph for ETrF-EF vs. NDVI is as follows (where the blue points are agricultural fields, while the red crosses are non-Agricultural fields):

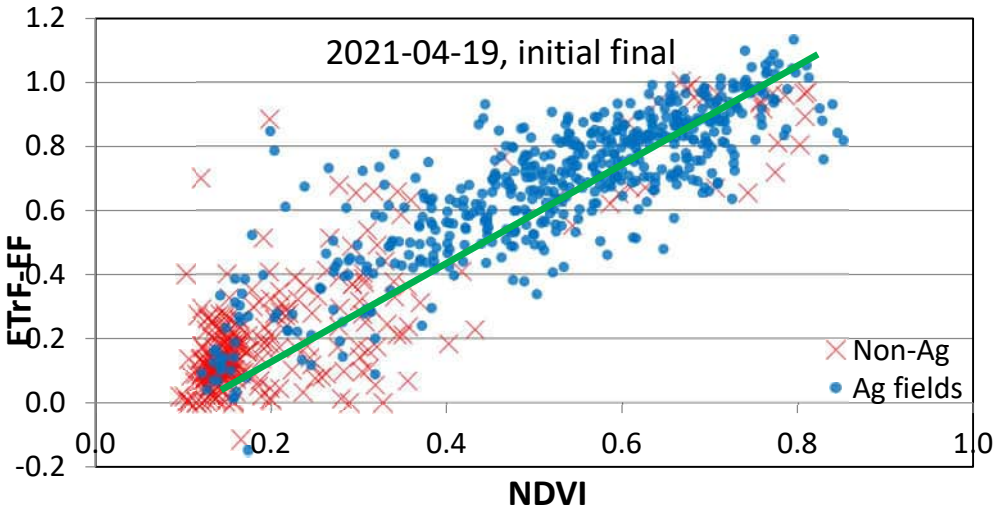

Based on the ETrF vs. NDVI plot and review of ETrF in the viewer, the lower end could be reduced by 0.05. The upper ETrF could be reduced by 0.10.

Path 38 Landsat 7 Images:

Since there were no clear Landsat 8 images from August 2 to September 3, Landsat 7 images were examined to process during that period. In addition, L8 images were cloudy during late March and early April so that the April 4 Landsat 7 image was process. The agricultural areas of interest are located near the edge of the Landsat 7 images and therefore SLC-off gaps are present. Landsat 7 images for August 10 and August 26 were good images, with 4% and 0% cloud percentages, respectively, according to the USGS assessment.

April 4, 2021

This was a good, clear Landsat 7 image with only 1% clouds overall, and with those occurring over the mountains. The agricultural area that we are interested was clear. Unfortunately there are SLC-off gaps over the agricultural areas that we are interested in. Also, because of the lower solar altitude in early April, this was an image that was challenging to calibrate. Wind speed at satellite overpass time was 2.3 m/s and ETr was 0.64 mm/h. There were 6.8 mm of precipitation from March 15 to March 17, 0.8 mm on March 20 and 1.5 mm precipitation from March 22 to March 23. After that, there was no rain for 11 days before the image date. Estimated Ke is 0.00 both for the satellite overpass date and for the previous day. ETrF at the cold pixel is set to 1.00 and at the hot pixel is set to 0.10. H at the hot pixel is 209 W/m^2 and at the cold pixel is 11 W/m^2.

The graph for de-lapsed surface temperature vs. NDVI is as follows (where the blue points are agricultural fields, and the red crosses are non-Agricultural fields):

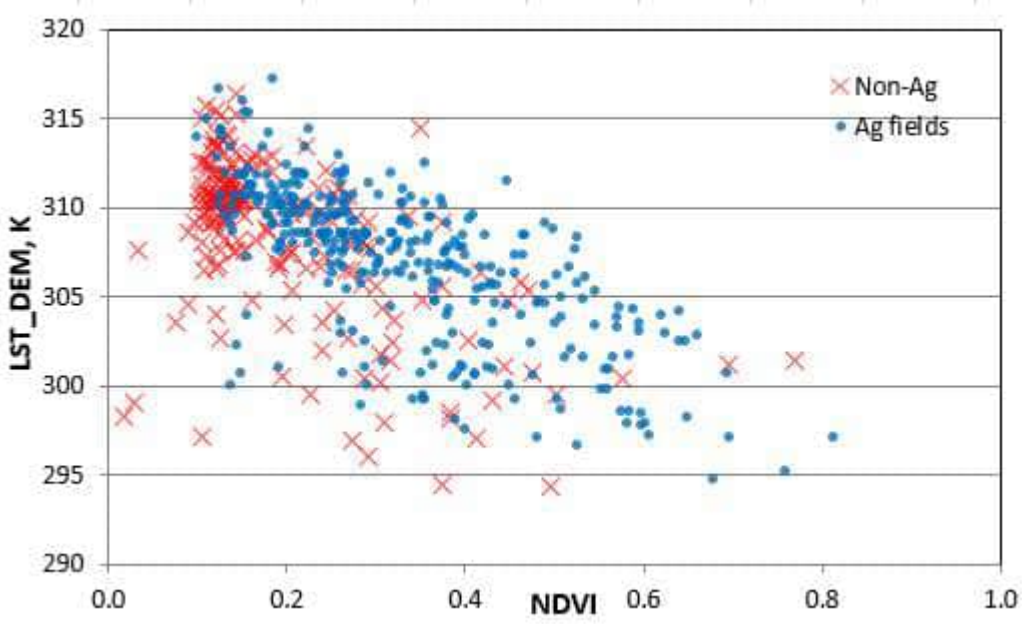

The graph for ETrF-EF vs. NDVI for the initial final calibration iteration, prior to final calibration adjustment, is as follows (where the blue points are agricultural fields, while the red crosses are non-Agricultural fields):

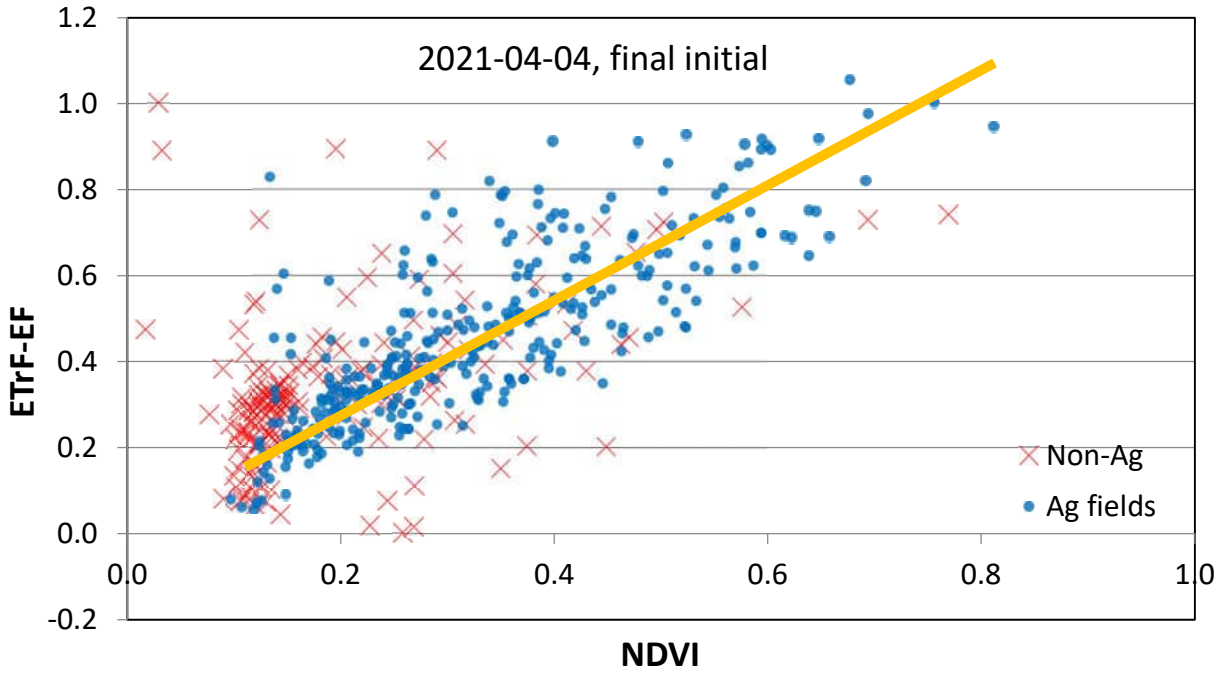

Based on the above figure, we have reduced the ETrF at the high end of NDVI by 0.10 and have reduced the ETrF at the low end of NDVI by 0.10.

August 10, 2021

This was a clear image with some clouds over the mountains. The agricultural areas that we are interested in were clear. Wind speed was very low at overpass time, at 0.78 m/s, and therefore, ETr was also low at 0.58 mm/h because of the low wind speed. There was an unusually high total of 61 mm of precipitation received between July 28 to August 1. After that, there was no rain for the 9 days before the image date. Estimated Ke is both 0.01 for the satellite overpass date and for the previous day, indicating that any bare soil should have dried down to nearly air dry by the overpass date. ETrF at the cold pixel was set to 1.00 and at the hot pixel was set to 0.10. H at the hot pixel is 261 W/m^2 and at the cold pixel is 56 W/m^2, indicating positive heat flux due to the low wind speeds and buoyancy effects.

The graph for de-lapsed surface temperature vs. NDVI is as follows (where the blue points are agricultural fields, and the red crosses are non-Agricultural fields):

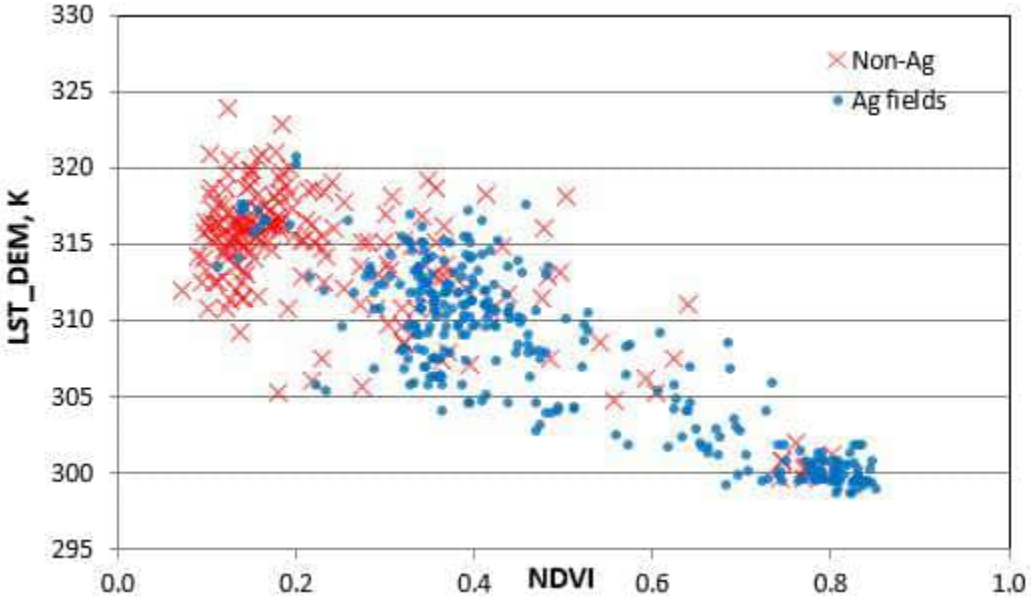

The graph for ETrF-EF vs. NDVI is as follows (where the blue points are agricultural fields, while the red crosses are non-Agricultural fields):

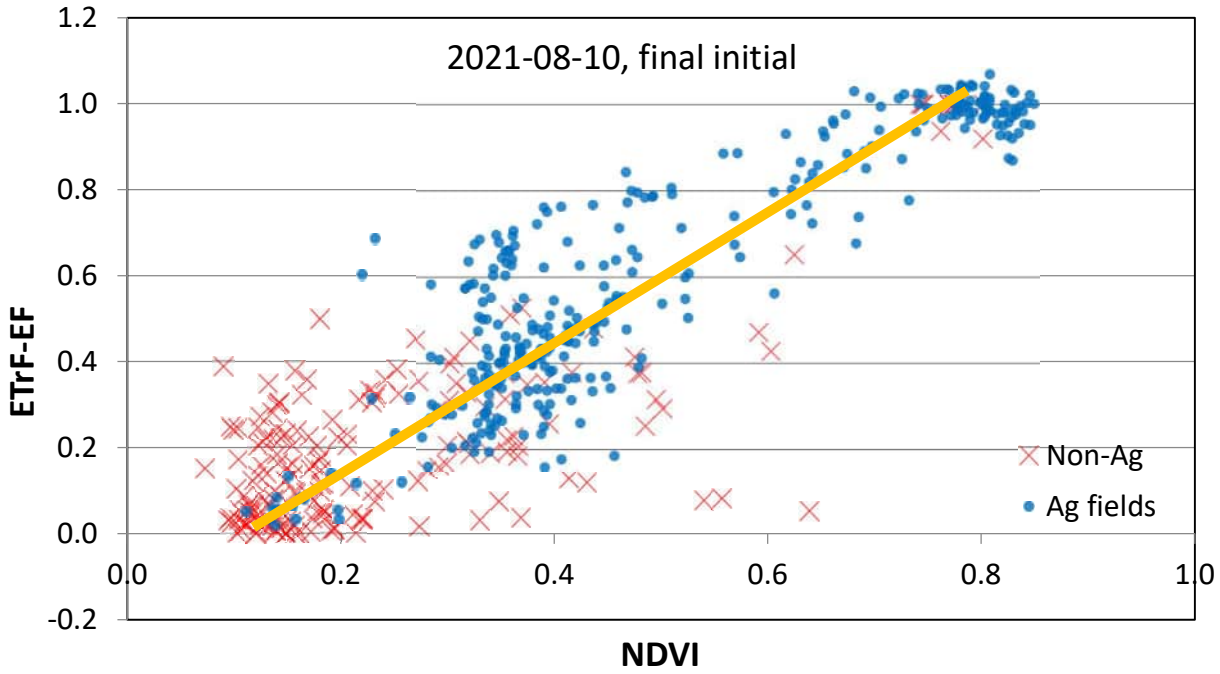

Based on the final calibration for the initial calibration step, as shown in the figure above, we accepted that calibration. The upper end could be reduced by about 0.03, but that amount is well within the uncertainty of the METRIC model.

August 26, 2021

This image is a clear Landsat 7 image with no clouds. Unfortunately there are SLC-off gaps over some of the agricultural areas that we are interested in. Wind speed was relatively low at 1.7 m/s and ETr was correspondingly low at 0.6 mm/h for Mid-August because of the low wind speed. There was 9.7 mm of precipitation on August 18 and 0.5 mm on August 19. Since then, there was no rain for 5 days before the image date. Estimated Ke is 0.00 both for the satellite overpass date and for the previous day, indicating that any exposed soil should be dry or nearly dry at overpass time. ETrF at the cold pixel is set to 1.05 and at the hot pixel is set to 0.10. H at the hot pixel is 192 W/m^2 and at the cold pixel is 1 W/m^2.

The graph for de-lapsed surface temperature vs. NDVI is as follows (where the blue points are agricultural fields, and the red crosses are non-Agricultural fields):

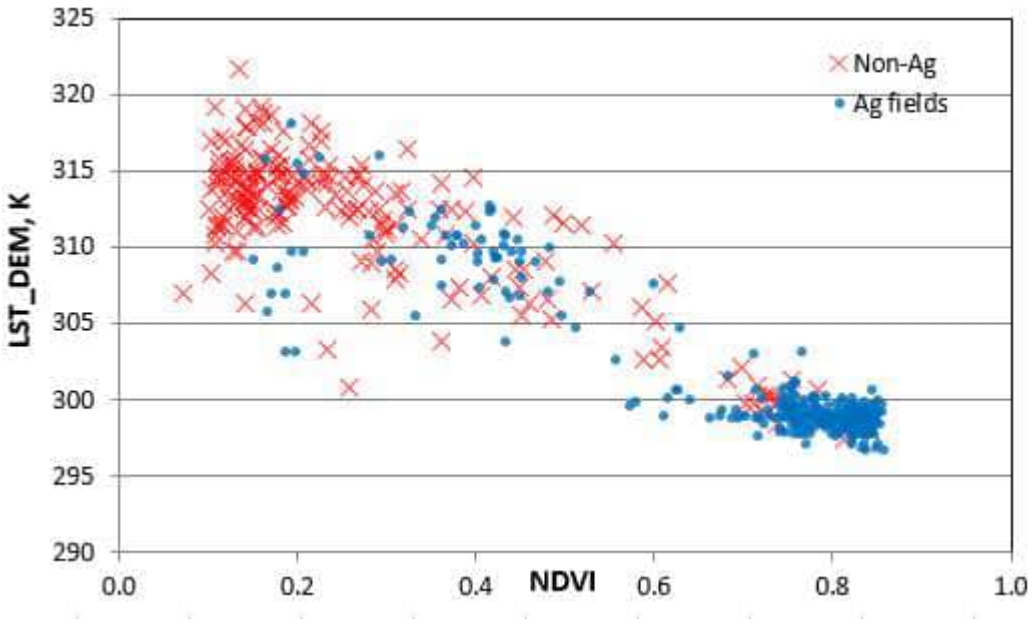

The graph for ETrF-EF vs. NDVI is as follows (where the blue points are agricultural fields, while the red crosses are non-Agricultural fields):

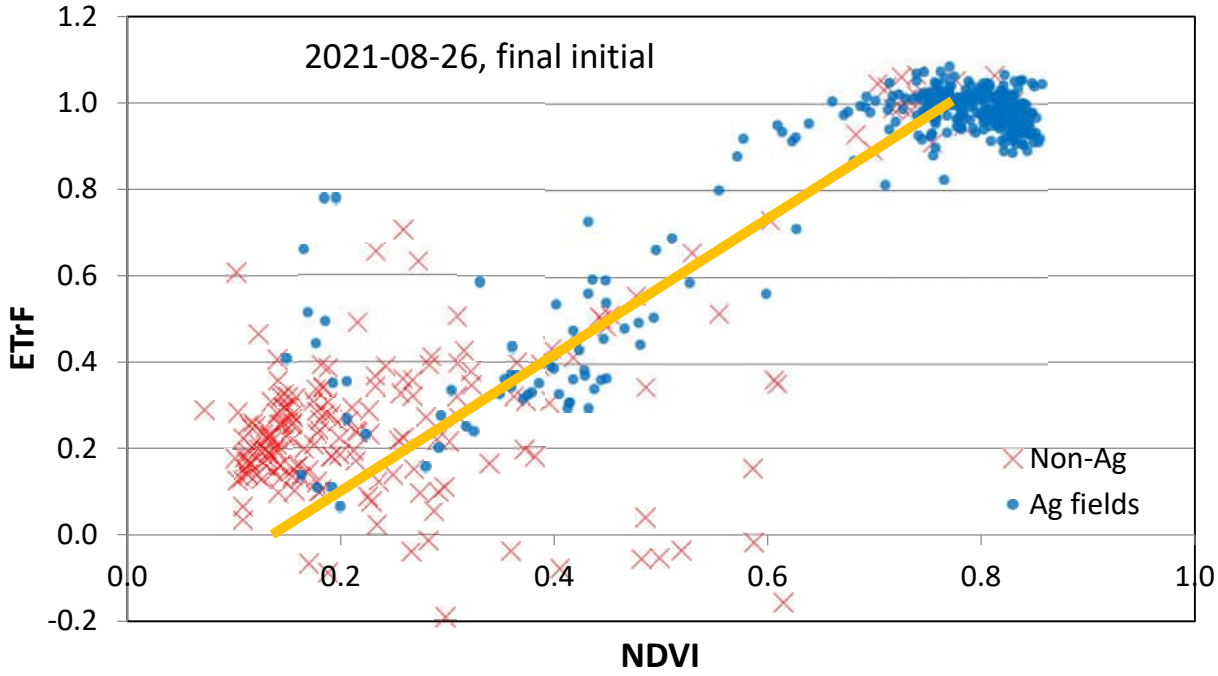

The upper end of ETrF agrees well with a 1.0 average ETrF for full cover conditions and the approximate lower end of ETrF intersects with approximately 0.0 representing the dry or near dry conditions for bare soil. Some residual evaporation was sampled (red symbols) for rangeland areas, indicating some response from shrubs or grasses due to the rains or some residual evaporation. The calibration is judged to be good.

September 27, 2021

This was a good, clear Landsat 7 image with only 1% clouding toward the east side of the image. The agricultural area that we are interested were clear. Unfortunately SLC-off gaps exists over the agricultural areas that we are interested in. Wind speed at overpass time was relatively low at 1.3 m/s and ETr was also low at 0.47 mm/h because of the low wind speed. There were 4.1 mm of precipitation from August 31 to September 1 and 3.8 mm precipitation on September 18. Since then, there was no rain for 7 days before the image date. Estimated Ke is 0.00 both for the satellite overpass date and for the previous day. ETrF at the cold pixel is set to 1.00 and at the hot pixel is set to 0.10. H at the hot pixel is 108 W/m^2 and at the cold pixel is 38 W/m^2.
The graph for de-lapsed surface temperature vs. NDVI is as follows (where the blue points are agricultural fields, and the red crosses are non-Agricultural fields):

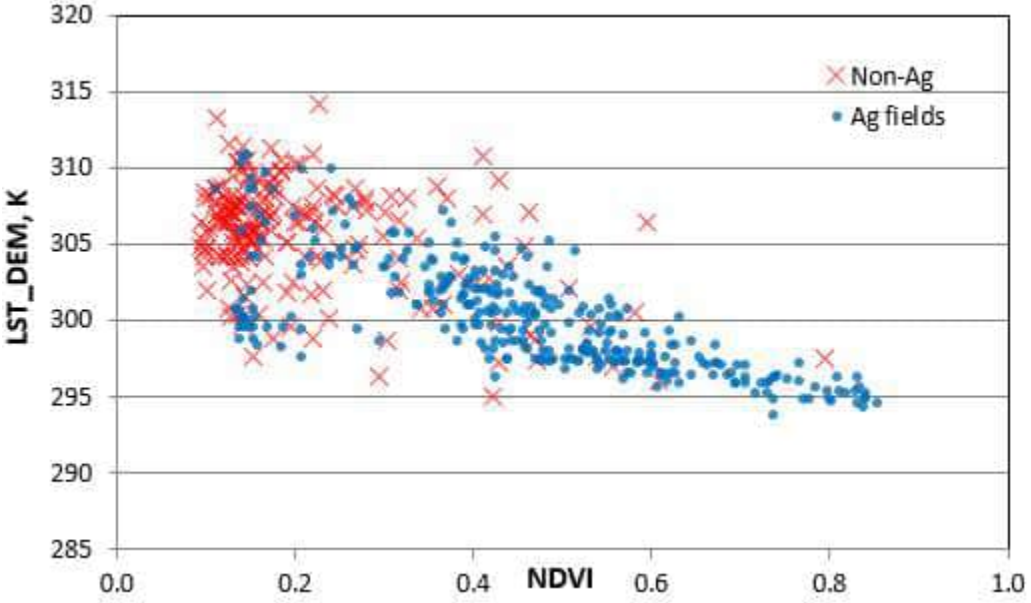

The graph for ETrF-EF vs. NDVI is as follows (where the blue points are agricultural fields, while the red crosses are non-Agricultural fields):

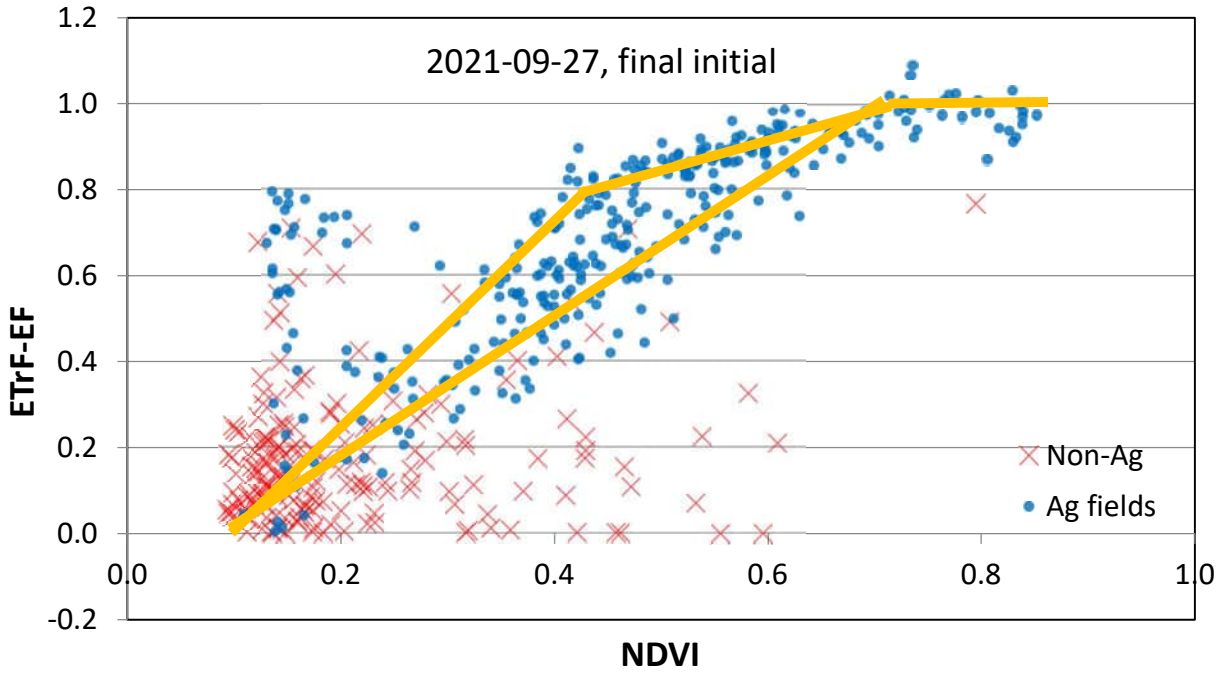

The calibration for ETrF for this date turned out relatively well, with an upper limit of ETrF. There was a plateau of ETrF ~ 1.0 for NDVI > 0.7, which is common and indicates a saturation of energy conversion and ET when NDVI is above that amount. An upper trend occurred for some sample points in the midrange of NDVI due either to corn or small grains that were showing reduced greenness and NDVI, but had continued transpiration at high levels, or had wet soil that contributed to ET.